USGS
science for a changing world

Prepared in Cooperation with South Dakota Department of Transportation, Federal Emergency Management Agency, City of Rapid City, and West Dakota Water Development District

Flood-Frequency Analyses from Paleoflood Investigations for Spring, Rapid, Boxelder, and Elk Creeks, Black Hills, Western South Dakota

Scientific Investigations Report 2011–5131

U.S. Department of the Interior
U.S. Geological Survey

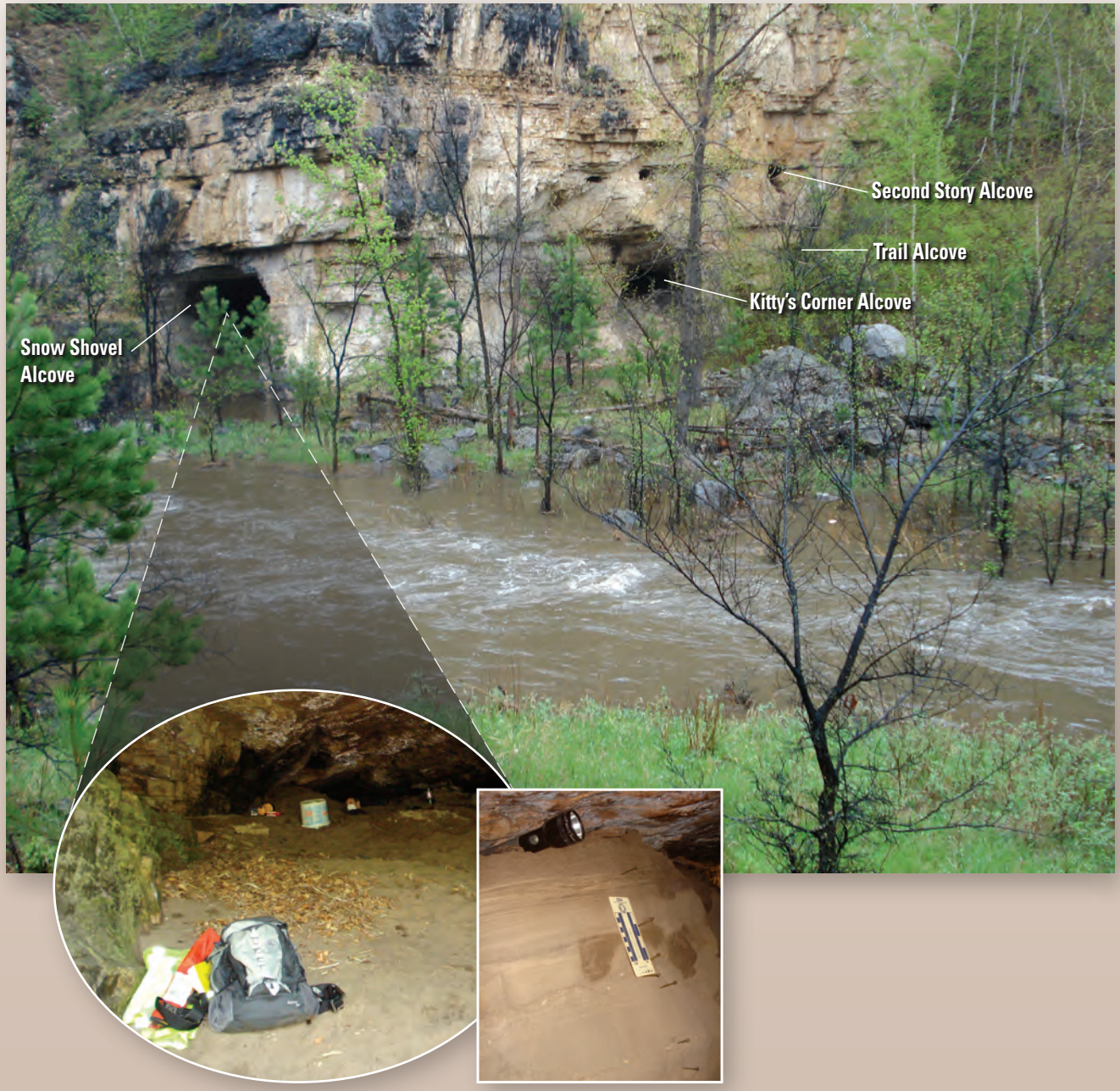

Front cover. High Alcove along downstream reach of Rapid Creek, with views of a flood deposit that recorded the largest known flood within any of the study reaches. This flood occurred about 440 years ago and had a flow of 128,000 cubic feet per second.

Inside front cover. Site of four alcoves for paleoflood investigations along downstream reach of Boxelder Creek where numerous large flows as much as 61,000 cubic feet per second were recorded by flood deposits. The flow of Boxelder Creek on this date was about 500 cubic feet per second. Insets show pit B of Snow Shovel Alcove about 50 feet to left of Kitty's Corner Alcove.

Flood-Frequency Analyses from Paleoflood Investigations for Spring, Rapid, Boxelder, and Elk Creeks, Black Hills, Western South Dakota

By Tessa M. Harden, Jim E. O'Connor, Daniel G. Driscoll, and John F. Stamm

Prepared in Cooperation with South Dakota Department of Transportation,
Federal Emergency Management Agency, City of Rapid City, and
West Dakota Water Development District

Scientific Investigations Report 2011–5131

U.S. Department of the Interior
U.S. Geological Survey

U.S. Department of the Interior
KEN SALAZAR, Secretary

U.S. Geological Survey
Marcia K. McNutt, Director

U.S. Geological Survey, Reston, Virginia: 2011

For more information on the USGS—the Federal source for science about the Earth, its natural and living resources, natural hazards, and the environment, visit http://www.usgs.gov or call 1–888–ASK–USGS.

For an overview of USGS information products, including maps, imagery, and publications, visit http://www.usgs.gov/pubprod

To order this and other USGS information products, visit http://store.usgs.gov

Any use of trade, product, or firm names is for descriptive purposes only and does not imply endorsement by the U.S. Government.

Although this report is in the public domain, permission must be secured from the individual copyright owners to reproduce any copyrighted materials contained within this report.

Suggested citation:
Harden, T.M., O'Connor, J.E., Driscoll, D.G., and Stamm, J.F., 2011, Flood-frequency analyses from paleoflood investigations for Spring, Rapid, Boxelder, and Elk Creeks, Black Hills, western South Dakota: U.S. Geological Survey Scientific Investigations Report 2011–5131, 136 p.

ISBN 978-1-4113-3230-0

Contents

Abstract 1
Introduction 2
Study Area and Background Information 3
Geology of the Study Area 5
Hydrology of the Study Area 5
Methods of Investigation 7
Development of Long-Term Flood Chronologies 8
Development of Paleoflood Chronologies 8
Stratigraphic Analysis 8
Geochronology 8
Compiling Reach-Scale Paleoflood Chronologies 10
Development of Modern Peak-Flow Chronologies 11
Estimation of Flow Rates 11
Assumptions and General Considerations 11
Hydraulic Modeling 11
Other Approaches for Estimation of Flow Rates 16
Flood-Frequency Analysis 16
Models for Flood-Frequency Analysis 16
Outstanding Uncertainty Issues 18
Flood-Frequency Analyses from Paleoflood Investigations 18
Spring Creek 18
Hydraulic Analysis and Paleoflood Chronology 19
Flood-Frequency Analysis 27
Rapid Creek 35
Lower Rapid Creek 35
Hydraulic Analysis and Paleoflood Chronology 37
Flood-Frequency Analysis 41
Upper Rapid Creek 49
Hydraulic Analysis and Paleoflood Chronology 49
Flood-Frequency Analysis 51
Implications of Paleoflood Chronologies for Rapid Creek 52
Boxelder Creek 58
Hydraulic Analysis and Paleoflood Chronology for Upstream Subreach 61
Flood-Frequency Analysis for Upstream Subreach 66
Hydraulic Analysis and Paleoflood Chronology for Downstream Subreach 66
Flood-Frequency Analysis for Downstream Subreach 69
Elk Creek 76
Hydraulic Analysis and Paleoflood Chronology 76
Flood-Frequency Analysis 78
Central Black Hills Flood Frequency: Synopsis, Implications, and Application 84
Synopsis of Results and Regional Assessment 84
Synopsis of Flood-Frequency Results 84

Regional Assessment....85
Implications for Flood Generation....86
Application for Hazard Assessment....89
Appropriate Application Domains....89
Quantile and Large-Flow Normalization....89
Approaches for Extrapolation and 1972 Flood Recurrence....90
Extrapolation Within Study Basins....90
Extrapolation Beyond Study Basins....92
Outstanding Issues and Uncertainties....94
Summary....95
References Cited....98
Supplement 1. Age-Dating Tables....103
Supplement 2. Modern Peak-Flow Chronologies....110
Spring Creek....110
Rapid Creek....110
Boxelder Creek....111
Elk Creek....111
Supplement 3. Schematic Diagrams....128

Figures

1. Map showing distribution of hydrogeologic units within the Black Hills area, locations of detailed paleoflood site investigations, and locations of selected streamgages....4
2. Geologic cross section *A–A'*....6
3. Photographs showing examples of bedrock outcrops along selected study reaches....7
4. Map showing topographic information and selected details of hydraulic analysis for Spring Creek reach....20
5. Photographs showing examples of geomorphic setting along Spring Creek reach....21
6. Graph showing modern peak-flow chronology (gaged records) for Spring Creek....22
7. Graph showing results of hydraulic model simulations for Spring Creek reach....23
8. Photographs showing setting and examples of stratigraphy for Superscour Alcove, Spring Creek....24
9. Schematic diagram showing paleoflood information for Superscour Alcove, Spring Creek....25
10. Schematic diagram showing paleoflood information for Hailstorm Alcove, Spring Creek....26
11. Schematic diagram showing paleoflood information for John Doe Alcove, Spring Creek....28
12. Schematic diagram showing paleoflood information for Temple of Doom Alcove, Spring Creek....29
13. Channel cross section and relevant elevations for Temple of Doom Alcove, Spring Creek....30

14. Graphical representation of the long-term flood chronology for Spring Creek 32
15. Graphs showing flood-frequency analyses for Spring Creek of gaged records only, and all available data that incorporate the long-term flood chronology from figure 14 34
16. Map showing topographic information and selected details of hydraulic analysis for lower Rapid Creek reach 36
17. Graph showing modern peak-flow chronology (gaged and historical records) for lower Rapid Creek reach 37
18. Graph showing results of hydraulic model simulations for lower Rapid Creek reach 38
19. Schematic diagram showing paleoflood information for Outhouse Alcove, lower Rapid Creek reach 39
20. Schematic diagram showing paleoflood information for Spider Alcove, lower Rapid Creek reach. 40
21. Schematic diagram showing paleoflood information for Meister Alcove, lower Rapid Creek reach 41
22. Schematic diagram showing paleoflood information for High Alcove, lower Rapid Creek reach 42
23. Schematic diagram showing paleoflood information for Lost Alcove, lower Rapid Creek reach 43
24. Schematic diagram showing paleoflood information for Black Socks Alcove, lower Rapid Creek reach 44
25. Graphical representation of the long-term flood chronology for lower Rapid Creek reach 45
26. Graphs showing flood-frequency analyses for lower Rapid Creek reach for gaged records only, and all available data that incorporate the long-term flood chronology from figure 25. 48
27. Graph showing modern peak-flow chronology for upper Rapid Creek reach 49
28. Channel cross section and relevant elevations for Gage House Alcove, upper Rapid Creek reach 50
29. Channel cross section and relevant elevations for Schist and Blue Ribbon Alcoves, upper Rapid Creek reach 52
30. Schematic diagram showing paleoflood information for Schist and Blue Ribbon Alcoves, upper Rapid Creek reach 53
31. Schematic diagram showing paleoflood information for Gage House Alcove, upper Rapid Creek reach 54
32. Graphical representation of the long-term flood chronology for upper Rapid Creek reach 55
33. Graphs showing flood-frequency analyses for upper Rapid Creek reach for gaged records only, and all available data that incorporate the long-term flood chronology from figure 32 57
34. Map showing topographic information and selected details of hydraulic analysis for Boxelder Creek reach 59
35. Graph showing modern peak-flow chronology (gaged records) for upstream subreach of Boxelder Creek 60
36. Graph showing modern peak-flow chronology (gaged records) for downstream subreach of Boxelder Creek 60
37. Graph showing results of hydraulic model simulations for Boxelder Creek reach 62

38. Schematic diagram showing paleoflood information for Joan's Alcove, upstream subreach of Boxelder Creek 63
39. Schematic diagram showing paleoflood information for Enob Alcove, upstream subreach of Boxelder Creek 64
40. Graphical representation of the long-term flood chronology for upstream subreach of Boxelder Creek 65
41. Graphs showing flood-frequency analyses for upstream subreach of Boxelder Creek for gaged records only, and all available data that incorporate the long-term flood chronology from figure 40 68
42. Schematic diagram showing paleoflood information for Custer Gap Alcove, downstream subreach of Boxelder Creek 69
43. Schematic diagram showing paleoflood information for Second Story Alcove, downstream subreach of Boxelder Creek 70
44. Schematic diagram showing paleoflood information for Trail Alcove, downstream subreach of Boxelder Creek 71
45. Schematic diagram showing paleoflood information for pit C in Kitty's Corner Alcove, downstream subreach of Boxelder Creek 72
46. Graphical representation of the long-term flood chronology for downstream subreach of Boxelder Creek 73
47. Graphs showing flood-frequency analyses for downstream subreach of Boxelder Creek for gaged records only, and all available data that incorporate the long-term flood chronology from figure 46 75
48. Graph showing modern peak-flow chronology (gaged records) for Elk Creek 76
49. Channel cross sections and relevant elevations for Dracula's Ledge, Elk Creek reach 77
50. Schematic diagram showing paleoflood information for Dracula's Ledge, Elk Creek 79
51. Graphical representation of the long-term flood chronology for Elk Creek 80
52. Graphs showing flood-frequency analyses for Elk Creek for gaged records only, and all available data that incorporate the long-term flood chronology from figure 51 83
53. Graph showing Black Hills paleofloods and maximum gaged flows for selected stream reaches, relative to national and regional envelope curves 87
54. Graph showing results of peak-flow frequency analyses for selected stream reaches, relative to regional envelope curve 88

Tables

1. Drainage areas and periods of peak-flow record for selected streamgages and for selected locations within and near study reaches 12
2. Modern peak-flow chronologies (gaged and historical records) for paleoflood study reaches 13
3. Summary of critical-flow computations for Temple of Doom Alcove, Spring Creek 30
4. Summary of long-term flood chronology used in flood-frequency analysis for Spring Creek 31
5. Flood-frequency analyses for Spring Creek 33
6. Summary of long-term flood chronology used in flood-frequency analysis for lower Rapid Creek reach 46
7. Flood-frequency analyses for lower Rapid Creek reach 47
8. Summary of Manning equation computations for selected locations along upper Rapid Creek reach 51
9. Summary of long-term flood chronology used in flood-frequency analysis for upper Rapid Creek reach 55
10. Flood-frequency analyses for upper Rapid Creek reach 56
11. Summary of long-term flood chronology used in flood-frequency analysis for upstream subreach of Boxelder Creek 65
12. Flood-frequency analyses for upstream subreach of Boxelder Creek 67
13. Summary of long-term flood chronology used in flood-frequency analysis for downstream subreach of Boxelder Creek 73
14. Flood-frequency analyses for downstream subreach of Boxelder Creek 74
15. Summary of critical-flow computations for Dracula's Ledge, Elk Creek 78
16. Summary of long-term flood chronology used in flood-frequency analysis for Elk Creek 81
17. Flood-frequency analyses for Elk Creek 82
18. Summary of flood-frequency analyses and large flows for paleoflood study reaches 85
19. Summary of normalized values for peak-flow estimates and selected large flows for paleoflood study reaches 91
20. Flood-frequency analyses scaled to drainage areas for selected streamgages 93
21. Summary of example flood-frequency computations for Cleghorn Canyon 94

Conversion Factors and Datums

Inch/Pound to SI

Multiply	By	To obtain
	Length	
inch (in.)	2.54	centimeter (cm)
inch (in.)	25.4	millimeter (mm)
foot (ft)	0.3048	meter (m)
mile (mi)	1.609	kilometer (km)
yard (yd)	0.9144	meter (m)
	Area	
square mile (mi^2)	259.0	hectare (ha)
square mile (mi^2)	2.590	square kilometer (km^2)
	Flow rate	
foot per second (ft/s)	0.3048	meter per second (m/s)
cubic foot per second (ft^3/s)	0.02832	cubic meter per second (m^3/s)
	Mass	
ounce, avoirdupois (oz)	28.35	gram (g) used in table S1–3 (Cesium)
pound, avoirdupois (lb)	0.4536	kilogram (kg)

Vertical coordinate information is referenced to the National Geodetic Vertical Datum of 1929 (NGVD 29) or the North American Vertical Datum of 1988 (NAVD 88).

Horizontal coordinate information is referenced to the North American Datum of 1983 (NAD 83).

Elevation, as used in this report, refers to distance above the vertical datum.

Water year is the 12-month period, October 1 through September 30, and is designated by the calendar year in which it ends. Thus, the water year ending September 30, 2009, is called the "2009" water year.

Under the downstream order system for streamgages, identification numbers increase in the downstream direction.

Symbols, Abbreviations, and Acronyms

α	significance criterion
~	approximately
±	plus or minus
1-σ	one standard deviation or 1-sigma
2-σ	two standard deviations or 2-sigma
^{12}C	carbon-12
^{14}C	carbon-14
EMA	expected moments algorithm
n	Manning's roughness coefficient
OSL	optically stimulated luminescence
SDDOT	South Dakota Department of Transportation
USGS	U.S. Geological Survey

Flood-Frequency Analyses from Paleoflood Investigations for Spring, Rapid, Boxelder, and Elk Creeks, Black Hills, Western South Dakota

By Tessa M. Harden, Jim E. O'Connor, Daniel G. Driscoll, and John F. Stamm

Abstract

Flood-frequency analyses for the Black Hills area are important because of severe flooding of June 9–10, 1972, that was caused by a large mesoscale convective system and caused at least 238 deaths. Many 1972 peak flows are high outliers (by factors of 10 or more) in observed records that date to the early 1900s. An efficient means of reducing uncertainties for flood recurrence is to augment gaged records by using paleohydrologic techniques to determine ages and magnitudes of prior large floods (paleofloods). This report summarizes results of paleoflood investigations for Spring Creek, Rapid Creek (two reaches), Boxelder Creek (two subreaches), and Elk Creek. Stratigraphic records and resulting long-term flood chronologies, locally extending more than 2,000 years, were combined with observed and adjusted peak-flow values (gaged records) and historical flood information to derive flood-frequency estimates for the six study reaches. Results indicate that (1) floods as large as and even substantially larger than 1972 have affected most of the study reaches, and (2) incorporation of the paleohydrologic information substantially reduced uncertainties in estimating flood recurrence.

Canyons within outcrops of Paleozoic rocks along the eastern flanks of the Black Hills provided excellent environments for (1) deposition and preservation of stratigraphic sequences of late-Holocene flood deposits, primarily in protected slack-water settings flanking the streams; and (2) hydraulic analyses for determination of associated flow magnitudes. The bedrock canyons ensure long-term stability of channel and valley geometry, thereby increasing confidence in hydraulic computations of ancient floods from modern channel geometry.

Stratigraphic records of flood sequences, in combination with deposit dating by radiocarbon, optically stimulated luminescence, and cesium-137, provided paleoflood chronologies for 29 individual study sites. Flow magnitudes were estimated from elevations of flood deposits in conjunction with hydraulic calculations based on modern channel and valley geometry. Reach-scale paleoflood chronologies were interpreted for each study reach, which generally entailed correlation of flood evidence among multiple sites, chiefly based on relative position within stratigraphic sequences, unique textural characteristics, or results of age dating and flow estimation.

The FLDFRQ3 and PeakfqSA analytical models (assuming log-Pearson Type III frequency distributions) were used for flood-frequency analyses for as many as four scenarios: (1) analysis of gaged records only; (2) gaged records with historical information; (3) all available data including gaged records, historical flows, paleofloods, and perception thresholds; and (4) the same as the third scenario, but "top fitting" the distribution using only the largest 50 percent of gaged peak flows. The PeakfqSA model is most consistent with procedures adopted by most Federal agencies for flood-frequency analysis and thus was (1) used for comparisons among results for study reaches, and (2) considered by the authors as most appropriate for general applications of estimating low-probability flood recurrence.

The detailed paleoflood investigations indicated that in the last 2,000 years all study reaches have had multiple large floods substantially larger than in gaged records. For Spring Creek, stratigraphic records preserved a chronology of at least five paleofloods in approximately (~) 1,000 years approaching or exceeding the 1972 flow of 21,800 cubic feet per second (ft^3/s). The largest was ~700 years ago with a flow range of 29,300–58,600 ft^3/s, which reflects the uncertainty regarding flood-magnitude estimates that was incorporated in the flood-frequency analyses.

In the lower reach of Rapid Creek (downstream from Pactola Dam), two paleofloods in ~1,000 years exceeded the 1972 flow of 31,200 ft^3/s. Those occurred ~440 and 1,000 years ago, with flows of 128,000–256,000 and 64,000–128,000 ft^3/s, respectively. Five smaller paleofloods of 9,500–19,000 ft^3/s occurred between ~200 and 400 years ago. In the upper reach of Rapid Creek (above Pactola Reservoir), the largest recorded floods are substantially smaller than for lower Rapid Creek and all other study reaches. Paleofloods of ~12,900 and 12,000 ft^3/s occurred ~1,000 and 1,500 years ago. One additional paleoflood (~800 years ago) was similar in magnitude to the largest gaged flow of 2,460 ft^3/s.

Boxelder Creek was treated as having two subreaches because of two tributaries that affect peak flows. During the last ~1,000 years, paleofloods of ~39,000–78,000 ft^3/s and 40,000–80,000 ft^3/s in the upstream subreach have exceeded the 1972 peak flow of 30,800 ft^3/s. One other paleoflood was similar to the second largest gaged flow (16,400 ft^3/s in 1907). For the downstream subreach, paleofloods of 61,300–123,000 ft^3/s and 52,500–105,000 ft^3/s in the last ~1,000 years have substantially exceeded the 1972 flood (50,500 ft^3/s). Four additional paleofloods had flows between 14,200 and 33,800 ft^3/s.

The 1972 flow on Elk Creek (10,400 ft^3/s) has been substantially exceeded at least five times in the last 1,900 years. The largest paleoflood (41,500–124,000 ft^3/s) was ~900 years ago. Three other paleofloods between 37,500 and 120,000 ft^3/s occurred between 1,100 and 1,800 years ago. A fifth paleoflood of 25,500–76,500 ft^3/s was ~750 years ago.

Considering analyses for all available data (PeakfqSA model) for all six study reaches, the 95-percent confidence intervals about the low-probability quantile estimates (100-, 200-, and 500-year recurrence intervals) were reduced by at least 78 percent relative to those for the gaged records only. In some cases, 95-percent uncertainty intervals were reduced by 99 percent or more. For all study reaches except the two Boxelder Creek subreaches, quantile estimates for these long-term analyses were larger than for the short-term analyses.

The 1972 flow for the Spring Creek study reach (21,800 ft^3/s) corresponds with a recurrence interval of ~400 years. Recurrence intervals are ~500 years for the 1972 flood magnitudes along the lower Rapid Creek reach and the upstream subreach of Boxelder Creek. For the downstream subreach of Boxelder Creek, the large 1972 flood magnitude (50,500 ft^3/s) exceeds the 500-year quantile estimate by about 35 percent. The recurrence interval of ~100 years for 1972 flooding along the Elk Creek study reach is small relative to other study reaches along the eastern margin of the Black Hills.

All of the paleofloods plot within the bounds of a national envelope curve, indicating that the national curve represents exceedingly rare floods for the Black Hills area. Elk Creek, lower Rapid Creek, and the downstream subreach of Boxelder Creek all have paleofloods that plot above a regional envelope curve; in the case of Elk Creek, by a factor of nearly two. The Black Hills paleofloods represent some of the largest known floods, relative to drainage area, for the United States. Many of the other largest known United States floods are in areas with physiographic and climatologic conditions broadly similar to the Black Hills—semiarid and rugged landscapes that intercept and focus heavy precipitation from convective storm systems.

The 1972 precipitation and runoff patterns, previous analyses of peak-flow records, and the paleoflood investigations of this study support a hypothesis of distinct differences in flood generation within the central Black Hills study area. The eastern Black Hills are susceptible to intense orographic lifting associated with convective storm systems and also have high relief, thin soils, and narrow and steep canyons—factors favoring generation of exceptionally heavy rain-producing thunderstorms and promoting runoff and rapid concentration of flow into stream channels. In contrast, storm potential is smaller in and near the Limestone Plateau area, and storm runoff is further reduced by substantial infiltration into the limestone, gentle topography, and extensive floodplain storage.

Results of the paleoflood investigations are directly applicable only to the specific study reaches and in the case of Rapid Creek, only to pre-regulation conditions. Thus, approaches for broader applications were developed from inferences of overall flood-generation processes, and appropriate domains for application of results were described. Example applications were provided by estimating flood quantiles for selected streamgages, which also allowed direct comparison with results of at-site flood-frequency analyses from a previous study.

Several broad issues and uncertainties were examined, including potential biases associated with stratigraphic records that inherently are not always complete, uncertainties regarding statistical approaches, and the unknown applicability of paleoflood records to future watershed conditions. The results of the paleoflood investigations, however, provide much better physically based information on low-probability floods than has been available previously, substantially improving estimates of the magnitude and frequency of large floods in these basins and reducing associated uncertainty.

Introduction

Estimates of the frequency of large riverine flows (peak-flow or flood-frequency estimates) serve many purposes, including (1) design of dams, highways, and many other types of infrastructure; (2) land-use planning and zoning; and (3) establishment of rates for flood insurance and other floodplain management purposes. Consequently, the importance of flood-frequency estimates has motivated substantial work, mainly involving statistical techniques, toward improving estimates of the magnitude and frequency of especially large and rare (low-probability) floods. An inherent limitation of nearly all such approaches, however, is that estimates of infrequent phenomena are needed and the observational records generally are short (typically less than 100 years for the Black Hills area) relative to the recurrence of low-probability floods. In this study, observational and historical records of flooding are supplemented with stratigraphic evidence of large floods from the last 1,000 to 2,000 years for four drainage basins in the central and eastern Black Hills of South Dakota, thereby substantially lengthening the record of large floods and allowing for much more confident prediction of the magnitude and frequency of low-probability floods for these streams.

Flood-frequency analyses for the Black Hills of western South Dakota are technically challenging and of substantial local interest and importance, chiefly because of the

large and damaging flooding of June 9–10, 1972, along the eastern flanks of the Black Hills. Flooding was caused by a large mesoscale convective system and resulted in at least 238 deaths and more than $160 million (about $664 million in 2002 dollars) in damage (Carter and others, 2002). Flooding was especially severe within Rapid City (Schwarz and others, 1975), where a 10-mile (mi) long corridor along Rapid Creek was devastated (Larimer, 1973). Exceptional flooding also affected Battle and Spring Creeks to the south, and Boxelder, Elk, and Bear Butte Creeks to the north (fig. 1).

As of 2011, peak flows from the 1972 flooding still remain as peaks of record for 14 streamgages in the Black Hills area (Driscoll and others, 2010). Despite streamflow records (observational records or gaged records) that date back to the early 1900s for some of the affected river systems, the 1972 peak flow exceeds the next largest flow by a factor of 10 for 8 of these streamgages, and by almost 20 times for 2 streamgages. As described by Sando and others (2008), such disparities or high outliers create substantial uncertainty for peak-flow frequency analyses for affected streams. Without additional information, it is difficult to reasonably estimate the frequency of such large flows: Is the record of the last 100 years typical? Alternatively, are flows such as 1972 exceptionally rare, recurring only at a millennial or even rarer frequency?

These questions recently were highlighted by severe thunderstorms on August 17, 2007, which caused heavy precipitation and flash flooding near Hermosa and Piedmont in the eastern Black Hills. As described by Driscoll and others (2010), the 2007 storm system caused the most substantial flooding in the Black Hills area since 1972 and resulted in a peak flow along Battle Creek near Hermosa that was only slightly smaller than the record 1972 flood at the same location. The 2007 storm area was much smaller, however, than for the 1972 storm, and severe flooding was restricted to the Hermosa area. In reporting on this event, Driscoll and others (2010) also compiled and examined a history of storm and flood events since 1877 for the Black Hills area (U.S. Geological Survey, 2010a).

In appropriate environments, an efficient means of reducing uncertainties regarding probabilities of flood recurrence is to augment observational and historical peak-flow records by using paleohydrologic techniques (Costa, 1978; Hosking and Wallis, 1986; Stedinger and Baker, 1987; Frances and others, 1994; Webb and others, 2002)—typically using geologic and paleobotanical evidence to determine the ages and magnitudes of floods that occurred before collection of observational records (paleofloods). During 2005–07, the U.S. Geological Survey (USGS) and South Dakota Department of Transportation (SDDOT) cooperated on a reconnaissance-level study (South Dakota Department of Transportation, 2010) confirming that such paleohydrologic techniques likely could improve estimates of the magnitude and frequency of low-probability floods in the Black Hills area (O'Connor and Driscoll, 2007). That study was followed in 2008 by a more comprehensive study in cooperation with the SDDOT, and included additional support from the Federal Emergency Management Agency, city of Rapid City, and West Dakota Water Development District. The primary purpose of this more comprehensive study was to improve flood-frequency characterization of low-probability floods for major streams in the central Black Hills through paleoflood investigations, which included analyses of stratigraphic evidence, timing, and magnitudes for large floods on Spring Creek, Rapid Creek (two reaches), Boxelder Creek (two subreaches), and Elk Creek. The stratigraphic records and resulting long-term flood chronologies, locally extending back more than 2,000 years, were combined with observed peak-flow records and historical flood observations to derive flood-frequency estimates. This report summarizes flood-frequency analyses from paleoflood investigations for each of the six study reaches.

Many individuals and entities supported this study. Special thanks are extended to numerous landowners who graciously provided access to private land. Gerardo Benito of the Centro de Ciencias Medioambientales of Spain assisted with stratigraphic interpretation. Several USGS scientists contributed to geochronologic analyses, including Shannon Mahan, Marci Marot, and John McGeehin.

Study Area and Background Information

The study area consists of the Spring, Rapid, Boxelder, and Elk Creek drainage basins within the central part of the Black Hills (fig. 1). Long-term frequency analyses were developed for 6 stream reaches within these basins: 1 reach on Spring Creek; 2 reaches on Rapid Creek, 1 upstream and 1 downstream from Pactola Reservoir; 2 adjacent subreaches along Boxelder Creek; and 1 reach along Elk Creek. For each of these reaches, paleoflood investigations and resulting flood-frequency assessments were based on multiple sites of stratigraphic analysis in conjunction with geochronology and hydraulic modeling.

The primary evidence for past large and infrequent floods consists of stratigraphic records formed of fine-grained sediment deposits preserved in slack-water environments. These deposits accumulate and can record multiple floods throughout several thousand years where (1) velocities are relatively low, which can allow deposition of suspended sediment; and (2) conditions are suitable for preservation. As described by O'Connor and Driscoll (2007) and in more detail in the "Methods of Investigation" section, numerous locations in canyons along the eastern flanks of the Black Hills provide excellent environments for (1) deposition and preservation of stratigraphic sequences of late-Holocene flood deposits, primarily in overhanging ledges, alcoves, and small caves flanking the streams; and (2) hydraulic analyses for determination of associated flow magnitudes.

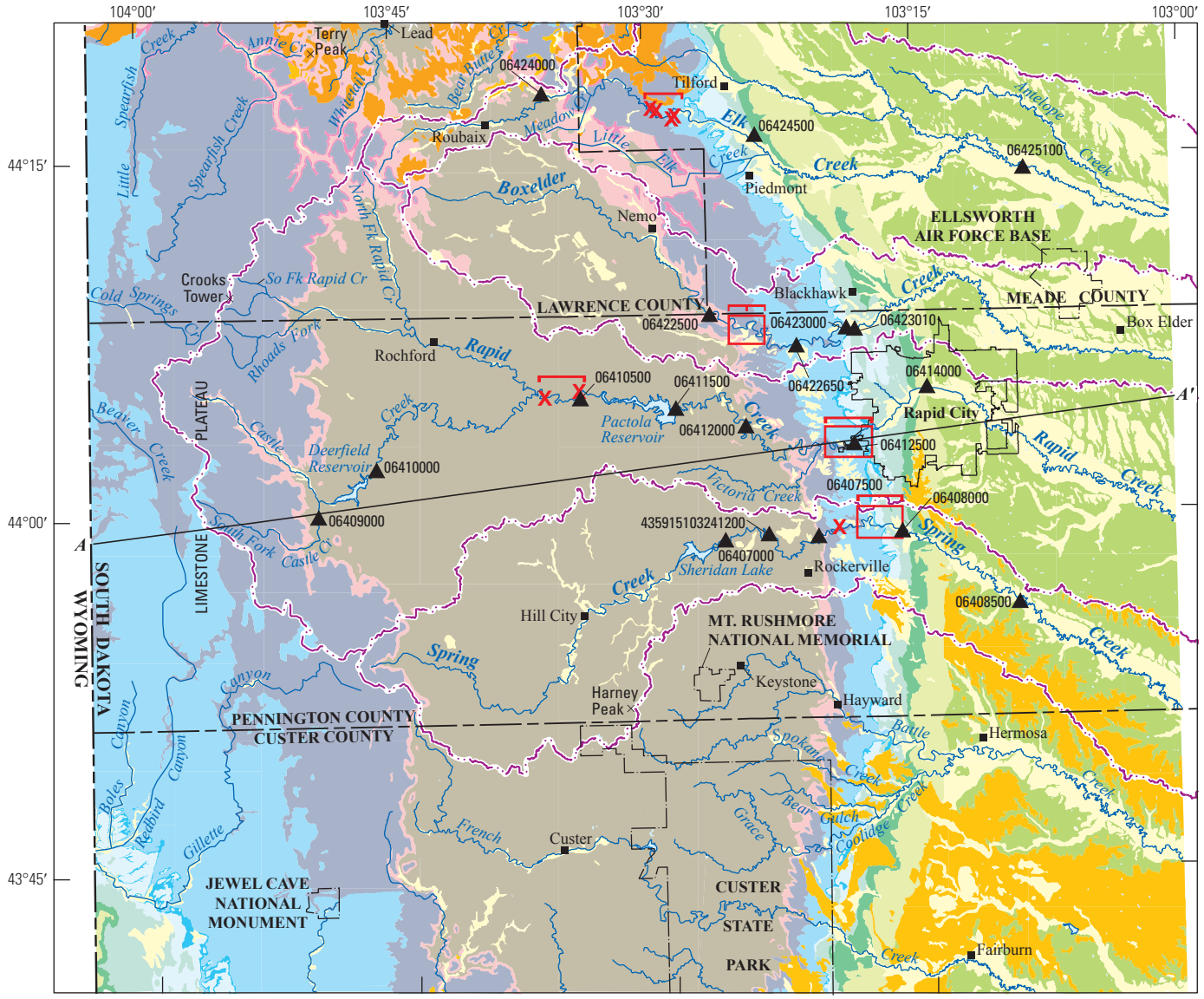

Hydrogeologic units modified from Strobel and others, 1999

Base modified from U.S. Geological Survey digital data, 1977–85, 1:100,000
Rapid City, Office of City Engineer map, 1996, 1:18,000
Universal Transverse Mercator projection, Zone 13

0 2 4 6 8 10 MILES
0 2 4 6 8 10 KILOMETERS

EXPLANATION

- Study reach or subreach
- Reach of detailed paleoflood site investigations and hydraulic analysis
- Boundary of study basin
- A A′ Line of geologic section (fig. 2)
- X Location of detailed paleoflood site investigation
- 06408500 ▲ Streamgage and identification number

Hydrogeologic units	Stratigraphic units	Map units
Unconsolidated units	QTac	Alluvium and colluvium, undifferentiated
White River aquifer	Tw	White River Group
Tertiary intrusive units	Tui	Undifferentiated intrusive igneous rocks
Cretaceous-sequence confining unit	Kps	Pierre Shale to Skull Creek Shale, undifferentiated
Inyan Kara aquifer	Kik	Inyan Kara Group
Jurassic-sequence semiconfining unit	Ju	Morrison Formation to Sundance Formation, undifferentiated
Spearfish confining unit	TRPs	Spearfish Formation
Minnekahta aquifer	Pmk	Minnekahta Limestone
Opeche confining unit	Po	Opeche Shale
Minnelusa aquifer	PIPm	Minnelusa Formation
Madison aquifer	MDme	Madison (Pahasapa) Limestone and Englewood Formation
Ordovician-sequence semiconfining unit	Ou	Whitewood Formation and Winnipeg Formation
Deadwood aquifer	O€d	Deadwood Formation
Precambrian igneous and metamorphic units	p€u	Undifferentiated igneous and metamorphic rocks

Figure 1. Distribution of hydrogeologic units within the Black Hills area, locations of detailed paleoflood site investigations, and locations of selected streamgages.

Geology of the Study Area

The successful paleoflood investigations in the Black Hills owe largely to the geologic and hydrologic environment. The Black Hills uplift formed as an elongated dome about 60 to 65 million years ago during the Laramide orogeny (Redden and Lisenbee, 1996). The dome trends north-northwest and is about 120-mi long and 60-mi wide, with elevations ranging from 7,242 feet (ft) above National Geodetic Vertical Datum of 1929 at Harney Peak to about 3,000 ft in the adjacent plains. Erosion has exposed Precambrian-age igneous and metamorphic rock units in the central Black Hills (fig. 1), flanked by outward-tilted (fig. 2) Paleozoic carbonate and sedimentary rocks that include the Ordovician- and Cambrian-age Deadwood Formation through the Permian-age lower Spearfish Formation. Each of the four study basins heads at least in part within the Precambrian rocks before draining eastward through canyons and steep-sided valleys that are cut into progressively younger Paleozoic rocks and that exit onto the plains of western South Dakota at approximately the upper extent of the Paleozoic sequence.

Four of the six study reaches (all except the upstream reaches of Rapid and Boxelder Creeks) are where the streams cut through the Mississippian- and Devonian-age Madison Limestone and the Pennsylvanian- and Permian-age Minnelusa Formation (fig. 1). Both formations have local site conditions conducive for flood deposition and preservation of flood slack-water deposits. The Madison Limestone is cavernous, with many small caves and alcoves in canyon walls that flank the modern channels and provide many potential sites for accumulating and sheltering slack-water deposits. The Minnelusa Formation is not as cavernous, but erodes and weathers into ledgy outcrops with alcoves and overhangs that locally accumulate and preserve slack-water deposits. The upstream subreach of Boxelder Creek is within the Ordovician- and Cambrian-age Deadwood Formation, a sandstone and conglomerate that can erode into ledges and overhangs similar to the Minnelusa Formation. The upstream reach of Rapid Creek is within the Precambrian rocks.

The formation and identification of slack-water deposits is enhanced by the coarse-grained Precambrian metamorphic and igneous rocks within the headwaters of all study basins. Tertiary-age intrusive rock units also are exposed in parts of the Boxelder and Elk Creek Basins (fig. 1). The Tertiary rocks and the Precambrian granitic rocks, gneisses, and schists all weather to produce micaceous quartzofeldspathic sand fine enough to be readily entrained during large floods, and thereby creating large suspended-sediment loads, but sufficiently coarse to settle rapidly in slack-water environments producing depositional sequences. Additionally, within the five reaches in the Paleozoic sedimentary rocks, the distinctly micaceous sands derived from the upper parts of the four study basins allow for secure identification of main-stem flood deposits. In particular, the mica-rich sands derived from the Precambrian and Tertiary rocks in the upstream parts of the basin are unambiguously distinguishable within sediment accumulations from deposits of local tributaries, slopewash, or sediment spalling from cave and alcove ceilings and walls, none of which contains mica.

Another key geologic aspect of the Black Hills study reaches is the long-term stability of the channel and valley geometry, providing persistent sites of slack-water deposition and increasing confidence in hydraulic computations of ancient floods from modern channel geometry. All study reaches are in narrow valleys laterally constrained by steep bedrock slopes. Because of the narrow canyons, flood stages change markedly with flow magnitudes, therefore improving reliability of flow estimates derived from the elevations of flood deposits. Additionally, bedrock crops out locally in the channel thalweg for all study reaches, indicating that the streams are flowing on alluvial deposits that are less than a few tens of feet thick. Thus, potential for lateral erosion and channel scour during floods is limited by bedrock valley margins and thin alluvial cover in valley bottoms, which reduces uncertainty in the hydraulic computations owing to uncertain channel geometry. Photographs illustrating channel conditions along Spring and Elk Creeks are provided in figure 3.

Long-term regional rates of downcutting are consistent with the premise of overall channel stability for the last several thousand years. As illustrated in figure 2, more than 5,000 ft of bedrock overlies the Deadwood Formation east of the Black Hills. Uplift of the Black Hills area began about 60 to 65 million years ago (Redden and Lisenbee, 1996), indicating a long-term regional erosion rate of 0.08 ft per thousand years. Modern rates of regional downcutting may be different than long-term averages, but overall downcutting in the last 2,000–3,000 years—the maximum length of the stratigraphic records of flooding considered in this study—is almost certainly less than 1 ft.

Hydrology of the Study Area

Many investigators have described the hydrology of the study area relative to general water-resource considerations, and a comprehensive summary was provided by Driscoll and others (2002). Driscoll and Carter (2001) identified five hydrogeologic settings for the Black Hills area that distinctively affect general streamflow characteristics. Sando and others (2008) described effects of these hydrogeologic settings on peak-flow characteristics, one of which is a distinct reduction in peak-flow magnitudes for low-magnitude peaks within “loss zones” that exist within the Paleozoic canyon reaches (Hortness and Driscoll, 1998). Because of this effect, the Spring Creek, lower Boxelder Creek, and Elk Creek reaches frequently are dry, and flow may not occur during some years.

Driscoll and others (2010) examined climatological factors affecting generation of heavy rain-producing thunderstorms in the Black Hills area, which were identified as causing most of the measured and historically reported large floods in the area. That study documented a tendency for

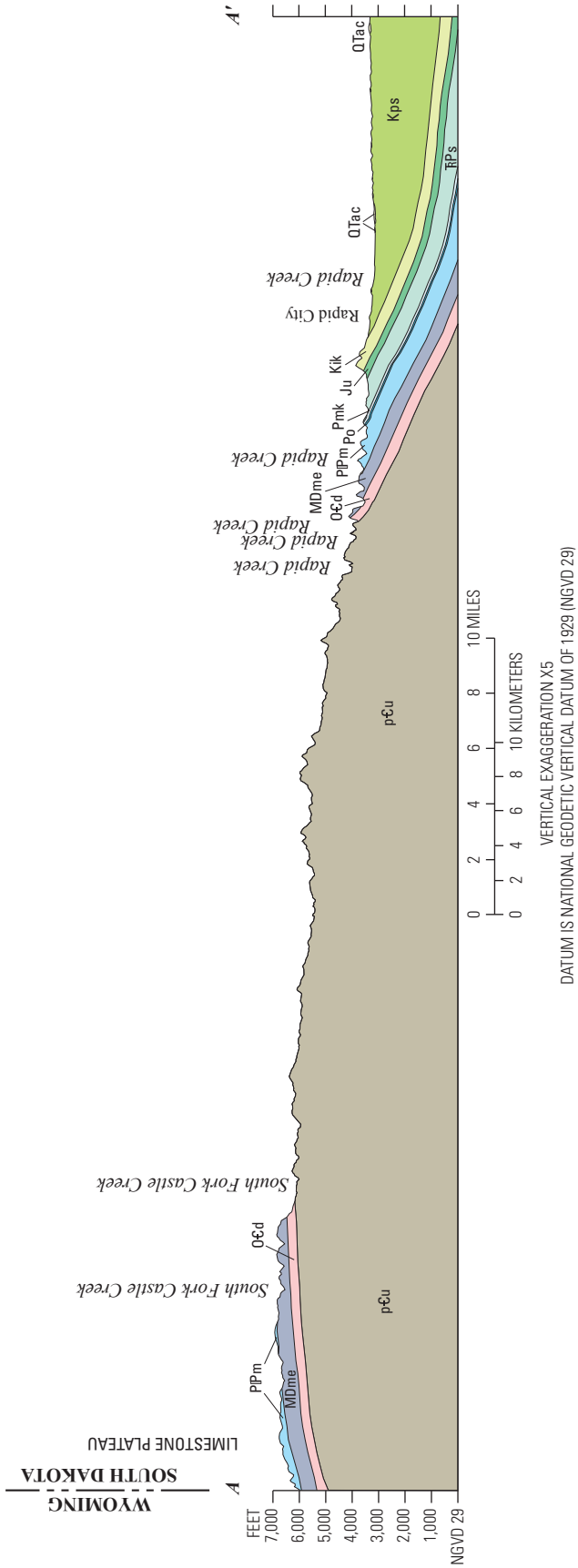

Figure 2. Geologic cross section *A–A′* (modified from Strobel and others, 1999). Location of section and abbreviations for stratigraphic intervals are shown on figure 1.

Figure 3. Examples of bedrock outcrops along selected study reaches. Photographs show *A*, outcrop of the Minnekahta Limestone along Spring Creek and *B*, outcrop of the Madison Limestone along Elk Creek.

exceptionally heavy precipitation east of the major axis of the Black Hills uplift, which generally coincides with a north/south trending escarpment along the contact between the Deadwood Formation and the Precambrian rocks about 10 to 15 mi east of the South Dakota/Wyoming border (fig. 1). The heaviest rain-producing thunderstorms generally occur east of this escarpment, with the greatest rainfall intensities and volumes along the eastern flanks of the Black Hills uplift and coinciding with areas of steepest slopes and greatest orographic uplift. Sando and others (2008) also identified this general area as having especially large flood potential owing to (1) rapid flow concentration by the steep topography and (2) limited attenuation of flood peaks within the narrow canyon reaches.

In comparing storms and flooding during 2007 and 1972, Driscoll and others (2010) provided examples of large and rapid changes in flow, which are typical of hydrographs for flash floods recorded for the Black Hills area. In conjunction with the flashy hydrographs, that study also documented large spatial variability in peak flows within short stream reaches for both floods. Such variability in spatial and temporal flow characteristics for these recent flows probably applies to floods recorded by slack-water deposits as well.

Driscoll and others (2010) also identified a gradient of increasing potential (from south to north) for contributions to large-scale floods from antecedent moisture conditions, which can include snowpack, soil moisture, high base flow, and runoff from previous precipitation events. Snowpack can contribute by way of both antecedent runoff (from snowmelt) and potential for melting during relatively warm rainfall events. The south to north gradient is consistent with (1) patterns for average annual precipitation, which increases from about 16 inches (in.) at the southern extent of the Black Hills to almost 30 in. near Lead in the northern Black Hills (Driscoll and others, 2000); and (2) seasonal precipitation patterns, which typically result in the heaviest snowpack accumulations for the northern Black Hills.

Land use and disturbance, especially from forest fires (for example, Agnew and others, 1997) can affect flood generation in the Black Hills. Driscoll and others (2004) documented increases in peak flows following the 1988 Galena Fire within the Battle Creek watershed. Some individual slack-water deposits investigated during this study contained abundant charcoal, indicating probable deposition shortly after large fires that may have enhanced basin runoff. Historical fire suppression probably has increased timber stand densities in the Black Hills (Progulske, 1974; Grafe and Horsted, 2002; Driscoll and others, 2004) with associated decreases in fire frequency, but increases in fire size and intensity (Brown and Sieg, 1996; Covington and More, 1994). For small urbanized basins, flood magnitudes certainly have increased since European settlement because of construction of impervious surface areas. However, overall flood potential before European settlement is not known to be substantially different than current flood potential as a consequence of land-cover changes for the largely undeveloped and forested basins of this study.

Methods of Investigation

The primary focus of this study was to characterize the frequency of recurrence of low-probability floods for six stream reaches within four basins of the central and eastern Black Hills (fig. 1). The main sources of information used in this study are stratigraphic records of large prehistoric floods, supplemented by existing peak-flow records and historical flood accounts. The overall approach for each reach consisted of (1) interpreting individual chronologies of flood stages from stratigraphic analysis and age dating of slack-water deposits for multiple sites within a study reach (detailed paleoflood site investigations); (2) estimating peak-flow magnitudes associated with elevations of flood evidence; (3) interpreting an overall paleoflood chronology for each study reach;

and (4) conducting quantitative flood-frequency analyses incorporating all relevant peak-flow information that includes paleoflood information, observational records, and historical flood accounts.

Development of Long-Term Flood Chronologies

Long-term flood chronologies primarily were derived from stratigraphic and geochronologic analysis of paleoflood deposits. Ensuing flood-frequency analyses also incorporated modern chronologies from observed peak-flow records and historical flood accounts.

Development of Paleoflood Chronologies

Paleoflood chronologies were derived primarily from stratigraphic analysis and age dating of flood slack-water deposits. This approach has been developed during the last three decades and is now a widely used method for quantifying unrecorded floods (Baker, 1987; Kochel and Baker, 1988; Ely and others, 1993; O'Connor and others, 1994; Sheffer and others, 2008). Flood slack-water deposits are composed of sand and silt suspended in large, high-velocity floods and deposited in channel margin areas where the sediment falls out of suspension because of reduced flow velocities. Typical sites where slack-water deposits are well preserved can include tributary mouths, rock shelters and alcoves, and bedrock caves (Kochel and Baker, 1982, 1988; Baker, 1987). Stable sites can yield information on numerous floods throughout thousands of years.

Stratigraphic Analysis

For this study, potential sites for stratigraphic analysis were identified by obtaining access permission and examining canyon walls and valley margins along most of the lengths of each of the study reaches where streams cut through geologic formations suitable for deposition and preservation of slack-water deposits (chiefly the Madison and Minnelusa Formations). In many locations, searches for appropriate sites were guided by visible flood evidence from 1972, which commonly could be distinguished from older evidence based on knowledge of the 1972 flow rate, deposit flotsam (particularly beverage containers, milled wood, and plastic debris), and the degree of weathering of the flood deposits or entrained organic material. For sites where reconnaissance indicated possible sediment accumulations from prehistoric floods, the stratigraphy was exposed by excavations. Pits typically were excavated through all the slack-water deposits to either bedrock or large and immovable rockfall. Where possible, several pits were excavated at each site in search for the most complete record. Also where possible, stratigraphic sequences were examined at multiple elevations at individual sites, as well as multiple sites within reaches, in order to more precisely define the frequency of deposition at different stages.

Upon excavation, pit stratigraphy was examined to determine the sequence of flood deposits. Individual flood deposits typically were separated from each other by evidence of temporal hiatus. Such evidence included layers or isolated clasts of local rockfall, bioturbated cave or alcove floor deposits, slopewash, in situ vegetation, and in some cases, evidence of cultural occupation or soil development. Identification of this evidence is key to the stratigraphic interpretations, and errors in inferences regarding breaks between individual flood deposits can lead to under- or over-estimates of the number of floods recorded in a sequence of deposits. Consequently, considerable effort was made to expose as much of the stratigraphy as possible and to carefully evaluate deposit stratigraphy for evidence of individual episodes of flood deposition. All observations and interpretations were recorded in detailed field notes and included measured thicknesses of all stratigraphic units, color, texture, grain size, degree of sorting, moisture content, amount of organic material, type of fluvial structures such as laminations or crossbedding if present, degree of bioturbation, and the nature of the contact between units.

Geochronology

The stratigraphy provided information on the number of floods and their relative ages, with more recent flood deposits on top of, or inset against, older deposits. Ages of individual flood deposits and the total length of record preserved in the stratigraphy were obtained by standard geochronologic techniques. The primary geochronologic approach used was radiocarbon analysis using carbon-14 (^{14}C) (Stuiver and Polach, 1977) of organic detritus, including charcoal, wood fragments, bark, pine cones and needles, and rodent fecal pellets that were deposited within and between individual flood deposits.

Organic samples were collected during examination and description of site stratigraphy. Samples were collected by hand, metal spatula, trowel, or knife and placed in sealable plastic bags. The nature of the material, its location in the section, and depth below the surface were recorded for each sample. For some flood deposits without visible organic material, bulk sediment samples were collected and later more closely examined to identify datable fragments of organic material. From all collected samples (more than 300), the 99 samples submitted for radiocarbon analysis were selected (1) on the basis of judgments regarding the relative importance of individual deposit sequences for understanding the overall flood history; (2) to obtain ages for the largest floods; and (3) to determine the length of depositional records at key sites, typically by selecting samples from near the base of deposit sequences. Results from basal ages guided selection of additional analyses. Additionally, multiple samples from some individual flood deposits (or intervening layers) were submitted to confirm key ages or to reduce ambiguity for cases where ages from previously analyzed samples were inconsistent with stratigraphy. Submitted samples were converted to graphite (Vogel and others, 1984) at the USGS Radiocarbon Dating Laboratory in Reston, Va. (U.S. Geological Survey, 2010b)

and dated by accelerator mass spectrometry at either the Center for Mass Spectrometry, Lawrence Livermore National Laboratory in Livermore, Calif. (Center for Accelerator Mass Spectrometry, 2011) or at the Arizona Accelerator Mass Spectrometry Laboratory in Tucson, Ariz. (Accelerator Mass Spectrometry Laboratory, 2011). Ages were calculated according to the methods of Stuiver and Polach (1977).

Results of radiocarbon analyses can have inherent ambiguity. Plants incorporate atmospheric ^{14}C through photosynthesis, and systematic loss of ^{14}C from the plant tissue occurs by radioactive decay beginning when the plant dies. Thus, radiocarbon dating yields the time of death of the plant. Consequently, an inherent assumption is that time of death of organic material associated with a flood deposit closely approximates the time of the flood. More precisely, however, the radiocarbon age of organic material within a flood deposit is a maximum limiting age for the flood, and organic materials associated with subaerial surfaces that accumulated materials between floods, provide a maximum limiting age for the flood deposit overlying the surface. To reduce potential errors resulting from dating materials substantially older than the associated flood deposits, selected samples for dating typically were those not expected to persist long in open environments, such as small plant fragments, pine needles, and leaves. In certain situations, however, the only available datable materials were of types that could have persisted for many years, even centuries, before being entrained into a flood deposit. Charcoal and large wood fragments are particularly susceptible to yielding erroneously old ages because of their potential persistence and reworking by multiple floods (Blong and Gillespie, 1978). For many sites, multiple samples were analyzed for key flood deposits to reduce the possibility of these types of errors affecting the final flood chronologies.

In addition to uncertainty introduced by stratigraphic context of the sample, the ratio of ^{14}C to carbon-12 (^{12}C) in the atmosphere, biosphere, and hydrosphere has varied; consequently, radiocarbon ages based on the historical ratio diverge from true calendar ages. For this reason, all radiocarbon ages were converted to calendar ages. For radiocarbon ages less than about 300 years, the resulting uncertainties in the calendar age are especially large because of the large and varying quantities of ^{12}C released into the atmosphere by anthropogenic burning of fossil fuels (Walker, 2005). Samples of organic materials photosynthesizing after A.D. 1950 have particularly high ^{14}C levels because of substantial ^{14}C introduction into the atmosphere by aboveground nuclear testing, and such post-1950 ages are simply noted as “modern.” As a consequence of these variations, radiocarbon ages of between 60 and about 300 years before present (2010) cannot typically be distinguished from each other, hindering precise dating of individual flood deposits from this time period (Taylor, 2001).

Radiocarbon results for 99 analyzed samples are reported in table S1–1 in the “Supplement 1. Age-Dating Tables” section. Reported results include the uncalibrated radiocarbon age plus or minus (±) the analysis error of one standard deviation (1-σ or 1-sigma). Also reported are the calibrations in calendar years [and the resulting two standard deviation (2-σ or 2-sigma) uncertainties] as determined by the radiocarbon calibration program Oxcal version 4.1 (Bronk Ramsey and others, 2001; Bronk Ramsey, 2009; Reimer and others, 2009). Because of fluctuations in the atmospheric ^{14}C content, some radiocarbon ages equate to multiple calendar-year periods. A “median” age derived (using the Oxcal calibration program) from the single or multiple age ranges also is reported.

The radiocarbon dating generally resulted in internally consistent results, with younger ages obtained from deposits stratigraphically above deposits with older ages. However, a few cases of widely divergent ages from the same stratigraphic deposit, and inconsistencies among dates relative to stratigraphic position probably resulted from (1) old charcoal or wood being entrained into a flood deposit; (2) bioturbation by plants or burrowing animals, resulting in movement of organic matter between stratigraphic units; (3) mistakenly sampling roots instead of detrital organic materials; and (4) errors in interpretation of the stratigraphic context of the sample in the overall deposit stratigraphy. Judging from the overall consistency of results, however, such issues were uncommon, and most of the few observed inconsistencies probably are because of old detrital material being incorporated into younger flood deposits.

Optically stimulated luminescence (OSL) was used for dating deposits less than about 300 years old, which cannot be precisely dated by radiocarbon analyses, and for deposits with insufficient organic material for radiocarbon dating. Sediment containing (or proximal to) naturally occurring radioactive isotopes, such as uranium, thorium, and potassium-40, are subject to low levels of radiation (Walker, 2005). OSL dating relies on the accumulation of free electrons derived from the decay of such radioisotopes within structural defects in the crystal lattice of a mineral grain. The longer a mineral grain is exposed to a radiation source, such as being buried in sediment with radioactive isotopes, the more trapped electrons accumulate (Bradley, 1999; Walker, 2005). When a mineral grain is exposed to light, the electrons are stimulated and released from the crystal lattice. Under laboratory conditions, the number of electrons released can be measured and correlated to the amount of time the crystal has been buried, thus giving a burial age. Flood sediments considered for this study primarily are derived from upstream igneous or metamorphic rocks containing naturally occurring radioactive isotopes. Additionally, the sediment contains abundant quartz grains, which accumulate free electrons from radioactive decay in their crystal lattices. If sediment entrained by a flood is exposed to light (“bleached”) before or during entrainment, the electron traps will be emptied, only to begin accumulation when buried within a flood deposit. In such cases, the measured age as indicated by subsequent electron accumulation represents the age of the depositing flood.

All OSL samples were collected using 1- or 2-in diameter metal or plastic tubes. The tubes were hammered horizontally into freshly exposed flood sediments in locations chosen to avoid large rocks and post-depositional disturbances such as

bioturbation, root penetration, or desiccation cracks. Aluminum foil was packed into the exposed end of the tube in order to minimize sample movement in the tube during transit. Tubes were capped, wrapped in aluminum foil, and sealed with opaque tape to prevent light exposure. When necessary, an opaque cloth was used during sample collection to shield the excavation from light. Bulk sediment samples of 1.3 pounds or larger also were collected in sealable plastic bags for measurement of water content and dose-rate. In all, 20 samples were collected, with 11 samples analyzed (Duller, 2008) by the USGS Luminescence Dating Laboratory in Lakewood, Colorado (U.S. Geological Survey, 2010c). Dates derived using OSL analyses are provided in table S1–2 in the "Supplement 1. Age-Dating Tables" section.

The OSL sample ages generally were consistent with the ^{14}C analyses, when both types of dating were applied, and provided improved resolution for floods within the last 300 years. In a few cases, the OSL samples were older than corresponding ^{14}C ages or older than the known age of 1972 flood sediments. These discrepancies probably owe to incomplete bleaching of sediment during flood entrainment and deposition, a plausible scenario for the high turbidities and low-light conditions associated with typical late-afternoon thunderstorm genesis and nighttime flood peaks for the Black Hills area (Driscoll and others, 2010).

Cesium-137 analyses were used in several cases to determine if uppermost flood deposits were from 1972 flooding. Atmospheric cesium-137 was produced during atmospheric nuclear weapons tests, with smaller amounts from nuclear reactor waste and accidental releases such as Chernobyl (U.S. Environmental Protection Agency, 2010). Thus, cesium-137 production and deposition began about 1945 and peaked about 1963 (Holmes, 1998). The cesium-137 that reaches the land surface is fixed strongly to the surface deposits. For the purpose of this study, the cesium-137 analyses did not return actual ages for flood units, but presence or absence of cesium-137 indicates whether or not a deposit pre- or post-dates 1945. If cesium-137 is detected in a deposit, the emplacing flood must have been after 1945; if cesium-137 is not detected, the flood was before 1945. This provided a reliable and economical means to distinguish 1972 flood sediments from those of slightly older (but pre-1945) floods, such as those of 1907 (Honerkamp, 1978), which likely approached 1972 flow rates in some drainages.

The cesium-137 samples were collected with a metal trowel and stored in sealable plastic bags. Freshly exposed samples were extracted from the middle of the flood units, or if the unit was thick, in 4-in unit-depth intervals. Moist samples were air dried and then sent to the USGS Radioisotope Laboratory (U.S. Geological Survey, 2010d) in St. Petersburg, Florida, for analysis. Results of cesium-137 analyses are provided in table S1–3 in the "Supplement 1. Age-Dating Tables" section.

Compiling Reach-Scale Paleoflood Chronologies

For the six study reaches, the stratigraphy and geochronology from analyzed sites were distilled into an interpreted chronology of the number, magnitude, and timing of large floods for each reach. These interpretations required extracting and combining information from multiple sites within a reach and using judgments and inferences regarding the stratigraphic relations among the sites. This process generally entailed selecting a "benchmark" site for each reach (typically one with a particularly long and complete record) to which all paleoflood information for the reach was compiled. Such compilation primarily was derived from the stratigraphic record at the benchmark site, supplemented by stratigraphic records, dating, and flow-magnitude information from other sites within the reach. Interpretations required correlation of flood evidence among multiple sites, chiefly based on relative position within stratigraphic sequences, unique textural characteristics, or results of age dating and flow estimation.

The collective approaches used for interpreting flood sequences at individual sites and for correlating among sites within a reach could possibly lead to underestimating the number of floods in the stratigraphic record. A fundamental premise is that deposition of flood sediment requires exceedance of the deposit elevation by flood stage; however, it is possible that a flood exceeding a deposit elevation may do so barely, or for some other reason may not leave a recognizable deposit. Because the protocol for stratigraphic analysis requires evidence of temporal hiatus in distinguishing individual flood deposits, multiple deposits from floods separated by short intervals can potentially be counted as a single flood unit if such evidence of hiatus is not observed. Correlations among sites were additionally conservative in that stratigraphic records from sites within a reach were considered to be completely overlapping unless compelling stratigraphic or geochronologic information indicated otherwise, again possibly leading to undercounting the total number of floods because stratigraphic records at some sites may include evidence of floods not preserved at other sites because of various circumstances. Potential biases were minimized by (1) selecting benchmark sites with relatively complete (as inferred by being in low-energy and passive depositional environments) and long-duration records and (2) focusing ensuing flood-frequency analyses on the largest, rarest, and most recent (generally within the last 1,000 years) floods, for which bias because of closely spaced or inconsistent deposition patterns are less likely to affect results. For example, it is unlikely that two very large floods are so closely spaced in time that no evidence of temporal hiatus is preserved. By contrast, it is more likely that smaller floods will fail to leave consistent records from site to site than it is for especially large floods.

Development of Modern Peak-Flow Chronologies

For computation of long-term flood-frequency analyses, the paleoflood chronologies derived from the stratigraphy and geochronology were combined with observational records and historical accounts of peak flows, which were compiled and adjusted to be directly comparable to the paleoflood chronologies determined for each study reach. Modern chronologies for each study reach were developed primarily from available systematic USGS peak-flow records (U.S. Geological Survey, 2010e) for selected streamgages (table 1), and the adjusted peak-flow values are referred to as gaged records within this report. Historical flood accounts pre-dating gaged records also were incorporated in analyses for Rapid Creek and Elk Creek.

Modern peak-flow chronologies (through water year 2009) for the study reaches are provided in table 2. Details regarding development of the modern chronologies are described in the "Supplement 2. Modern Peak-Flow Chronologies" section. This section includes tables S2–1 through S2–5 that provide peak-flow records and historical information (by stream reach) for all streamgages considered. The modern chronologies for both reaches of Rapid Creek are derived for streamgage locations that were coincident with the study reaches. For all other cases, however, gaged and historical records were adjusted on the basis of drainage area to be comparable with the paleoflood study reaches. Drainage areas for the streamgages and for selected locations within the study reaches are provided in table 1. Adjustments relative to drainage area were performed using an equation adapted from Burr and others (1996):

$$Q_t = Q_g\,(A_t/A_g)^{0.6},$$

where Q_t and A_t are peak-flow values and areas, respectively, for a target location, and Q_g and A_g are peak-flow values and areas for a gaged location. Various approaches can be used for selection of the exponent (Burr and others, 1996; Sando, 1998), and 0.6 is consistent with analyses of Sando and others (2008) in which large peak-flow values for the Black Hills area were normalized relative to drainage area. Many of the derived values in table 2 are reported with unrealistic precision (numbers of significant figures) for use in subsequent flood-frequency analyses, with appropriate rounding reported in the final flood-frequency analyses.

Estimation of Flow Rates

A key aspect of any paleoflood record is estimation of flow magnitudes for floods preserved in the stratigraphic records. Flow estimates derive from the elevations of slack-water deposits or other flood evidence in conjunction with hydraulic calculations based on modern channel and valley geometry.

Assumptions and General Considerations

The elevation of a slack-water deposit represents a minimum value for the peak stage of the emplacing flood (Baker, 1987; Kochel and Baker, 1998). Additionally, the highest deposits may closely approximate the peak stage (Webb and others, 2002), although maximum flood stages may exceed the highest deposits in many cases. For purposes of hydraulic calculations, stage evidence is related to modern channel and valley geomorphology, which introduces an additional assumption that changes in geometry have been sufficiently small for the time represented by the stratigraphic record so as to not substantially affect calculations of flow rate. This assumption likely is satisfied in the rock-bound study reaches, where the common presence of bedrock in channels (fig. 3) and along valley margins is indicative of overall stability, especially with respect to hydraulic controls on stages of large floods.

Although overall changes in channel and valley geometry probably are small for the length of the paleoflood records (generally 2,000 years or less), it is likely that minor mass wasting and downed timber locally have affected flow hydraulics. No evidence, however, of large-scale mass wasting was discovered during the reach surveys, so it is unlikely that such events have substantially affected results. Log jams and large boulder bars from 1972 flooding were evident in many study reaches, but resulting blockages were small relative to overall canyon geometry and likely had little effect on reach-scale flood hydraulics within the steep channels of the study reaches.

Hydraulic Modeling

The primary method for estimating peak-flow magnitudes was application of the one-dimensional, steady-flow River Analysis System (HEC-RAS) model developed by the Hydrologic Engineering Center of the U.S. Army Corps of Engineers (2008a, 2008b). Simulations using the HEC-RAS model, in conjunction with detailed topographic data, were used to estimate flows for the study reaches along Spring Creek, Boxelder Creek, and the reach of Rapid Creek located downstream from Pactola Reservoir and just west of Rapid City (fig. 1). For Rapid Creek, an existing digital topographic coverage (5-ft contour interval) was provided by the city of Rapid City (Dan Jarvenin, written commun., March 2009). For Spring and Boxelder Creeks, SDDOT provided digital topographic coverages (2-ft contour interval) developed from high-resolution photogrammetry acquired specifically for this study (South Dakota Department of Transportation, written commun., 2009). For these reaches, high-water evidence from 1972 flooding and all sites of stratigraphic analysis were surveyed using a combination of survey-grade Global Positioning System and standard leveling equipment. Elevations

Table 1. Drainage areas and periods of peak-flow record for selected streamgages and for selected locations within and near study reaches.

[--, not applicable]

Streamgage number	Streamgage name or location of relevant feature or study reach	Drainage area (square miles)[1]	Period of record considered (water years)[2]
	Spring Creek drainage basin		
06407000	Spring Creek near Hill City, S. Dak.	151	1938–1940
435915103241200	Spring Creek below Bitter Creek, S. Dak.	157	1972
06407500	Spring Creek near Keystone, S. Dak.	163	1946–47, 1987–2009
--	Upstream extent of Spring Creek study reach	170	--
--	Downstream extent of Spring Creek study reach	172	--
06408000	Spring Creek near Rapid City, S. Dak.	175	1904–05, 1946–47, 1972
06408500	Spring Creek near Hermosa, S. Dak.	206	1950–2004
	Rapid Creek drainage basin		
06409000	Castle Creek above Deerfield Reservoir near Hill City, S. Dak.	79.3	1949–2009
--	Deerfield Dam	92.4	[3]1945
06410000	Castle Creek below Deerfield Dam near Hill City, S. Dak.	92.5	1947–2009
--	Upstream extent of upper Rapid Creek study reach	290	--
06410500	Rapid Creek above Pactola Reservoir at Silver City, S. Dak.[4]	294	1954–2009
--	Pactola Dam	321	[3]1956
06411500	Rapid Creek below Pactola Dam, S. Dak.	322	1929–42, 1947–2009,
06412000	Rapid Creek at Big Bend near Rapid City, S. Dak.	339	1915–17, 1932–42, 1998–2009
--	Upstream extent of lower Rapid Creek study reach	367	--
06412500	Rapid Creek above Canyon Lake near Rapid City, S. Dak.	375	1947–2009
--	Downstream extent of lower Rapid Creek study reach	384	--
06414000	Rapid Creek at Rapid City, S. Dak.	414	1905–06, 1943–2009
	Boxelder Creek drainage basin		
06422500	Boxelder Creek near Nemo, S. Dak.	94.4	1907, 1946–47, 1966–2009
--	Upstream extent of Boxelder Creek study reach	98	--
--	Boxelder Creek between two subreaches (subreach break is about 0.2 miles downstream from confluence with Bogus Jim Creek)	111	--
--	Downstream extent of Boxelder Creek study reach	112	--
06422650	Boxelder Creek at Doty School near Blackhawk, S. Dak.	116	1972, 1978–80
06423000	Boxelder Creek at Blackhawk, S. Dak.	126	1904–05, 1946–47
06423010	Boxelder Creek near Rapid City, S. Dak.	126	1981–2009
	Elk Creek drainage basin		
06424000	Elk Creek near Roubaix, S. Dak.	21.6	1946–47, 1992–2009
--	Elk Creek paleoflood study reach	40	--
06424500	Elk Creek above Piedmont, S. Dak.	47.6	1945–47, 1972
06425100	Elk Creek near Rapid City, S. Dak.	211	1979–2009
06425500	Elk Creek near Elm Springs, S. Dak.	549	1950–2009

[1]Includes entire drainage area, regardless of effects of regulating structures.

[2]Includes entire period of record, regardless of effects of regulating structures.

[3]Water year of first storage within regulating structure.

[4]Approximates downstream extent of upper Rapid Creek study reach.

Table 2. Modern peak-flow chronologies (gaged and historical records) for paleoflood study reaches.

[Values in ***bold italics*** indicate special computations for the lower Rapid Creek reach, as noted in the "Supplement 2. Modern Peak-Flow Chronologies" section. Gray-shaded rows signify a gap in the chronology. ft³/s, cubic feet per second; %, estimated uncertainty, in percent, for use in selected flood-frequency analyses; (H), historical value; --; no data]

Water year	Spring Creek		Rapid Creek				Boxelder Creek				Elk Creek	
			Lower reach		Upper reach		Upstream subreach		Downstream subreach			
	Annual peak flow (ft³/s)	%	Annual peak flow (ft³/s)	%	Annual peak flow (ft³/s)	%	Annual peak flow (ft³/s)	%	Annual peak flow (ft³/s)	%	Annual peak flow (ft³/s)	%
1878	--	--	7,060 (H)	50	--	--	--	--	--	--	--	--
1883	--	--	7,900 (H)	50	--	--	--	--	--	--	--	--
1904	493	20	--	--	--	--	533	10	578	15	--	--
1905	691	20	2,350	15	--	--	559	10	606	15	--	--
1906	--	--	922	15	--	--	--	--	--	--	--	--
1907	--	--	12,200 (H)	50	--	--	16,400	33	17,700	33	10,400 (H)	50
1915	--	--	654	15	566	20	--	--	--	--	--	--
1916	--	--	217	15	187	20	--	--	--	--	--	--
1917	--	--	287	15	248	20	--	--	--	--	--	--
1920	--	--	7,540 (H)	50	--	--	--	--	--	--	--	--
1929	--	--	870	15	752	20	--	--	--	--	--	--
1930	--	--	213	15	184	20	--	--	--	--	--	--
1931	--	--	170	15	147	20	--	--	--	--	--	--
1932	--	--	747	15	646	20	--	--	--	--	--	--
1933	--	--	1,690	15	1,460	20	--	--	--	--	--	--
1934	--	--	128	15	111	20	--	--	--	--	--	--
1935	--	--	479	15	414	20	--	--	--	--	--	--
1936	--	--	110	15	95	20	--	--	--	--	--	--
1937	--	--	92	15	80	20	--	--	--	--	--	--
1938	539	20	94	15	81	20	--	--	--	--	--	--
1939	638	20	68	15	59	20	--	--	--	--	--	--
1940	260	20	268	15	232	20	--	--	--	--	--	--
1941	--	--	592	15	511	20	--	--	--	--	--	--
1942	--	--	448	15	387	20	--	--	--	--	--	--
1943	--	--	882	15	--	--	--	--	--	--	--	--
1944	--	--	254	15	--	--	--	--	--	--	--	--
1945	--	--	359	15	--	--	--	--	--	--	1,630	20
1946	346	20	943	15	--	--	1,210	10	1,310	15	1,220	20
1947	690	20	950	15	903	20	380	10	412	15	314	20
1948	--	--	245	15	235	20	--	--	--	--	--	--
1949	--	--	290	15	221	20	--	--	--	--	--	--
1950	100	20	209	15	221	20	--	--	--	--	--	--

Table 2. Modern peak-flow chronologies (gaged and historical records) for paleoflood study reaches.—Continued

[Values in ***bold italics*** indicate special computations for the lower Rapid Creek reach, as noted in the "Supplement 2. Modern Peak-Flow Chronologies" section. Gray-shaded rows signify a gap in the chronology. ft³/s, cubic feet per second; %, estimated uncertainty, in percent, for use in selected flood-frequency analyses; (H), historical value; --; no data]

Water year	Spring Creek		Rapid Creek				Boxelder Creek				Elk Creek	
			Lower reach		Upper reach		Upstream subreach		Downstream subreach			
	Annual peak flow (ft³/s)	%	Annual peak flow (ft³/s)	%	Annual peak flow (ft³/s)	%	Annual peak flow (ft³/s)	%	Annual peak flow (ft³/s)	%	Annual peak flow (ft³/s)	%
1951	30	20	77	15	92	20	--	--	--	--	--	--
1952	627	20	2,600	15	2,460	20	--	--	--	--	--	--
1953	240	20	152	15	152	20	--	--	--	--	--	--
1954	418	20	140	15	106	20	--	--	--	--	--	--
1955	29	20	326	15	1,520	20	--	--	--	--	--	--
1956	33	20	203	15	175	20	--	--	--	--	--	--
1957	340	20	***595***	15	181	20	--	--	--	--	--	--
1958	33	20	131	15	113	20	--	--	--	--	--	--
1959	30	20	169	15	146	20	--	--	--	--	--	--
1960	33	20	135	15	117	20	--	--	--	--	--	--
1961	29	20	111	15	96	20	--	--	--	--	--	--
1962	544	20	***1,700***	15	390	20	--	--	--	--	--	--
1963	389	20	827	15	715	20	--	--	--	--	--	--
1964	88	20	735	15	635	20	--	--	--	--	--	--
1965	390	20	2,380	15	2,060	20	--	--	--	--	--	--
1966	54	20	174	15	150	20	31	10	33	15	89	20
1967	825	20	726	15	627	20	972	10	1,050	15	510	20
1968	49	20	123	15	106	20	63	10	69	15	104	20
1969	398	20	246	15	213	20	147	10	160	15	141	20
1970	34	20	1,150	15	995	20	663	10	718	15	372	20
1971	390	20	353	15	305	20	226	10	245	15	176	20
1972	21,800	33	31,200	33	252	20	30,800	33	50,500	33	10,400	50
1973	127	20	196	15	169	20	120	10	130	15	129	20
1974	33	20	***476***	15	54	20	24	10	25	15	86	20
1975	43	20	253	15	219	20	437	10	473	15	271	20
1976	401	20	***1,220***	15	614	20	1,490	10	1,620	15	744	20
1977	379	20	216	15	187	20	174	10	188	15	153	20
1978	204	20	498	15	430	20	308	10	334	15	213	20
1979	34	20	200	15	173	20	99	10	107	15	120	20
1980	418	20	87	15	75	20	36	10	39	15	91	20
1981	31	20	96	15	83	20	27	10	29	15	87	20
1982	394	20	384	15	332	20	278	10	301	15	200	20
1983	223	20	303	15	262	20	182	10	197	15	157	20
1984	283	20	229	15	198	20	220	10	238	15	174	20
1985	43	20	87	15	75	20	132	10	143	15	134	20
1986	42	20	142	15	123	20	84	10	91	15	113	20
1987	123	20	115	15	99	20	126	10	136	15	132	20

Table 2. Modern peak-flow chronologies (gaged and historical records) for paleoflood study reaches.—Continued

[Values in ***bold italics*** indicate special computations for the lower Rapid Creek reach, as noted in the "Supplement 2. Modern Peak-Flow Chronologies" section. Gray-shaded rows signify a gap in the chronology. ft³/s, cubic feet per second; %, estimated uncertainty, in percent, for use in selected flood-frequency analyses; (H), historical value; --; no data]

Water year	Spring Creek		Rapid Creek				Boxelder Creek				Elk Creek	
			Lower reach		Upper reach		Upstream subreach		Downstream subreach			
	Annual peak flow (ft³/s)	%	Annual peak flow (ft³/s)	%	Annual peak flow (ft³/s)	%	Annual peak flow (ft³/s)	%	Annual peak flow (ft³/s)	%	Annual peak flow (ft³/s)	%
1988	25	20	80	15	69	20	34	10	37	15	90	20
1989	32	20	64	15	55	20	31	10	33	15	89	20
1990	96	20	108	15	93	20	30	10	32	15	89	20
1991	299	20	487	15	421	20	410	10	444	15	259	20
1992	32	20	64	15	55	20	54	10	59	15	22	20
1993	294	20	1,000	15	867	20	300	10	325	15	223	20
1994	66	20	227	15	196	20	128	10	139	15	149	20
1995	940	20	1,020	15	879	20	1,170	10	1,260	15	745	20
1996	1,000	20	823	15	711	20	845	10	915	15	255	20
1997	531	20	***1,090***	15	524	20	474	10	513	15	289	20
1998	315	20	1,490	15	1,290	20	621	10	673	15	285	20
1999	315	20	698	15	603	20	334	10	362	15	192	20
2000	109	20	264	15	228	20	182	10	197	15	178	20
2001	68	20	131	15	113	20	53	10	58	15	56	20
2002	32	20	159	15	137	20	48	10	52	15	224	20
2003	64	20	243	15	210	20	102	10	111	15	145	20
2004	14	20	67	15	58	20	19	10	21	15	41	20
2005	28	20	61	15	53	20	25	10	27	15	65	20
2006	24	20	104	15	90	20	105	10	114	15	221	20
2007	35	20	177	15	153	20	205	10	222	15	191	20
2008	175	20	***1,000***	15	1,640	20	661	10	716	15	434	20
2009	71	20	277	15	239	20	376	10	408	15	188	20

were related to a high-resolution topographic network developed for the Rapid City area (City of Rapid City, 2010), with internal checks indicating that surveyed elevations for most sites of stratigraphic analysis have errors less than 0.1 ft.

All topographic data were converted to triangular irregular networks (TINs) using the spatial analysis tools in ArcMAP (Environmental Systems Research Institute, 2010). Cross sections for HEC-RAS analyses were placed and oriented to reflect conveyance during flood stages and thus are not always perpendicular to low-water channels. Cross sections include all areas of inferred down-valley flow conveyance, including overbank areas, but exclude areas likely to be occupied by eddies and stagnant flow during high stages, such as at tributary mouths and behind large rock protrusions. Cross sections were spaced at intervals of 100 ft or less for all of the study reaches.

The HEC-RAS model uses the step-backwater method for estimating water-surface elevations corresponding to specified flow rates. The method is based on the one-dimensional energy equation to determine energy-balanced water-surface profiles for flows that are steady (in time), gradually varied, and for slopes less than about 0.1 ft/ft (U.S. Army Corps of Engineers, 2008b). Step-backwater models have been used extensively to estimate paleoflood magnitudes in multiple studies globally (O'Connor and Webb, 1988; Enzel and others, 1994; Wohl and others, 1994; Hosman and others, 2003; Sheffer and others, 2008).

Average channel gradients in the three simulated reaches are 0.007, 0.008, and 0.01 ft/ft for Rapid, Spring, and Boxelder Creeks, respectively. Critical-flow conditions were identified in many sections of the simulated reaches, which is

consistent with conditions described in a subsequent section titled "Other Approaches for Estimation of Flow Rates."

Results of the HEC-RAS simulations for all simulated reaches were "calibrated" by checking simulation output against known flow values and high-water evidence associated with 1972 flooding, including tree scars, flotsam lines, flood debris piles, and geomorphic evidence. These data allowed evaluation of values for Manning's roughness coefficient (Manning's *n*) and provided confidence regarding digital topographic coverages and overall model functionality. High-water marks documented by the U.S. Army Corps of Engineers (1973) were available for part of the reach of lower Rapid Creek and were supplemented by 1972 high-water accounts obtained from local residents in this reach.

Selection of the final (calibrated) HEC-RAS model for each simulated reach was accomplished by comparing simulation output to a water-surface profile based on 1972 estimated flow rates and high-water marks. Cross sections and model input parameters including Manning's *n* were adjusted accordingly. Roughness coefficients and channel geometry are inherently subject to change with time; however, these variables were assumed constant in the absence of other information. Water-surface elevations were calculated for a range of Manning's *n* values (±25 percent of final values) to determine the sensitivity of the reaches to roughness and to obtain a range of flow values likely associated with each water-surface elevation. Once appropriate water-surface elevations corresponding to specific flow rates were established, rating curves (relation between flow rate and stage) were constructed for each paleoflood site. For all paleoflood sites, uncertainties in simulated flow rates resulting from the ±25-percent range of Manning's *n* values were substantially smaller than overall uncertainties assigned to paleoflood flow estimates, as described in a subsequent section "Models for Flood-Frequency Analyses."

Other Approaches for Estimation of Flow Rates

The HEC-RAS model and the required reach-scale topographic surveys were not justified for Elk Creek and the upstream reach of Rapid Creek, where paleoflood evidence was sparser than for other study reaches. Instead, flow estimates were derived by applying the Manning equation or critical-flow equation for a cross section at each site of stratigraphic analysis. The Manning equation (Barnes, 1967; Benson and Dalrymple, 1967) is an established relation for estimating flow rate; $Q = 1.49n^{-1}AS^{1/2}R^{2/3}$, where Q is flow rate (in cubic feet per second), n is the Manning's roughness coefficient (dimensionless), A is the cross-section area (in square feet), S is the energy gradient (typically assumed equivalent to channel slope, in feet divided by feet), and R is the hydraulic radius, which is the wetted perimeter divided by area (in feet). The critical-flow equation is based on the observation that flows in steep-gradient channels tend toward a state of minimum specific energy, thereby allowing calculation of flow from cross-section geometry alone (Grant, 1997). This condition is satisfied for $Q = (gA^3T^{-1})^{1/2}$, where g is the acceleration of gravity (32.174 feet per second squared), and T is flow top width (in feet). Alternatively, velocity (V, in feet per second) can be computed as $V = (gHD)^{0.5}$, where HD (hydraulic depth, in feet) is computed as area divided by top width, which allows computation of flow rate as area times velocity.

An advantage of the critical-flow equation is that it does not rely on judgments regarding Manning's *n*, and on the assumption that measured channel slope is equivalent to the energy gradient. There may be uncertainty as to whether flow is indeed close to critical conditions—an uncertainty that can only be addressed completely by more sophisticated hydraulic analysis. However, Jarrett and England (2002) indicated that peak flow computed by the critical-flow equation generally was within about ±15 percent of flow rates computed using direct current meter measurement methods for 35 stream reaches with slopes exceeding about 0.01 ft/ft, as is the case for the applicable study reaches in this report. Additional confidence in the applicability of the critical-flow equation was obtained by inspection of numerous slope-area measurements (method described by Benson and Dalrymple, 1967) conducted by the USGS for large flows events in the Black Hills area, including many measurements reported by Schwarz and others (1975) for sites with large 1972 flows. These measurements commonly indicated Froude numbers approaching or exceeding 1.0 (indicative of critical-flow conditions), with computed flow conditions vacillating between sub- and super-critical conditions for multiple cross sections within computational reaches.

Flood-Frequency Analysis

Paleoflood information provides tangible information on the occurrence and magnitude of large and infrequent floods, which when considered in a statistically appropriate manner, can substantially reduce uncertainties in frequency and magnitude estimates of rare floods (Hosking and Wallis, 1986; Costa, 1978; Stedinger and Baker, 1987; Frances and others, 1994; Webb and others, 2002). The increasing global application of paleoflood studies has prompted development of new techniques to efficiently consider such information in frequency analyses (Stedinger and Cohn, 1986; Cohn and others, 1997; Levish, 2002; O'Connell and others, 2002).

Models for Flood-Frequency Analysis

Two analytical models with capabilities for incorporating paleoflood data in flood-frequency estimation were applied: (1) the FLDFRQ3 model (O'Connell, 1999; O'Connell and others, 2002), and (2) the PeakfqSA model (Cohn and others, 1997, 2001; Griffis and others, 2004). Both models allow specification of dates, flow rates, and perception thresholds for peak-flow events. Perception thresholds provide constraining information regarding known (or presumed) exceedances (or non-exceedances) of especially large flood magnitudes

within specified timeframes. For example, for several study reaches historical accounts indicate that the 1972 flood was the largest flood since 1907 even in the absence of complete gaged records dating to 1907. Thus, the 1907 flood can be used as a threshold for the period 1907–2009 because the 1907 flow has been exceeded once in the intervening 102 years. Similarly, estimates of timing and magnitude for some of the paleofloods within a reach can be used as perception thresholds, based on the assumption that subsequent larger floods would have left evidence.

For both models and all reaches, flood-frequency analyses were computed assuming log-Pearson Type III frequency distributions and were performed for as many as four flood-record scenarios: (1) analysis of gaged annual peak flows only; (2) gaged peak flows in combination with historical flow information (when available), including historical thresholds; (3) all available data, which may include the gaged peak flows, historical flows and thresholds, and paleofloods and thresholds; and (4) the same as the third scenario, but "top fitting" the distribution by arbitrarily including only the largest 50 percent of the gaged peak flows (that is, those larger than the median of the gaged flows). The Weibull plotting position (Weibull, 1939) was used for graphical representations of results of flood-frequency analyses for all scenarios.

Scenarios 1 and 2 (using only gaged flows and historical information) were conducted as baseline analyses and provided a basis for comparison of incremental effects when including all available data (scenario 3). The top-fitting analyses (scenario 4) could be conducted only with the PeakfqSA model (because of the complexity of the datasets) and enabled consideration of the general sensitivity of the analytical approach to inclusion of relatively small flows that dominate typical gaged peak-flow records. The small flows may result from flood-generation processes with different statistical properties, and thus may adversely affect fitting of the frequency distribution, especially with respect to low-probability floods. Top-fitting strategies similar to scenario 4 ultimately may provide the most robust flood-frequency analyses for rare floods; however, more rigorous evaluation of potential approaches first would be more appropriate. Consequently, analyses resulting from scenario 3, which include all observational, historical, and paleoflood records, are considered to provide the best estimates of flood recurrence (flood-frequency estimates) for low-probability floods. Within this report, flood-frequency estimates are provided only for recurrence intervals of 25 years or larger (annual exceedance probabilities of 0.04 or smaller, which means a flow with a 4-percent chance of being exceeded in any given year). Results are not reported for smaller recurrence intervals because several study reaches are within loss-zone settings described by Sando and others (2008), and accurate characterization would require additional analyses beyond the scope of this study.

The FLDFRQ3 model uses a Bayesian approach (O'Connell and others, 2002) with a maximum likelihood method (Stedinger and Cohn, 1986). The FLDFRQ3 model allows for specification of uncertainties for magnitudes and timing of hydrologic events and for thresholds derived from paleoflood data that arise because of flow-rate, stratigraphic, and chronologic uncertainties. Additionally, the FLDFRQ3 model allows for specification of uncertainties in the gaged record, with uncertainties assigned (table 2) on the basis of general reliability of the datasets. For this study, uncertainties of ±10 percent were assigned for the most reliable peak-flow records (recent gaged records from locations near the benchmark sites). Progressively larger uncertainties (as much as 33 percent) were assigned for flow values derived using various methods of estimation as described in the previous section "Development of Modern Peak-Flow Chronologies." Especially large flow values generally were assigned uncertainties of ±33 or 50 percent, depending on professional judgment regarding factors such as sources of data and extrapolation required for applicability to study reaches. The specified uncertainties in table 2 do not necessarily reflect semi-quantitative ratings of data quality that typically are assigned to measurements at streamgages.

In the maximum likelihood approach used by the FLDFRQ3 model, especially large flows can be used as constraints, or perception thresholds, on the magnitude and timing of the peak flows. When incorporating perception thresholds for paleofloods, a range of ages can be used. In most analyses, thresholds were based on stratigraphic and geochronologic evidence. In order to be consistent with the input values of the PeakfqSA model, threshold ranges varied only slightly (there is not a substantial difference between the minimum and maximum values), with age ranges corresponding to calibrated radiocarbon or OSL ages, reported in years before present (2010). Ages of all paleofloods also were input as years before present. In most cases, the median age from radiocarbon dating (table S1–1) was used as the most likely age of the paleoflood. When multiple age estimates were associated with a specific flood deposit, the youngest age was used, consistent with the condition that detrital organic materials provide maximum ages for the enclosing flood deposits.

For FLDFRQ3 model input, plausible flow ranges for specific floods generally were specified using three values: (1) a minimum being the flow required to inundate any given flood unit, (2) a maximum assumed to be twice the minimum value, and (3) a most likely value assumed as 1.5 times the minimum value. These specified values are based on a general observation that the known 1972 flow rates (mainly from indirect measurements obtained immediately after 1972 flooding) commonly are about twice the flow rates derived by HEC-RAS simulations for elevations of preserved 1972 flood deposits. To accommodate the structure of the Bayesian approach, the three specified values defining this range were each assigned an equal probability weighting.

The PeakfqSA model (Cohn and others, 1997; Cohn and others, 2001; Griffis and others, 2004) also can accommodate paleoflood information; however, the primary difference from the FLDFRQ3 model is use of the expected moments algorithm (EMA), which has an iterative procedure for computing method-of-moments parameter estimates (Cohn

and others, 1997). The EMA can use interval data (such as paleofloods and thresholds) efficiently (Cohn and others, 1997) and provides a method to compute accurate confidence intervals (Cohn and others, 2001). A primary advantage of the PeakfqSA model is that it maintains the overall structure and moments-based approach of procedures recommended in Bulletin 17B "Guidelines for Determining Flood Flow Frequency" (Interagency Advisory Council on Water Data, 1982; hereinafter referred to as Bulletin 17B), while using additional components to improve upon known shortcomings such as the inability to properly utilize paleoflood data. Consequently, this approach is most consistent with procedures adopted by most Federal agencies for flood-frequency analysis. For this reason, analyses using the PeakfqSA model are used as the primary basis of comparison among results for the six study reaches. A disadvantage of the PeakfqSA model is that it does not allow specification of flow uncertainties associated with gaged records, perhaps resulting in confidence intervals that incompletely consider all uncertainties in the observations. Flow uncertainties associated with paleofloods are defined by the minimum and maximum flows used in the FLDFRQ3 model. The slightly different structures of the two models precluded exact comparisons of identical input datasets between the two approaches for both the gaged and gaged-plus-paleoflood records, but the analyses were conducted as similarly as possible.

Outstanding Uncertainty Issues

The PeakfqSA and FLDFRQ3 analytical models both account for standard statistical uncertainties in sampling populations and for additional user-specified uncertainties in the timing and magnitude of individual paleofloods. The FLDFRQ3 model allows for user-specified characterization of the probability distribution function for flood-frequency analysis and for specifying uncertainty in the observational record. Neither model, however, can explicitly account for other factors or conditions that may affect both the analyses and the future recurrence of low-probability floods. Results of flood-frequency analyses for both models may be affected by biases inherent in the stratigraphic approach, as conducted for this study, that possibly result in underestimating the number of recognized floods (by requiring positive stratigraphic evidence of individual floods) and their associated magnitudes (by using minimum flow rate required for sediment deposition). Both factors collectively result in flood-frequency analyses possibly biased towards underestimating magnitudes of floods associated with specific recurrence intervals. Such biases are minimized, however, by development of accurate and complete stratigraphic records of floods; a condition enabled in this study by the large number of sites, extensive geochronology, and favorable environmental conditions in the Black Hills area for estimating paleoflood magnitudes.

This study does not address uncertainties related to nonstationary climatic trends or long-term changes in geomorphic and land-cover conditions. Thus, the flood-frequency estimates resulting from this study may not perfectly describe future flood recurrence. Another source of uncertainty meriting investigation is the adequacy of the log-Pearson Type III frequency distribution used in both flood-frequency analytical models for reasonably representing the true population of low-probability floods.

Flood-Frequency Analyses from Paleoflood Investigations

For each study reach, paleoflood investigations involved hydraulic analyses, interpretation of paleoflood chronologies from stratigraphic investigations, and flood-frequency analyses, which together allowed understanding of the history and recurrence of low-probability floods. These investigations were conducted for each of the six reaches within the four basins of the study area. The resulting flood chronologies and flood-frequency estimates indicate that (1) floods as large as and even substantially larger than 1972 previously have affected most of these stream reaches, and (2) incorporation of the paleohydrologic information can reduce uncertainties substantially in estimating recurrence of low-probability floods. This section describes key analyses for each reach. Additional synthesis of the reach-specific results in relation to each other, local and broader-scale flood processes, and approaches for application are described in a subsequent section "Central Black Hills Flood Frequency: Synopsis, Implications, and Application."

Spring Creek

Detailed stratigraphic investigations were conducted at four locations (five individual sites) within a 2-mi reach of Spring Creek (fig. 4). Additional information from the Temple of Doom Alcove located about 2 mi farther upstream supplemented the stratigraphic records of the primary study reach.

The primary study reach is a meandering canyon about 200 to 500 ft wide (fig. 4) flanked by near-vertical walls of Minnelusa Formation, as much as several hundred feet high, except at the downstream end where Spring Creek exits the canyon reach after passing through the Minnekahta Limestone (fig. 1) about 0.5 mi upstream from Highway 16. This reach is within a loss zone where flow occurs only during prolonged wet conditions. The channel substrate (fig. 5) consists of cobble-gravel, sand, and locally bedrock. No large tributaries enter the study reach—the drainage area increases from 170 to 172 square miles (mi^2) throughout the reach (table 1). The valley bottom is vegetated with grass, shrubs, ponderosa pine, and various deciduous trees. This reach is privately owned and primarily used for pasture. No structures or developed roads are within the study reach. The Temple of Doom Alcove is within a much narrower canyon carved into the cavernous

Madison Limestone about 2 mi upstream from the primary study reach (fig. 4).

The 1972 flood had a peak flow of 21,800 cubic feet per second (ft^3/s), as measured for streamgage 06408000 (Schwarz and others, 1975; U.S. Geological Survey, 2010e), which is located at the downstream extent of the study reach (fig. 1). The 1972 flow is the largest (by more than a factor of 20) in the 67 years of non-contiguous gaged records for Spring Creek that date back to 1904 (table 2, fig. 6). As for all study reaches, the gaged records (modern chronologies) as applied to the study reach were derived from records for multiple streamgages that were adjusted for the location of the study reach (as described in detail in the "Supplement 2. Modern Peak-Flow Chronologies" section). The 1972 flood locally deposited boulder and gravel bars along the channel as well as large accumulations of woody debris. Along the canyon margins, the 1972 flood deposited abundant flotsam (which provides high-water evidence along the length of the study reach) and fine-grained slack-water deposits. The sites of stratigraphic analysis are in locations where slack-water sediment from the 1972 flood and previous large floods has accumulated in alcoves and under overhangs formed in the canyon walls.

Hydraulic Analysis and Paleoflood Chronology

Paleoflood magnitudes were derived from simulations using the HEC-RAS model based on a digital (2-ft contour interval) topographic coverage (fig. 4). Calibration of the hydraulic model was based on elevations of 1972 high-water evidence (fig. 7) that were surveyed within the reach and by assuming a 1972 peak flow of 21,800 ft^3/s for the reach (table 2). Simulations using the calibrated hydraulic model were used for estimating flow magnitudes for elevations of paleoflood evidence at locations of detailed site investigations within the reach (figs. 4 and 7). Relations between flow rate and elevation are nonlinear because of typical exponential relations between flow rate and stage.

The benchmark site for the Spring Creek reach is the Superscour Alcove (fig. 8), which is located along a channel margin near the center of the reach (fig. 4). This site has the most comprehensive paleoflood record within the reach, but is supplemented by key stratigraphic and geochronologic evidence at three additional sites.

Three separate pits at Superscour Alcove had slightly different elevations and depositional environments and therefore contained different stratigraphic records (fig. 9). Pit A (fig. 8*C*) is the lowest and contained evidence of five floods since A.D. 1272–1391 (laboratory identification number ww5976; table S1–1), of which the most recent flood unit was inferred to be from 1972 on the basis of fresh-appearing flotsam within and on top of the deposit. Flow estimates required for inundation for pit A (fig. 9) range from 4,000 ft^3/s for the oldest flood unit (V) to 6,600 ft^3/s for the uppermost (1972) flood unit (I). These flow estimates are small relative to that of 1972 (21,800 ft^3/s) because of the relatively low elevation of the pit. Pit B is just upstream from pit A and provided evidence of three floods within the last several hundred years. Radiocarbon analyses indicate that the oldest flood unit (III) is dated between A.D. 1640 and 1806 (laboratory identification number ww7069; table S1–1), consistent with an OSL date of A.D. 1785–1815 (table S1–2). Minimum flows required for inundation at pit B range from 12,000 ft^3/s for the oldest flood unit to 14,200 ft^3/s for the most recent (1972) flood unit (I). Pit C (slightly upstream from pit B and higher) provided evidence of two floods. The most recent is the 1972 flood. The older flood unit (II) was not dated but presumably correlates to flood units in pits A and B.

Flotsam from 1972 in alcove along Spring Creek.

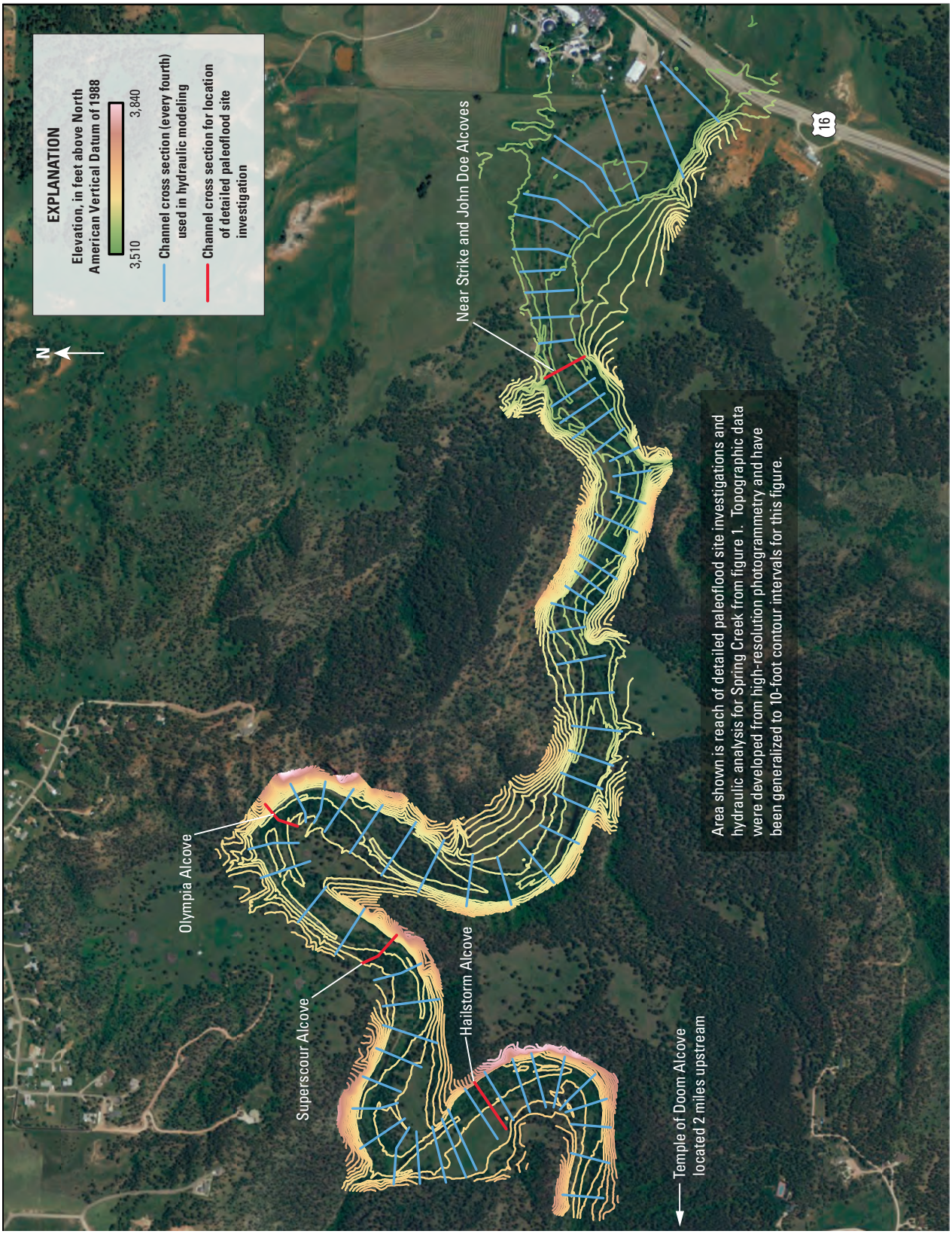

Figure 4. Topographic information and selected details of hydraulic analysis for Spring Creek reach.

Additional flood sands left by the 1972 flood were found at an elevation more than 2 ft higher than the excavated pits at this site, requiring a flow of about 23,000 ft^3/s for deposition. This flow rate is consistent with the estimated 1972 flow rate for this reach and within the simulated flow range of 15,000–30,000 ft^3/s from the HEC-RAS analysis for the 1972 high-water evidence in the vicinity of Superscour Alcove (fig. 7). It is interpreted that the three floods at pit B correlate with three of the floods in pit A based on unit age and stratigraphic context. Similarly, the two flood units of pit C probably correlate with two of the flood units in pit A.

Two pits were excavated 0.5 mi upstream from Superscour Alcove at Hailstorm Alcove (fig. 10). Pit A provided evidence of three floods since 382–192 B.C. The middle flood unit (II) was dated to A.D. 1296–1410 and is likely the same flood as described later in this section for the Temple of Doom Alcove. The most recent flood deposit in pit A is from 1972, with its relatively low elevation requiring a flow of 10,000 ft^3/s for inundation. Pit B had evidence of two floods, the most recent being from 1972. The oldest flood unit (II) in pit B likely correlates with flood unit II in pit A. Because pit B is lower than pit A, corresponding flow values are smaller for pit B, thus limiting the utility of this pit in developing the overall flood chronology. A thin layer of flood sands that were dated to A.D. 1486–1644 was identified in a small crevice about 3 ft higher that pit A. The corresponding flow for deposition of these sands is about 18,200 ft^3/s. This layer of flood sands likely correlates with a flood unit in pit A at Superscour Alcove.

Two pits were excavated in the John Doe Alcove (fig. 11), the most downstream site in the reach. Pit B is slightly higher than pit A and provided evidence of four floods. The flow required for inundation of the oldest flood unit (IV) in pit B is 7,500 ft^3/s, and the age of the flood unit, for which a datable sample was not obtained, is constrained between A.D. 892 and 1253 by ages for the underlying and overlying deposits.

Figure 5. Examples of geomorphic setting along Spring Creek reach. Photographs show *A*, outcrop of the Minnelusa Formation in the channel (looking downstream towards Olympia Alcove); *B*, looking upstream at a localized scour hole at the Superscour Alcove; and *C*, looking downstream towards the Superscour Alcove.

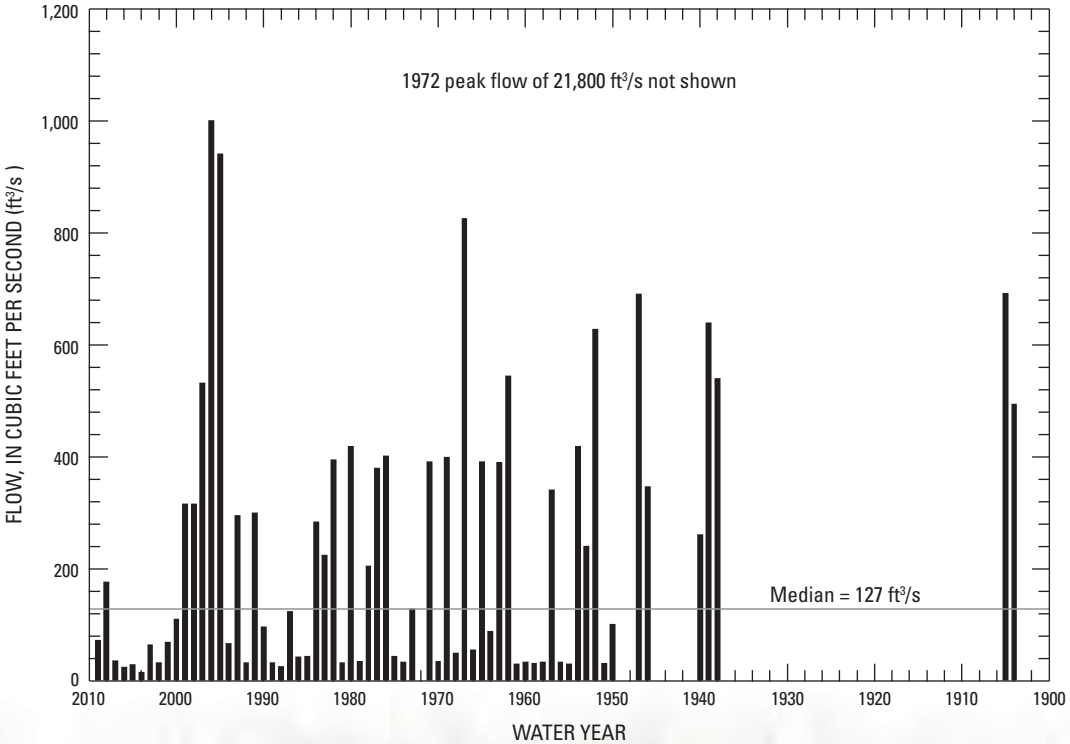

Figure 6. Modern peak-flow chronology (gaged records) for Spring Creek. Values are from table 2.

Logjam from 1972 flood along Spring Creek. This is the largest logjam observed within the study reaches.

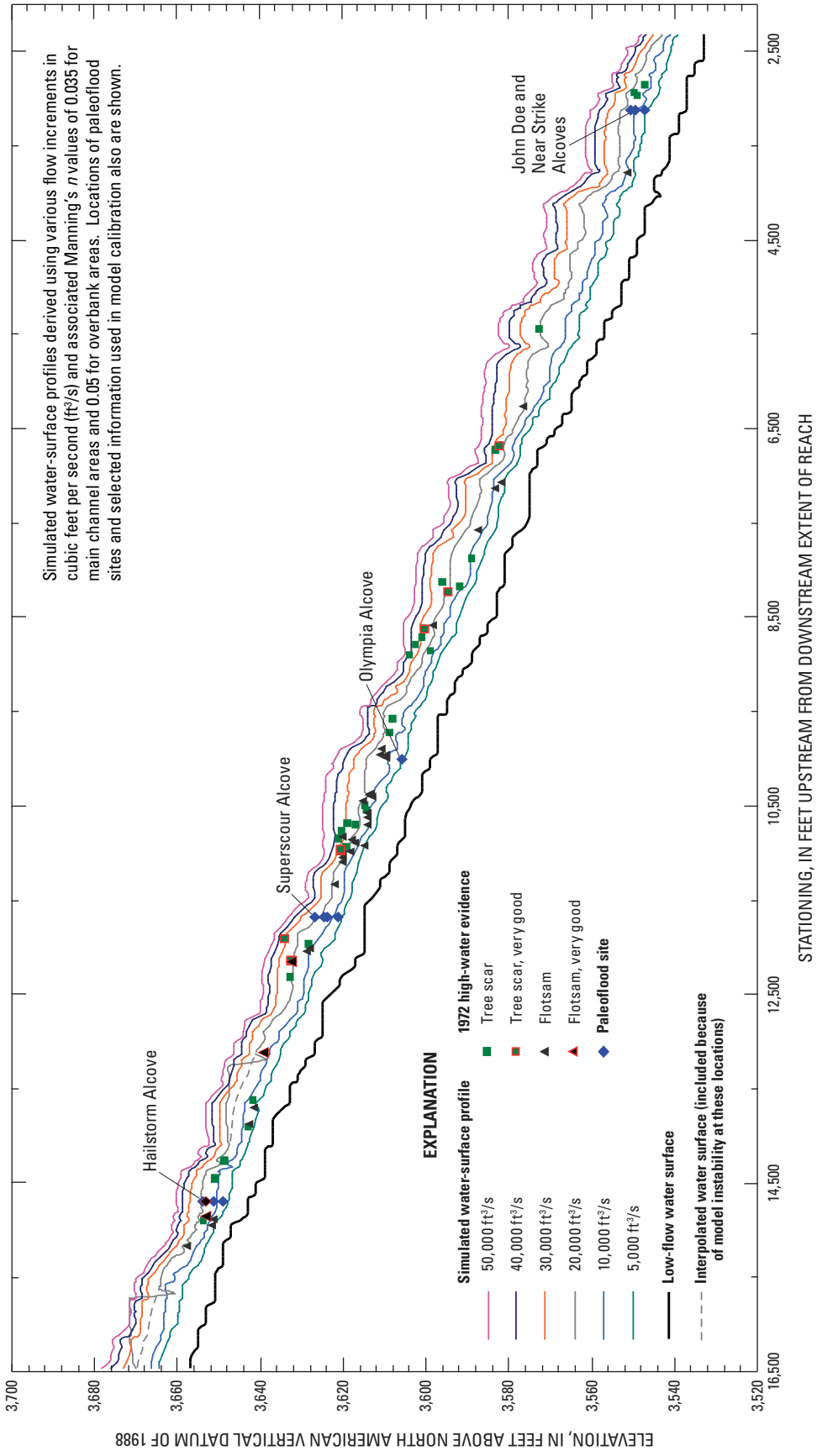

Figure 7. Results of hydraulic model simulations for Spring Creek reach.

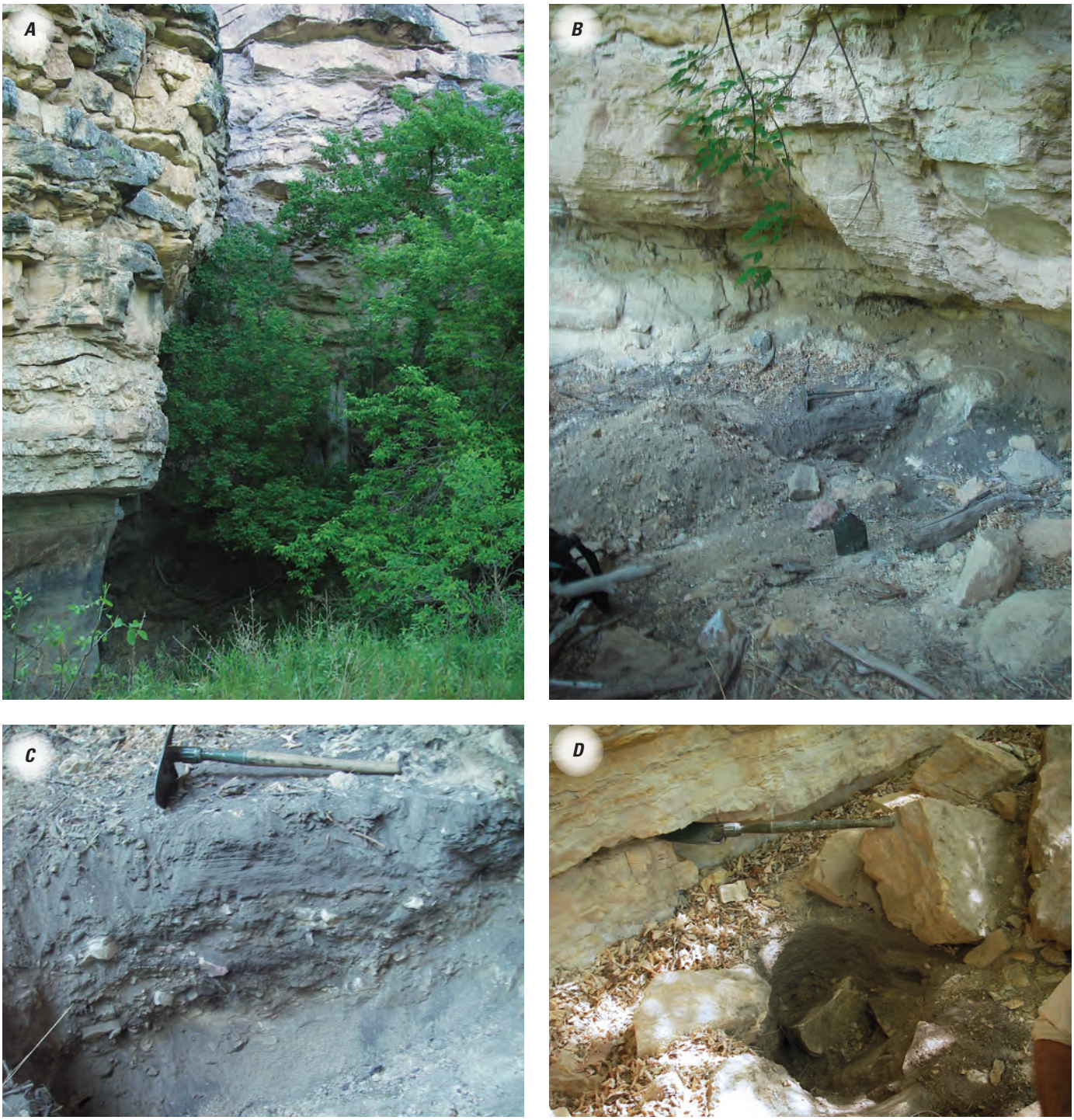

Figure 8. Setting and examples of stratigraphy for Superscour Alcove, Spring Creek. Photographs show *A,* a large cliff shielding the site; *B,* pit B, which exposes three flood units; *C,* pit A, which exposes five flood units; and *D,* pit D, which exposes two flood units. Detailed stratigraphy for pits is shown in figure 9.

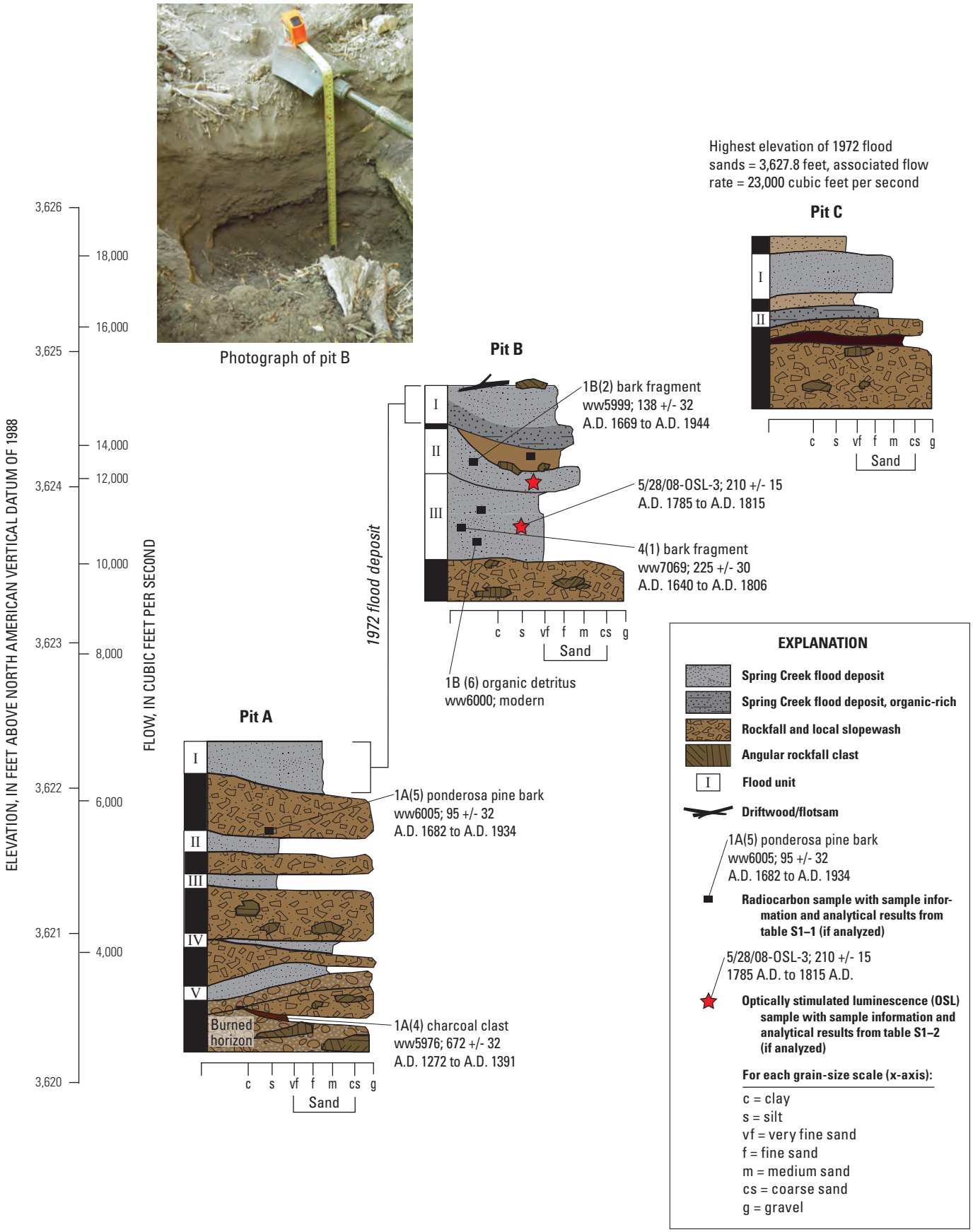

Figure 9. Schematic diagram showing paleoflood information for Superscour Alcove, Spring Creek.

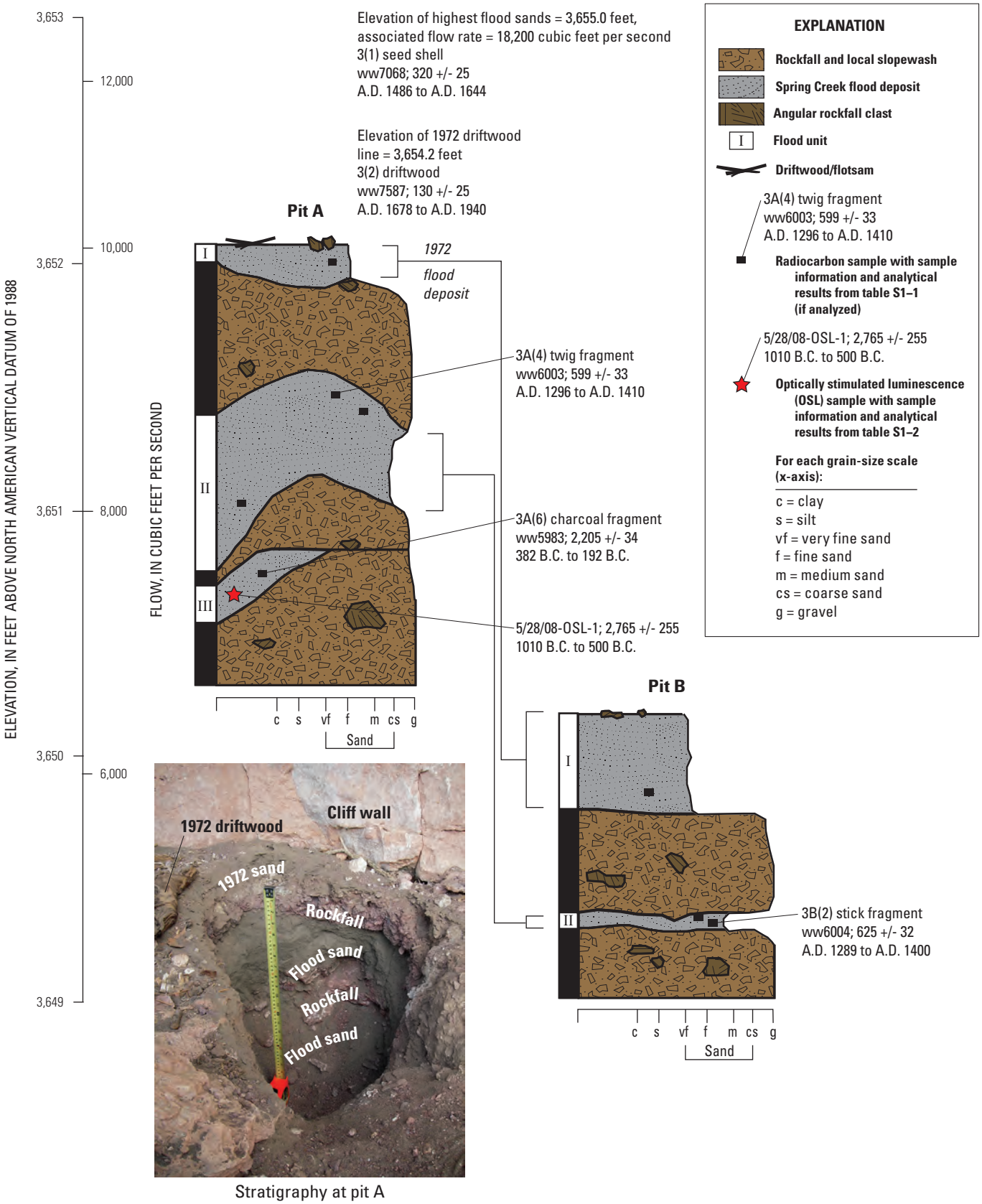

Figure 10. Schematic diagram showing paleoflood information for Hailstorm Alcove, Spring Creek.

The next youngest flood unit (III) in pit B was dated to A.D. 1052–1253 and required a flow of 8,750 ft^3/s for inundation. The two most recent floods units (I and II) occurred in the last few hundred years and likely correlate with flood units II and III in pit B at Superscour Alcove. Pit A (fig. 11) provided a similar flood history; the oldest flood unit (V) was dated to A.D. 1048–1225 and likely correlates with flood unit III in pit B. The three to four other flood units in pit A likely correspond to flood units in pit B at John Doe and pit A at Superscour Alcove.

The Temple of Doom Alcove is 2 mi upstream from the main study reach (fig. 1) and consists of driftwood and flood sediment deposited in small caves in the Madison Limestone. The channel near this alcove is only about 100 ft wide, resulting in high stages during large floods. Sampled wood from a small driftwood accumulation in a cavern 19.9 ft above the channel thalweg was dated between A.D. 1267 and 1392 (fig. 12). On the basis of this age, this deposit likely correlates with flood unit II in pit A and flood unit II in pit B at Hailstorm Alcove. In an adjacent small cavern 25.9 ft above the thalweg, bedded flood deposits indicated an even higher flood stage, although the lack of datable material precludes correlation to floods inferred from stratigraphy at other sites. It is most likely that this sediment was deposited by the same flood that deposited the A.D. 1267–1392 driftwood in the adjacent cavern, or by an earlier and possibly larger flood, because a younger flood presumably would have removed the lower driftwood.

Because the Temple of Doom site was outside the area of high-resolution topographic information for Spring Creek, flows rates for elevations of deposits were determined using a critical-flow computation, which was justified by the steep channel slope of 0.013 ft/ft. Computations were performed after first subdividing the cross section at a topographic break located about 89 ft from the left bank (fig. 13). Computations are summarized in table 3, and the computed flows were 56,400 and 29,300 ft^3/s for elevations 25.9 ft and 19.9 ft above the thalweg, respectively. Therefore, the Temple of Doom stratigraphy and flow computations indicate at least a single A.D. 1267–1392 flood of at least 29,300 ft^3/s, and possibly as large as 56,400 ft^3/s. Evidence supporting the occurrence of two unique floods at this site was not sufficient (nor corroborated by evidence at other sites) to justify interpretation as separate flood units.

Stratigraphic investigations also were conducted at Olympia Alcove located several hundred yards downstream from Superscour Alcove and at the Near Strike Alcove located a few tens of yards upstream from John Doe Alcove (fig. 4). For these sites, however, all inferred flood units possibly correlate with units for other sites previously described. Consequently, these sites do not unambiguously add additional information to the overall flood chronology for Spring Creek. For completeness, schematic diagrams for these sites are included as figures S3–1 and S3–2 respectively in the "Supplement 3. Schematic Diagrams" section.

Summarizing interpretations for all of the Spring Creek paleoflood sites (table 4), a chronology of at least five paleofloods with magnitudes approaching or exceeding that of 1972 was preserved by stratigraphic records extending back approximately (~) 1,000 years. The 1972 flow of 21,800 ft^3/s was exceeded by a paleoflood of ~700 years ago with a flow range of 29,300–58,600 ft^3/s (P4 in table 4), which reflects the uncertainty incorporated into the flood-magnitude estimates, as previously described in the section "Models for Flood-Frequency Analysis." A paleoflood ~450 years ago had a flow of 18,200–36,400 ft^3/s (P3). Three paleofloods (P5, P2, and P1) about 800, 210, and 200 years ago had flows of 8,750–17,500, 12,000–24,000, and 13,900–27,800 ft^3/s, respectively.

Flood-Frequency Analysis

For flood-frequency analyses, the gaged and paleoflood information was structured into specific events and perception thresholds as summarized in figure 14 and table 4. For these analyses, only the most complete part of the stratigraphic record encompassing about the last 1,000 years was considered, for which the largest flows and their timing, as well as reliable perception thresholds could most confidently be identified. In total, five specific paleofloods were included in the flood-frequency analyses, with flows possibly as large as 58,600 ft^3/s, and dates as old as A.D. 1048, which represents the lower end of the age range for the oldest flood unit dated at the John Doe Alcove. Three perception thresholds (based on stratigraphic evidence and geochronology) also were formulated: (1) flows equal to that of Superscour Alcove pit B unit III have been exceeded only three times in the last ~200 years; (2) flows equal to that which deposited the highest sands at Hailstorm Alcove probably have not been exceeded since A.D. 1487; and (3) only one flood has exceeded 29,300 ft^3/s since A.D. 1048. The more than 2,000-year-old flood unit

Tree scars (foreground and background) from 1972 flooding along Spring Creek.

(III) at Hailstorm Alcove pit A (fig. 10) lends confidence that if a large flood occurred after A.D. 1048, it would have left evidence.

Flood-frequency analyses for Spring Creek (table 5) were performed using the FLDFRQ3 and PeakfqSA flood-frequency models for three scenarios: (1) gaged records only, (2) all available data (including paleoflood chronologies and perception thresholds), and (3) top-fitting analysis (PeakfqSA only). No historical peak-flow data (beyond the gaged records) are available for Spring Creek. The analysis of the gaged records only (fig. 6) provided baseline results from which to compare analyses incorporating the paleoflood information.

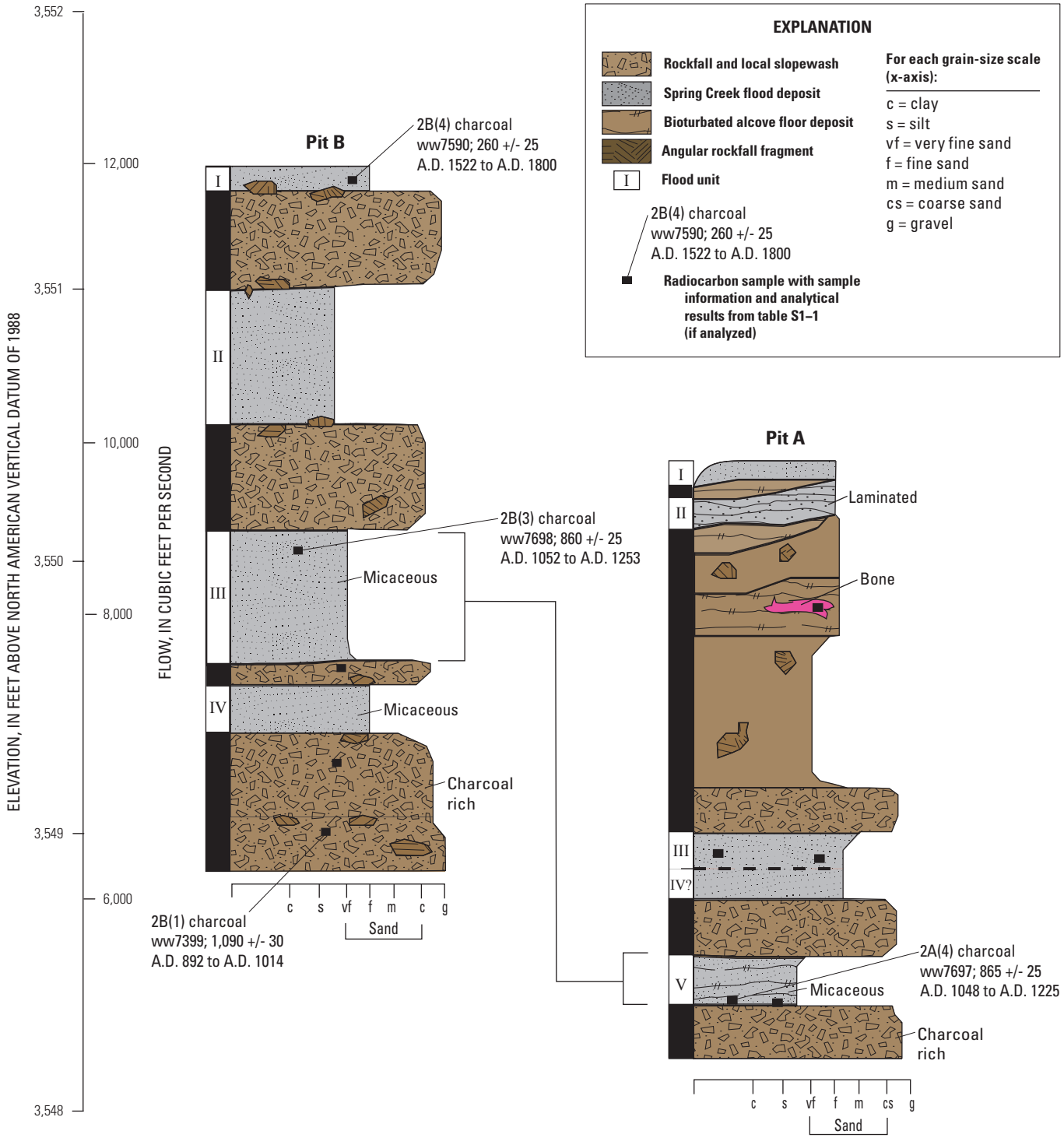

Figure 11. Schematic diagram showing paleoflood information for John Doe Alcove, Spring Creek.

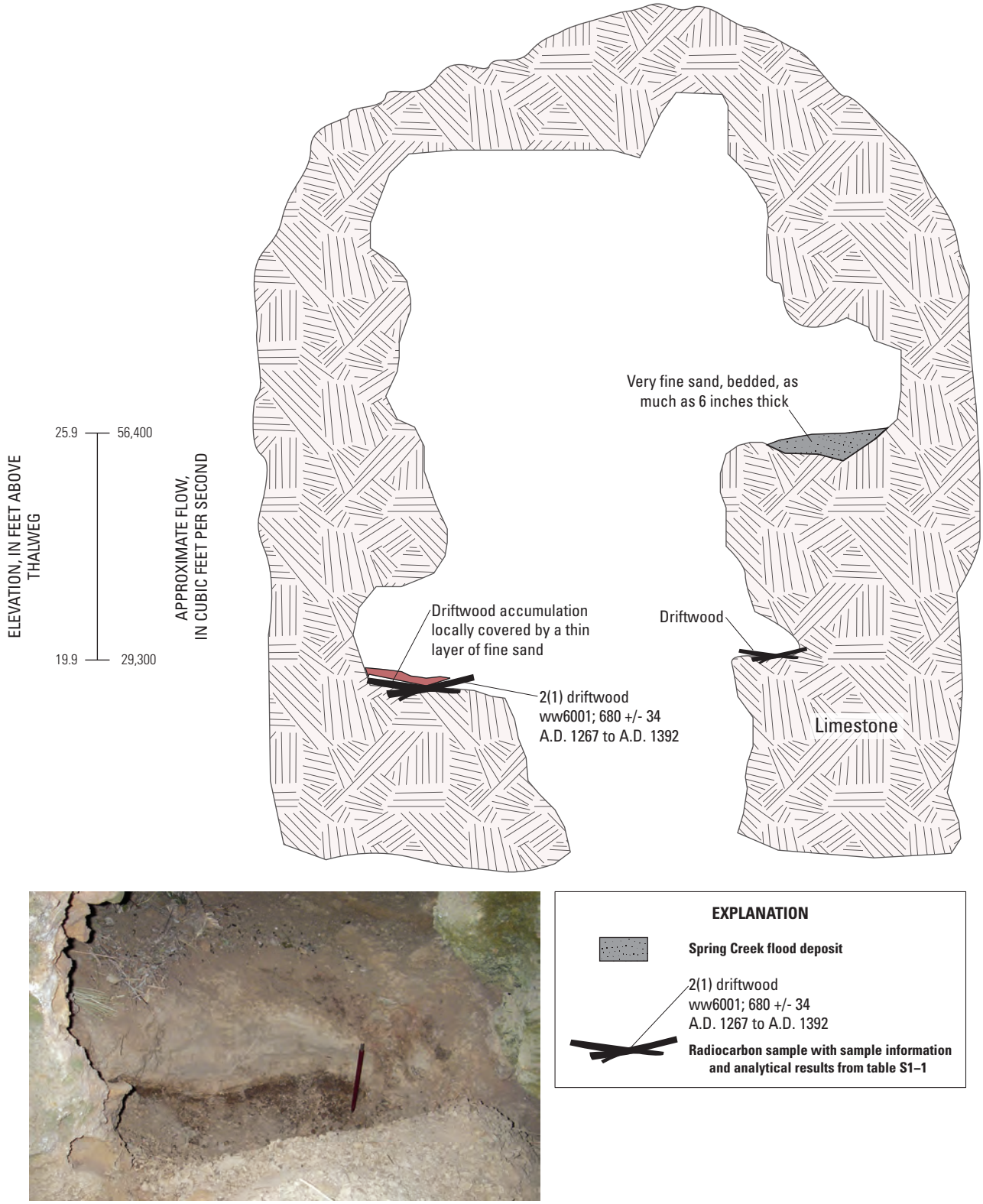

Figure 12. Schematic diagram showing paleoflood information for Temple of Doom Alcove, Spring Creek.

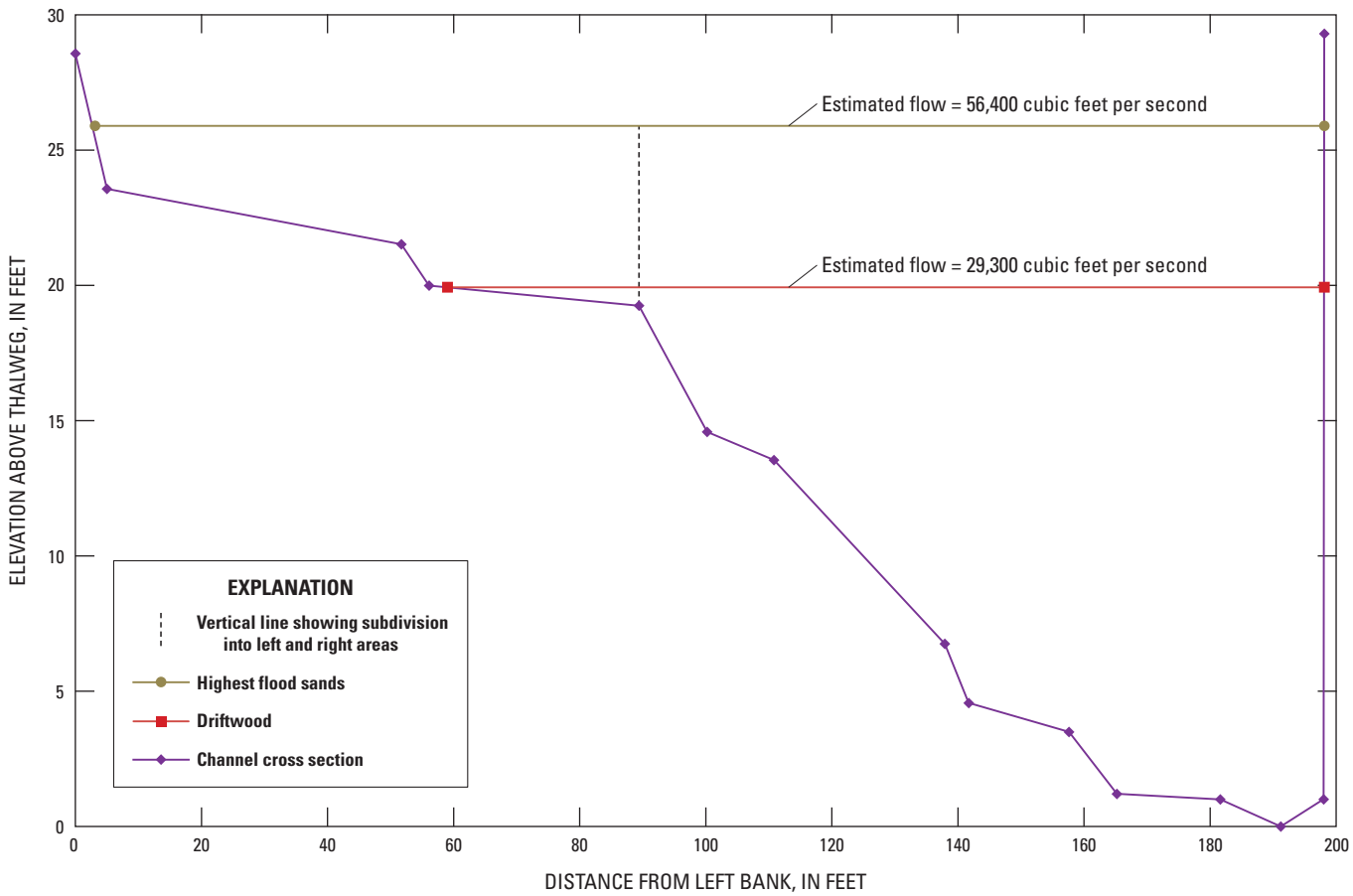

Figure 13. Channel cross section and relevant elevations for Temple of Doom Alcove, Spring Creek. Cross section is view looking downstream.

Table 3. Summary of critical-flow computations for Temple of Doom Alcove, Spring Creek.

[--, computation not applicable]

Computational unit	Elevation above thalweg (feet)	Top width (feet)	Area (square feet)	Hydraulic depth (feet)	Velocity (feet per second)	Flow rate (cubic feet per second)
Upper elevation, left bank subdivision	25.93	86.8	394	4.54	12.1	4,800
Upper elevation, left bank subdivision	25.93	108.7	2,080	19.1	24.8	51,600
Total flow rate for both subdivisions	--	--	--	--	--	56,400
Lower elevation, left bank subdivision	19.93	30.4	10.3	.34	3.3	34
Lower elevation, left bank subdivision	19.93	108.7	1,428	13.1	20.5	29,300
Total flow rate for both subdivisions	--	--	--	--	--	29,300

For the FLDFRQ3 model, which allows specification of uncertainty for gaged records, uncertainties of ±20 percent were assigned for all gaged peak-flow values except that of 1972 (table 2), for which ±33 percent was assigned because of larger uncertainty associated with especially large flows. For the top-fitting analysis, only the 33 annual peak flows greater than the median value of 127 ft^3/s in the gaged records were included. Flood-frequency analyses provided in table 5 include (1) computed peak-flow magnitudes (quantile estimates) for selected recurrence intervals ranging from 25 to 500 years (equivalent to annual exceedance probabilities ranging from 0.04 to 0.002); and (2) associated 95-percent confidence limits for all quantile estimates.

Flood-frequency analyses for all scenarios (fig. 15, table 5) indicate that the addition of the paleoflood information markedly improves estimates of low-probability floods—most clearly indicated by substantial narrowing (relative to results for the gaged record) of the range of the 95-percent confidence limits (especially for the largest recurrence intervals). Magnitudes from flood-frequency analyses were similar between the FLDFRQ3 and PeakfqSA models when paleoflood data were included with the gaged records. Additionally, the top-fitting analysis (PeakfqSA model only) yielded peak-flow magnitudes that were similar to those for the analysis with all available data; however, the 95-percent confidence intervals generally were somewhat larger because fewer data points were included.

As described in the previous section "Models for Flood-Frequency Analysis," the flood-frequency analysis using the PeakfqSA model (accounting for all gaged and paleoflood information without top fitting) is considered by the authors as most appropriate for general applications where estimates of low-probability peak flows are needed. This assessment primarily is based on the analytical approach of the PeakfqSA model, which conforms more closely than that of the FLDFRQ3 model to guidelines recommended for use by Federal agencies in Bulletin 17B (Interagency Advisory Council on Water Data, 1982). Additionally, the approach adopted for top fitting (including the largest 50 percent of gaged flows) is arbitrary, was mainly applied to determine

Table 4. Summary of long-term flood chronology used in flood-frequency analysis for Spring Creek.

[ID, identification; min, minimum; max, maximum; PT, perception threshold; --, not applicable]

ID for figure 14	Data description	Flow values, in cubic feet per second, for flood-frequency analysis			Flood or perception threshold dates, in calendar years A.D.			
		Min	Max	Most likely	Flood date	PT min	PT max	PT date
				Perception thresholds				
PT1	Superscour Alcove, pit B unit III	--	--	12,000	--	2009	1800	1860
PT2	Hailstorm Alcove, highest sands	--	--	18,200	--	1799	1487	1563
PT3	Temple of Doom Alcove/Hailstorm Alcove, pit A unit II and pit B unit II	--	--	29,300	--	1486	1048	1187
				Paleoflood chronology				
P1	Superscour Alcove, pit B unit II	13,900	27,800	20,800	1810	--	--	--
P2	Superscour Alcove, pit B unit III	12,000	24,000	18,000	1800	--	--	--
P3	Hailstorm Alcove, highest sands	18,200	36,400	27,300	1563	--	--	--
P4	Temple of Doom/Hailstorm Alcove, pit A unit II and pit B unit II	29,300	58,600	44,000	1347	--	--	--
P5	John Doe Alcove, pit A unit V and pit B unit III	8,750	17,500	13,100	1187	--	--	--
				Gaged records				
1972	1972 flood	14,600	29,000	21,800	--	--	--	--
Gaged record	1904–05, 1938–40, 1946–47, 1950–2009 (excluding 1972). Uncertainty for flow values is plus or minus 20 percent (not shown). (Top-fitting analysis excludes values less than 127 cubic feet per second)	14	10,000	--	--	--	--	--

model sensitivity, had little overall effect, and might be improved by more rigorous statistical evaluation.

Based on this assessment, the following summary comparisons for Spring Creek focus on quantile estimates from the PeakfqSA model derived using all available data without top fitting relative to quantile estimates derived using only gaged records. For the analysis derived using all available data, the 100-year quantile estimate was 7,960 ft^3/s (table 5), with 95-percent confidence limits of 4,160 and 14,500 ft^3/s. By contrast, the analysis of gaged records only produced a smaller 100-year quantile estimate of 6,290 ft^3/s, but with a much larger 95-percent confidence interval of 2,600–102,000 ft^3/s. The addition of the paleoflood data to the gaged records increased the magnitude of the 100-year flood by about 27 percent and reduced the 95-percent confidence interval by about 90 percent. Similarly, consideration of the paleoflood data increased the magnitude of the 500-year flood by about 29 percent and reduced the 95-percent confidence interval by about 95 percent.

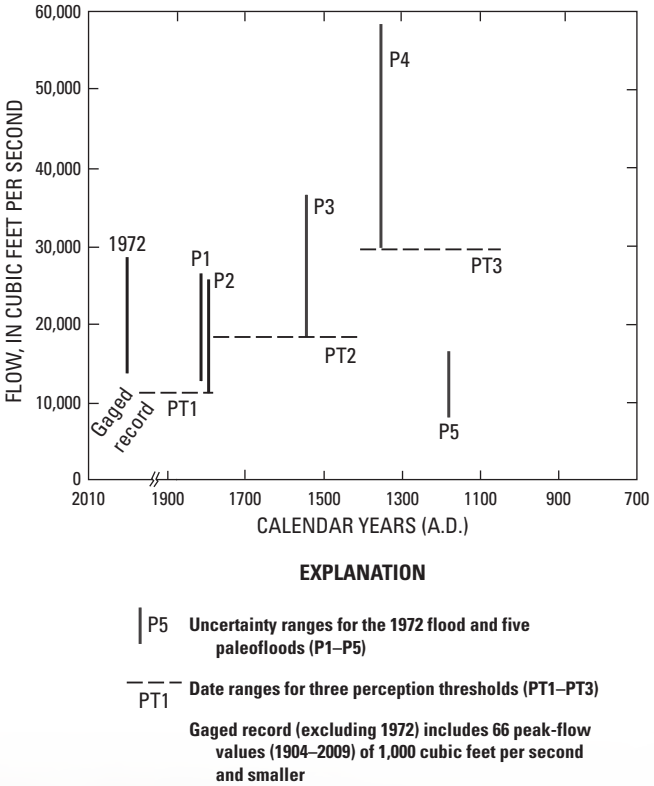

Figure 14. Long-term flood chronology for Spring Creek (from table 4).

View (looking downstream) of Hailstorm Alcove along Spring Creek. Flotsam is from 1972 flood.

Table 5. Flood-frequency analyses for Spring Creek.

[% reduction, percent reduction in confidence interval for analysis with all available data, relative to analysis for gaged records only]

Peak-flow magnitudes and 95-percent confidence limits and intervals, in cubic feet per second, for associated recurrence interval (annual exceedance probability)					
Data description	**25 years (0.04)**	**50 years (0.02)**	**100 years (0.01)**	**200 years (0.005)**	**500 years (0.002)**
PeakfqSA model, gaged records only					
Magnitude	2,010	3,620	6,290	10,700	20,800
Lower limit	1,080	1,710	2,600	3,830	6,150
Upper limit	9,750	35,200	102,000	295,000	1,190,000
Interval	8,670	33,500	99,400	291,000	1,180,000
PeakfqSA model, all available data					
Magnitude	2,480	4,530	7,960	13,600	26,900
Lower limit	1,500	2,550	4,160	6,580	11,600
Upper limit	3,850	7,440	14,500	28,600	71,300
Interval	2,350	4,890	10,300	22,000	59,700
% reduction	72.9	85.4	89.6	92.4	94.9
PeakfqSA model, all data with top fitting					
Magnitude	2,630	4,700	8,070	13,500	25,600
Lower limit	1,430	2,490	4,100	6,640	12,000
Upper limit	4,390	7,740	14,200	29,500	96,000
Interval	2,960	5,250	10,100	22,900	84,000
FLDFRQ3 model, gaged records only					
Magnitude	2,510	5,060	9,950	19,200	45,000
Lower limit	1,150	1,910	3,020	4,600	7,730
Upper limit	8,800	24,800	69,300	190,000	721,000
Interval	7,650	22,900	66,300	185,000	713,000
FLDFRQ3 model, all available data					
Magnitude	2,290	4,360	8,080	14,600	31,200
Lower limit	1,470	2,670	4,630	7,710	14,500
Upper limit	3,590	7,300	14,800	30,200	77,400
Interval	2,120	4,630	10,200	22,500	62,900
% reduction	72.3	79.8	84.6	87.8	91.2

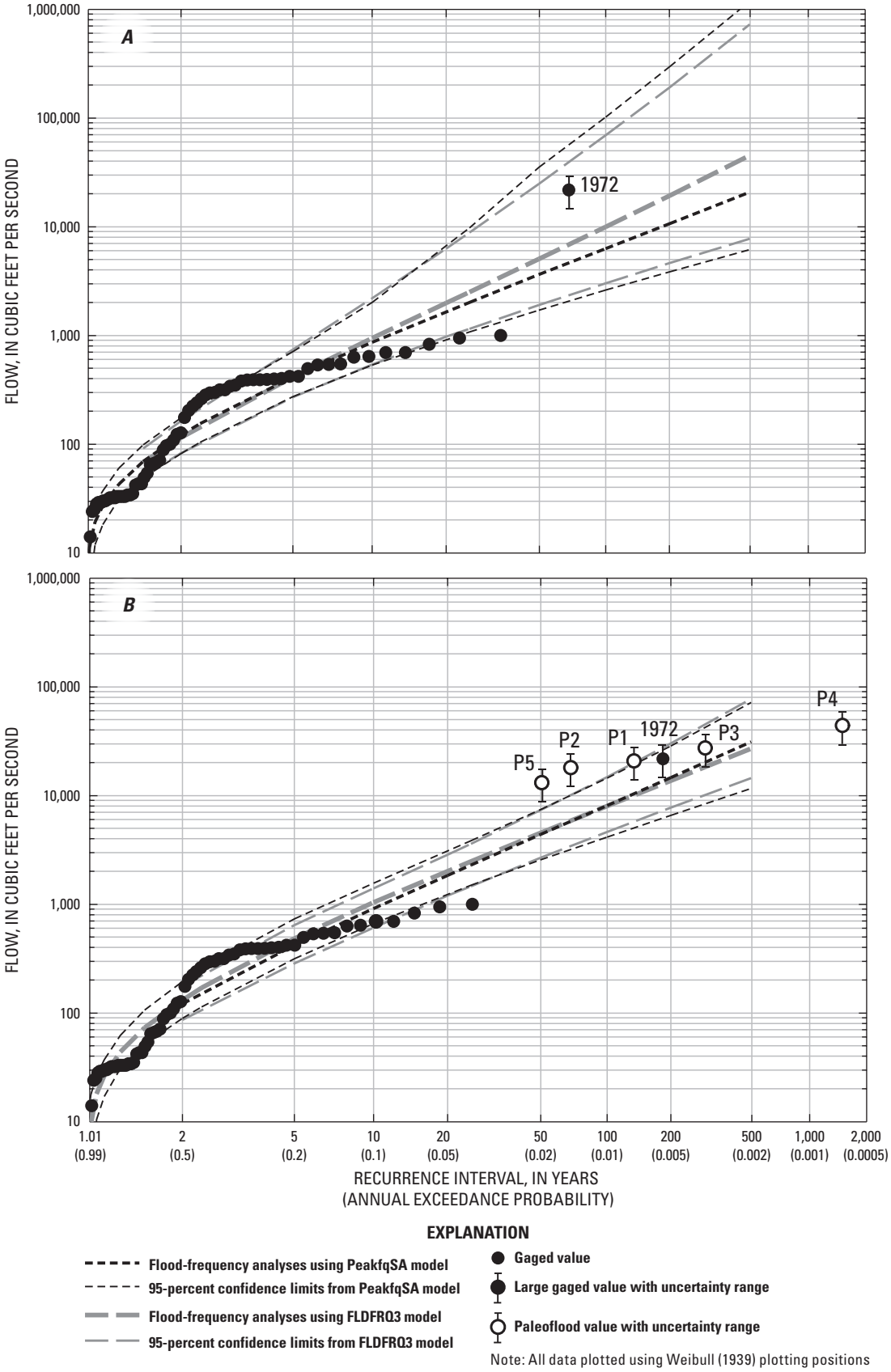

Figure 15. Flood-frequency analyses for Spring Creek for *A*, gaged records only, and *B*, all available data that incorporate the long-term flood chronology from figure 14.

Rapid Creek

The flood history for the reach of Rapid Creek downstream from Pactola Dam (fig. 1) is of particular interest because of proximity to urban populations. However, the available paleoflood chronology for this "lower" reach predates construction of Pactola Dam, which regulates 321 mi^2 of the drainage area for this reach (367–384 mi^2; table 1). Thus, paleoflood investigations also were conducted in an "upper" reach (upstream from Pactola Reservoir). Implications regarding peak-flow characterization for modern conditions (subsequent to dam construction) are described in a subsequent section on "Implications of Paleoflood Chronologies for Rapid Creek."

Lower Rapid Creek

Stratigraphic investigations were conducted at seven sites within the lower Rapid Creek study reach. The reach (figs. 1 and 16) extends from just downstream from the confluence of Victoria Creek to near the confluence of Cleghorn Canyon. No major tributaries enter the reach—the largest (7 mi^2) is Cleghorn Canyon. The study reach is a narrow canyon about 200 to 800 ft wide flanked by near-vertical walls of the Madison Limestone and Minnelusa Formation (fig. 1), as much as several hundred feet high. The valley bottom widens near the downstream end of the reach where it exits the Minnelusa Limestone. The channel substrate consists of cobble-gravel, sand, and locally bedrock. The valley bottom is vegetated with grass, shrubs, ponderosa pine, and various deciduous trees. Most of this reach is privately owned, and homes flank the channel in several locations. Roads parallel the channel throughout the reach.

The 1972 flood had a peak flow of 31,200 ft^3/s at streamgage 06412500 (Schwarz and others, 1975; U.S. Geological Survey, 2010e). This streamgage is located near the center of the study reach (unregulated drainage area downstream from Pactola Dam = 54 mi^2, table 1) about 0.5 mi upstream from Cleghorn Canyon (fig. 16). This is the largest flow (by more than a factor of 10) in the 86 years of non-contiguous gaged records for lower Rapid Creek that date back to 1905 (fig. 17, table 2). The 1972 flow also was substantially larger than four historical floods (1878, 1883, 1907, and 1920; as described in "Supplement 2. Modern Peak-Flow Chronologies") of about 7,000 to 12,000 ft^3/s, and is documented in accounts of Driscoll and others (2010) as the largest flow since 1878.

The 1972 flood locally destroyed many houses in the study reach, as marked by foundations in many locations. The flood also left abundant flotsam, tree scars, and fine-grained slack-water deposits along the channel margins. The sites of stratigraphic analysis are in locations where slack-water sediment from the 1972 flood and previous large floods has accumulated in alcoves and shallow caves formed in the canyon walls. One site, Black Socks Alcove, is near the downstream end of the reach and consists of sediment accumulated along an outcrop of the Minnelusa Formation. The other sites within the study reach are in small caves or alcoves formed in the Madison Limestone.

Upstream view of Madison Limestone outcrop near the Church Mug and High Alcoves along lower Rapid Creek.

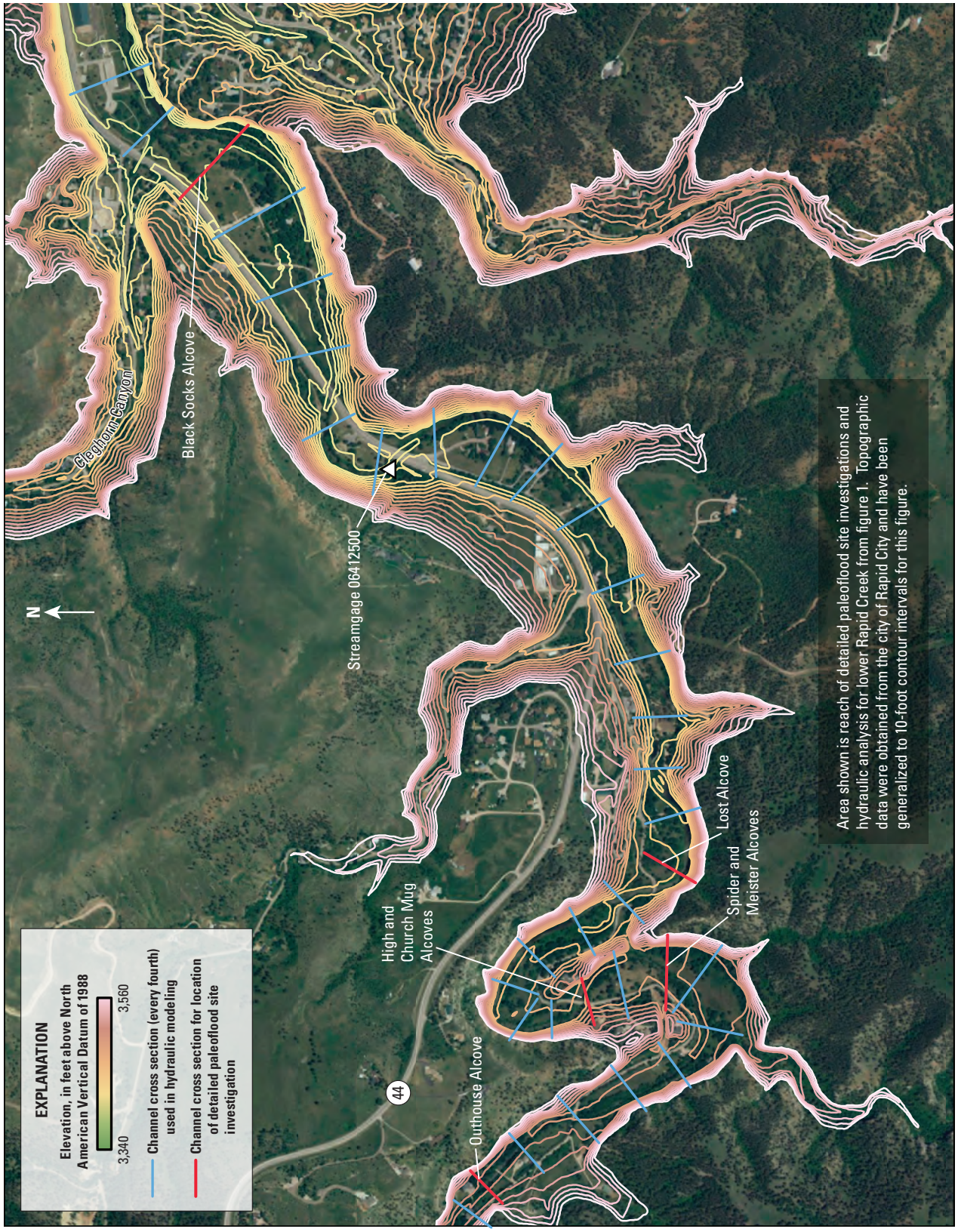

Figure 16. Topographic information and selected details of hydraulic analysis for lower Rapid Creek reach.

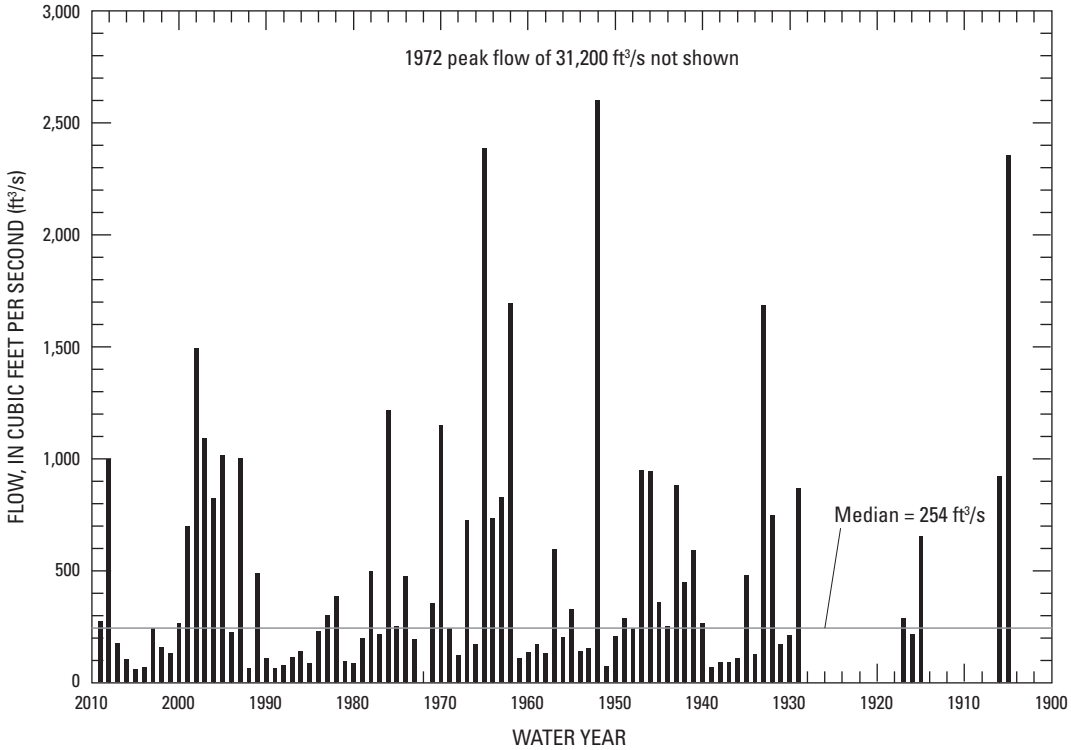

Figure 17. Modern peak-flow chronology (gaged and historical records) for lower Rapid Creek reach. Values are from table 2.

Hydraulic Analysis and Paleoflood Chronology

A HEC-RAS hydraulic model (fig. 18) based on a digital (5-ft contour interval) topographic coverage (fig. 16) was used for estimating peak-flow magnitudes for paleofloods along lower Rapid Creek. Calibration of the hydraulic model was accomplished by using surveyed elevations for 1972 high-water evidence (fig. 18) within the reach. Calibration primarily was based on the 1972 peak-flow value of 31,200 ft^3/s for streamgage 06412500. The drainage area increases by only 17 mi^2 throughout the reach, relative to an area of 384 mi^2 at the downstream extent of the reach (table 1); thus, most tributaries within this reach are small and flow adjustments for calibration purposes were minor. However, a higher flow value of 40,000–50,000 ft^3/s for the 1972 flood was inferred for the short reach downstream from Cleghorn Canyon (fig. 16), which contributed about 12,600 ft^3/s to Rapid Creek during the 1972 flood (Schwarz and others, 1975).

Slack-water deposits from paleofloods were investigated at seven different sites along lower Rapid Creek. One pit excavated at the upstream-most site, Outhouse Alcove (fig. 19), provided stratigraphic evidence of four floods. The oldest flood unit (IV) was dated between A.D. 124 and 318, and required a flow of at least 5,250 ft^3/s for inundation. The second oldest flood unit (III) was dated to A.D. 1039–1215, with a flow of at least 7,700 ft^3/s required for inundation. A thick unit of very fine sand comprised flood unit II, which required a flow of 11,300 ft^3/s for inundation. This flood unit provided no datable organics for radiocarbon analysis; however, the age was constrained as younger than about 1,000 years by the underlying flood unit. The age was further constrained as older than about 200 years based on a wood fragment from an overlying colluvium unit that was dated to A.D. 1527–1954. Although of limited use alone, this constraint is useful for correlating flood deposits among different sites. The youngest flood unit (I) at this site is from 1972 the flood, with an associated flow of about 15,100 ft^3/s for the elevation.

The Spider and Meister Alcoves are about 0.5 mi farther downstream and are close enough (about 100 ft) to be represented on a single HEC-RAS cross section (fig. 16). Stratigraphic evidence of one flood was found at the Spider Alcove (fig. 20), which is farthest upstream and in a small cave in the Madison Limestone. Two radiocarbon samples were analyzed from colluvium directly below the flood unit. Both samples returned ages within 20 years of each other adding confidence to an age estimate for the flood of A.D. 1016–1180, which spans the range of the two samples. The corresponding flow for this flood unit exceeds 64,000 ft^3/s, which is about twice that of the 1972 flood at the same location. The Meister Alcove is lower than the Spider Alcove and provided evidence

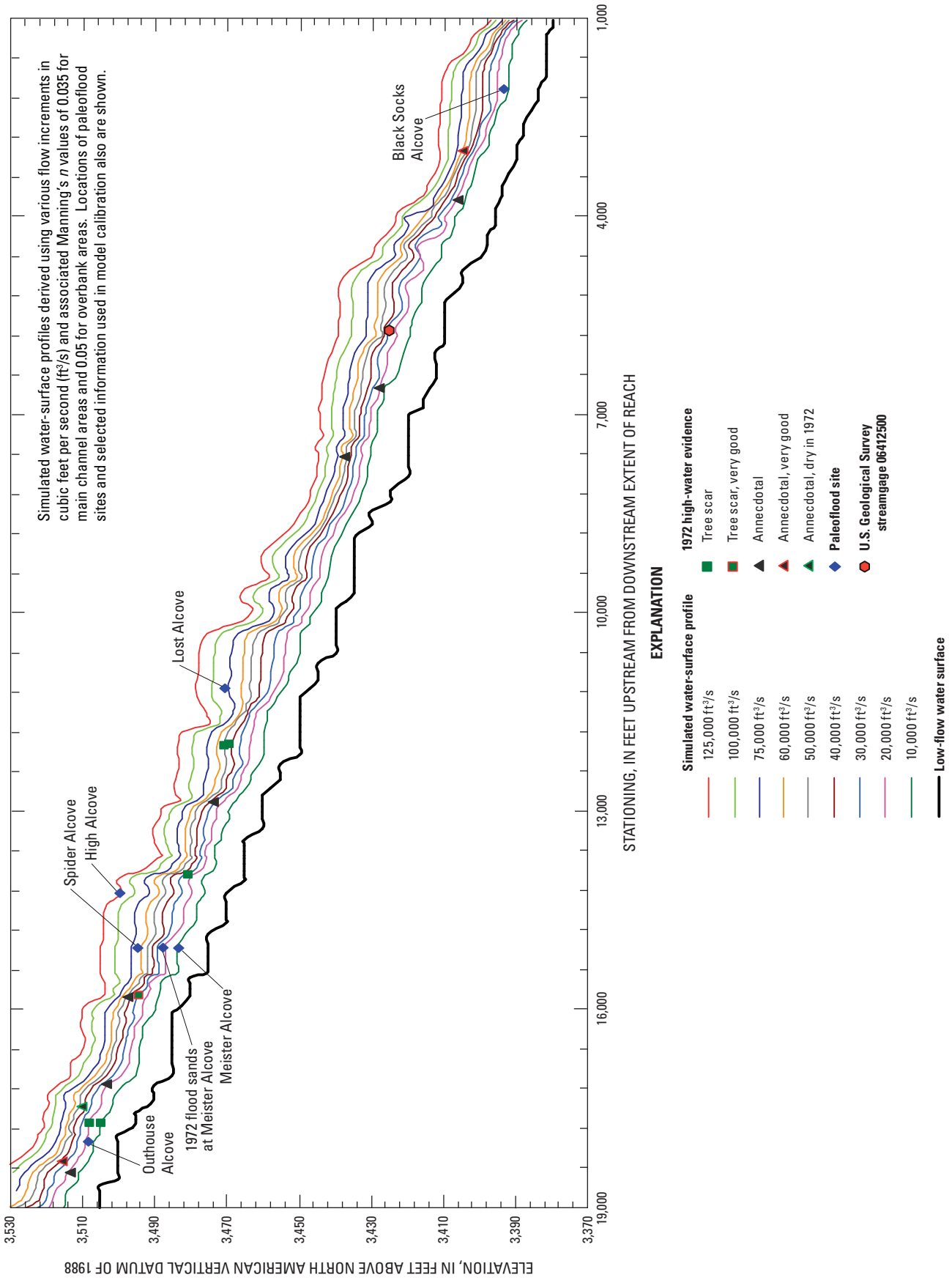

Figure 18. Results of hydraulic model simulations for lower Rapid Creek reach.

of four floods (fig. 21). The oldest flood unit (IV) was dated to A.D. 708–947, and required a flow of 7,000 ft^3/s for inundation. The contact between the two uppermost flood units (I and II) is unclear because of extensive bioturbation; however, all three overlying flood units (I to III) were deposited within the last several hundred years and have corresponding flow rates between 7,200 and 9,000 ft^3/s. Flood unit II or III at Meister Alcove likely correlates to flood unit II at Outhouse Alcove based on the age dating and stratigraphic context. Additional flood evidence at Meister Alcove consisted of a thin silt deposit in the alcove wall about 5 ft above the excavated pit and was presumed to be from 1972 flooding. The associated flow for the elevation of this silt is 27,000 ft^3/s, which is consistent with the simulated flow range of 20,000–30,000 ft^3/s (fig. 18) and abundant evidence of the approximate 1972 flood elevation in this reach.

The site highest in elevation relative to the channel thalweg along lower Rapid Creek is High Alcove, located in a small limestone cave several hundred feet downstream from Spider and Meister Alcoves. High Alcove contained stratigraphic evidence of one flood that was dated using OSL analysis as A.D. 1545–1595 (fig. 22) and has an associated flow exceeding 128,000 ft^3/s. This is the largest known flood in the Rapid Creek paleoflood chronology in the last 2,000 years, and also is the largest known flood within all four drainages in the study area.

One pit was excavated at Church Mug Alcove (fig. S3–3) located just downstream from High Alcove, but at a much lower elevation. This site contained multiple flood deposits; however, these flood units had small corresponding flow rates and correlate with flood units at other sites along lower Rapid Creek. Thus, additional information could not be incorporated

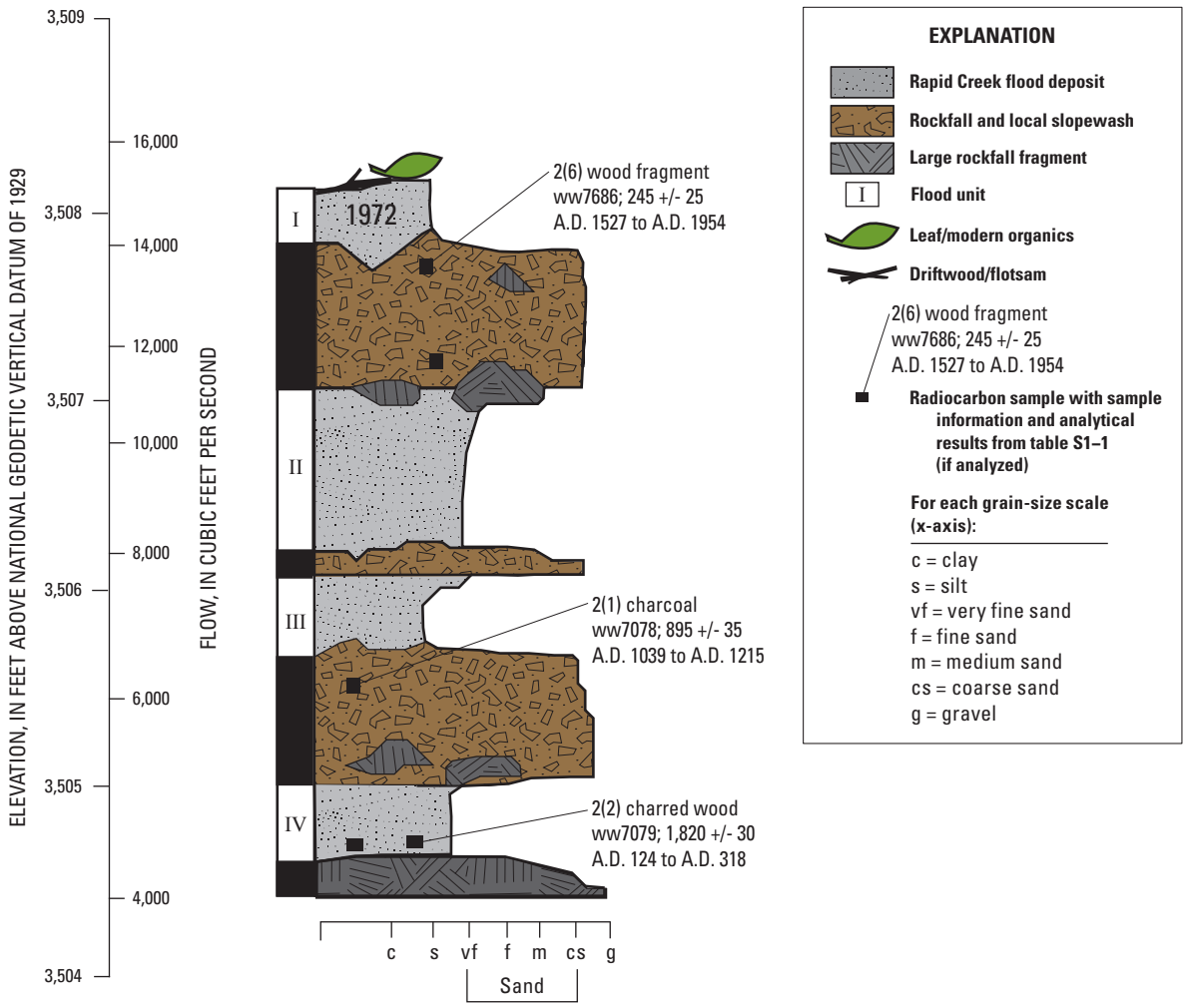

Figure 19. Schematic diagram showing paleoflood information for Outhouse Alcove, lower Rapid Creek reach.

in the paleoflood chronology for Rapid Creek from this site without possibly counting single floods more than once.

The Lost Alcove is 0.25 mi farther downstream and provided stratigraphic evidence of 12 to 14 especially large floods, all between about 2,400 and 1,200 years ago (fig. 23). Minimum flows for the associated floods are between 66,000 and 79,000 ft³/s. This exceptional paleoflood record was not used in the flood-frequency analyses because it may represent a period of remarkably high flows distinct from the last ~1,000 years. The reason for this is uncertain but may owe to large fires in the basin (many of the flood deposits contain abundant charcoal) or possibly a period of local aggradation (the flood deposits sit directly on round-cobble channel gravel about 22 ft above the modern channel thalweg). The youngest flood at Lost Alcove (79,000 ft³/s between about A.D. 720 and 944) probably does not correlate with the large flood at Spider Alcove (64,000 ft³/s between about A.D. 1016 and 1180) or the younger flood at High Alcove (128,000 ft³/s between about A.D. 1545 and 1595).

The Black Socks Alcove is farthest downstream along lower Rapid Creek and provided stratigraphic evidence of 9 or 10 floods in the last 600 years (fig. 24). The oldest flood unit (X) was dated to A.D. 1400–1466 (youngest of two samples) and required a flow of at least 5,300 ft³/s for inundation. The youngest flood unit (I) is from 1972 and required a flow of 13,800 ft³/s for inundation. Radiocarbon samples

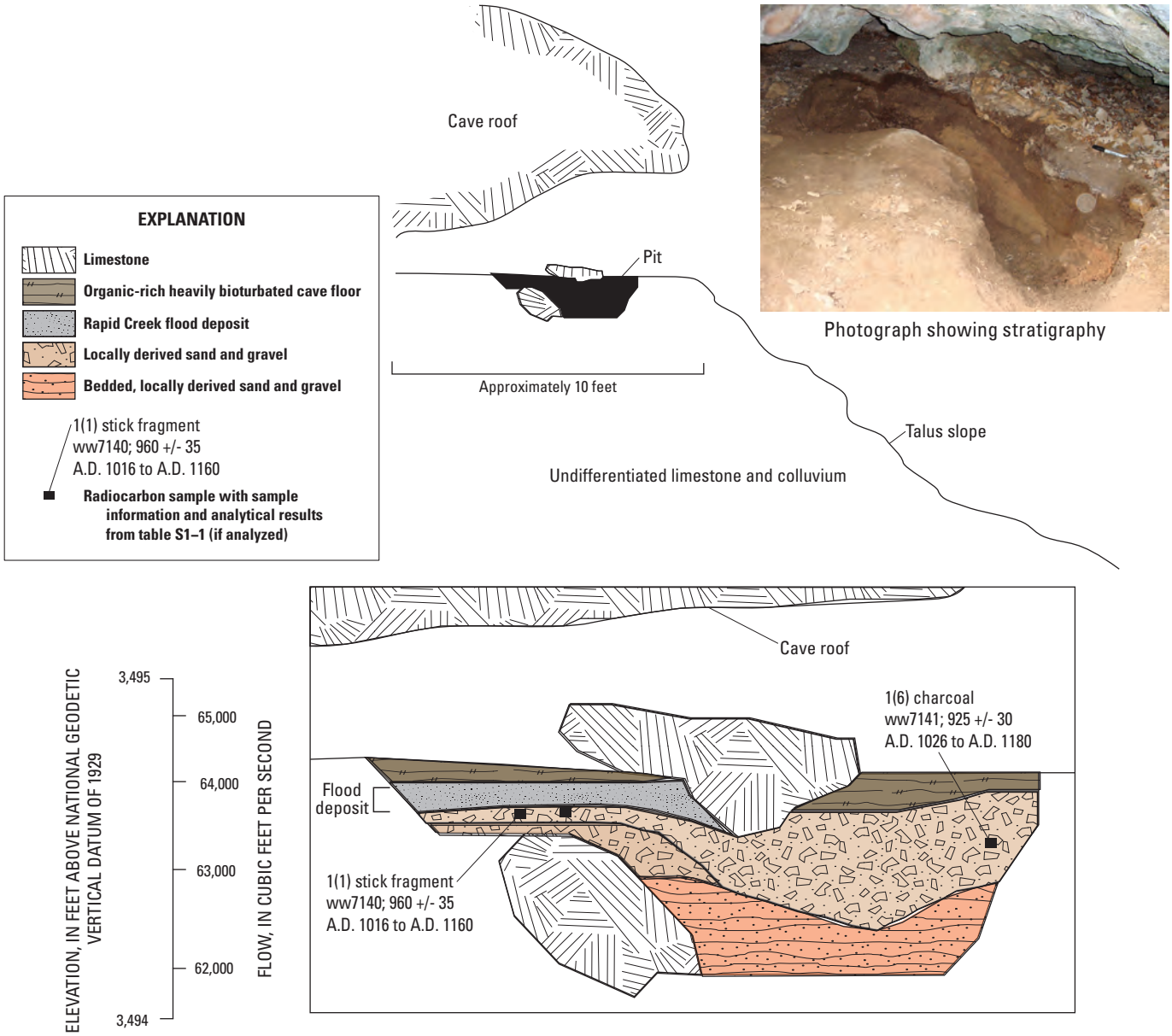

Figure 20. Schematic diagram showing paleoflood information for Spider Alcove, lower Rapid Creek reach.

indicated dates of A.D. 1665 or younger for underlying flood units II through VII. A charcoal sample from a colluvium unit dated to A.D. 410–558, but its stratigraphic position indicates contamination by older carbon (likely from bioturbation). Some or all of the historical peak flows of 1878, 1883, 1907, and 1920 (table 2) for lower Rapid Creek (about 7,000 to 12,000 ft^3/s) may be represented in the stratigraphy at Black Socks Alcove (and possibly Meister and Church Mug Alcoves).

In summary, lower Rapid Creek has experienced two paleofloods in the last ~1,000 years exceeding the 1972 flow of 31,200 ft^3/s (fig. 25, table 6). The largest paleoflood (P6) left deposits in High Alcove about 440 years ago and had a flow of 128,000–256,000 ft^3/s. Another large paleoflood (recorded in Spider Alcove) was about 1,000 years ago and had a flow of 64,000–128,000 ft^3/s. Five smaller paleofloods (Black Socks Alcove) of 9,500–19,000 ft^3/s (P1–P5) occurred between about 200 and 400 years ago.

Flood-Frequency Analysis

Flood-frequency analyses for lower Rapid Creek are based on a long-term paleoflood chronology than spans ~1,000 years in conjunction with information on four historical floods of 1878, 1883, 1907, and 1920 (H1–H4, respectively, in fig. 25) and the gaged records (fig. 17). Flow values and associated uncertainties for gaged and historical flows are shown in table 2. The paleoflood chronology (table 6) includes the two large floods recorded at High and Spider Alcoves, and five smaller paleofloods recorded at Black Socks Alcove. Based on elevations and flow simulations, the five young paleofloods at Black Socks Alcove were all inferred to have minimum flows of 9,500 ft^3/s. More precise resolution of these paleoflood flows was not possible because of the ambiguous relation between the stratigraphy and historical flood records, which include four peak flows of similar magnitude between 1878 and 1920 (table 2).

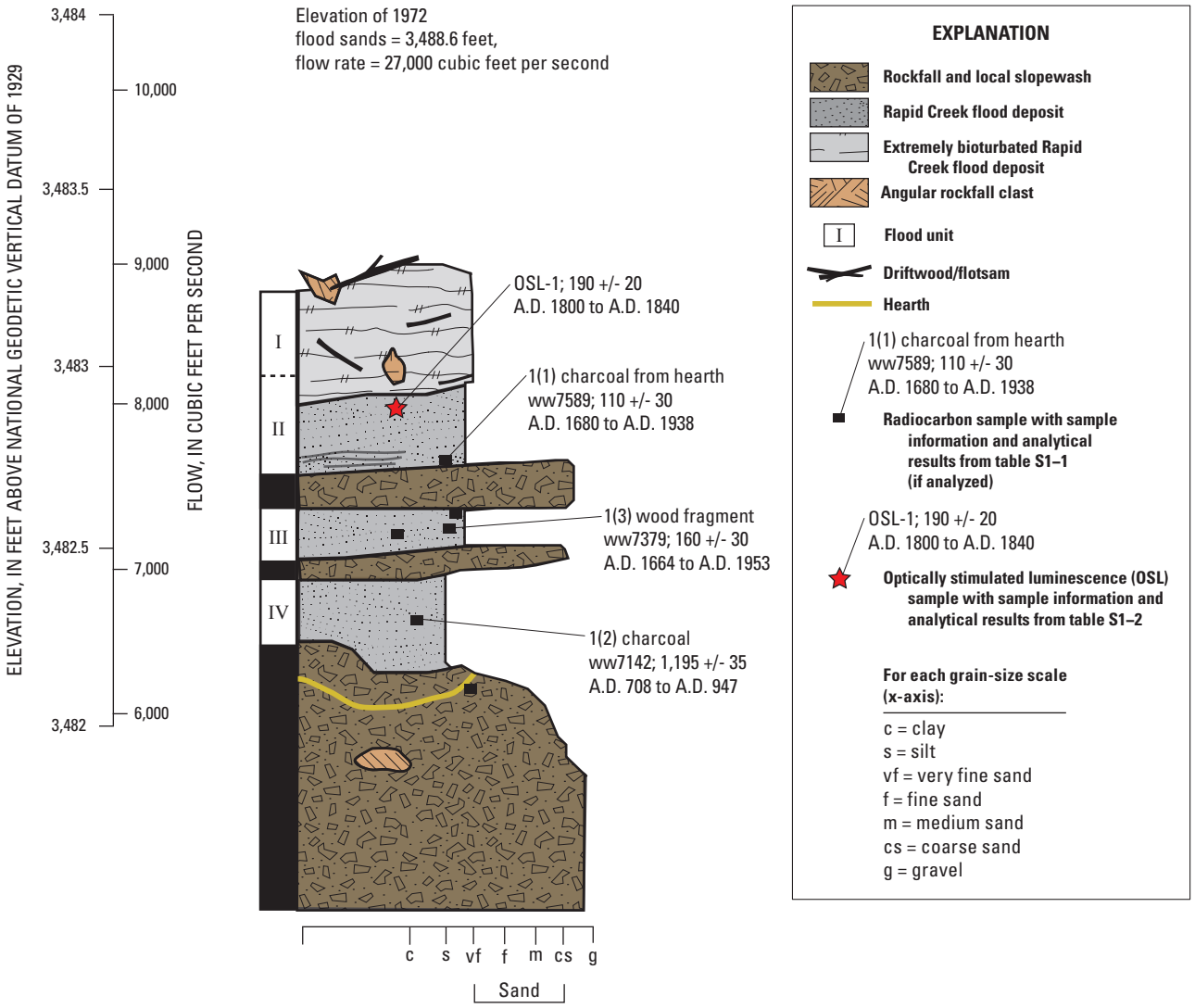

Figure 21. Schematic diagram showing paleoflood information for Meister Alcove, lower Rapid Creek reach.

Four perception thresholds were specified for the flood-frequency analyses (fig. 25, table 6). The 1878 historical flood was treated as a threshold since 1875 (PT1). The five small paleofloods at Black Socks Alcove were incorporated into one threshold (PT2). The third threshold (PT3) was set to the flow for the flood unit preserved at Spider Alcove and the fourth threshold (PT4) was set equal to the flow for the youngest flood unit at Lost Alcove. This threshold begins at A.D. 720 because that is the age of the youngest flood unit, and if a larger flood occurred after this time, it is likely that evidence of it would have been preserved. For the top-fitting analysis, only the 43 values greater than the median value of 254 ft^3/s in the gaged peak-flow record were included.

As was done for Spring Creek, flood-frequency analyses were performed for multiple scenarios (table 7), with the analysis of the gaged records only providing a basis for comparison with various longer-term analyses that include historical floods, the paleoflood chronology, and appropriate perception thresholds. The 100-, 200-, and 500-year quantile estimates for the analysis with all available data are substantially larger than the quantile estimates for the analyses of the gaged records only and for the gaged records plus historical

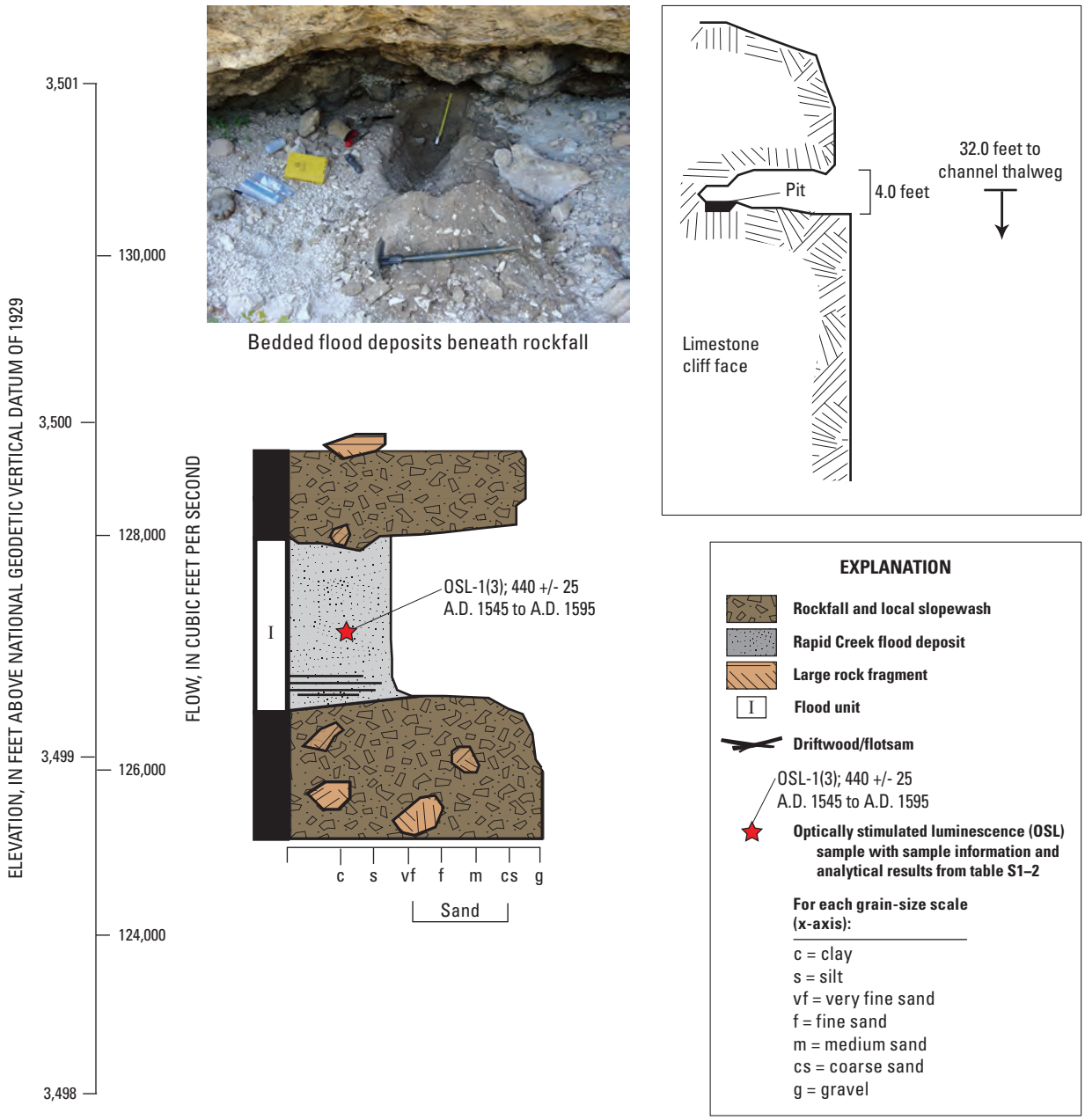

Figure 22. Schematic diagram showing paleoflood information for High Alcove, lower Rapid Creek reach.

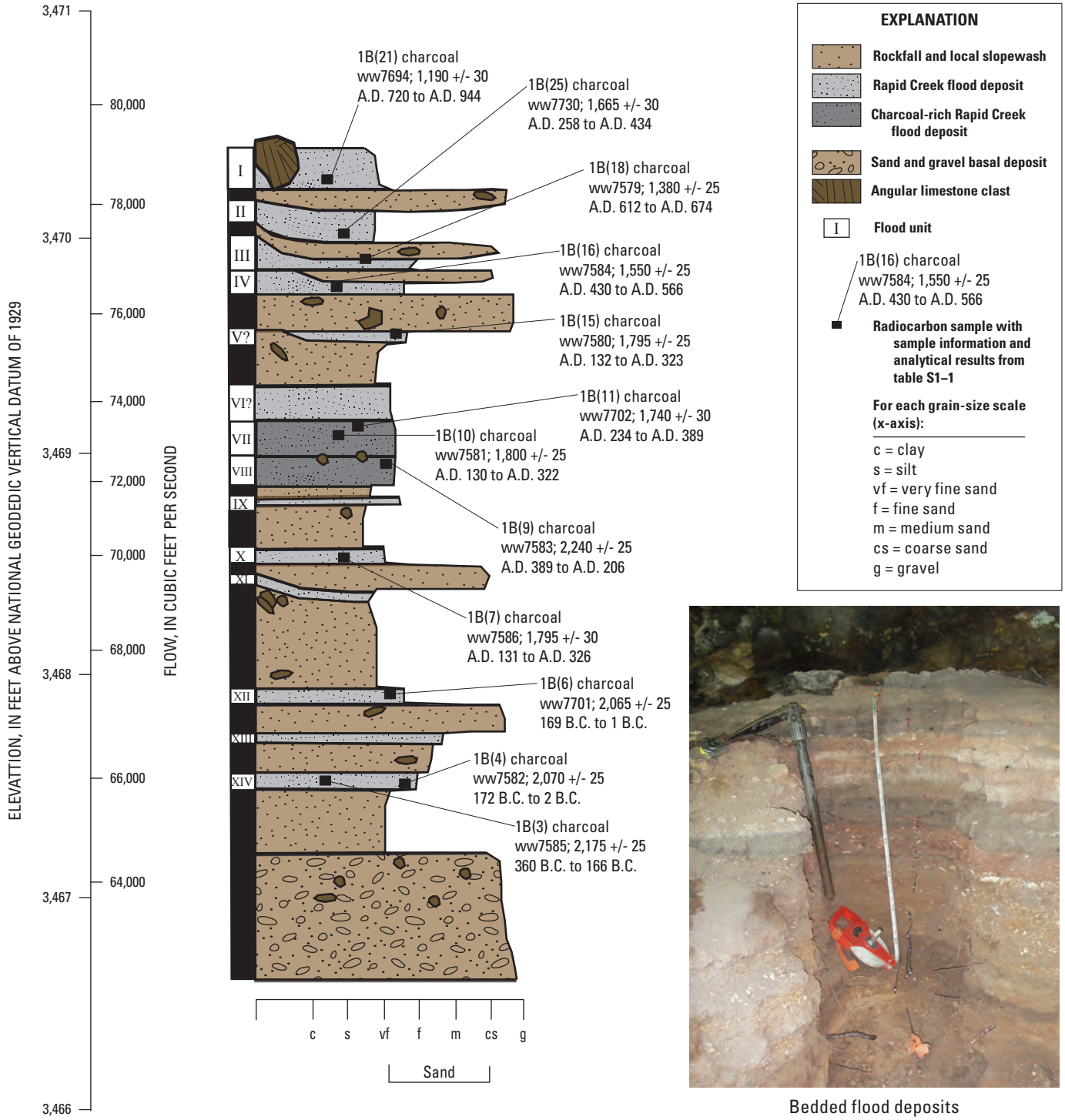

Figure 23. Schematic diagram showing paleoflood information for Lost Alcove, lower Rapid Creek reach.

data, reflecting the evidence for the paleofloods in this reach. Incorporation of all available data greatly reduced uncertainties for low-probability floods (fig. 26), with 95-percent confidence intervals for the 100-, 200-, and 500-year PeakfqSA quantile estimates decreasing by more than 80 percent, relative to analyses for gaged records only (table 7). The modern peak-flow chronology for the lower Rapid Creek study reach (described in "Supplement 2. Modern Peak-Flow Chronologies") was developed to estimate pre-regulation conditions, which is consistent with the paleoflood chronology obtained for the reach. Thus, the resulting flood-frequency analyses are not consistent with the modern post-regulation conditions. Perspectives regarding application of results relative to modern conditions are described in a subsequent section "Central Black Hills Flood Frequency: Synopsis, Implications, and Application."

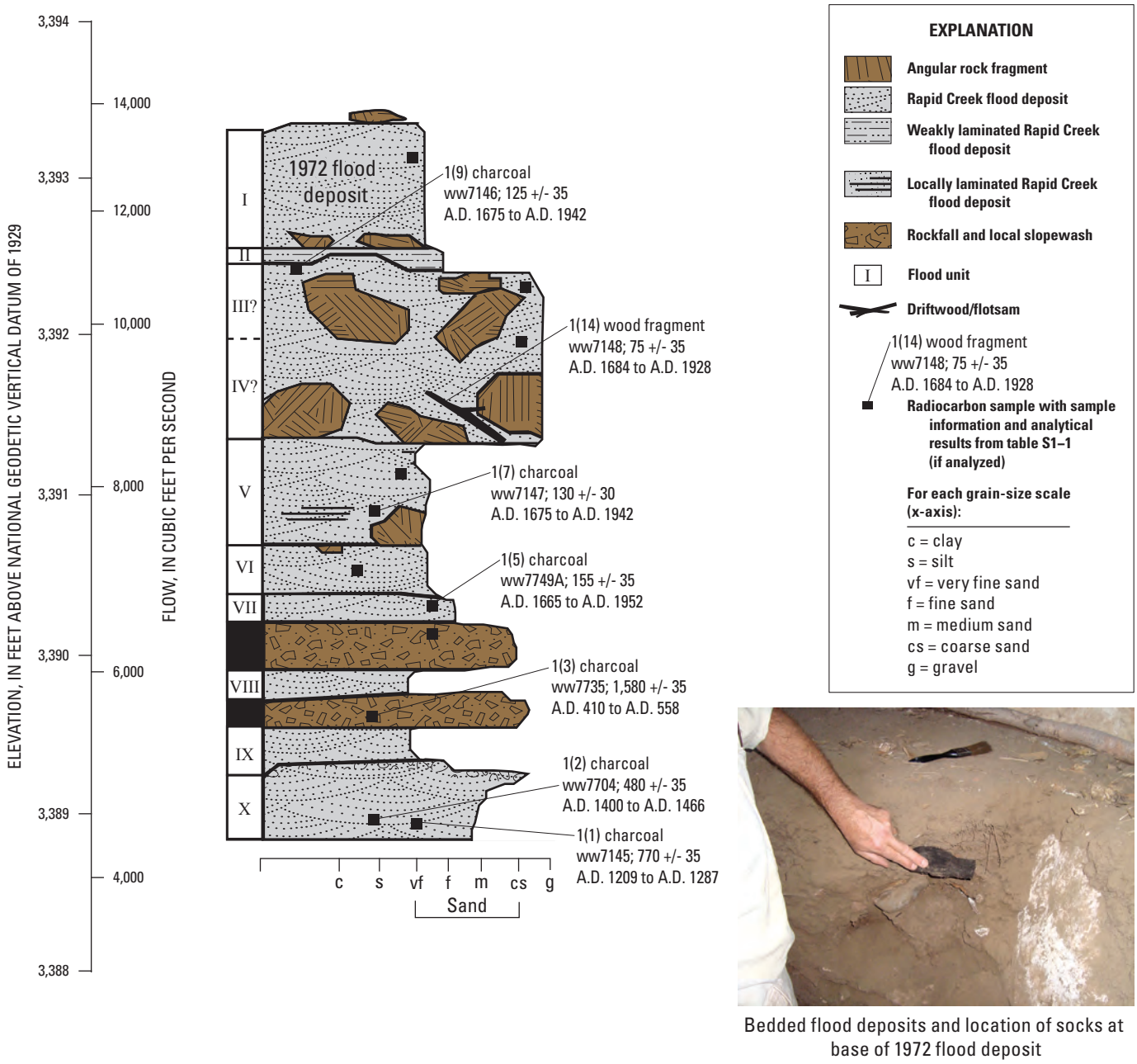

Bedded flood deposits and location of socks at base of 1972 flood deposit

Figure 24. Schematic diagram showing paleoflood information for Black Socks Alcove, lower Rapid Creek reach.

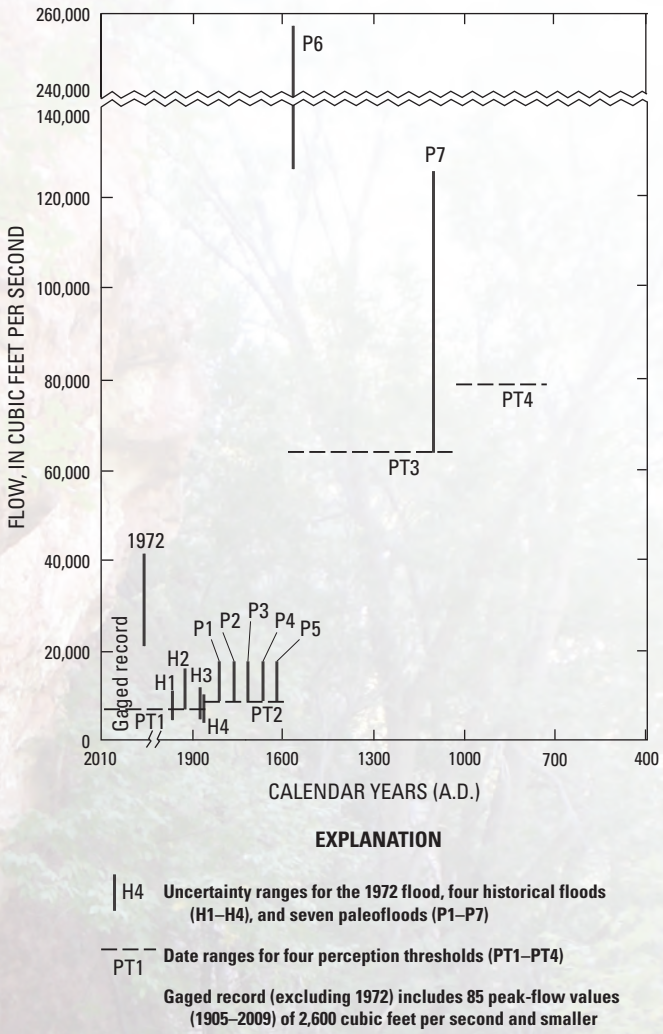

Figure 25. Long-term flood chronology for lower Rapid Creek reach (from table 6).

View (looking upstream) of Black Socks Alcove along the lower Rapid Creek reach.

Table 6. Summary of long-term flood chronology used in flood-frequency analysis for lower Rapid Creek reach.

[ID, identification; min, minimum; max, maximum; PT, perception threshold; --, not applicable]

ID for figure 25	Data description	Flow values, in cubic feet per second, for flood-frequency analysis			Flood or perception threshold dates, in calendar years A.D.			
		Min	Max	Most likely	Flood date	PT min	PT max	PT date
			Perception thresholds					
PT1	1878 historical flood	--	--	7,090	--	2009	1875	1920
PT2	Black Socks Alcove (paleofloods 1 through 5)	--	--	9,500	--	1874	1595	1740
PT3	Spider Alcove	--	--	64,000	--	1594	1016	1300
PT4	Lost Alcove	--	--	79,000	--	1015	720	900
			Paleoflood chronology					
P1	Black Socks Alcove	9,500	19,000	14,300	1810	--	--	--
P2	Black Socks Alcove	9,500	19,000	14,300	1760	--	--	--
P3	Black Socks Alcove	9,500	19,000	14,300	1710	--	--	--
P4	Black Socks Alcove	9,500	19,000	14,300	1660	--	--	--
P5	Black Socks Alcove	9,500	19,000	14,300	1610	--	--	--
P6	High Alcove	128,000	256,000	192,000	1570	--	--	--
P7	Spider Alcove	64,000	128,000	96,000	1103	--	--	--
			Historical floods					
H1	1920	3,770	11,300	7,540	1920	--	--	--
H2	1907	6,100	18,300	12,200	1907	--	--	--
H3	1883	3,950	11,800	7,900	1883	--	--	--
H4	1878	3,530	10,600	7,060	1878	--	--	--
			Gaged records					
1972	1972 flood	29,900	41,500	31,200	--	--	--	--
Gaged record	1905–06, 1915–17, 1929–2009 (excluding 1972). Uncertainty for flow values is plus or minus 15 percent (not shown). (Top-fitting analysis excludes values less than 254 cubic feet per second)	61	2,600	--	--	--	--	--

Table 7. Flood-frequency analyses for lower Rapid Creek reach.

[% reduction, percent reduction in confidence interval for analysis with all available data, relative to analysis for gaged records only]

Peak-flow magnitudes and 95-percent confidence limits and intervals, in cubic feet per second, for associated recurrence interval (annual exceedance probability)					
Data description	**25 years (0.04)**	**50 years (0.02)**	**100 years (0.01)**	**200 years (0.005)**	**500 years (0.002)**
PeakfqSA model, gaged records only					
Magnitude	2,990	5,160	8,720	14,500	27,900
Lower limit	1,780	2,730	4,070	5,910	9,440
Upper limit	11,800	37,100	104,000	294,000	1,170,000
Interval	10,000	34,400	100,000	288,000	1,160,000
PeakfqSA model, gaged records and historical data					
Magnitude	3,840	6,770	11,600	19,600	38,400
Lower limit	2,330	3,680	5,630	8,390	13,800
Upper limit	9,840	28,000	87,400	262,000	957,000
Interval	7,510	24,300	81,800	254,000	943,000
PeakfqSA model, all available data					
Magnitude	4,410	7,950	14,000	24,100	48,300
Lower limit	3,000	5,110	8,350	13,200	23,400
Upper limit	6,330	12,300	24,600	50,300	133,000
Interval	3,330	7,220	16,200	37,100	110,000
% reduction	66.7	79.0	83.8	87.1	90.5
PeakfqSA model, all data with top fitting					
Magnitude	4,670	8,350	14,400	24,300	46,900
Lower limit	2,880	5,200	8,740	13,800	23,500
Upper limit	6,810	12,700	25,000	54,200	169,000
Interval	3,930	7,500	16,300	40,400	146,000
FLDFRQ3 model, gaged records only					
Magnitude	3,270	5,850	10,300	17,900	36,400
Lower limit	1,830	2,830	4,250	6,240	10,200
Upper limit	8,010	18,400	41,800	93,800	272,000
Interval	6,180	15,600	37,600	87,600	262,000
FLDFRQ3 model, gaged records and historical data					
Magnitude	3,620	6,570	11,700	20,600	42,200
Lower limit	2,220	3,590	5,610	8,550	14,600
Upper limit	6,930	15,000	32,400	69,000	187,000
Interval	4,710	11,400	26,800	60,400	172,000
FLDFRQ3 model, all available data					
Magnitude	3,580	6,580	12,000	21,600	46,700
Lower limit	2,580	4,490	7,640	12,800	24,500
Upper limit	5,020	9,860	19,500	38,900	97,000
Interval	2,440	5,370	11,900	26,100	72,500
% reduction	60.5	65.6	68.4	70.2	72.3

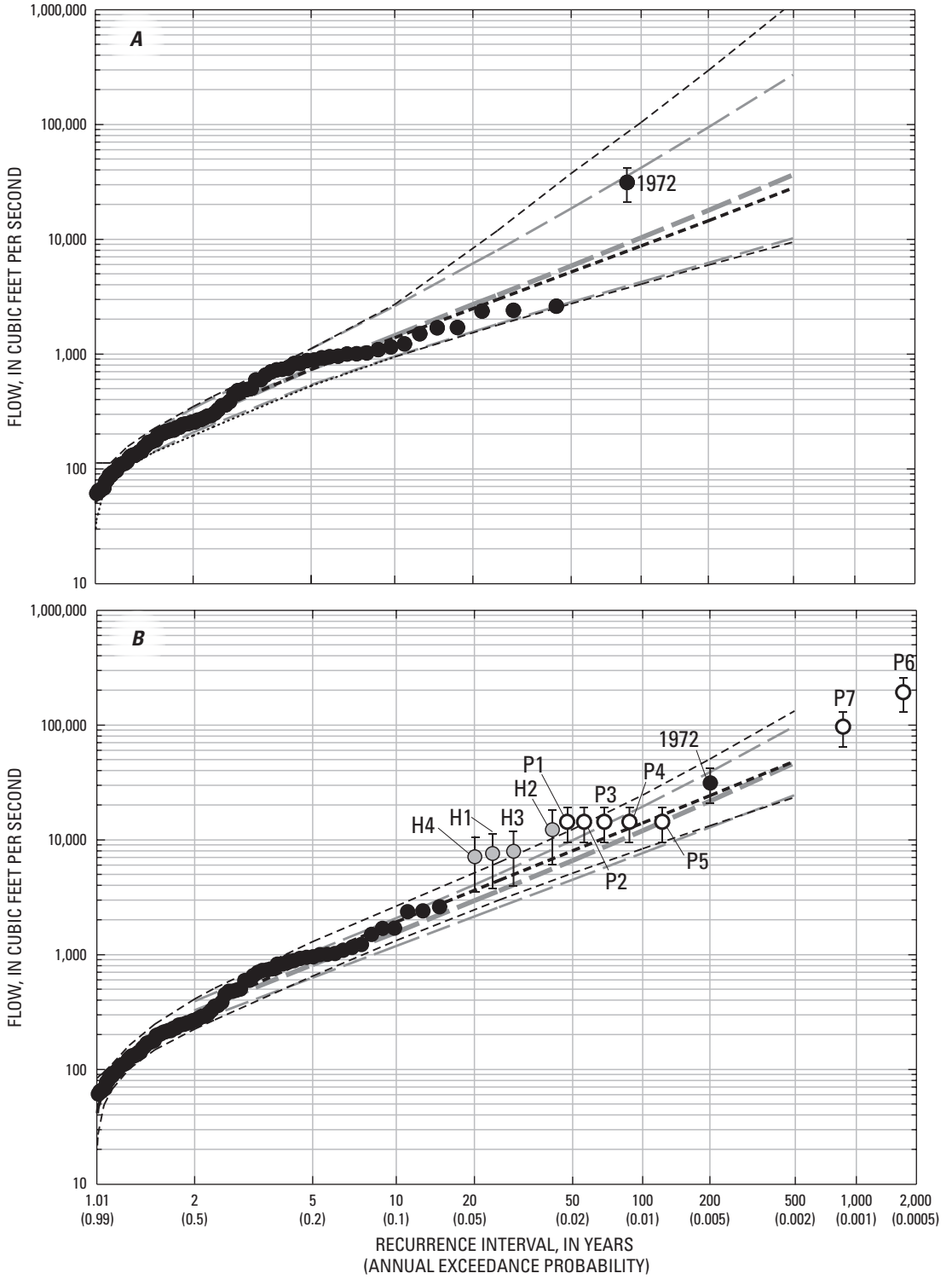

EXPLANATION

- Flood-frequency analyses using PeakfqSA model
- 95-percent confidence limits from PeakfqSA model
- Estimated 95-percent confidence limits from PeakfqSA model
- Flood-frequency analyses using FLDFRQ3 model
- 95-percent confidence limits from FLDFRQ3 model
- Gaged value
- Large gaged value with uncertainty range
- Historical value with uncertainty range
- Paleoflood value with uncertainty range

Note: All data plotted using Weibull (1939) plotting positions

Figure 26. Flood-frequency analyses for lower Rapid Creek reach for *A*, gaged records only, and *B*, all available data that incorporate the long-term flood chronology from figure 25.

Upper Rapid Creek

The upper reach of Rapid Creek is completely within the Precambrian-age metamorphic rock units and includes no major tributaries (fig. 1, table 1). Suitable sites where slackwater deposits can be preserved are uncommon in this reach because of the general absence of caves and alcoves in the schistose bedrock. Thus, the reach is defined by the only two sites where well-preserved paleoflood evidence was found: (1) two adjacent alcoves (Schist and Blue Ribbon Alcoves) about 1 mi downstream from the confluence of Castle and Rapid Creeks and (2) a site 2 mi farther downstream at streamgage 06410500 (Gage House Alcove). In this reach, the valley bottom ranges from about 100 to 300 ft wide and is bounded by steep, bedrock hillslopes. Thus, similar to the other study reaches that are situated within sedimentary canyons, large flows are well constrained to main channel proximities and large flood stages are sensitive to flow magnitude. The channel substrate consists of cobble-gravel, sand, and locally bedrock. This reach of Rapid Creek is primarily under U.S. Forest Service ownership and is largely undeveloped. The valley bottom is vegetated with grass, shrubs, ponderosa pine, and various deciduous trees. The 1972 peak flow was only 252 ft^3/s in this reach (fig. 27, table 2). The largest flow in the 80 years of non-contiguous (1915–2009) gaged records was 2,460 ft^3/s in 1952, but this flow did not leave substantial geomorphic evidence.

Hydraulic Analysis and Paleoflood Chronology

Application of the Manning equation provided flow estimates for paleoflood deposits preserved at both sites along upper Rapid Creek. The cross section for the downstream site (Gage House Alcove) was sufficiently close to streamgage 06410500 so that resulting flow estimates could be compared with the rating curve for the streamgage. A peak flow of 1,640 ft^3/s was recorded (from the rating curve) on July 7, 2008, at the streamgage. This flow has been exceeded during the period of gaged record only by flows of 2,460 and 2,060 ft^3/s in 1952 and 1965, respectively (fig. 27; table 2). The rating curve for this site was substantiated by a current meter measurement made on July 8, 2008.

A channel cross section (fig. 28) was surveyed on August 11, 2008, and a high-water mark from the July 7, 2008, peak flow was used as a point of reference for the hydraulic analysis. The flow derived from a trial critical-depth computation was 2,990 ft^3/s, largely exceeding the rated flow of 1,640 ft^3/s. Application of the Manning equation for the reach slope of 0.005 ft/ft and a Manning's *n* value of 0.04 yielded a computed flow of 1,670 ft^3/s, which is close to the value of 1,640 ft^3/s recorded for the streamgage. Two pits were excavated at the Gage House site (pits A and B), and associated flows of 5,620 and 1,050 ft^3/s for the highest flood deposits, respectively, were computed using the aforementioned application of the Manning equation (table 8).

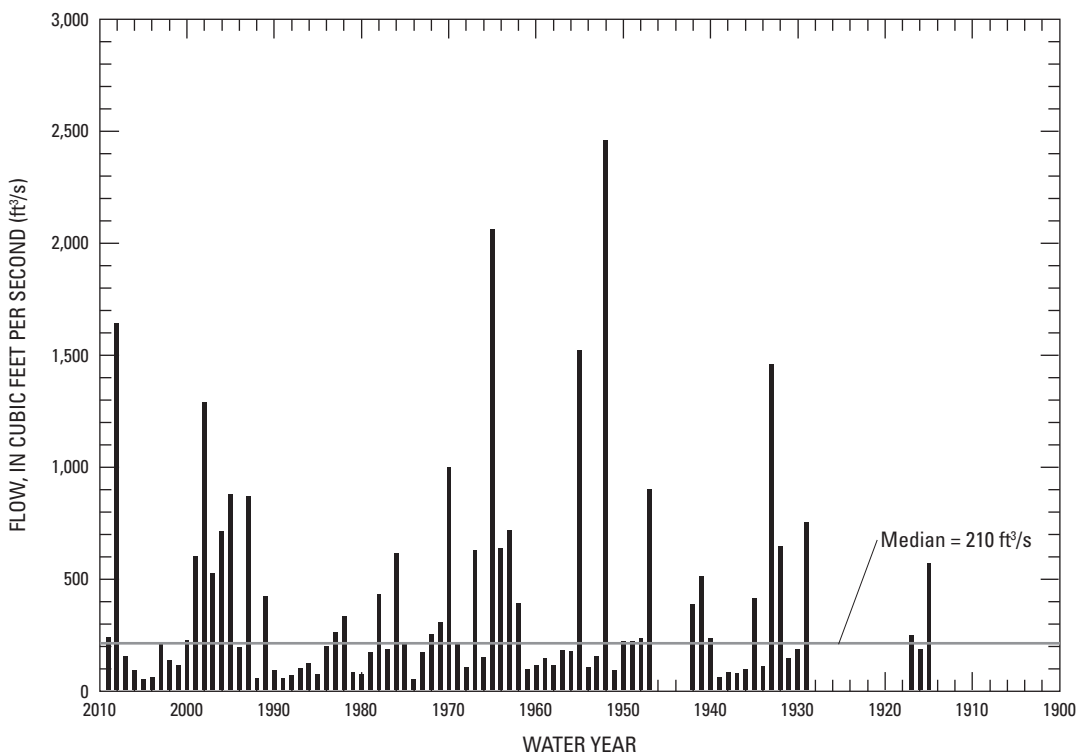

Figure 27. Modern peak-flow chronology (gaged records) for upper Rapid Creek reach. Values are from table 2.

A channel cross section (fig. 29) also was surveyed on August 11, 2008, at the location of the Schist and Blue Ribbon Alcoves at the upstream end of the upper Rapid Creek reach (fig. 1). Similar to the Gage House Alcove, flow estimates were made using the Manning equation (table 8). In this case, a flow value of 1,850 ft^3/s was computed for the 2008 peak flow, which was slightly larger than the 1,670 ft^3/s recorded farther downstream at streamgage 06410500. This is a reasonable difference, however, because the primary storm cell was located upstream (Driscoll and others, 2010) and the peak flow probably attenuated in the 2 mi between measurement locations. Flow values for elevations of slack-water deposits also are shown in table 8.

The benchmark site for the upper Rapid Creek reach consists of the Schist and Blue Ribbon Alcoves (fig. 30). The Schist Alcove is the higher of the two alcoves and provided stratigraphic evidence of two floods. The most recent flood unit (I) was dated to A.D. 895–1021 and required a flow exceeding 12,900 ft^3/s for inundation (table 8). The older flood unit (II) did not contain sufficient datable organic material, and an OSL sample could not be obtained because the flood unit was too thin and contained abundant metamorphic clasts not suitable for OSL analysis. It is likely that the older flood occurred between 100 and 1,000 years before the younger flood at Schist Alcove based on its associated flow rate and the thickness of the colluvium between the two flood deposits. For the purpose of incorporating the most complete paleoflood record at this site, it was assumed that the older flood was about 500 years before the younger flood and had a flow rate of 12,000 ft^3/s. The lower alcove, Blue Ribbon, provided evidence of one flood that was dated to A.D. 1185–1278, which required a flow of about 2,100 ft^3/s for inundation.

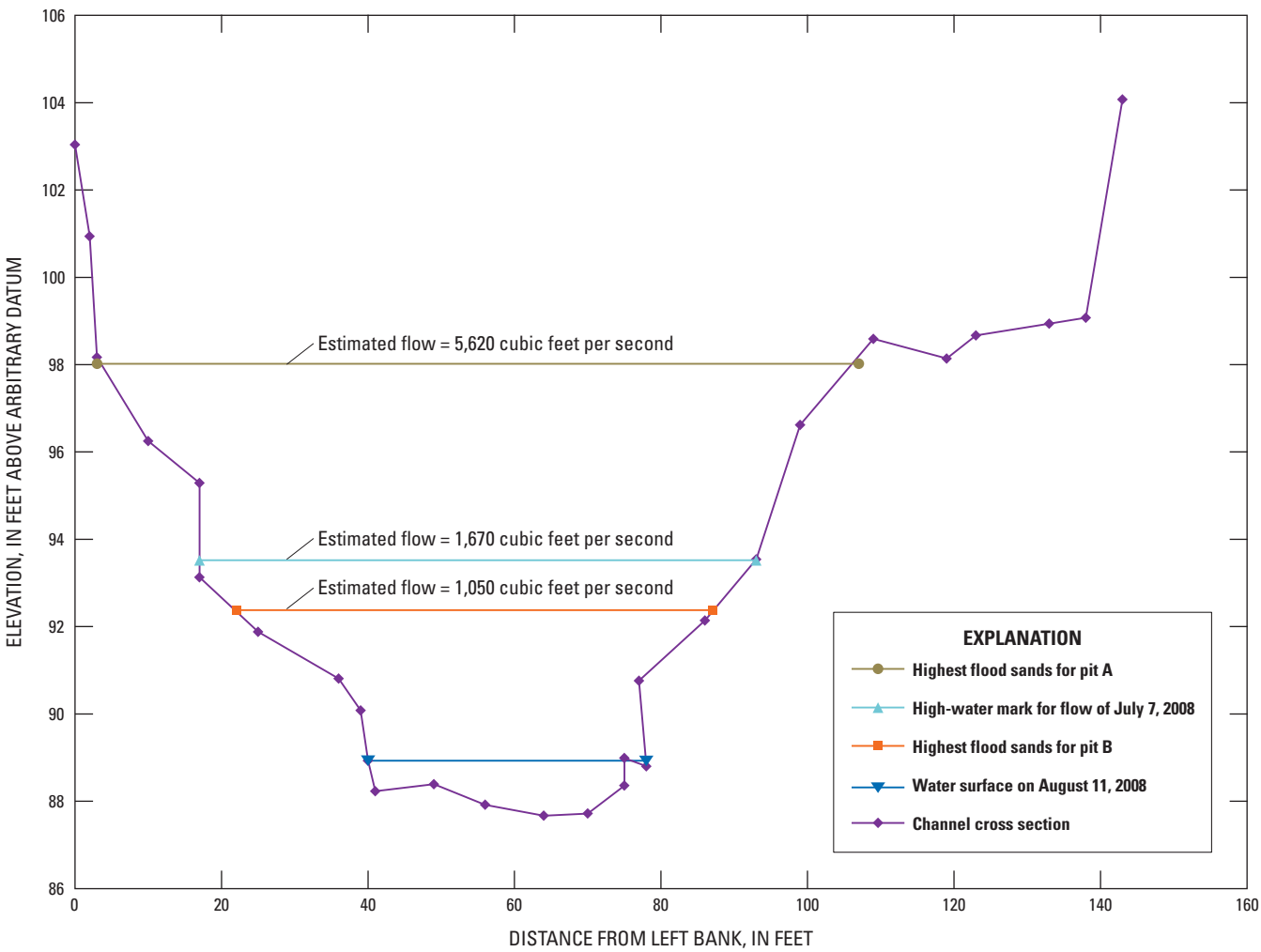

Figure 28. Channel cross section and relevant elevations for Gage House Alcove, upper Rapid Creek reach. Cross section is view looking downstream.

Two pits were excavated at the Gage House Alcove (fig. 31) at the downstream end of the reach. The upper pit (A) contained stratigraphic evidence of at least two floods. The most recent flood unit (I) required a minimum flow of 5,620 ft^3/s for inundation and had a maximum age of A.D. 722–950 based on the age of the underlying local slope-wash. Because this flood unit likely correlates with the most recent flood unit (I) at the Schist Alcove, it was not included as an additional flood in the flood-frequency analysis. The second (and oldest) flood unit (II) in pit A likely had evidence of more than one flood because of its thickness; however, unit contacts were not distinguishable. Radiocarbon dating for this unit returned a modern date, indicating contamination from younger carbon, probably from root penetration. Pit B contained evidence of at least four floods, with a flow of at least 1,050 ft^3/s required for inundation of the uppermost flood unit (unit I; table 8). This stratigraphic record essentially overlaps with the gaged records for the site, which contain six peak-flow values of 1,290 ft^3/s or larger since 1915 (table 2).

In summary, stratigraphic evidence for two paleofloods (P2 and P3) of about 12,000–13,000 ft^3/s about 1,000 and 1,500 (estimated) years ago constitute most of the paleoflood chronology for upper Rapid Creek (fig. 32, table 9). Both paleofloods are substantially larger than the largest flow in the gaged records of about 2,460 ft^3/s in 1952 (fig. 27). Only one additional paleoflood (P1), about 800 years ago and similar in magnitude to the 1952 flow rate, could be confidently identified for inclusion in the paleoflood chronology. Compared to lower Rapid Creek and all of the other study reaches, the largest floods along upper Rapid Creek are substantially smaller.

Flood-Frequency Analysis

No historical flood accounts are available for upper Rapid Creek; thus, the long-term flood chronology (fig. 32, table 9) considered for the flood-frequency analyses includes only gaged records (fig. 27) and three paleofloods. Uncertainties of ±20 percent are assigned for the gaged records (table 2) because of minor regulatory effects of Deerfield Dam upstream (described in “Supplement 2. Modern Peak-Flow Chronologies”). The largest flow in the gaged record (1952) was used as a perception threshold since 1914 (PT1). An additional perception threshold (PT2) was based on the older of the two paleofloods recorded in the Schist Alcove. For the top-fitting analysis, only the 40 values greater than the median value of 210 ft^3/s in the gaged peak-flow records were included.

Results of flood-frequency analyses for several scenarios are summarized in table 10 with results from analyses of the gaged records only and the analyses of all available data shown in figure 33. Because of the sparse evidence for large paleofloods, the 100-, 200-, and 500-year quantile estimates resulting from incorporation of paleoflood data into the PeakfqSA model are less than 10 percent larger than the quantile estimates for the analysis of the gaged records only. Because the paleoflood record spans at least 1,000 years, the corresponding 95-percent confidence intervals for the paleoflood analysis using the PeakfqSA model are much smaller than those from the analysis of the gaged records only, with reductions of 78 percent or more for recurrence periods of 100 years and larger (table 10).

Table 8. Summary of Manning equation computations for selected locations along upper Rapid Creek reach.

[--, not computed]

Computational unit	Relative elevation (feet)	Manning's *n* value	Slope (feet per foot)	Area (square feet)	Wetted perimeter (feet)	Hydraulic radius (feet)	Flow rate (cubic feet per second)
Summary of computations for Gage House Alcove							
Uppermost deposits (unit I) at pit A	98.02	0.04	0.005	653	110.5	5.91	5,620
High-water mark for July 7, 2008, peak flow	93.52	.04	.005	275	78.5	3.50	1,670
Uppermost deposits (unit I) at pit B	92.38	.04	.005	196	68.0	2.88	1,050
Summary of computations for Schist and Blue Ribbon Alcoves							
Uppermost deposits (unit I) at Schist Alcove	103.24	0.04	0.005	1,300	178.6	7.28	12,900
Penultimate deposits (unit II) at Schist Alcove	103.00	--	--	--	--	--	[1]12,000
Uppermost deposits (unit I) at Blue Ribbon Alcove	97.55	.04	.005	398	139	2.86	2,110
High-water mark for July 7, 2008, peak flow	97.32	.04	.005	367	138.5	2.65	1,850

[1]Estimated on basis of computed flow for uppermost deposits.

Implications of Paleoflood Chronologies for Rapid Creek

The paleoflood chronologies for lower and upper Rapid Creek are distinctively different, with an especially rich history of very large floods for lower Rapid Creek and a much sparser record with much smaller flows for upper Rapid Creek. The distinctive differences in chronologies and resulting flood-frequency analyses raise questions regarding (1) regional peak-flow characteristics relative to climate, geology, and physiography; and (2) the more pragmatic issue of how to apply results of flood-frequency analyses downstream from Pactola Dam.

Some of the differences in chronologies may owe to less than optimum conditions along upper Rapid Creek for accumulation and preservation of slack-water sediments (few alcoves and caves flank this reach), thereby resulting in incomplete records. More plausible, however, is that the physiography and climate of the upper part of Rapid Creek result in small peak flows, relative to downstream reaches. As postulated by Sando and others (2008), with reinforcement and refinement by Driscoll and others (2010), the Limestone Plateau area (fig. 1) and other parts of the upper Rapid Creek reach probably produce relatively small peak flows because of substantial infiltration into the limestone, relatively gentle topography, extensive floodplain storage, and reduced potential for exceptionally heavy rain-producing thunderstorms, relative to downstream reaches. Additional perspectives regarding application of flood-frequency results for both reaches of Rapid Creek are provided in a subsequent section "Central Black Hills Flood Frequency: Synopsis, Implications, and Application."

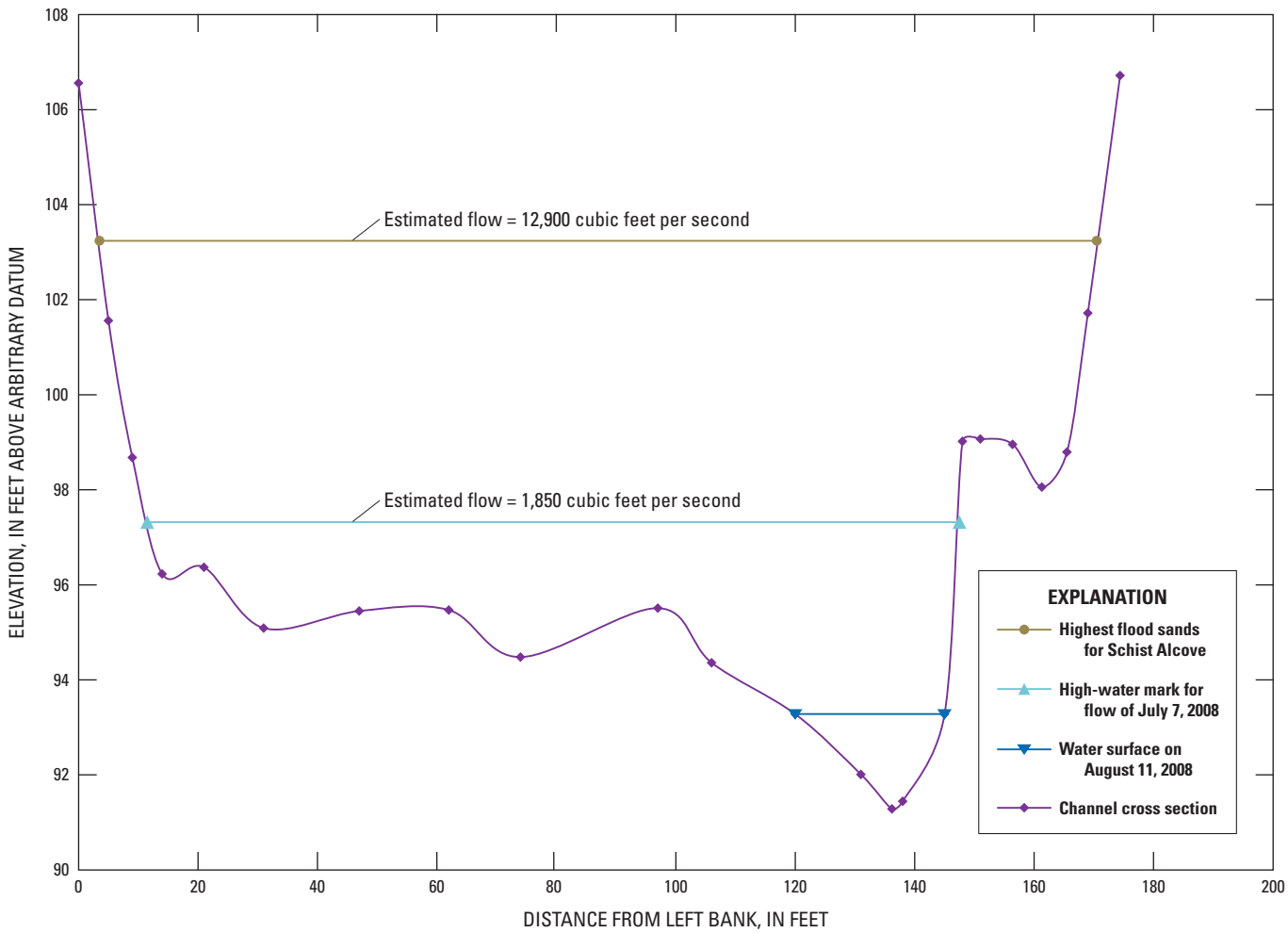

Figure 29. Channel cross section and relevant elevations for Schist and Blue Ribbon Alcoves, upper Rapid Creek reach. Cross section is view looking downstream.

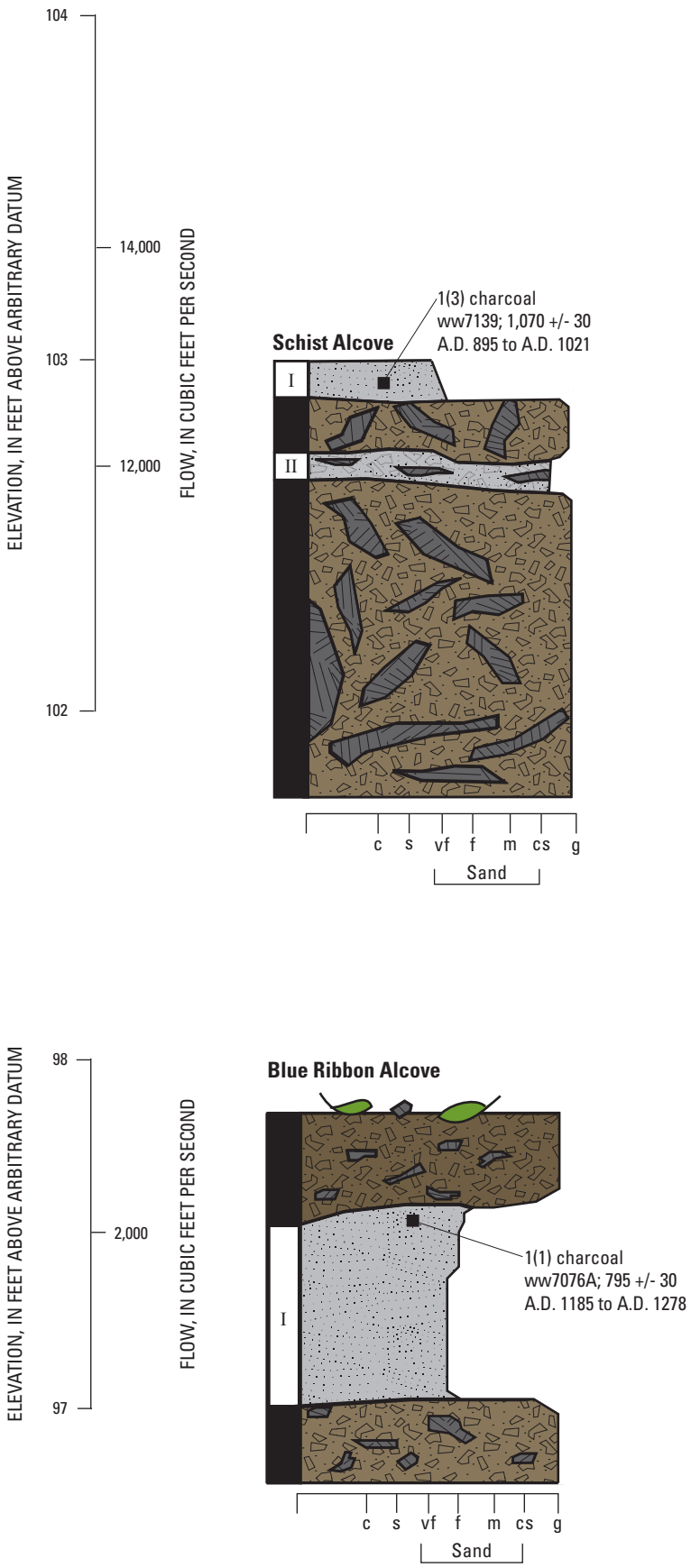

Bedded flood deposits intermixed with metamorphic clasts

EXPLANATION

- **Rockfall and local slopewash**
- **Rapid Creek flood deposit**
- **Large angular (schist) rockfall clast**
- I **Flood unit**
- **Leaf/modern organics**
- 1(3) charcoal ww7139; 1,070 +/- 30 A.D. 895 to A.D. 1021 — **Radiocarbon sample with sample information and analytical results from table S1–1**

For each grain-size scale (x-axis):

c = clay
s = silt
vf = very fine sand
f = fine sand
m = medium sand
cs = coarse sand
g = gravel

Flood deposit in Blue Ribbon Alcove

Figure 30. Schematic diagram showing paleoflood information for Schist and Blue Ribbon Alcoves, upper Rapid Creek reach.

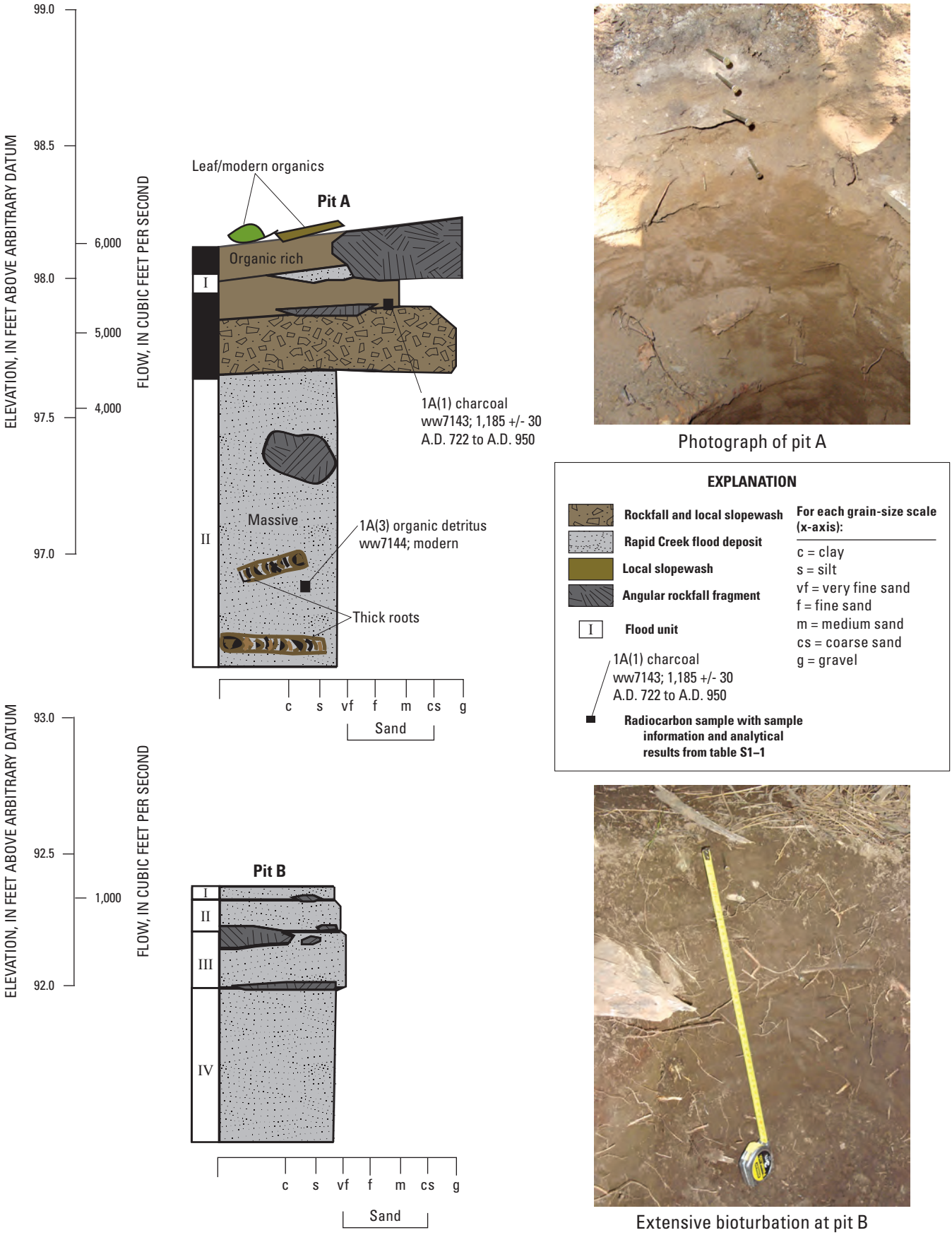

Figure 31. Schematic diagram showing paleoflood information for Gage House Alcove, upper Rapid Creek reach.

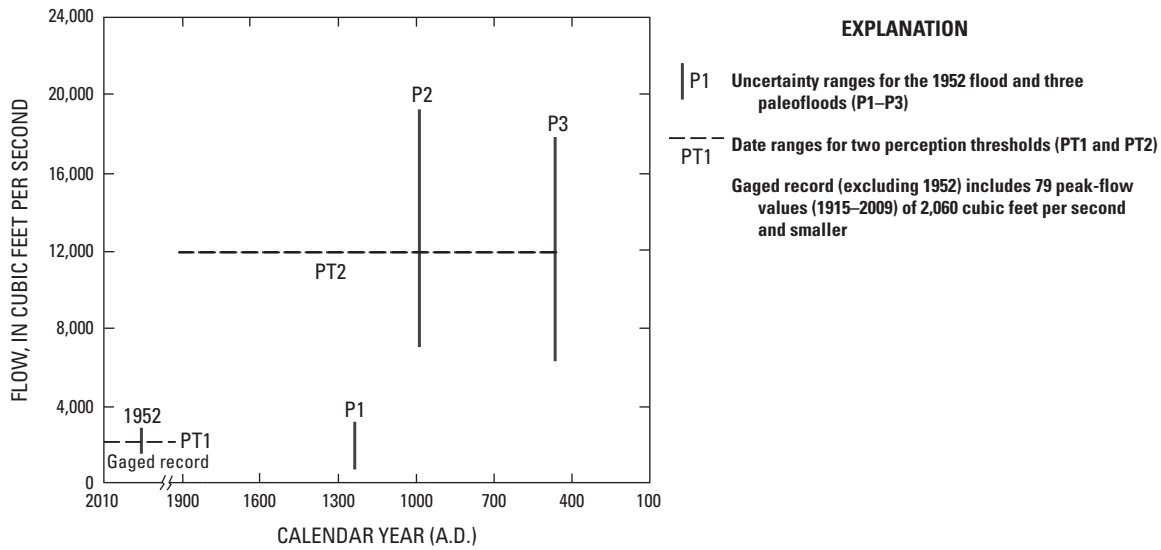

Figure 32. Long-term flood chronology for upper Rapid Creek reach (from table 9).

Table 9. Summary of long-term flood chronology used in flood-frequency analysis for upper Rapid Creek reach.

[ID, identification; min, minimum; max, maximum; PT, perception threshold; --, not applicable]

ID for figure 32	Data description	Range of flow values, in cubic feet per second, for flood-frequency analysis			Flood or perception threshold dates, in calendar years A.D.			
		Min	Max	Most likely	Flood date	PT min	PT max	PT date
			Perception thresholds					
PT1	1952 flood	--	--	2,460	--	2009	1914	1920
PT2	Schist Alcove unit II	--	--	12,000	--	1913	450	1300
			Paleoflood chronology					
P1	Blue Ribbon Alcove	1,060	3,160	2,110	1232	--	--	--
P2	Schist Alcove unit I	6,450	19,400	12,900	958	--	--	--
P3	Schist Alcove unit II	6,000	18,000	12,000	458	--	--	--
			Gaged record					
1952	1952	1,650	3,270	2,460	--	--	--	--
Gaged record	1915–17, 1929–42, 1947–2009 (excluding 1952). Uncertainty for flow values is plus or minus 20 percent (not shown). (Top-fitting analysis excludes values less than 210 cubic feet per second)	53	2,060	--	--	--	--	--

Table 10. Flood-frequency analyses for upper Rapid Creek reach.

[% reduction, percent reduction in confidence interval for analysis with all available data, relative to analysis for gaged records only]

Peak-flow magnitudes and 95-percent confidence limits and intervals, in cubic feet per second, for associated recurrence interval (annual exceedance probability)					
Data description	**25 years (0.04)**	**50 years (0.02)**	**100 years (0.01)**	**200 years (0.005)**	**500 years (0.002)**
PeakfqSA model, gaged records only					
Magnitude	1,500	2,200	3,160	4,450	6,850
Lower limit	1,010	1,380	1,830	2,370	3,230
Upper limit	3,420	7,090	15,000	30,400	70,500
Interval	2,410	5,710	13,200	28,000	67,300
PeakfqSA model, all available data					
Magnitude	1,590	2,350	3,390	4,770	7,340
Lower limit	1,130	1,550	2,080	2,720	3,790
Upper limit	2,160	3,280	4,950	7,450	12,800
Interval	1,030	1,730	2,870	4,730	9,000
% reduction	57.3	69.7	78.3	83.1	86.6
PeakfqSA model, all data with top fitting					
Magnitude	1,810	2,630	3,670	4,990	7,220
Lower limit	1,130	1,650	2,240	2,850	3,820
Upper limit	2,610	3,790	5,300	7,390	12,200
Interval	1,480	2,140	3,060	4,540	8,400
FLDFRQ3 model, gaged records only					
Magnitude	1,830	3,030	4,930	7,910	14,500
Lower limit	1,080	1,550	2,160	2,940	4,290
Upper limit	4,280	8,950	18,700	38,400	99,400
Interval	3,200	7,400	16,500	35,500	95,100
FLDFRQ3 model, all available data					
Magnitude	1,570	2,450	3,740	5,660	9,590
Lower limit	1,130	1,670	2,380	3,320	4,990
Upper limit	1,100	2,100	3,960	7,300	62,900
Interval	1,100	2,100	3,960	7,300	15,900
% reduction	65.6	71.6	76.0	79.4	83.3

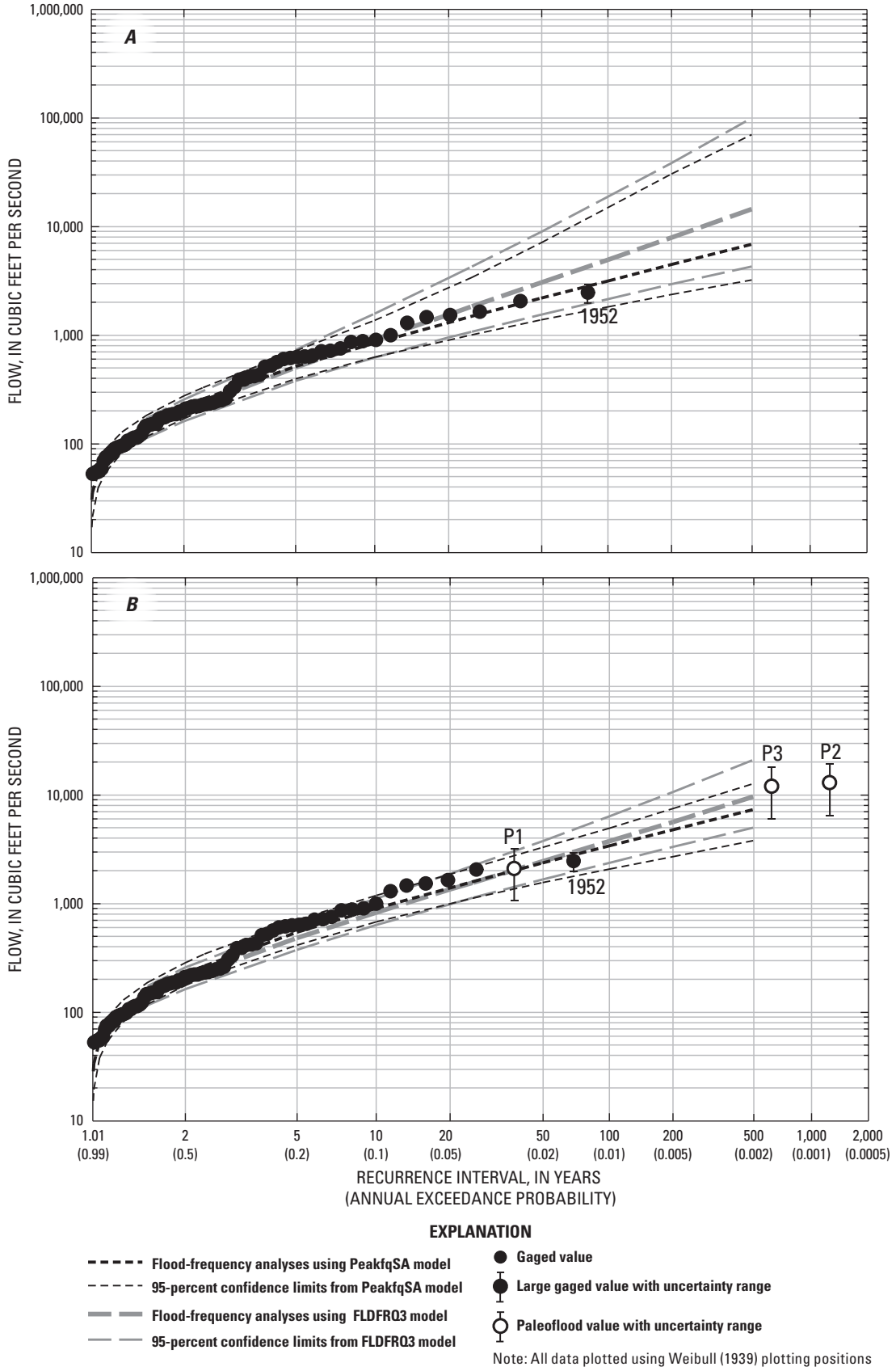

Figure 33. Flood-frequency analyses for upper Rapid Creek reach for *A*, gaged records only, and *B*, all available data that incorporate the long-term flood chronology from figure 32.

Boxelder Creek

The Boxelder Creek study reach (figs. 1 and 34) encompasses two distinct subreaches separated by Bogus Jim Creek and an un-named tributary about 0.2 mi farther downstream. The two tributaries comprise most of the 14 mi^2 of intervening drainage area between the upstream and downstream extents of the study reach (table 1) and can substantially affect peak-flow conditions and characteristics within the reach. The upstream subreach is primarily within the locally conglomeratic Deadwood Formation. The downstream subreach is primarily within the Madison Limestone.

The upstream subreach is in a low canyon about 100–500 ft wide flanked by near-vertical bedrock walls locally separated by gentler colluvial slopes. The bedrock outcrops are about 30–200 ft high. The channel in this reach generally consists of bedrock locally covered by gravels, cobbles, and boulders as large as about 10 ft in diameter. The narrow valley bottom is vegetated with grass, shrubs, and riparian trees, primarily ponderosa pine. Land ownership is a mix of U.S. Forest Service and private land, with only several houses present within this subreach. A highway parallels the channel, primarily on the left bank.

The 1972 flood had an estimated peak flow of 30,800 ft^3/s (fig. 35, table 2) in the upstream subreach, which was based on the peak flow of 30,100 ft^3/s for streamgage 06422500 (Schwarz and others, 1975; U.S. Geological Survey, 2010e) located 2 mi upstream from the study reach (fig. 1). This is the largest flow in the 49 years of non-contiguous record for this streamgage, and is nearly twice as large the next highest flow of 16,400 ft^3/s recorded in 1907. Remaining evidence of the 1972 flood in the upstream subreach includes flotsam, tree scars, and fine-grained slack-water deposits along the channel margins.

The downstream subreach is about 100–500 ft wide and flanked in most locations by near-vertical walls of Madison Limestone, as much as several hundred feet high (fig. 34). A Holocene-age terrace locally flanks the channel within the downstream part of the reach. The channel substrate consists of cobble-gravel, sand, bedrock, and large boulder bars. This subreach is downstream from the two tributaries that divide the reach and is located primarily within a loss zone where zero-flow conditions are common. The narrow valley bottom is vegetated with grass, shrubs, and riparian trees, primarily ponderosa pine. The reach is largely undeveloped with road access only at the upstream end.

For the downstream subreach, the 1972 peak flow was estimated as 50,500 ft^3/s (fig. 36, table 2), based on a flow estimate for streamgage 06422650 (table S2–4) about 2 mi downstream from the study reach (fig. 1). This flow was much larger than for the upstream subreach because of large inflows from the two intervening tributaries. The 1907 flow estimate (17,700 ft^3/s) was based on a drainage-area adjustment (table S2–4) for upstream streamgage 06422550 and thus is only slightly larger than the flow estimate of 16,400 ft^3/s for the upstream subreach. The 1972 flood locally deposited abundant woody debris, anthropogenic flotsam (metal debris, milled wood), and boulder bars. Tree scars and fine-grained slack-water deposits along the channel margins also persist.

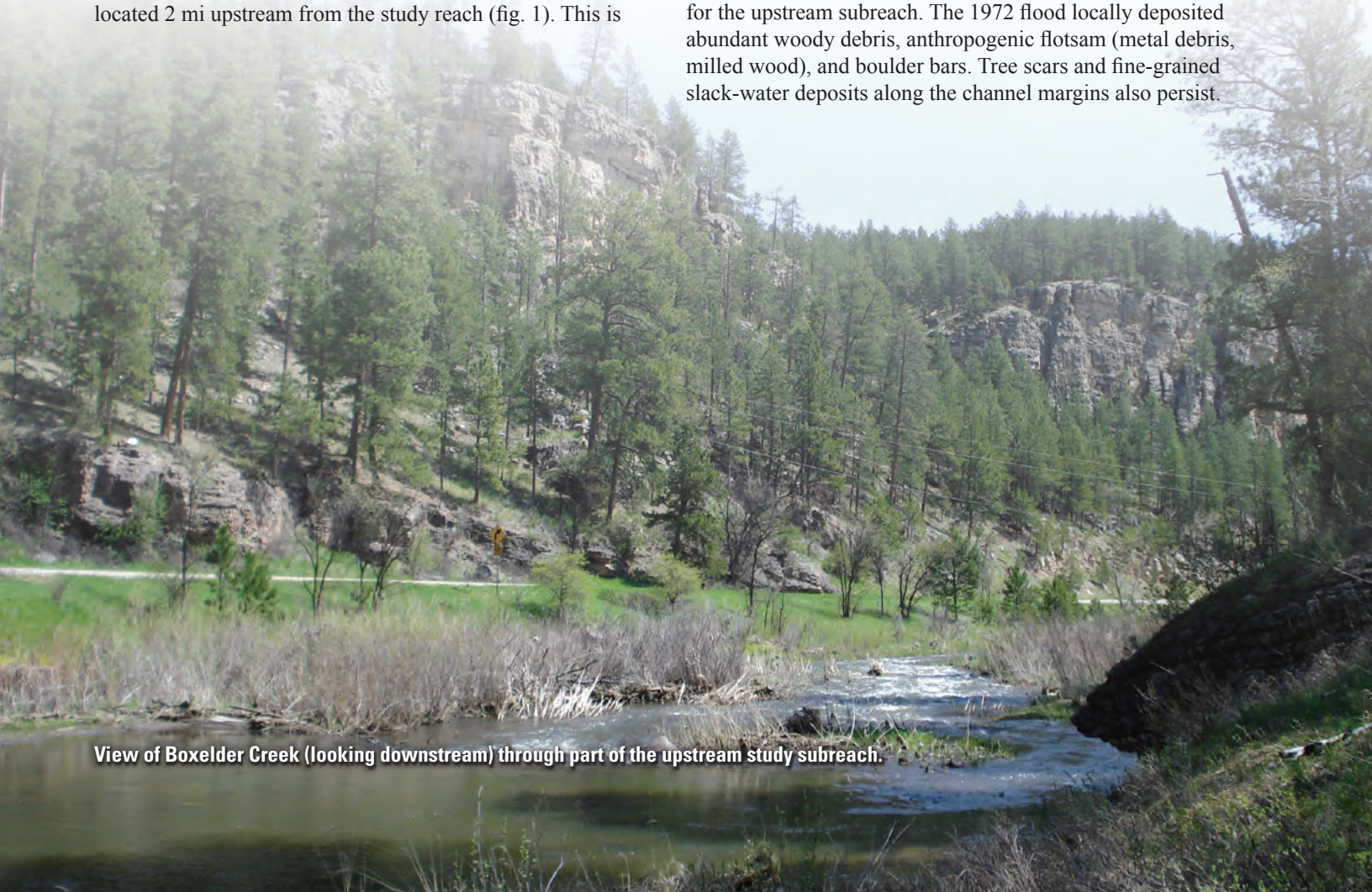

View of Boxelder Creek (looking downstream) through part of the upstream study subreach.

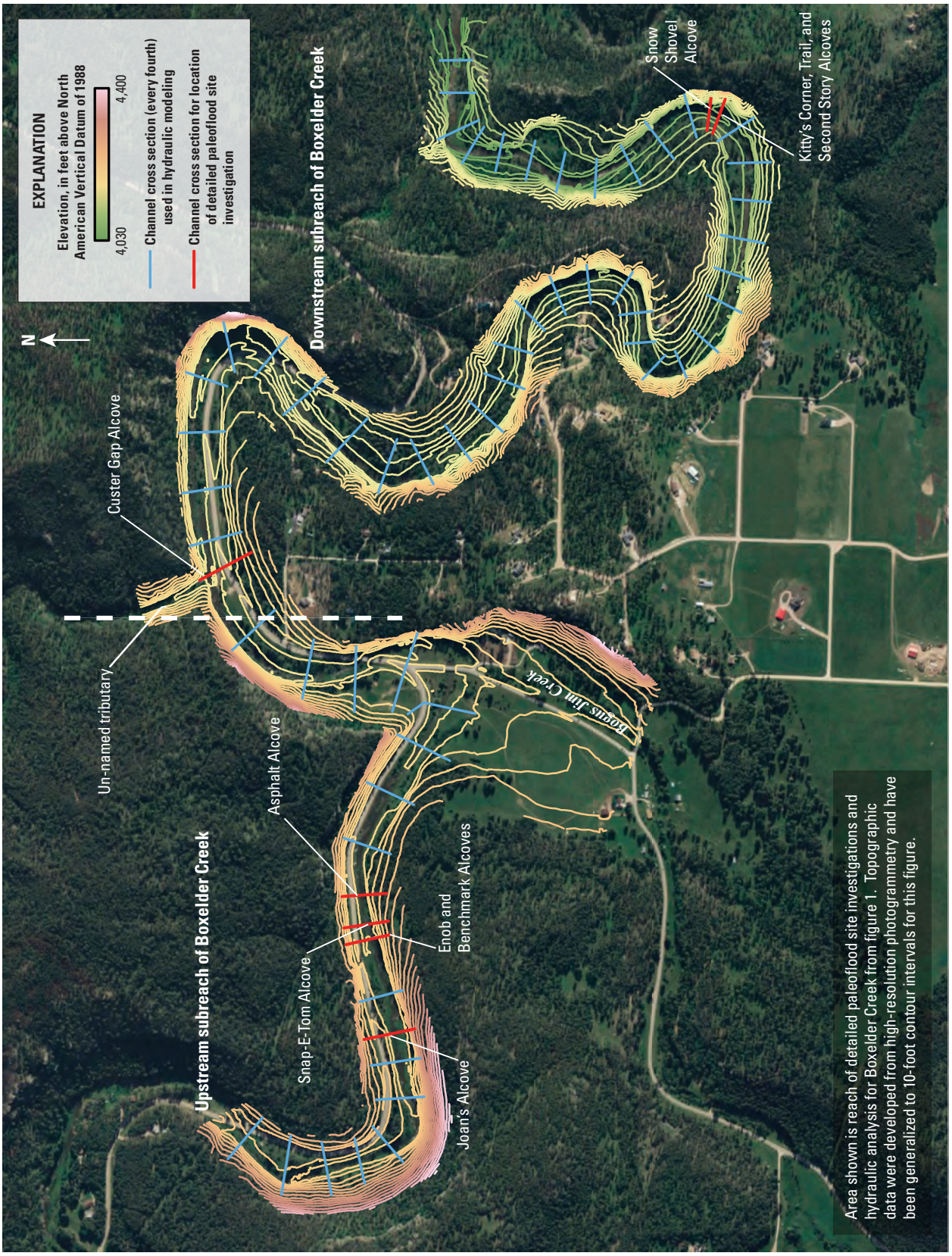

Base modified from Environmental Systems Research Institute (ESRI®) digital data, Lambert Conformal Conic projection North American Datum of 1983 (NAD 83)

Figure 34. Topographic information and selected details of hydraulic analysis for Boxelder Creek reach.

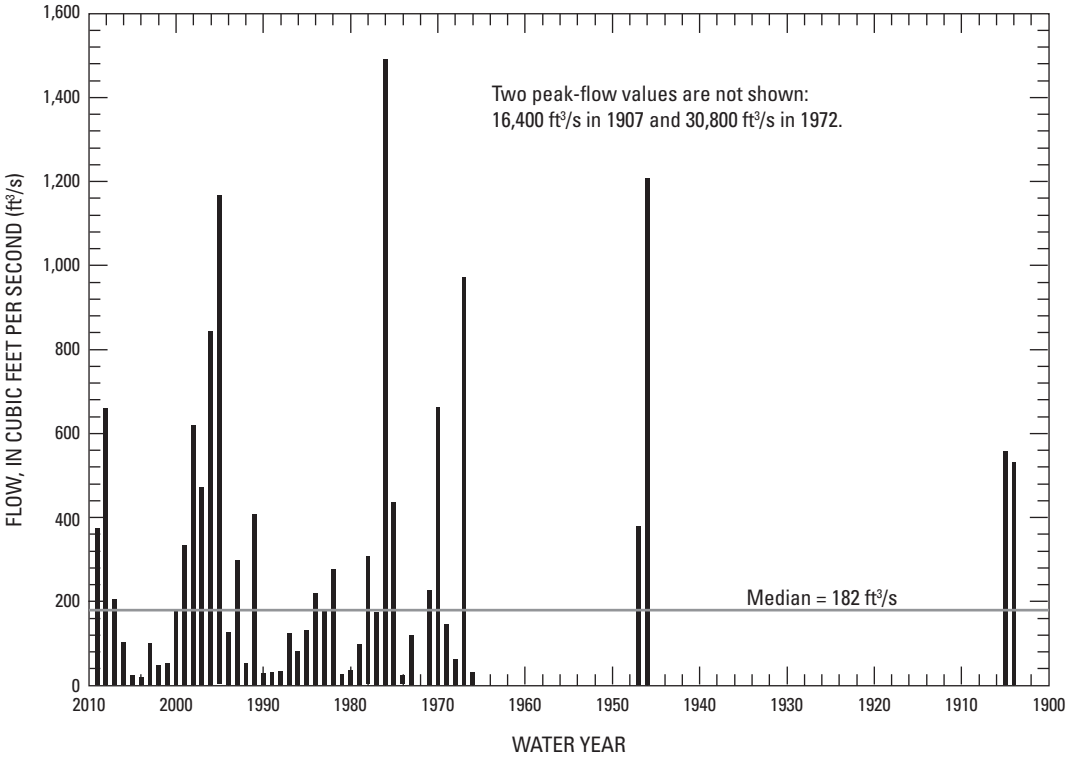

Figure 35. Modern peak-flow chronology (gaged records) for upstream subreach of Boxelder Creek. Values are from table 2.

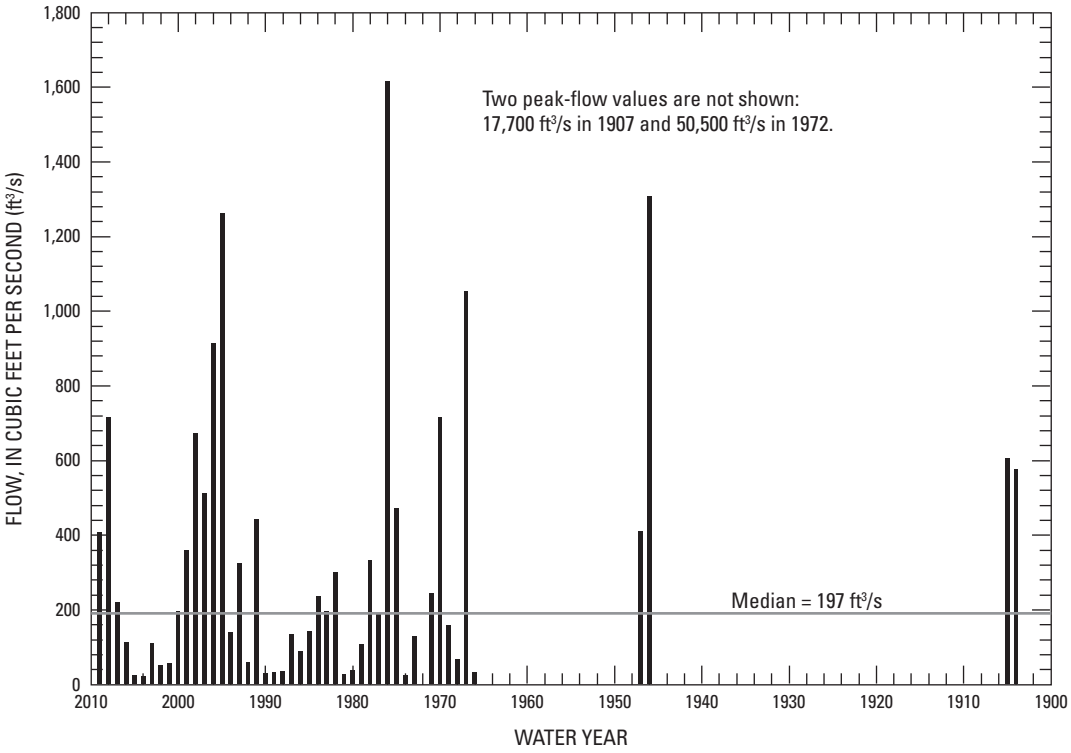

Figure 36. Modern peak-flow chronology (gaged records) for downstream subreach of Boxelder Creek. Values are from table 2.

Hydraulic Analysis and Paleoflood Chronology for Upstream Subreach

Peak-flow magnitudes associated with the elevations of paleoflood deposits were determined by HEC-RAS hydraulic simulations based on a digital (2-ft contour interval) topographic coverage (fig. 34). The hydraulic model was calibrated by using surveyed elevations for 1972 high-water evidence (fig. 37) and by assuming 1972 peak-flow values of about 30,800 and 50,500 ft^3/s for the upstream and downstream subreaches, respectively (table 2). Hydraulic simulations were complicated by valley-bottom grading associated with highway construction within the upstream subreach of Boxelder Creek. For analysis and calibration purposes, the modern (modified) topography was assumed for calibrating the hydraulic model with the 1972 flood conditions, but for simulating the paleofloods, the topographic coverage was adjusted to reflect estimated conditions before road construction and grading.

Stratigraphic investigations were conducted at five sites in the upstream subreach of Boxelder Creek. The most upstream site was Joan's Alcove, where two pits were excavated (fig. 38). The more complete record in pit B provided evidence of four flood units, the oldest of which (unit IV) was dated to between A.D. 972 and 1149 and required at least 11,300 ft^3/s for inundation and emplacement. The next three floods were in the last ~500 years; flood unit III was dated to A.D. 1520–1794, unit II was dated to A.D. 1666–1953, followed by the 1972 flood (unit I). A minimum flow of 14,800 ft^3/s is associated with the 1972 flood deposit for this pit, and the two older deposits in the last several hundred years required slightly smaller flows of 12,800 ft^3/s and 12,000 ft^3/s for inundation. Pit A contained evidence of only two floods, the most recent being the 1972 flood (unit I), and the older flood (unit II) likely correlates to a flood unit in pit B.

The next site downstream, Enob Alcove, is the benchmark site for the upstream subreach. A single pit provided stratigraphic evidence of two large floods within the last several hundred years (fig. 39). The oldest deposit (flood unit II) was dated to A.D. 1515–1798 and required a minimum flow of 39,000 ft^3/s for inundation. The most recent flood unit (I) was dated to A.D. 1668–1891 and required a minimum flow of 40,000 ft^3/s. This dark gray deposit contained abundant charcoal and had a distinctive fine blocky texture, enabling correlation to deposits at other sites in this reach. Flood deposits from the 1972 flood were not present at Enob Alcove, which along with the flow rate required for inundation, indicate that both deposits in Enob Alcove required floods larger than that of 1972. Flood units II and III in pit B of Joan's Alcove plausibly correlate with the two flood units at Enob Alcove. This correlation is bolstered by the presence of the similar high charcoal content and distinct fine blocky texture of flood unit II at Joan's Alcove, indicating correlation with flood unit I at Enob Alcove.

View across Boxelder Creek showing location of four alcoves.

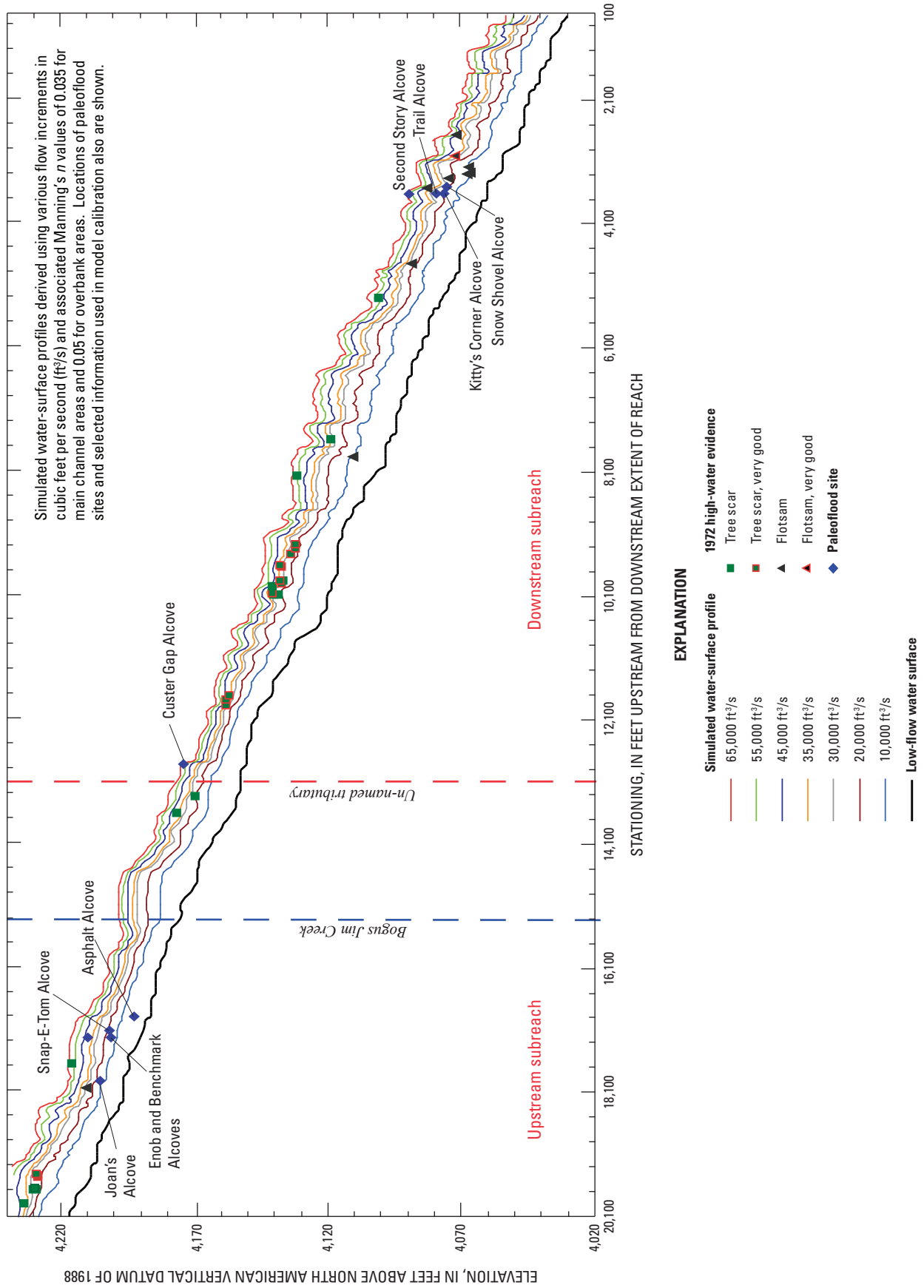

Figure 37. Results of hydraulic model simulations for Boxelder Creek reach.

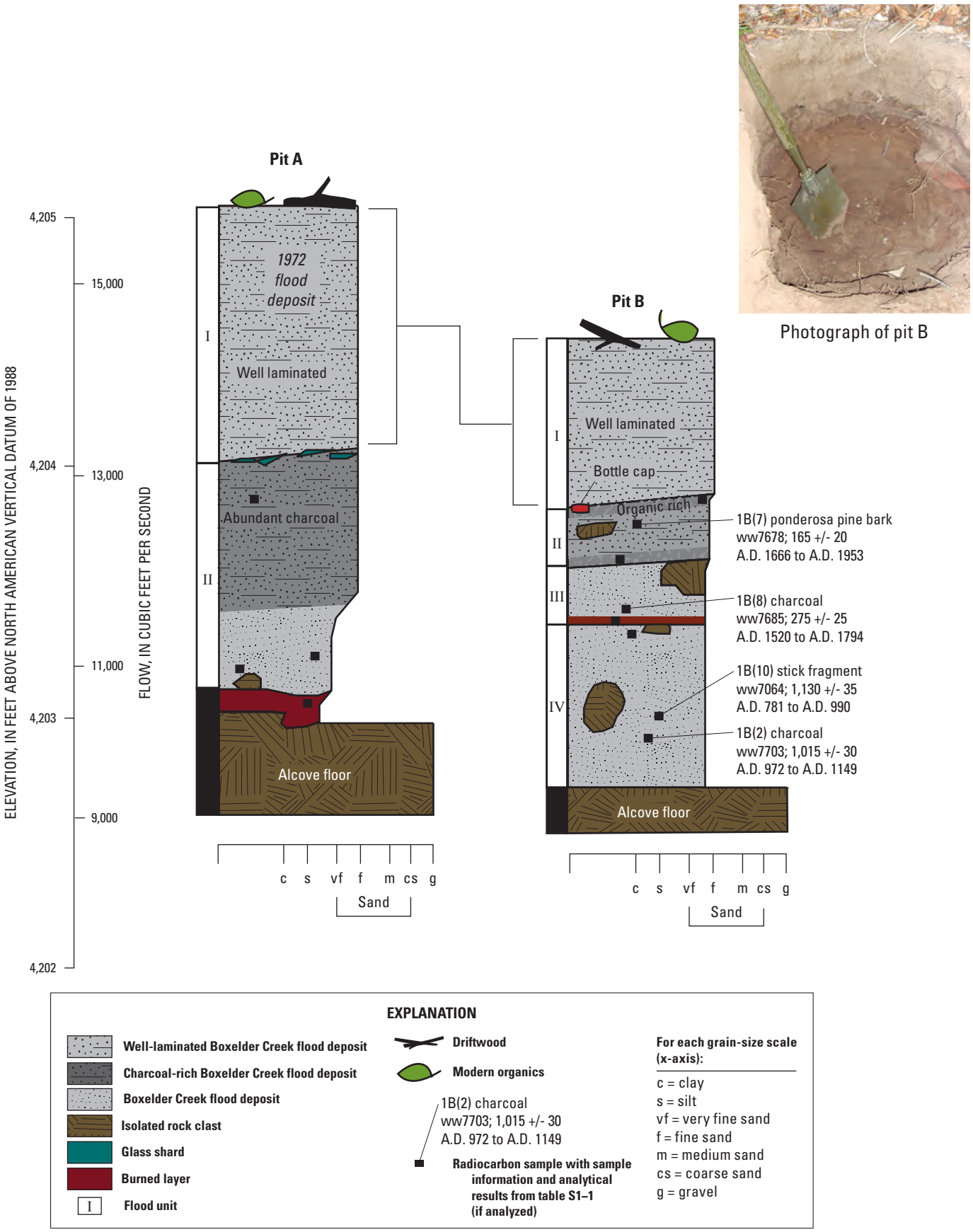

Figure 38. Schematic diagram showing paleoflood information for Joan's Alcove, upstream subreach of Boxelder Creek.

Stratigraphic investigations also were conducted at Benchmark, Snap-E-Tom, and Asphalt Alcoves, all of which are located within a few hundred yards of Enob Alcove. Stratigraphic records from these sites did not provide additional information beyond that recorded in Joan's and Enob Alcoves. Consequently, records derived from these alcoves were not included in the flood-frequency analyses; however, stratigraphy for these alcoves is shown in figures S3–4 through S3–6. All three sites, however, contained multiple flood deposits, including deposits of 1972 and the charcoal-rich deposit with the fine blocky texture found at Enob Alcove (flood unit I; A.D. 1668–1891). The oldest dated flood deposit in this reach (400–231 B.C.) was at Snap-E-Tom Alcove (flood unit IV in fig. S3–5), although it is unlikely that the stratigraphic record for this low alcove (containing evidence for only four floods) is complete back to that date.

In summary, for a period spanning the last ~1,000 years, two paleofloods in the upstream subreach of Boxelder Creek have exceeded the 1972 peak flow of 30,800 ft^3/s (table 2), both within the last ~500 years (fig. 40, table 11). The associated flow estimates for these two paleofloods (P1 and P2) are 39,000–78,000 ft^3/s and 40,000–80,000 ft^3/s. One other paleoflood that was similar to the second largest flow of record (16,400 ft^3/s in 1907) was almost 1,000 years ago (P3) and had an associated flow of 11,300–22,600 ft^3/s.

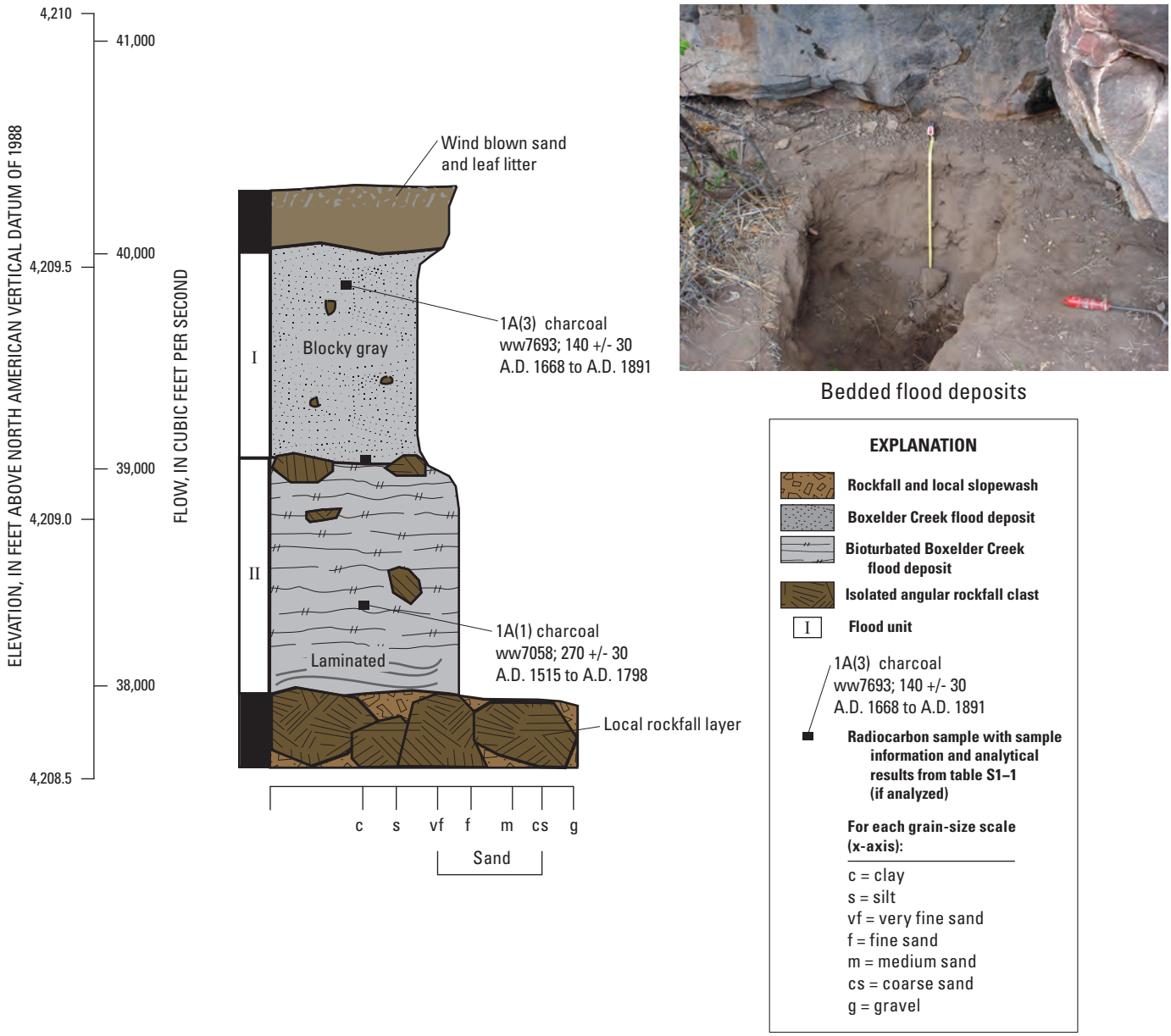

Figure 39. Schematic diagram showing paleoflood information for Enob Alcove, upstream subreach of Boxelder Creek.

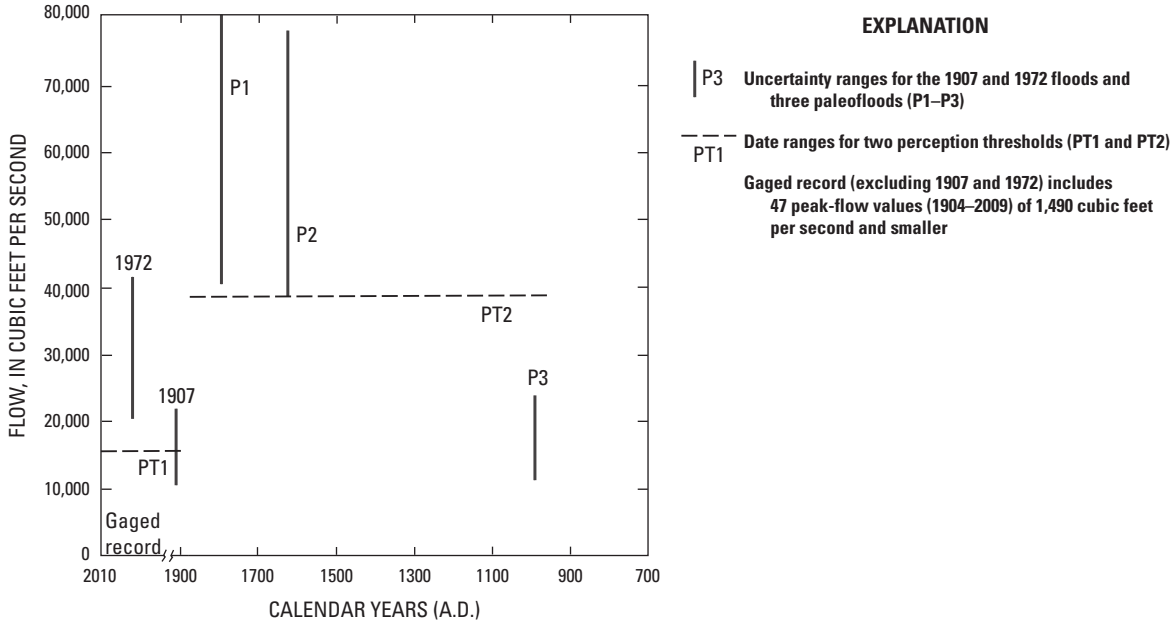

Figure 40. Long-term flood chronology for upstream subreach of Boxelder Creek (from table 11).

Table 11. Summary of long-term flood chronology used in flood-frequency analysis for upstream subreach of Boxelder Creek.

[ID, identification; min, minimum; max, maximum; PT, perception threshold; --, not applicable]

ID for figure 40	Data description	Range of flow values, in cubic feet per second, for flood-frequency analysis			Flood or perception thresholds date, in calendar years A.D.			
		Min	Max	Most likely	Flood date	PT min	PT max	PT date
			Perception thresholds					
PT1	1907 flood	--	--	16,400	--	2009	1884	1907
PT2	Enob Alcove unit II	--	--	39,000	--	1883	972	1610
			Paleoflood chronology					
P1	Enob Alcove unit I	40,000	80,000	60,000	1808	--	--	--
P2	Enob Alcove unit II	39,000	78,000	58,500	1633	--	--	--
P3	Joan's Alcove pit B unit IV	11,300	22,600	17,000	1013	--	--	--
			Gaged records					
1907	1907 flood	11,000	21,800	16,400	--	--	--	--
1972	1972 flood	20,600	41,000	30,800	--	--	--	--
Gaged record	1904–05, 1946–47, 1966–2009 (excluding 1972). Uncertainty for flow values is plus or minus 10 percent (not shown). (Top-fitting analysis excludes values less than 182 cubic feet per second)	19	1,490	--	--	--	--	--

Flood-Frequency Analysis for Upstream Subreach

The flood-frequency analyses of the gaged records only for the upstream subreach of Boxelder Creek included large floods for 1907 and 1972 (fig. 35). Uncertainties of ±33 percent were assigned for the large peak-flow values of 1907 and 1972 and uncertainties of ±10 percent were assigned for the rest of the gaged peak-flow values (table 2). The flood-frequency analyses that considered all available data (fig. 40, table 11) also included the gaged records, with additional consideration of the 1907 flood as a perception threshold since 1884 (PT1) based on accounts from Driscoll and others (2010). Three paleofloods from the last ~1,000 years—two large paleofloods recorded at Enob Alcove (flood units I and II) and the oldest flood unit (IV) from Joan's Alcove—were included in the flood-frequency analyses that incorporated all available data. A second perception threshold (PT2) was based on stratigraphic evidence with the assumption that the second highest flood deposit (unit II) at Enob Alcove and its associated minimum flow of 39,000 ft^3/s have been exceeded only once in the last ~1,000 years. Joan's Alcove provided a stratigraphic record starting about 1,000 years ago and records the same two large floods at Enob Alcove; this lends confidence that if a large flood had occurred in the last 1,000 years, evidence of it would have been recorded at Joan's or Enob Alcoves. For the top-fitting analysis, only the 25 values greater than the median value of 182 ft^3/s in the gaged peak-flow record were included.

Incorporation of all available data into the flood-frequency analyses for the upstream subreach of Boxelder Creek reduced the 100-, 200-, and 500-year quantile estimates by about 50 to 65 percent as determined using the PeakfqSA model, compared to the similar analysis of the gaged record only (table 12, fig. 41). Similar to the other study reaches, incorporation of the paleoflood information greatly reduced the uncertainty in the estimates for recurrence intervals of 100 years and larger, in this case by more than 99 percent.

Hydraulic Analysis and Paleoflood Chronology for Downstream Subreach

Stratigraphic investigations were conducted at five sites in the downstream subreach of Boxelder Creek (fig. 34). The Custer Gap Alcove is located about 100 yards from the main channel of Boxelder Creek in an un-named tributary canyon at the upstream extent of the subreach and provided evidence of three large floods (fig. 42), the most recent (flood unit I) from 1972. Charcoal from the flood unit II was dated to A.D. 686–870. The oldest flood unit (III) at this site was slightly younger (A.D. 720–944). The inconsistency in ages of these two flood units likely can be attributed to incorporation of old charcoal into flood unit II. Minimum flows required for deposition of the three flood units range from 52,500 to 57,500 ft^3/s. Flow estimates for this site may have more uncertainty than for most other paleoflood sites because of backwater effects in the tributary, and complicated mixing hydraulics if the tributary contributed substantial flow during flood events.

About 1 mi downstream from Custer Gap Alcove, stratigraphic investigations were performed at the Trail, Second Story, Kitty's Corner, and Snow Shovel Alcoves. All except the Snow Shovel Alcove are within about 50 ft and thus were associated with the same HEC-RAS cross section (fig. 34). One high flood deposit was found at Second Story Alcove (fig. 43) that required a flow of 61,300 ft^3/s for inundation. A stick fragment at the contact between this unit and the underlying colluvium unit was dated to A.D. 1218–1296. Trail Alcove, located directly below Second Story Alcove provided evidence from three floods, with flows of between 23,300 and 25,000 ft^3/s required for inundation (fig. 44). The most recent flood deposit was the 1972 flood based on the presence of cesium-137 (table S1–3). The second youngest flood unit was dated to A.D. 1288–1396, and the oldest flood unit at this site was dated to A.D. 1039–1208. Although imprecision in age dating precludes direct correlations among the sites that had the largest flows (Custer Gap, Trail, and Second Story Alcoves), the most conservative assumption is that the three flood units at Trail Alcove (including the 1972 flow) correspond with the three floods recorded at Custer Gap Alcove. Thus, the middle flood unit at Trail Alcove (A.D. 1288–1396) was assumed to be deposited by the same large flood that deposited the sediment in Second Story Alcove (A.D. 1218–1296), as well as flood unit II at Custer Gap Alcove, for which the associated age is considered unreliable.

Three pits were excavated at Kitty's Corner Alcove (fig. 45), the benchmark site for the downstream subreach, located below Trail and Second Story Alcoves. Kitty's Corner Alcove is a small cave in the Madison Limestone that narrows from about 10 ft in diameter at the mouth to about 3 ft in diameter nearly 100 ft beyond the mouth. Pit A was located near the mouth of the cave, pit B was located about 5 ft farther back along the cave wall, and pit C was located near the back of the cave. Pits A and B provided evidence of 4 and 5 floods, respectively, whereas pit C provided evidence of 10 floods. It is interpreted from stratigraphic correlations and age dating that the flood units in pits A and B also are represented in pit C. Thus, the analysis focused on the stratigraphic record contained in pit C, and schematic diagrams were not constructed for pits A and B.

Pit C of Kitty's Corner Alcove (fig. 45) contained 10 flood units deposited during the last ~2,000 years, including 7 floods within about the last ~1,000 years. The uppermost flood unit (I) probably is from 1972, based on the associated flow (17,000 ft^3/s) and the presence of cesium-137 in three samples from unit I of pit C (table S1–3). Because the floods recorded at Custer Gap, Trail, and Second Story Alcoves were all within the last ~1,000 years, interpretation of the pit C flood chronology was restricted to the last 1,000 years. Of the seven youngest floods, three likely correlate with the three large floods at Custer Gap, Trail, and Second Story

Alcoves, leaving four floods recorded in Pit C that were not recorded at the higher sites and thereby providing additional evidence of large floods during the last ~1,000 years. Based on deposit elevations and the hydraulic simulations, these four floods required flows exceeding 14,200 to 16,900 ft^3/s. The exact ages of these additional floods are not known because all individual flood deposits cannot be correlated from site to site, but plausible estimates of median dates from the age dating (radiocarbon and OSL) for pit C were estimated to be A.D. 995, 1098, 1445, and 1563 (table 13). For the flood-frequency analyses, however, the exact ages are less important than the understanding of the total number of floods during the time period of interest.

Stratigraphic investigations also were conducted at Snow Shovel Alcove (fig. S3–7) located about 50 ft downstream from Kitty's Corner Alcove. The flood units at Snow Shovel Alcove, however, likely correlate with deposits at other sites, thereby providing no additional information other than corroborating the records obtained from the other sites.

In summary, two paleofloods with flows substantially larger than the 1972 flood (50,500 ft^3/s) have occurred in the last ~1,000 years in the downstream subreach of Boxelder Creek (fig. 46, table 13). The largest paleoflood was about 700 years ago with a flow of 61,300–123,000 ft^3/s (P3 in table 13 and fig. 46); whereas, the second largest paleoflood (P4; ~900 years ago) had a flow of 52,500–105,000 ft^3/s.

Table 12. Flood-frequency analyses for upstream subreach of Boxelder Creek.

[% reduction, percent reduction in confidence interval for analysis with all available data, relative to analysis for gaged records only]

Peak-flow magnitudes and 95-percent confidence limits and intervals, in cubic feet per second, for associated recurrence interval (annual exceedance probability)					
Data description	**25 years (0.04)**	**50 years (0.02)**	**100 years (0.01)**	**200 years (0.005)**	**500 years (0.002)**
PeakfqSA model, gaged records only					
Magnitude	4,680	9,980	20,600	41,700	103,000
Lower limit	1,930	3,430	5,810	9,510	17,500
Upper limit	81,800	419,000	2,190,000	11,600,000	107,000,000
Interval	79,800	416,000	2,180,000	11,600,000	107,000,000
PeakfqSA model, all available data					
Magnitude	3,350	6,120	10,800	18,500	36,500
Lower limit	1,860	3,160	5,120	8,070	14,200
Upper limit	5,460	10,300	19,700	38,500	95,800
Interval	3,600	7,140	14,600	30,400	81,600
% reduction	95.5	98.3	99.3	99.7	99.9
PeakfqSA model, all data with top fitting					
Magnitude	3,210	5,860	10,400	18,000	36,200
Lower limit	1,480	2,660	4,470	7,380	14,300
Upper limit	5,960	10,600	19,200	39,500	141,000
Interval	4,480	7,940	14,700	32,100	127,000
FLDFRQ3 model, gaged records only					
Magnitude	5,590	12,500	27,100	57,300	151,000
Lower limit	2,020	3,520	5,830	9,280	16,400
Upper limit	37,800	146,000	562,000	2,140,000	12,500,000
Interval	35,800	142,000	556,000	2,130,000	12,500,000
FLDFRQ3 model, all available data					
Magnitude	3,980	7,830	14,900	27,500	60,300
Lower limit	2,270	4,200	7,330	12,300	22,900
Upper limit	7,060	15,400	33,600	73,800	209,000
Interval	4,790	11,200	26,300	61,500	186,000
% reduction	86.6	92.1	95.3	97.1	98.5

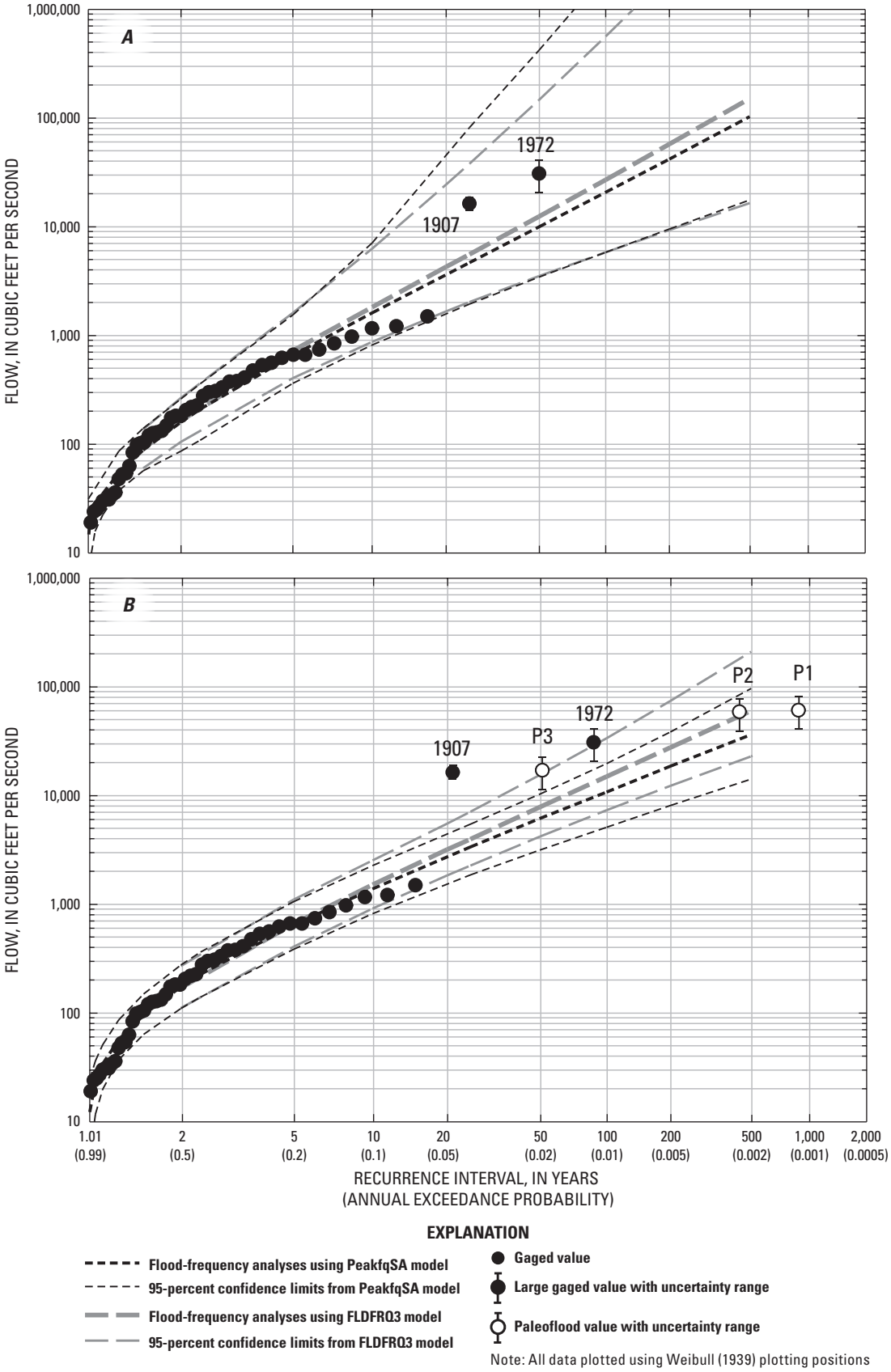

Figure 41. Flood-frequency analyses for upstream subreach of Boxelder Creek for *A*, gaged records only, and *B*, all available data that incorporate the long-term flood chronology from figure 40.

Four additional paleofloods between about 450 and 1,000 years ago had flows between about 14,200 and 33,800 ft^3/s.

Flood-Frequency Analysis for Downstream Subreach

Flood-frequency analyses of the gaged records only for the downstream subreach of Boxelder Creek include the large floods for 1907 and 1972 (fig. 36), for which uncertainties of ±33 percent were assigned (table 2). Uncertainties assigned for the rest of the gaged records were ±15 percent, which were larger than uncertainties assigned to gaged records for the upstream subreach because of the uncertain effect of intervening tributaries and flow diminishment within the loss zone of the downstream subreach. Analyses for all available data (fig. 46, table 13) included the gaged records and six paleofloods, two of which exceeded the 1972 flood magnitude. A perception threshold associated with the smallest paleoflood for Kitty's Corner Alcove (PT1) also was included.

The quantile estimates derived with the PeakfqSA model using all available data for the downstream subreach of Boxelder Creek (table 14, fig. 47) are nearly identical to those independently determined for the upstream subreach (table 12, fig. 41). Similar to the upstream subreach, the quantile estimates for all available data for the downstream subreach are much smaller than those derived using the gaged records only, with quantile estimates reduced by 60 percent or more for recurrence intervals of 100 years and larger. The 95-percent confidence intervals for these recurrence intervals were reduced by more than 99 percent. The quantile estimates derived using the FLDFRQ3 model are notably larger than those derived using the PeakfqSA model for both comparable scenarios (gaged records only and all available data) and both subreaches (tables 12 and 14). Evaluation of the differences in the analytical approaches used in the two statistical models is beyond the scope of this report.

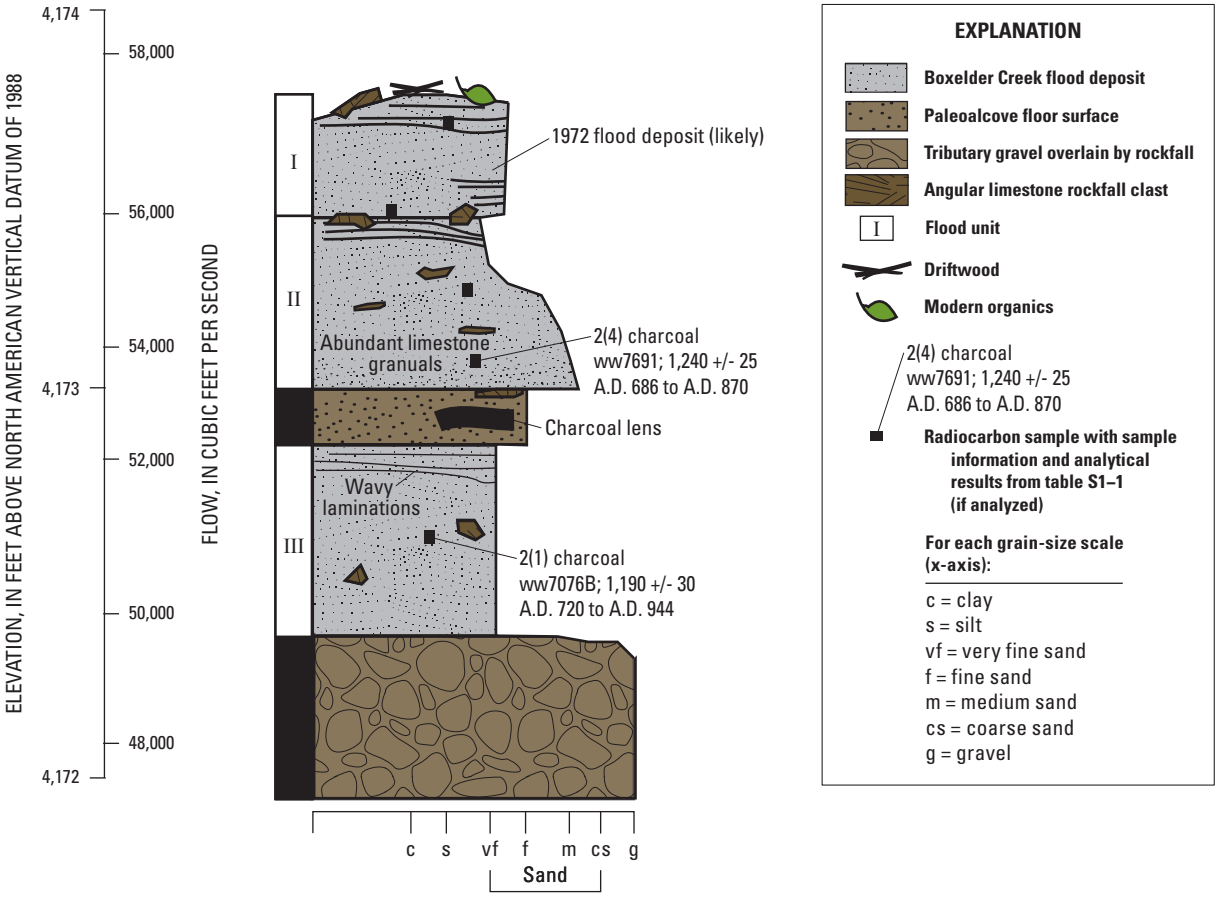

Figure 42. Schematic diagram showing paleoflood information for Custer Gap Alcove, downstream subreach of Boxelder Creek.

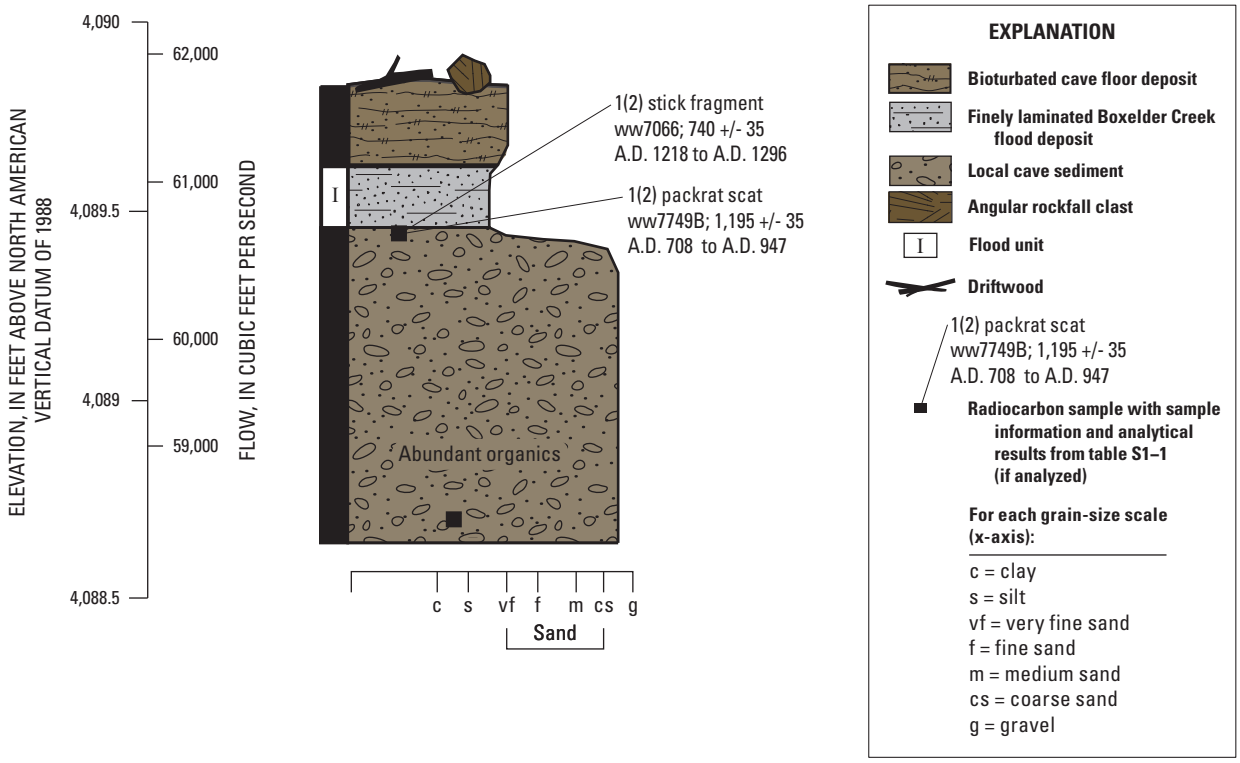

Figure 43. Schematic diagram showing paleoflood information for Second Story Alcove, downstream subreach of Boxelder Creek.

Bedded flood deposits in Custer Gap Alcove. Note small "silt cap" just left of trowel.

Looking from above Second Story Alcove at erosional scar, exposed alluvium, and exposed bedrock along Boxelder Creek. Flow direction is to the right.

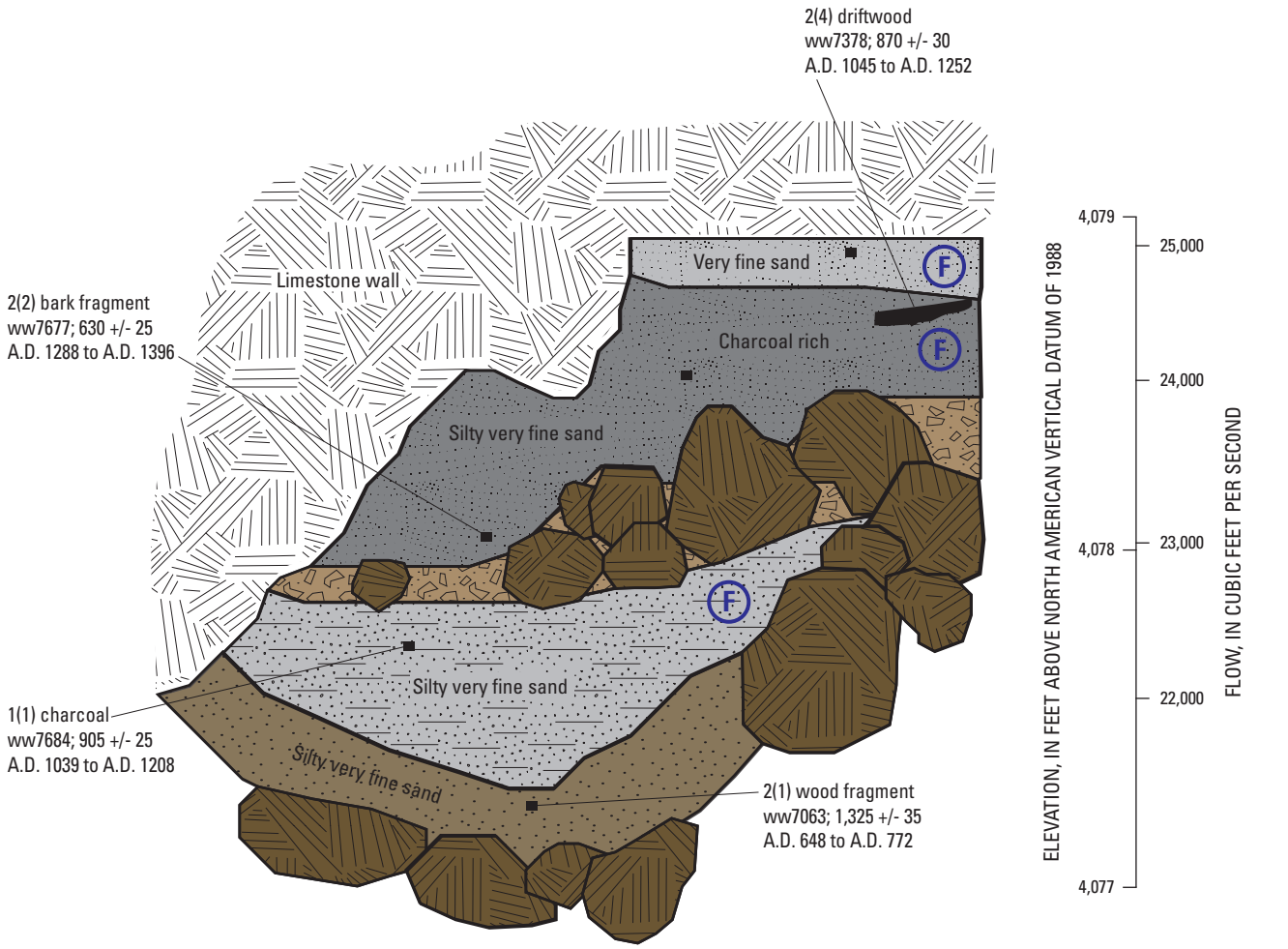

Bedded flood deposits

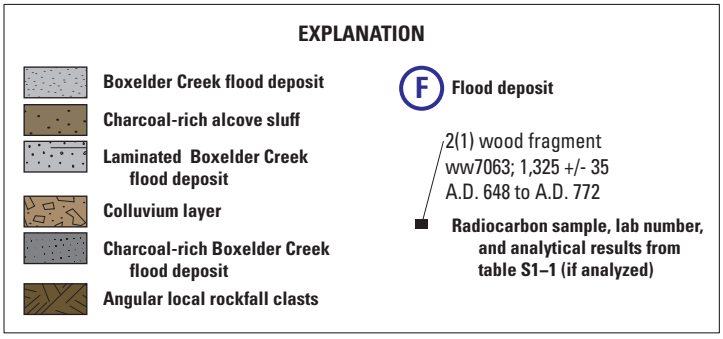

Figure 44. Schematic diagram showing paleoflood information for Trail Alcove, downstream subreach of Boxelder Creek.

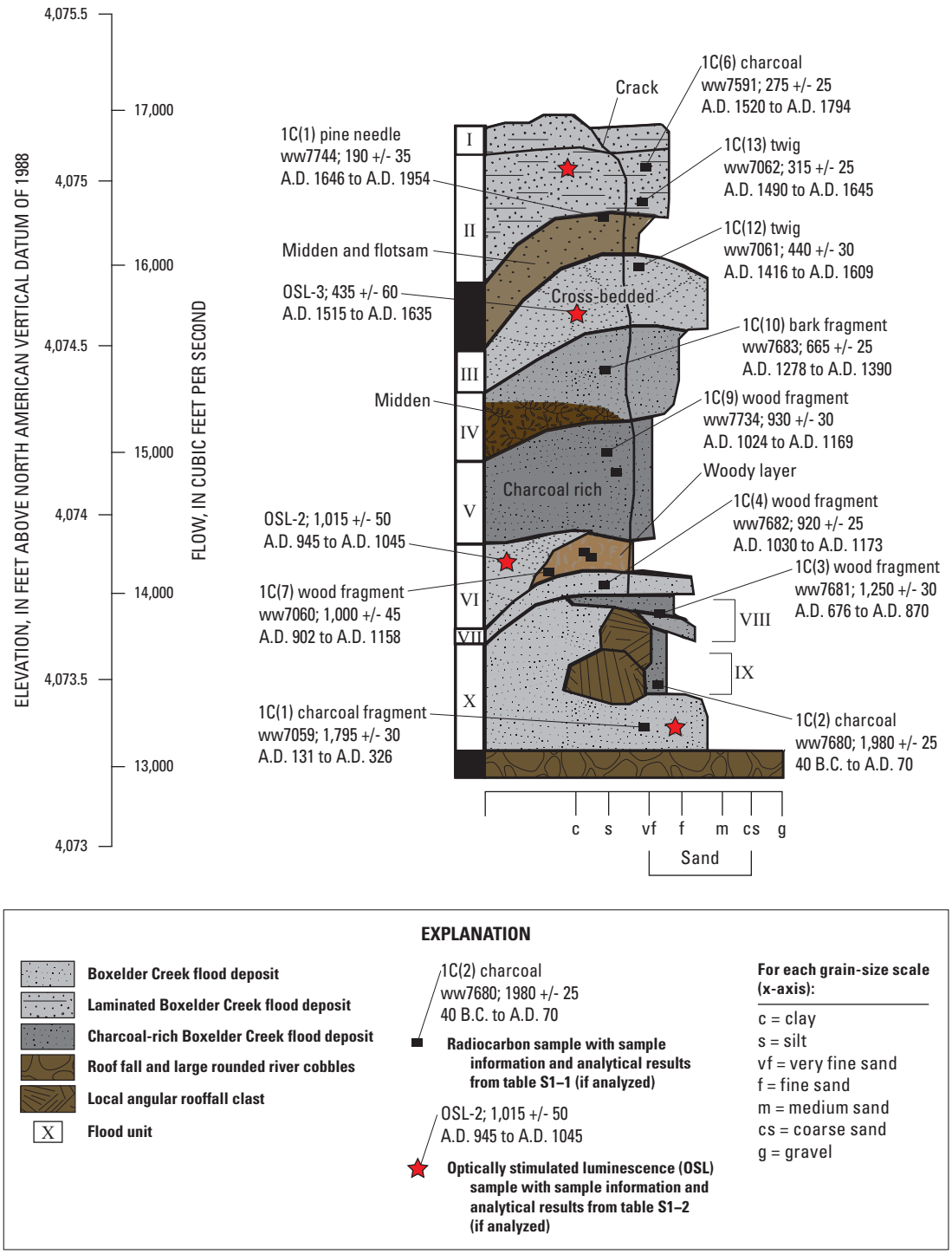

Figure 45. Schematic diagram showing paleoflood information for pit C in Kitty's Corner Alcove, downstream subreach of Boxelder Creek. Schematic diagrams for pits A and B are not provided.

Figure 46. Long-term flood chronology for downstream subreach of Boxelder Creek (from table 13).

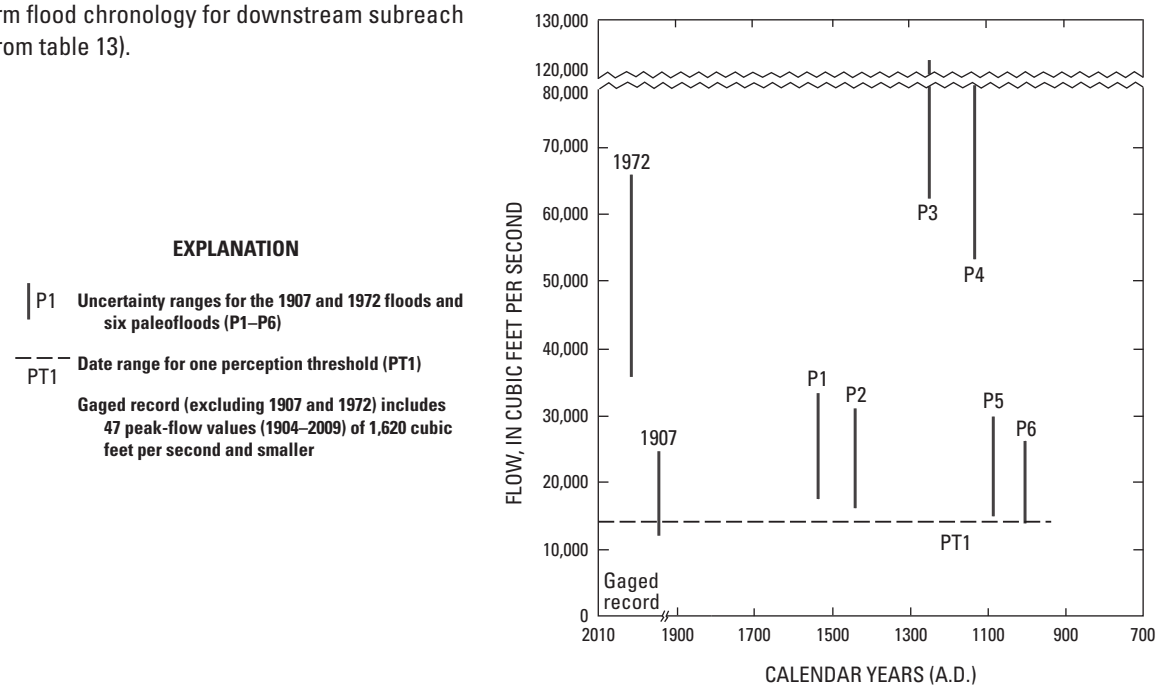

Table 13. Summary of long-term flood chronology used in flood-frequency analysis for downstream subreach of Boxelder Creek.

[ID, identification; min, minimum; max, maximum; PT, perception threshold; --, not applicable;]

ID for figure 46	Data description	Flow value, in cubic feet per second, for flood-frequency analysis			Flood or perception threshold date, in calendar years A.D.			
		Min	Max	Most likely	Flood date	PT min	PT max	PT date
			Perception thresholds					
PT1	Kitty's Corner Alcove pit C	--	--	14,200	--	2009	945	1510
			Paleoflood chronology					
P1	Kitty's Corner Alcove pit C	16,900	33,800	25,400	1563	--	--	--
P2	Kitty's Corner Alcove pit C	15,900	31,800	23,900	1445	--	--	--
P3	Second Story Alcove	61,300	123,000	92,000	1268	--	--	--
P4	Custer Gap Alcove unit III, Trail Alcove unit III	52,500	105,000	78,800	1111	--	--	--
P5	Kitty's Corner Alcove pit C	15,300	30,600	23,000	1098	--	--	--
P6	Kitty's Corner Alcove pit C	14,200	28,400	21,300	995	--	--	--
			Gaged record					
--	1907 flood	11,900	23,500	17,700	--	--	--	--
--	1972 flood	33,800	67,200	50,500	--	--	--	--
Gaged record	1904–05, 1946–47, 1966–2009 (excluding 1972). Uncertainty for flow values is plus or minus 15 percent (not shown). (Top-fitting analysis excludes values less than 197 cubic feet per second)	24	1,620	--	--	--	--	--

Table 14. Flood-frequency analyses for downstream subreach of Boxelder Creek.

[% reduction, percent reduction in confidence interval for analysis with all available data, relative to analysis for gaged records only; --, data not reported]

Peak-flow magnitudes and 95-percent confidence limits and intervals, in cubic feet per second, for associated recurrence interval (annual exceedance probability)					
Data description	**25 years (0.04)**	**50 years (0.02)**	**100 years (0.01)**	**200 years (0.005)**	**500 years (0.002)**
PeakfqSA model, gaged records only					
Magnitude	5,750	12,800	27,900	59,300	157,000
Lower limit	2,260	4,140	7,240	12,200	23,500
Upper limit	124,000	738,000	4,510,000	28,000,000	325,000,000
Interval	122,000	734,000	4,500,000	27,000,000	325,000,000
PeakfqSA model, all available data					
Magnitude	3,200	5,920	10,600	18,500	37,400
Lower limit	1,960	3,590	6,280	10,500	19,500
Upper limit	4,690	8,980	18,100	38,600	111,000
Interval	2,730	5,390	11,800	28,100	91,500
% reduction	97.8	99.3	99.7	99.9	100
PeakfqSA model, all data with top fitting					
Magnitude	2,980	5,540	10,100	18,200	38,900
Lower limit	919	2,420	5,400	10,600	--
Upper limit	4,630	8,510	18,400	84,700	--
Interval	4,480	7,940	14,700	32,100	--
FLDFRQ3 model, gaged records only					
Magnitude	6,440	14,700	32,600	71,100	195,000
Lower limit	2,270	4,040	6,830	11,100	20,500
Upper limit	44,300	176,000	694,000	2,730,000	16,500,000
Interval	42,000	172,000	687,000	2,720,000	16,500,000
FLDFRQ3 model, all available data					
Magnitude	4,130	8,270	16,000	30,200	68,300
Lower limit	2,540	4,830	8,680	14,900	28,600
Upper limit	6,800	15,000	33,700	75,700	219,000
Interval	4,260	10,200	25,000	60,800	190,000
% reduction	89.9	94.1	96.4	97.8	98.8

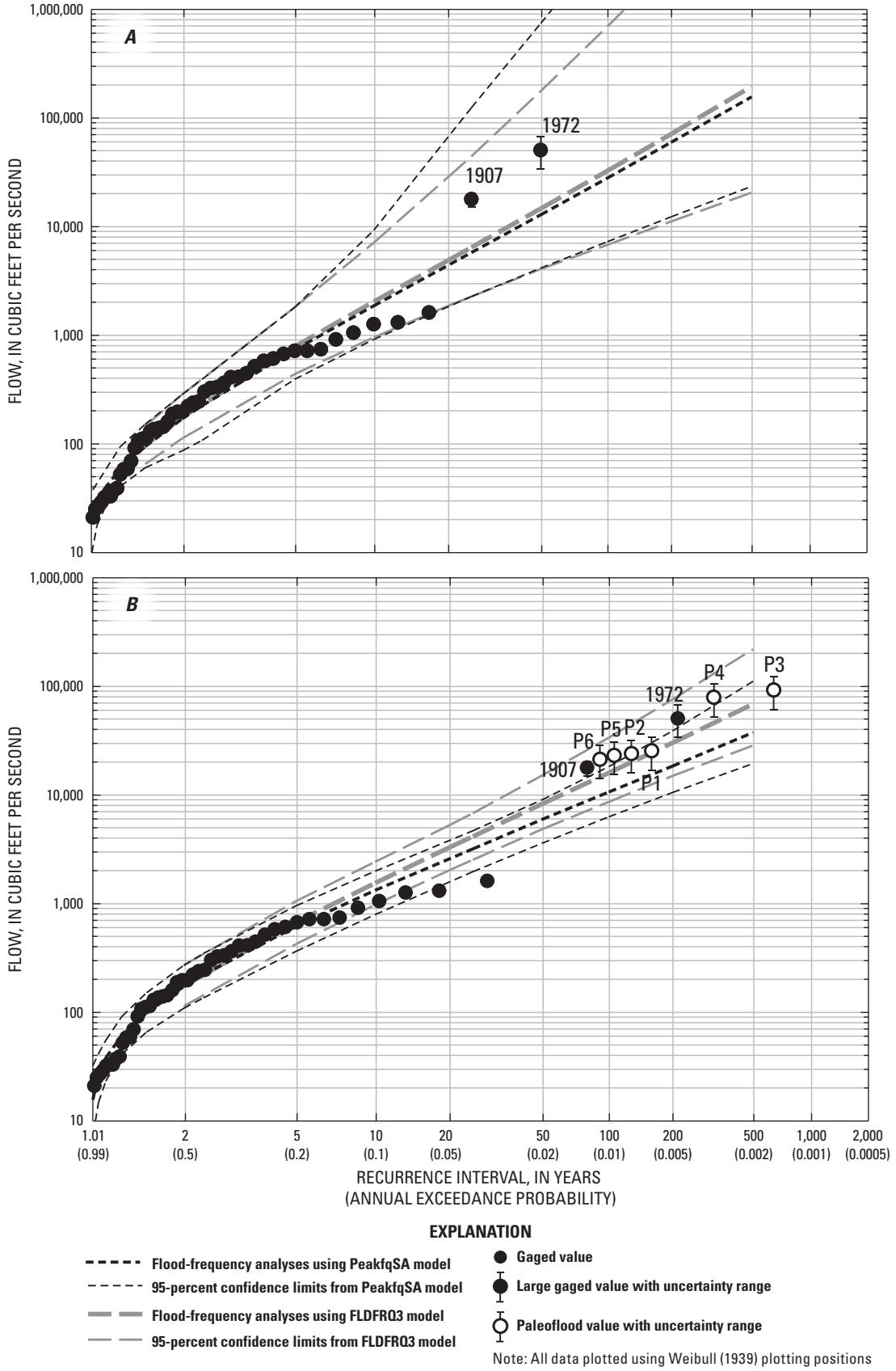

Figure 47. Flood-frequency analyses for downstream subreach of Boxelder Creek for *A*, gaged records only, and *B*, all available data that incorporate the long-term flood chronology from figure 46.

Elk Creek

Sites of paleoflood deposits are sparse along Elk Creek. As a consequence, the paleoflood chronology for Elk Creek was based on a single benchmark site, Dracula's Ledge, located within the outcrop of the Madison Limestone (fig. 1). Stratigraphic investigations also were conducted at the Sand Wall Alcove (upstream from Dracula's Ledge) and the Flat Rock and Bird's Nest Alcoves (both downstream from Dracula's Ledge); however, information provided by these sites (figs. S3–8 through S3–10) could not be used to expand the chronology. Dracula's Ledge is about 5 mi upstream from streamgage 06424500 where the 1972 flood had a peak flow of 11,600 ft^3/s (adjusted to 10,400 ft^3/s for the study reach; tables 2 and S2–5). The 1972 peak-flow value is the largest flow in 47 years of non-contiguous data for Elk Creek (1945–2009; fig. 48), although substantial flooding in 1907 is well documented in historical accounts (Driscoll and others, 2010).

Elk Creek in the vicinity of the Dracula's Ledge site is in an incised meandering and narrow canyon about 100 to 200 ft wide flanked by tall (as much as several hundred feet high) and near-vertical walls of Madison Limestone and steep colluvial sideslopes. The channel and valley bottom consist of exposed bedrock, thin alluvial deposits, and boulder fields (fig. 3). Flow is ephemeral in this reach, commonly with no flow for prolonged periods. Fine-grained sediments are less abundant in Elk Creek than in the other drainages in the study area, and large accumulations of slack-water sediments are uncommon within most of the Elk Creek valley bottom. No large tributaries enter the study reach. The 1972 flood deposited boulder and gravel bars along the channel bottom as well as accumulations of woody debris. The canyon bottom is densely vegetated with shrubs and stands of small ponderosa pines that generally post-date 1972. This reach is under U.S. Forest Service management, undeveloped, and without roads. Remnants of a narrow gauge railroad line locally flank the channel, but the line was badly damaged by the large 1907 flood and abandoned at that time (Honerkamp, 1978).

Hydraulic Analysis and Paleoflood Chronology

Peak flows associated with flood deposits at the Dracula's Ledge site along Elk Creek were estimated by critical-flow computations for two cross sections located about 10 ft upstream and downstream from the alcove location (fig. 49, table 15). The channel slope is about 0.038 ft/ft in this reach, justifying use of the critical-flow method. Both cross sections show the abandoned railroad grade; however, an estimate of smoothed pre-grading topography was used for computations. Computations for each cross section were performed for three elevations (relative to the thalweg elevation). The computed flow rates for each cross section were within 2 percent of each other for each elevation, so the values were averaged, as shown in table 15, to form the basis for the flow-rate scale shown on figure 50.

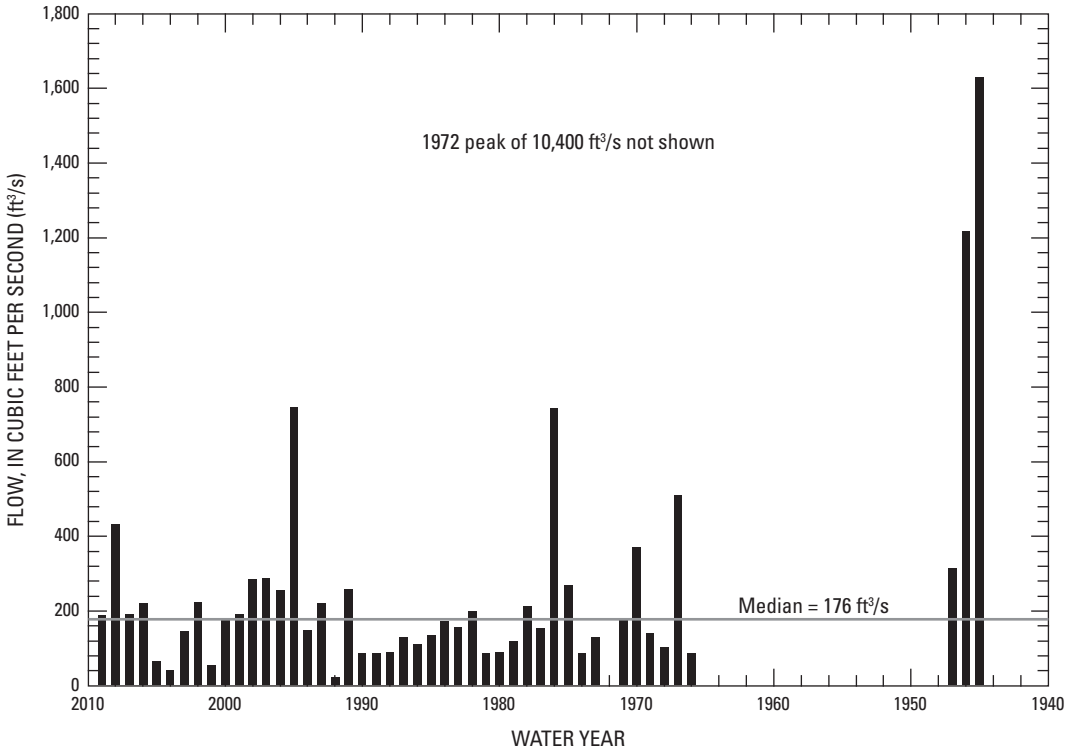

Figure 48. Modern peak-flow chronology (gaged records) for Elk Creek. Values are from table 2.

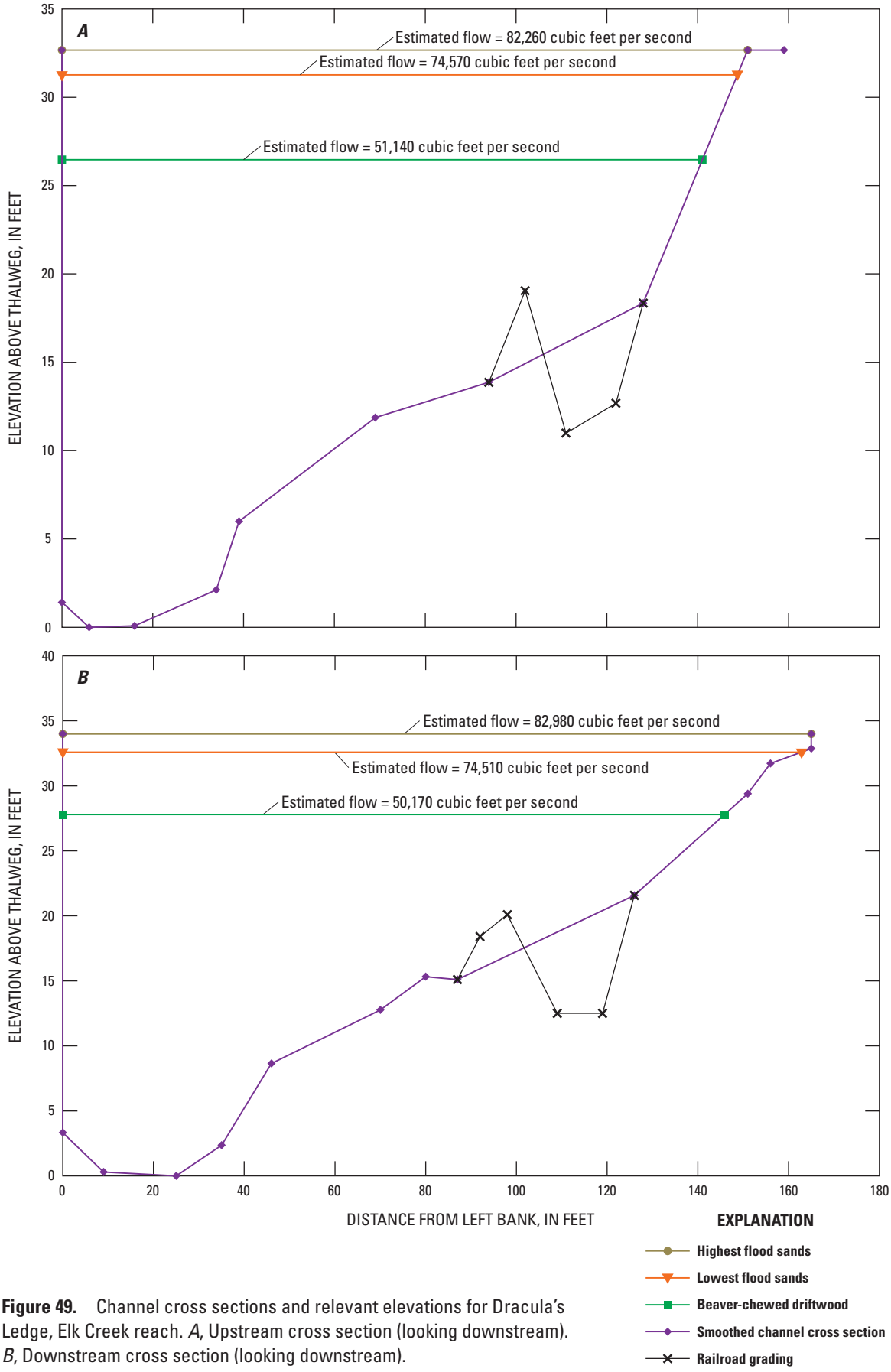

Figure 49. Channel cross sections and relevant elevations for Dracula's Ledge, Elk Creek reach. *A*, Upstream cross section (looking downstream). *B*, Downstream cross section (looking downstream).

Table 15. Summary of critical-flow computations for Dracula's Ledge, Elk Creek.

[--, computation not applicable]

Computational unit	Elevation above thalweg (feet)	Top width (feet)	Area (square feet)	Hydraulic depth (feet)	Velocity (feet per second)	Flow rate (cubic feet per second)
Highest elevation, upstream section	32.67	151.0	3,164	21.0	26.0	82,260
Highest elevation, downstream section	33.99	161.0	3,254	20.2	25.5	82,980
Average flow rate for two cross sections	--	--	--	--	--	82,620
Intermediate elevation, upstream section	31.27	149.5	2,959	19.8	25.2	74,570
Intermediate elevation, downstream section	32.59	161.0	3,029	18.8	24.6	74,510
Average flow rate for two cross sections	--	--	--	--	--	74,540
Lowest elevation, upstream section	26.47	114.5	2,273	15.7	22.5	51,140
Lowest elevation, downstream section	27.79	149.8	2,270	15.2	22.2	50,170
Average flow rate for two cross sections	--	--	--	--	--	50,660

The Dracula's Ledge site had slack-water deposits from four exceptionally large floods (fig. 50). The oldest flood unit (IV) was dated to A.D. 85–238 (younger of two samples) and required a flow exceeding 75,000 ft^3/s for inundation. The overlying flood unit (III) was dated to A.D. 242–393 and required a flow of about 77,000 ft^3/s. The second youngest flood unit (II) was dated to A.D. 869–1014 and required a flow of 80,000 ft^3/s. The youngest flood unit (I) was deposited about 900 years ago (A.D. 1016–1155) and has an associated flow of about 83,000 ft^3/s. A large beaver-chewed driftwood log was found in a rock crevice less than 30 yards upstream from the excavated pit. This log was radiocarbon dated to A.D. 1220–1284 (table S1–1), which is distinctively younger than the youngest slack-water deposit at the nearby pit. Given the context of the log's location, the only plausible explanation for placement was that it was carried there by a flood with a flow of at least 51,000 ft^3/s.

Investigations along Elk Creek included efforts to locate evidence for estimating the magnitude of the historical 1907 flood. No such evidence was found, nor was compelling evidence indicating the magnitude of the 1907 flood relative to that of 1972. Thus, in the absence of other information, the 1907 peak flow was assumed equal to the 1972 flood of 10,400 ft^3/s.

In summary, the 1972 flow on Elk Creek (10,400 ft^3/s) has been substantially exceeded at least five times in the last 1,900 years (fig. 51, table 16). The largest of these paleofloods (P2) was ~900 years ago and had a flow of 41,500–124,000 ft^3/s (83,000 ft^3/s ±50 percent). Three other paleofloods (P5, P4, and P3 in table 16) all between 37,500 and 120,000 ft^3/s occurred about 1,800, 1,700, and 1,100 years ago, respectively. The fifth large paleoflood (P1), recorded by the beaver-chewed driftwood log, was ~750 years ago and had a flow of 25,500–76,500 ft^3/s. The magnitude of the historical flood of 1907 is unknown, but for purposes of flood-frequency analysis is inferred to be similar to that of 1972.

Flood-Frequency Analysis

Flood-frequency analyses of the gaged records only for Elk Creek account for the large flood of 1972 and 46 other years of non-contiguous peak-flow data between 1945 and 2009 (fig. 48, table 2). The analyses incorporating all available data include the gaged records, five paleofloods (table 16), and the historical 1907 flood (fig. 51). Three perception thresholds were identified: (1) the 1972 flow rate (10,400 ft^3/s) likely has not been otherwise exceeded since A.D. 1907; (2) the flow rate represented by the beaver-chewed log has not been exceeded since A.D. 1155; and (3) the paleoflood of 75,000 ft^3/s recorded at the Dracula's Ledge site has been exceeded only four times since A.D. 76, as indicated by the length of the paleoflood chronology (~1,900 years) for the site. For the top-fitting analysis, only the 24 values greater than the median value of 176 ft^3/s in the gaged peak-flow records were included.

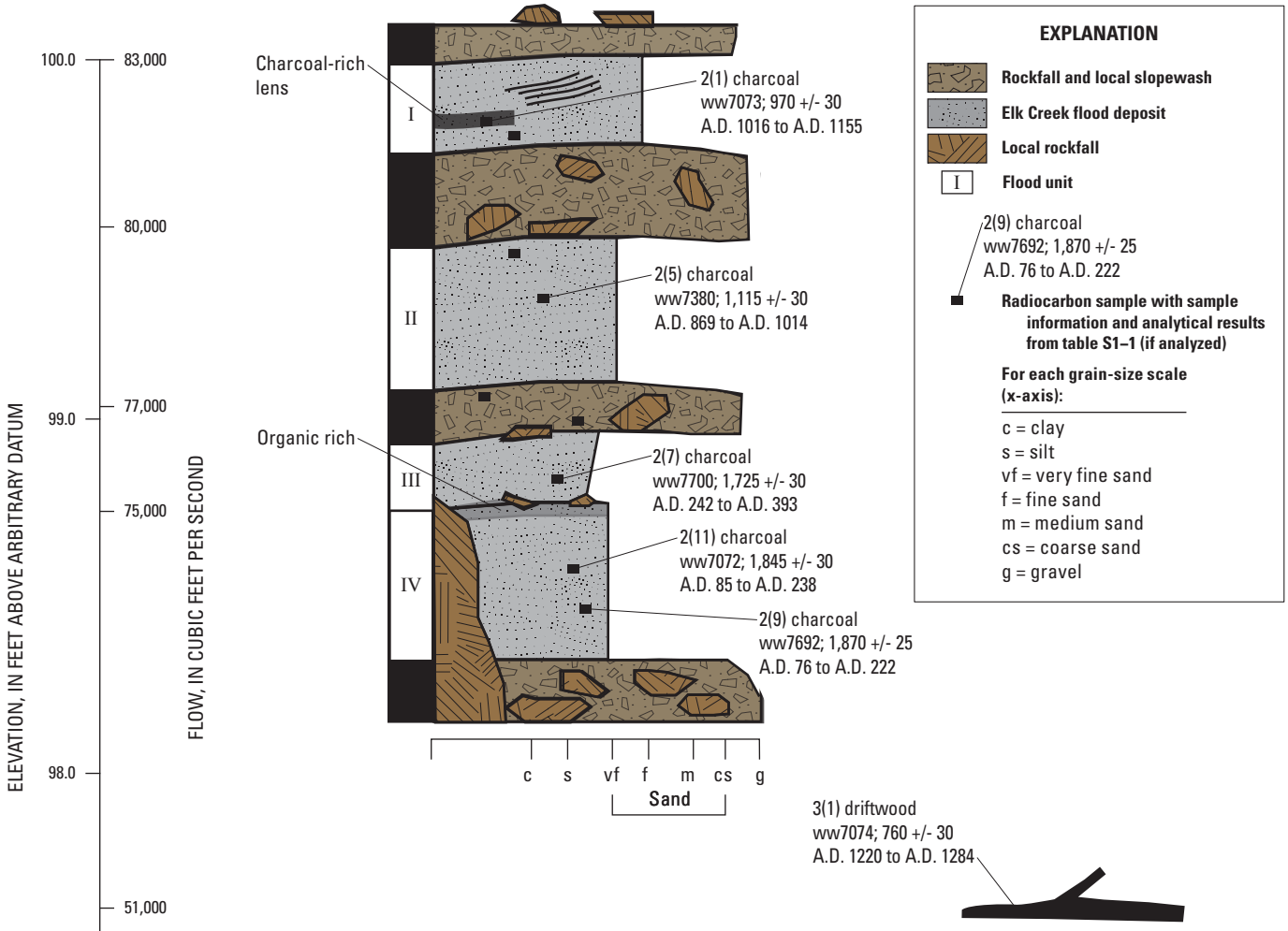

Pre-1907 grade stake from railroad construction (site's namesake) shown with bedded flood deposits

Beaver-chewed (right limb) driftwood log

Figure 50. Schematic diagram showing paleoflood information for Dracula's Ledge, Elk Creek.

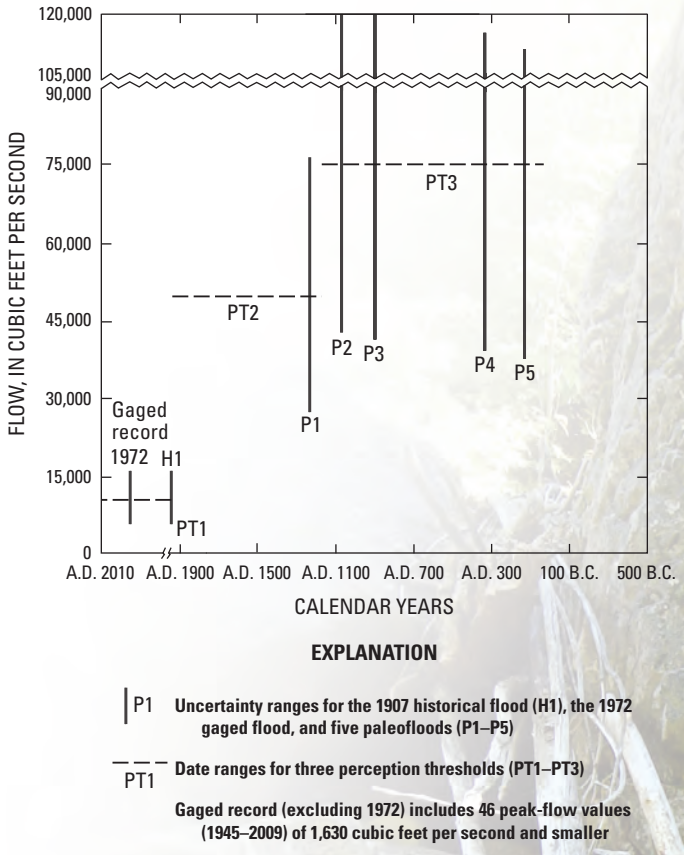

Figure 51. Long-term flood chronology for Elk Creek (from table 16).

The quantile estimates derived using all available data for the PeakfqSA model are more than twice as large as those derived using the gaged records only for all recurrence intervals (table 17, fig. 52). This result reflects the evidence of the five paleofloods of the last ~1,900 years that substantially exceeded the largest gaged and historical flows. Similar to all other study reaches, incorporation of the long-term flood chronology in the PeakfqSA model resulted in substantially reduced uncertainties for the flood-quantile estimates; in this case, the 95-percent confidence intervals were reduced by 96 percent or more for the 100-, 200-, and 500-year recurrence intervals (table 17). For the FLDFRQ3 model, uncertainties for estimates derived using all available data were greater than uncertainties for estimated derived using gaged records only because of the especially large increases in flow magnitudes.

Tie from pre-1907 railroad along Elk Creek

Table 16. Summary of long-term flood chronology used in flood-frequency analysis for Elk Creek.

[ID, identification; min, minimum; max, maximum; PT, perception threshold; --, not applicable]

ID for figure 51	Data description	Flow values, in cubic feet per second, for flood-frequency analysis			Flood or perception threshold dates, in calendar years A.D.			
		Min	Max	Most likely	Flood date	PT min	PT max	PT date
		Perception thresholds						
PT1	1907 historical flood	--	--	10,400	--	2009	1907	1930
PT2	Beaver-chewed log	--	--	51,000	--	1906	1155	1259
PT3	Dracula's Ledge unit IV	--	--	75,000	--	1154	76	260
		Paleoflood chronology						
P1	Beaver-chewed log	25,500	76,500	51,000	1259	--	--	--
P2	Dracula's Ledge unit I	41,500	124,000	83,000	1090	--	--	--
P3	Dracula's Ledge unit II	40,000	120,000	80,000	935	--	--	--
P4	Dracula's Ledge unit III	38,500	115,000	77,000	315	--	--	--
P5	Dracula's Ledge unit IV	37,500	112,000	75,000	171	--	--	--
		Historical floods						
H1	1907	5,200	15,600	10,400	1907	--	--	--
		Gaged records						
1972	1972 flood	6,970	13,800	10,400	--	--	--	--
Gaged record	1945–47, 1966–2009 (excluding 1972). Uncertainty for flow values is plus or minus 20 percent (not shown). (Top-fitting analysis excludes values less than 254 cubic feet per second)	22	1,630	--	--	--	--	--

Table 17. Flood-frequency analyses for Elk Creek.

[% reduction, percent reduction in confidence interval for analysis with all available data, relative to analysis for gaged records only; a negative value indicates a percent increase in confidence interval]

Peak-flow magnitudes and 95-percent confidence limits and intervals, in cubic feet per second, for associated recurrence interval (annual exceedance probability)					
Data description	**25 years (0.04)**	**50 years (0.02)**	**100 years (0.01)**	**200 years (0.005)**	**500 years (0.002)**
PeakfqSA model, gaged records only					
Magnitude	1,650	2,980	5,340	9,480	20,000
Lower limit	835	1,290	1,930	2,850	4,660
Upper limit	18,800	85,600	407,000	1,990,000	16,700,000
Interval	18,000	84,300	405,000	1,990,000	16,700,000
PeakfqSA model, gaged records and historical data					
Magnitude	1,900	3,470	6,230	11,100	23,400
Lower limit	941	1,460	2,220	3,310	6,740
Upper limit	7,010	31,400	159,000	625,000	3,020,000
Interval	6,070	29,900	157,000	622,000	3,010,000
PeakfqSA model, all available data					
Magnitude	3,510	6,670	12,400	22,500	48,300
Lower limit	1,960	3,570	6,150	10,300	19,800
Upper limit	5,680	10,900	21,300	42,700	113,000
Interval	3,720	7,330	15,200	32,400	93,200
% reduction	79.3	91.3	96.2	98.4	99.4
PeakfqSA model, all data with top fitting					
Magnitude	4,450	8,700	15,800	27,200	52,000
Lower limit	1,550	3,040	5,580	9,440	22,600
Upper limit	10,000	17,800	28,300	44,700	133,000
Interval	8,450	14,800	22,700	35,300	110,000
FLDFRQ3 model, gaged records only					
Magnitude	1,150	1,670	2,370	3,300	5,010
Lower limit	700	933	1,210	1,540	2,050
Upper limit	2,520	4,330	7,310	12,200	23,300
Interval	1,820	3,400	6,100	10,700	21,200
FLDFRQ3 model, gaged records and historical data					
Magnitude	1,520	2,340	3,540	5,230	8,600
Lower limit	886	1,250	1,710	2,290	3,280
Upper limit	3,200	5,800	10,300	18,000	37,300
Interval	2,310	4,550	8,590	15,700	34,000
FLDFRQ3 model, all available data					
Magnitude	3,410	6,340	11,500	20,400	42,400
Lower limit	2,140	3,750	6,360	10,500	19,800
Upper limit	5,440	10,700	20,900	40,400	95,100
Interval	3,300	6,950	14,500	29,900	75,300
% reduction	-81.3	-104	-138	-179	-255

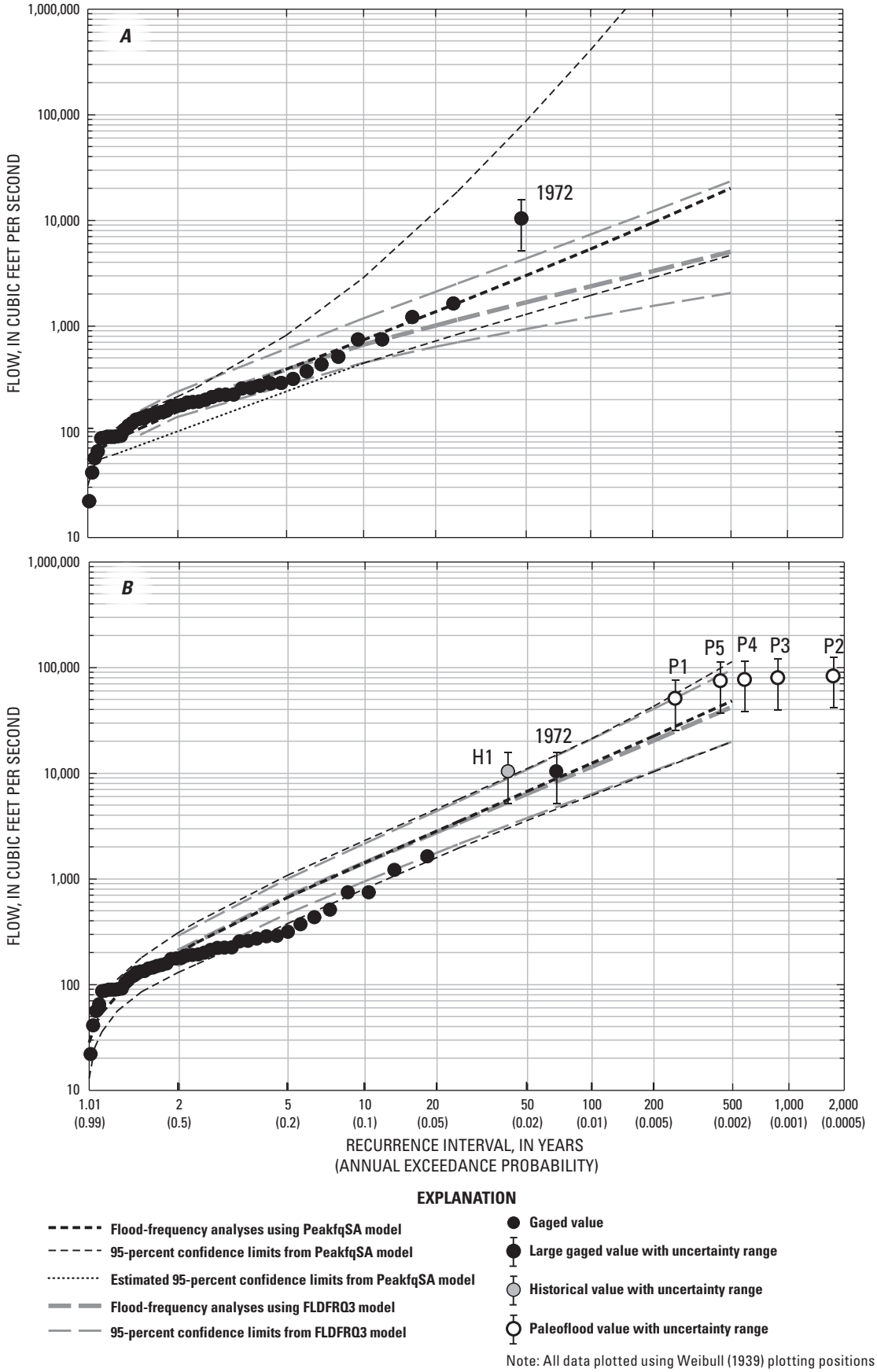

Figure 52. Flood-frequency analyses for Elk Creek for *A*, gaged records only, and *B*, all available data that incorporate the long-term flood chronology from figure 51.

Central Black Hills Flood Frequency: Synopsis, Implications, and Application

The paleoflood investigations, in conjunction with observational and historical records, provide a rich history of large floods locally extending back 2,000 years for Spring, Rapid, Boxelder, and Elk Creeks. In total, the flood-frequency analyses for the six study reaches account for 29 large paleofloods inferred from examination and interpretation of stratigraphic records at 29 sites, including 19 primary sites and 10 supplemental sites. For all study reaches, composited stratigraphic records extend back between about 1,000 and 2,000 years, substantially longer than gaged records (which extend to the early 1900s for some drainages) and historical accounts (which extend to 1878 for lower Rapid Creek and 1907 for Elk Creek).

The results of the paleoflood investigations provide better physically based information on low-probability floods than has been previously available, substantially improving estimates of the magnitude and frequency of large floods in central Black Hills and reducing associated uncertainties. Collectively, the results provide insights regarding regional flood-generation processes and their spatial controls, enable approaches for extrapolation of results for hazard assessment beyond specific study reaches, and provide a millennial-scale perspective on the 1972 flooding.

Synopsis of Results and Regional Assessment

Collective examination of flood-frequency results for all six study reaches allows comparisons among the reaches and regional-scale assessments regarding low-probability flooding in the central Black Hills. These analyses also provide context relative to national-scale information.

Synopsis of Flood-Frequency Results

Results of the paleoflood investigations provide improved flood-frequency estimates for each of the six study reaches and facilitate comparisons among and within individual drainage basins. For simplification, only the flood-frequency analyses from the PeakfqSA model are considered within this report section, although analyses from the FLDFRQ3 model generally are similar for most study reaches. Exceptions are the two subreaches of Boxelder Creek (tables 12 and 14). The 100-year quantile estimates (considering all available data) from the FLDFRQ3 model exceed those from the PeakfqSA model by 38 and 51 percent for the upstream and downstream subreaches, respectively, and the 500-year quantile estimates have differentials of 65 and 83 percent. In addition to providing a consistent basis for comparison, analyses from the PeakfqSA model accord most closely to established Federal procedures for flood-frequency analysis (Interagency Advisory Council on Water Data, 1982). The analyses considered herein consist of those from the PeakfqSA model for the short-term analyses (derived using only gaged peak-flow records) and long-term analyses (incorporating all available information including paleoflood, historical, and gaged records—with perception thresholds and without top fitting), which in the absence of additional analysis, probably provide the best available estimates of low-probability flood recurrence for the study reaches.

The overarching result of incorporating the paleoflood information is substantially narrowed confidence intervals, relative to those for the short-term flood-frequency analyses (table 18). In all cases, 95-percent confidence intervals about the low-probability quantile estimates (100-, 200-, and 500-year recurrence-intervals) are reduced by at least 78 percent relative to similar analyses of the gaged records only. In some cases, 95-percent uncertainty limits have been reduced by 99 percent or more. This result is the logical outcome of the much longer records of the large paleofloods provided by the stratigraphic records.

For all study reaches except the two Boxelder Creek subreaches, quantile estimates for the long-term flood-frequency analyses are larger than for the short-term analyses (table 18). The largest differences are for lower Rapid Creek and Elk Creek. For lower Rapid Creek, the 100-year quantile estimate increased by 61 percent (from 8,720 to 14,000 ft^3/s), and the 500-year quantile estimate increased by 73 percent (from 27,900 to 48,300 ft^3/s). For Elk Creek, the 100- and 500-year quantile estimates increased by about 130 and 140 percent, respectively. For Spring Creek and the upstream reach of Rapid Creek, increases in the quantile estimates were smaller. In all of these cases, the increases resulted from incorporation of paleofloods that were substantially larger than the largest gaged flows in the flood-frequency analyses.

For both subreaches of Boxelder Creek, quantile estimates for the long-term flood-frequency analyses were substantially smaller than for the short-term analyses (table 18). For the upstream subreach, the 100-year quantile estimate decreased by 48 percent, and the 500-year quantile estimate decreased by 65 percent. For the downstream subreach, the 100-year quantile estimate decreased by 62 percent, and the 500-year quantile estimate decreased by 76 percent. These decreases largely reflect the effect of the two large floods (1907 and 1972) in the gaged records on the short-term flood-frequency analyses—the short-term quantile estimates for both subreaches of Boxelder Creek are substantially larger than for the other study reaches (table 18). The paleoflood chronologies for the two subreaches of Boxelder Creek were independently determined, and although the stratigraphic records cannot be precisely correlated between the two subreaches, the general similarities between results help affirm the overall study approaches.

Regional Assessment

An assessment of the flood-frequency analyses in the context of regional information aids in comparisons among the reaches and evaluation of the results. “Envelope” curves bounding large observed flood measurements relative to drainage area provide an overall basis to assess the magnitudes of paleofloods and associated flood-frequency analyses (Enzel and others, 1993). In particular, such curves can guide assessment of the reasonableness of flood-magnitude inferences or observations in light of other observed floods at a variety of spatial scales. Flood measurements or observations that substantially exceed existing measurements and associated envelope curves merit extra scrutiny in regards to measurement procedure and validity, extraordinary watershed conditions, and possibly unusual processes in flood generation, such as floods involving debris flows or failures of natural dams (Wolman and Costa, 1984).

The “most-likely” values for all paleofloods incorporated in the flood-frequency analyses (tables 4, 6, 9, 11, 13, and 16) are plotted in figure 53 relative to envelope curves developed by Crippen and Bue (1977) for the United States

Table 18. Summary of flood-frequency analyses and large flows for paleoflood study reaches.

[All analyses from PeakfqSA model. Short-term analyses are for gaged records only. Long-term analyses incorporate all available information without top fitting. ft^3/s, cubic feet per second; --, not applicable; % reduction, percent reduction in 95-percent confidence interval for analysis with all available data, relative to analysis for gaged records only]

Data description	Peak-flow estimate, in ft^3/s for associated recurrence interval (annual exceedance probability)					Flow (ft^3/s) for selected paleofloods		Largest gaged flow (ft^3/s)
	25 years (0.04)	50 years (0.02)	100 years (0.01)	200 years (0.005)	500 years (0.002)	Largest	Second largest	
Spring Creek (drainage area = 171 square miles)								
Short-term	2,010	3,620	6,290	10,700	20,800	--	--	21,800
Long-term	2,480	4,530	7,960	13,600	26,900	56,400	18,200	--
% reduction	72.9	85.4	89.6	92.4	94.9	--	--	--
Lower reach of Rapid Creek (actual drainage area = 375 square miles; adjusted drainage area between streamgages 06410500 and 06412500 = 81 square miles)								
Short-term	2,990	5,160	8,720	14,500	27,900	--	--	31,200
Long-term	4,410	7,950	14,000	24,100	48,300	128,000	64,000	--
% reduction	66.7	79.0	83.8	87.1	90.5	--	--	--
Upstream reach of Rapid Creek (drainage area = 294 square miles)								
Short-term	1,500	2,200	3,160	4,450	6,850	--	--	2,460
Long-term	1,590	2,350	3,390	4,770	7,340	12,900	12,000	--
% reduction	57.3	69.7	78.3	83.1	86.6	--	--	--
Upstream subreach of Boxelder Creek (drainage area = 98 square miles)								
Short-term	4,680	9,980	20,600	41,700	103,000	--	--	30,800
Long-term	3,350	6,120	10,800	18,500	36,500	40,000	39,000	--
% reduction	95.5	98.3	99.3	99.7	99.9	--	--	--
Downstream subreach of Boxelder Creek (drainage area = 112 square miles)								
Short-term	5,750	12,800	27,900	59,300	157,000	--	--	50,500
Long-term	3,200	5,920	10,600	18,500	37,400	61,300	52,500	--
% reduction	97.8	99.3	99.7	99.9	100	--	--	--
Elk Creek (drainage area = 40 square miles)								
Short-term	1,650	2,980	5,340	9,480	20,000	--	--	10,400
Long-term	3,510	6,670	12,400	22,500	48,300	83,000	80,000	--
% reduction	79.3	91.3	96.2	98.4	99.4	--	--	--

(national envelope curve) and for "region 11" that includes the Black Hills area (regional envelope curve). All of the paleofloods plot within the bounds of the national envelope curve, indicating that the national curve represents exceedingly rare floods for the Black Hills area. Several Black Hills paleofloods plotted above the regional envelope curve, which is not surprising because the curve for region 11 is poorly constrained. Elk Creek, lower Rapid Creek, and the downstream subreach of Boxelder Creek had paleofloods exceeding the regional curve; in the case of Elk Creek, by a factor of nearly two. The Black Hills paleofloods represent some of the largest known floods, relative to drainage area, for the United States. Many of the other largest known United States floods (fig. 53; Costa, 1987; International Association of Hydrological Sciences, 2003; Costa and Jarrett, 2008) are in areas with physiographic and climatologic conditions broadly similar to the Black Hills—semiarid and rugged landscapes that intercept and focus heavy precipitation from convective storm systems (Costa, 1987; O'Connor and Costa, 2004).

The two largest paleofloods for each study reach (table 18) and the largest gaged flow (all of which are from 1972, with the exception of upper Rapid Creek) are shown in figure 54 relative to the low-probability quantile estimates from the long-term flood-frequency analyses and regional envelope curve. The paleoflood flow values (table 18 and fig. 54) are those that are associated with tops of flood-unit deposits and for some cases differ from the most-likely values that are plotted in figure 53. The largest gaged flow for lower Boxelder Creek (50,500 ft^3/s; tables 2 and 18) essentially coincides with one of the points (1972 flow of 51,600 ft^3/s for streamgage 06422650; table S2–4) used by Crippen and Bue (1977) in developing the regional envelope curve.

Two datasets are plotted for lower Rapid Creek (fig. 54)—one based on the whole drainage area and one based on an "adjusted" area of 81 mi^2, which is the intervening drainage area (table 1) between representative streamgages 06410500 and 06412500 at the two Rapid Creek study reaches. A key issue for this study is flood-frequency characterization for modern (regulated) conditions for lower Rapid Creek, as described in a previous section "Implications of Paleoflood Chronologies for Rapid Creek," and this area (81 mi^2) is postulated in ensuing interpretations as the primary contributing area for low-probability floods during pre-regulation conditions. The largest paleofloods and quantile estimates for upper Rapid Creek are about an order of magnitude smaller than for lower Rapid Creek and strongly support the hypothesis of distinctly different regimes for large-flood generation for the two reaches.

The area-adjusted quantile estimates for lower Rapid Creek (fig. 54) plot close to those for the two subreaches of Boxelder Creek, which are nearly identical, and magnitudes for all of these quantile estimates are similar to those for Elk Creek, for which the drainage area is less than one-half of that for all of the other study reaches. The 500-year quantile estimate for Elk Creek plots slightly above the regional envelope curve and is exceeded by the two largest paleofloods by a factor of almost two.

Implications for Flood Generation

The overall results from the paleoflood investigations and associated flood-frequency analyses, in conjunction with gaged records, historical records, and previous studies, support general observations of flood-generation processes in the Black Hills. Such observations are relevant for assessing general flood hazards and for extrapolating flood-frequency results from discrete study reaches to other appropriate locations in the Black Hills.

Driscoll and others (2010) postulated that potential for heavy rain-producing thunderstorms (storm potential) and associated flooding are smallest on the relatively flat top of the Limestone Plateau (fig. 1), with storm and flood potential increasing in an easterly direction. The eastern Black Hills are susceptible to intense orographic lifting associated with convective storm systems and also have high relief, thin soils, and narrow and steep canyons—factors favoring generation of exceptionally heavy rain-producing thunderstorms and promoting runoff and rapid concentration of flow into stream channels. In contrast, storm potential in and near the Limestone Plateau area is much lower than for the steeper flanks of the Black Hills. Storm runoff is further reduced by substantial infiltration into the limestone, gentle topography, and extensive floodplain storage.

The gradient in flood-generation processes is reflected in results of this study, for which some of the most compelling evidence is the disparity between results of the paleoflood investigations for the two Rapid Creek study reaches. Large parts of the upper Rapid Creek drainage basin are within the Limestone Plateau and other high-elevation areas where reduced flood potential is postulated (Driscoll and others, 2010; Sando and others, 2008). The upper reach composes about 78 percent of the drainage area of the lower reach, as defined by areas for associated streamgages (294 and 375 mi^2, respectively; table 1). Stratigraphic records for the upper reach indicate two paleofloods during the last 1,000 to 2,000 years of at least 12,000 and 12,900 ft^3/s, which substantially exceed the largest gaged flow of 2,460 ft^3/s (table 18). These floods are small, however, compared to the contributing drainage area and plot much lower than paleofloods recognized from deposits within all of the other study reaches (figs. 53 and 54). Moreover, the largest paleoflood of at least 128,000 ft^3/s for lower Rapid Creek is larger by a factor of about 10, despite having a drainage area that is less than 30 percent larger than that for the upper reach.

The disparity of the paleoflood chronology for upper Rapid Creek relative to other study reaches is consistent with characteristics of the June 9–10, 1972, storm and flooding (Schwarz and others, 1975). The 1972 flooding along Rapid Creek occurred exclusively downstream from Pactola Reservoir, with peak flows of 31,200 and 50,000 ft^3/s determined for streamgages 06412500 and 06414000, respectively (fig. 1, table S2–2). In contrast, the 1972 peak flow for streamgage 06410500 located upstream from Pactola Reservoir was only 252 ft^3/s.

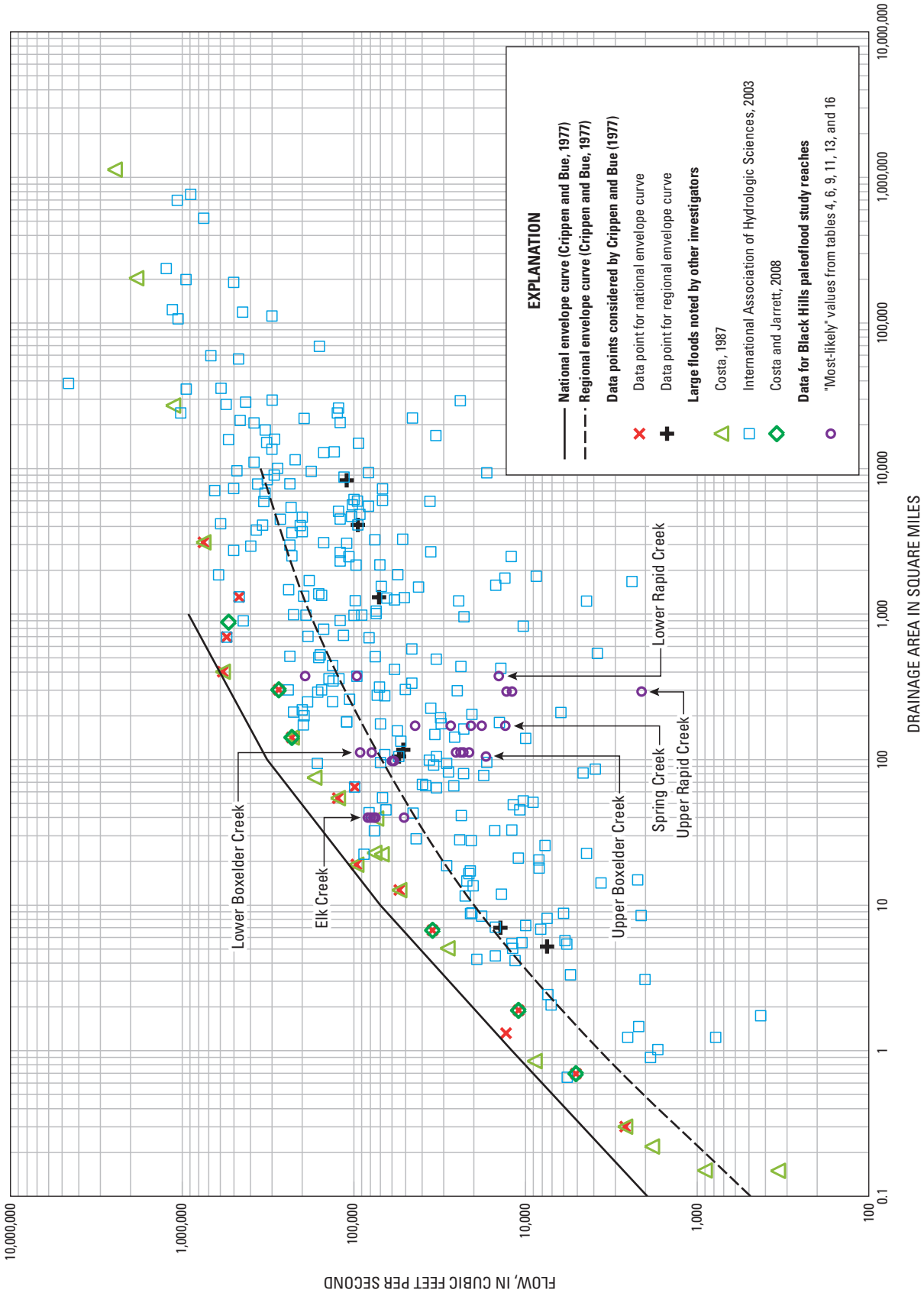

Figure 53. Black Hills paleofloods and maximum gaged flows for selected stream reaches, relative to national and regional envelope curves.

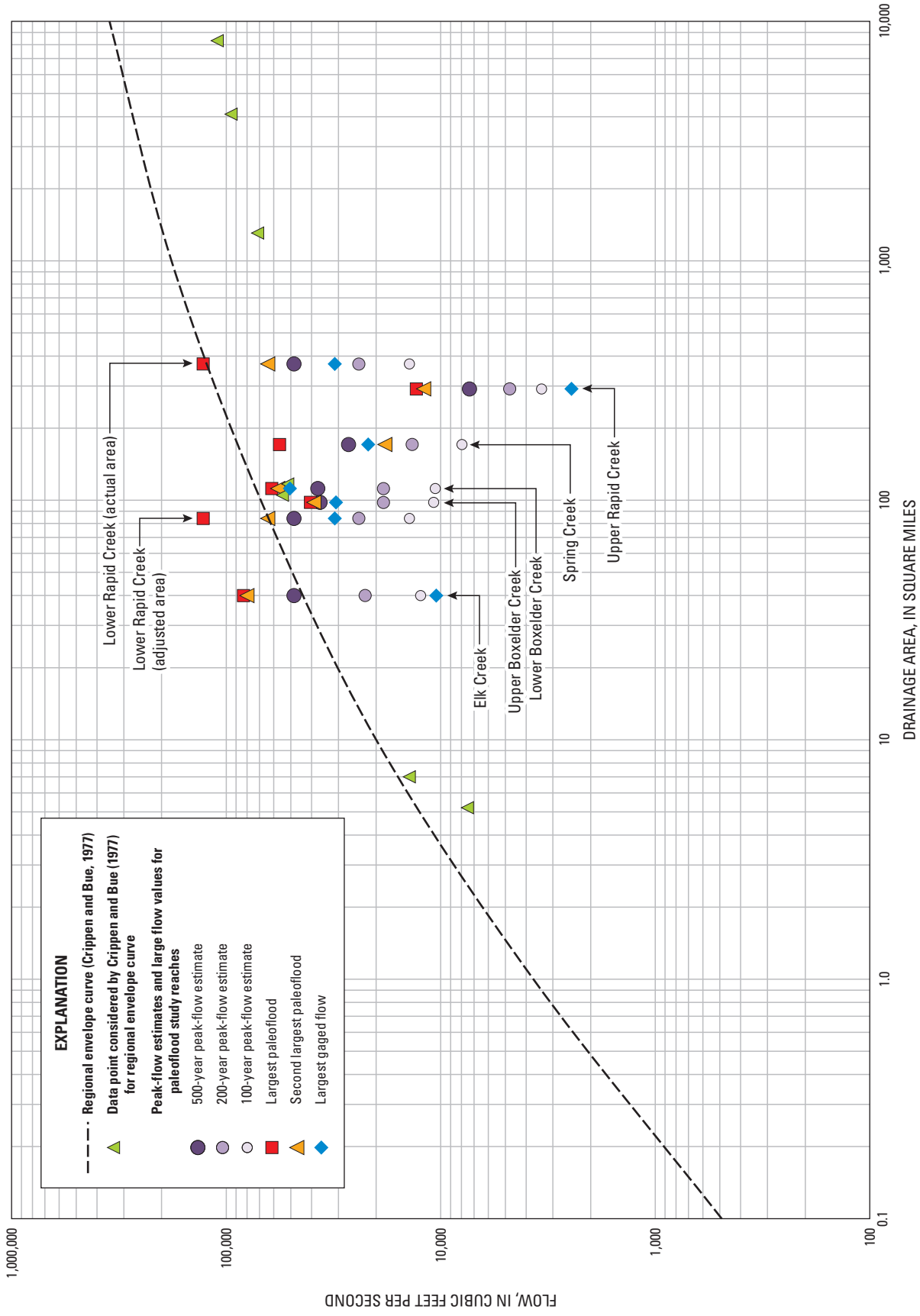

Figure 54. Results of peak-flow frequency analyses for selected stream reaches, relative to regional envelope curve.

The quantile estimates for Spring Creek are smaller than for all study reaches except upper Rapid Creek (fig. 54), despite having a relatively large drainage area. The Spring Creek drainage basin is long and like Rapid Creek has high-elevation headwaters extending close to the eastern extent of the Limestone Plateau (fig. 1). Consequently, it is plausible that the largest flows in Spring Creek are chiefly generated in the eastern part of the watershed. Consistent with this, documentation from Schwarz and others (1975) indicates that the Spring Creek watershed upstream from Hill City was not substantially affected by the 1972 storm.

Perhaps the most compelling evidence of enhanced flood generation in the eastern Black Hills is provided by Elk Creek, which has had four paleofloods exceeding 75,000 ft^3/s in the last 2,000 years from a drainage area of only 40 mi^2. The headwaters of Elk Creek are northeast of the contiguous geologic outcrops that compose the Limestone Plateau (fig. 1), and the whole upper basin drains the steep northeastern flanks of the Black Hills. In contrast to the three other (and larger) study basins, there is no ambiguity regarding the area contributing to the large Elk Creek flows, demonstrating that exceptional floods can be generated wholly within the eastern Black Hills.

Enhanced flood generation from the eastern Black Hills also is consistent with paleoflood and observed records for the two Boxelder Creek subreaches, which are contiguous but separated by two tributaries that compose most of the intervening drainage area that increases from 98 to 112 mi^2 across the two subreaches (table 1). The two largest paleofloods for the downstream subreach are disproportionately larger (relative to drainage area) than for the upstream subreach (table 18). The 1972 flood peak increased from 30,100 to 51,600 ft^3/s between streamgages 06422500 and 06422650, which are located slightly beyond the two ends of the overall study reach (fig. 1, table S2–4). Schwarz and others (1975) documented a 1972 peak flow of only 1,180 ft^3/s for another site along Boxelder Creek about 3.5 mi upstream from Nemo (drainage area = 37 mi^2). This peak flow indicates that primary contributions to the 1972 runoff came from the steep and dissected terrain in the downstream reach of Boxelder Creek that generally parallels the Paleozoic outcrops along the northeastern flank of the Black Hills and that minimal runoff came from the headwater reaches.

In summary, the 1972 precipitation and runoff patterns (Schwarz and others, 1975), previous analyses of peak-flow records (Sando and others, 2008), and results of paleoflood investigations of this study together indicate distinct differences in flood generation within the central Black Hills study area. The eastern flanks are underlain by dissected Paleozoic and Precambrian rocks and produce very large flood flows, contrasting with substantially less storm runoff in and near the Limestone Plateau region. This distinction results from the combined effect of climatology and physiography on peak-flow generation and is consistent with postulations of Driscoll and others (2010). Despite the developing understanding of these regional gradients of flood generation in the Black Hills, assessment of local and regional flood-hazard management would be further improved by quantitative studies of the spatial variability of such gradients throughout the Black Hills, the relative importance of climatology compared to physiography, and the complex interactions among many variables that can affect peak-flow generation.

Application for Hazard Assessment

Results of the paleoflood investigations provide substantially improved knowledge of low-probability flood recurrence for use in flood-hazard assessments. Results are directly applicable, however, only to the specific study reaches and in the case of Rapid Creek, only to pre-regulation conditions. Consequently, extrapolation is required for applications beyond the study reaches or for drainage basins not assessed for this study. In this section of the report, appropriate domains for application of results are described and approaches for broader applications are developed from inferences of overall flood-generation processes in the Black Hills area derived from this and previous studies. Many unresolved issues and uncertainties remain, however, and this section concludes with a description of some key opportunities for future research.

Appropriate Application Domains

Most of the paleoflood investigations were conducted along the eastern margin of the central Black Hills (fig. 1), where flood generation and runoff processes may be different than for upstream and downstream reaches. Consequently, the flood-frequency estimates are most applicable to sites near the study reaches. As described previously in the “Implications for Flood Generation” section, areas west of the eastern flank the of Black Hills, particularly in and near the Limestone Plateau area, likely are outside the area of most intense rainfall and peak-flow generation.

Downstream from the Minnekahta Limestone, which is the easternmost canyon-confining Paleozoic rock unit of the eastern Black Hills (fig. 1), floodplains widen substantially for all four main streams considered in this study. Consequently, flood peaks derived from convective storm systems affecting the Black Hills typically attenuate markedly once they pass into the plains east of the Black Hills (Driscoll and others, 2010). In contrast to uncertainties in applying paleoflood results upstream from study reaches, which primarily owe to uncertainties in spatial and climatological processes of flood generation, it may be feasible to extend flood-frequency estimates to downstream sites of interest by applying flood-routing approaches capable of assessing flood dynamics in steep channels.

Quantile and Large-Flow Normalization

Although the national and regional envelope curves (figs. 53 and 54) provide a visual approach for comparing results among study reaches, more rigorous “normalizing”

with respect to drainage area allows specific comparisons among basins and provides a basis for extrapolating results beyond the specific study reaches. For this analysis, the long-term quantile estimates (PeakfqSA model) and large flow values from table 18 are normalized by dividing by drainage area raised to the 0.6 power (table 19). This analysis follows that of Sando and others (2008), who normalized large flows in developing a "regional mixed-population" approach for flood-frequency estimation for the Black Hills area. This analysis includes consideration of the actual drainage areas for the lower Rapid Creek study reach as well as the "adjusted" area that represents the intervening area of 81 mi^2 downstream from the upper Rapid Creek reach. This area adjustment is consistent with the collective information indicating probable preferential peak-flow generation within this intervening reach for the unregulated condition before construction of Pactola Dam and is further supported by analyses presented in this section.

The normalized values (table 19) further illustrate the distinct flood regime of upper Rapid Creek, for which the largest normalized paleoflood value is only 17 percent of the next smallest values (Spring Creek and the upstream subreach of Boxelder Creek) and only about 5 percent of that for Elk Creek. Similarly, the normalized quantile estimates for all other study reaches are much larger than for upper Rapid Creek— by factors approaching or exceeding 10 for most cases. The next smallest normalized quantile estimates after upper Rapid Creek are for Spring Creek, which are exceeded by those for Elk Creek by a factor of 4.5 or less. The normalized quantile estimates for Elk Creek, the two subreaches of Boxelder Creek, and the area-adjusted reach of lower Rapid Creek are relatively similar, varying by less than a factor of 2.5. The largest normalized gaged flow value is for the downstream subreach of Boxelder Creek, which exceeds those for the upstream subreach and the area-adjusted reach of lower Rapid Creek by a factor of about 0.5.

Approaches for Extrapolation and 1972 Flood Recurrence

The normalized quantile estimates allow for extrapolation of low-probability flood recurrence within appropriate domains beyond the specific study reaches, especially along the eastern flanks of the Black Hills where the results are most applicable. Extrapolation of results allows assessment of 1972 flood recurrence for locations beyond the extent of the paleoflood study reaches.

Extrapolation Within Study Basins

Results of the paleoflood investigations are most applicable within the study basins and for locations near the paleoflood study reaches. An appropriate approach for extrapolation is to use the normalized quantile estimates from table 19 as index values that can be "scaled" to other locations of interest by multiplying by drainage area raised to the 0.6 power, which is the same exponent that was used for normalizing. This approach is similar to approaches described by Burr and Korkow (1996) and Sando (1998) for extrapolating at-site quantile estimates to ungaged locations.

An example application of such scaling is to estimate flood quantiles for selected streamgages (table 20), thereby allowing direct comparison with other at-site flood-frequency analyses. For comparison, table 20 also provides quantile estimates for the streamgages that were computed by Sando and others (2008) using a mixed-population analysis. That analysis involved defining a regional "high-outlier" probability distribution that was combined (using joint-probability theory) with site-specific probability distributions for individual streamgages. That approach resulted in divergence from the site-specific ("ordinary peaks") distributions to increasingly larger peak-flow estimates for recurrence intervals larger than about 50 to 100 years. In all cases except for the upper Rapid Creek reach, the quantile estimates derived from the paleoflood studies and scaled to the streamgage areas are larger than those estimated by Sando and others (2008) from the mixed-population analysis.

Extrapolation of results to streamgage locations also allows broader evaluation of recurrence intervals for the 1972 flooding and other large measured flows. For example, the 1972 flow for the Spring Creek study reach was 21,800 ft^3/s (largest gaged flow; table 18), which corresponds with a recurrence interval approaching 400 years (fig. 15*B*, table 18). For upstream streamgage 06407500, the scaled quantile estimates (table 20) are nearly identical to the long-term estimates for the study reach (table 18), and the 1972 flow estimate of 20,000 ft^3/s (table S2–1) similarly has a recurrence interval approaching 400 years. The 1972 flood peak along Spring Creek attenuated to about 13,400 ft^3/s for downstream streamgage 06408500 (table S2–1), and another large flow of 6,910 ft^3/s occurred in 1996. Recurrence intervals for these 1972 and 1996 flows are slightly less than 200 and 100 years, respectively, based on the scaled quantile estimates (table 20); whereas, recurrence intervals from Sando and others (2008) are much larger (substantially exceeding the 200-year quantile estimate) and seemingly are less reliable. Because streamgage 06408500 is located about 8 mi downstream from the outcrop of the Minnekahta Limestone (fig. 1), extrapolation within this domain may be considered questionable. However, this example illustrates the utility of considering information from multiple sources in evaluating low-probability flood recurrence.

Schwarz and others (1975) documented a 1972 peak flow of 5,630 ft^3/s for a site along Spring Creek just upstream from Sheridan Lake (fig. 1; drainage area = 127 mi^2). Extrapolation of the Spring Creek quantile estimates to this domain also may be considered slightly questionable, but would yield a quantile estimate of 6,660 ft^3/s for a recurrence interval of about 100 years. Extrapolation of quantile estimates is not considered appropriate for the 1972 peak flow of 14,900 ft^3/s for streamgage 435915103241200 (table S2–1; fig. 1). This streamgage is located just downstream from Sheridan Lake,

which is operated primarily as a pass-through system (Driscoll and Norton, 2009). However, effects of the reservoir pool on routing of the flood wave were not necessarily trivial and have not been quantified.

The scaled quantile estimates for two streamgages along lower Rapid Creek (table 20) are larger than those from Sando and others (2008) by factors ranging from about two to five. Quantile estimates for both streamgages were scaled relative to the adjusted area of 81 mi^2, which approximates the intervening drainage area between the two Rapid Creek paleoflood study reaches. Recurrence intervals for the 1972 peak flows of 31,200 and 50,000 ft^3/s for streamgages 06412500 and 06414000, respectively (table S2–2), are about 500 years relative to scaled quantile estimates for these two streamgages. In contrast, recurrence intervals for the 1972 peak flows largely exceed 500 years relative to the quantile estimates by Sando and others (2008). Schwarz and others (1975) documented a 1972 peak flow of 7,320 ft^3/s at a site along Rapid Creek about 20 miles downstream from Rapid City, which demonstrates attenuation potential sufficiently large that extrapolation of the quantile estimates is not considered appropriate.

The importance and challenges of estimating flood recurrence are exemplified by Rapid Creek, where many of the 238 deaths from the 1972 flooding occurred. The appropriateness of the drainage-area adjustment for resolving pre- and post-regulation conditions could not be explicitly evaluated. However, the scaled values for streamgages 06412500 and 06414000 (table 20), with unregulated drainage areas of 54 and 93 mi^2, are similar to values for the Elk Creek paleoflood study reach (table 18), for which the drainage area of 40 mi^2 is not affected by regulation and, for which four exceptionally large paleofloods (75,000–83,000 ft^3/s) were recorded by stratigraphic records.

Streamgage 06410500 along upper Rapid Creek is at the location of the paleoflood study reach (fig. 1); however, scaling (table 20) was performed relative to the unregulated area of 201.6 mi^2 downstream from Deerfield Reservoir (table 1), which is consistent with a drainage-area adjustment used by Sando and others (2008). The scaled quantile estimates reflect the absence of evidence for large paleofloods in this reach and are substantially smaller than those from Sando and others (2008), who stated that the mixed-population analysis "probably results in overestimation of peak flows for large recurrence intervals for stations where drainage areas are primarily within the limestone-headwater setting." The largest gaged flows in the observational record (~1,500–2,500 ft^3/s; table 2) for streamgage 06410500 have recurrence intervals between 25 and 100 years (table 20).

In developing their region 11 envelope curve, Crippen and Bue (1977) considered three data points from a 1955 storm and flood event along Castle Creek (fig. 1), upstream from the upper Rapid Creek paleoflood reach. The largest

Table 19. Summary of normalized values for peak-flow estimates and selected large flows for paleoflood study reaches.

[--, not applicable]

Paleoflood study reach	Area[1] raised to the 0.6 power	Normalized[2] long-term peak-flow estimate (from table 18) for associated recurrence interval (annual exceedance probability)					Normalized[2] paleoflood and gaged flow values (from table 18)		
		25 years (0.04)	50 years (0.02)	100 years (0.01)	200 years (0.005)	500 years (0.002)	Largest paleoflood	Second largest paleoflood	Largest gaged flow
Spring Creek	21.9	113	207	364	622	1,230	2,580	832	997
Lower reach of Rapid Creek (actual area)	35.0	126	227	400	688	1,380	3,650	1,830	890
Lower reach of Rapid Creek (adjusted area)	14.0	316	569	1,000	1,730	3,460	9,160	4,580	2,230
Upper Rapid Creek	30.3	53	78	112	158	242	426	396	81
Upstream subreach of Boxelder Creek	15.7	214	391	690	1,180	2,330	2,590	2,490	1,970
Downstream subreach of Boxelder Creek	17.0	189	349	625	1,090	2,200	3,610	3,390	2,980
Elk Creek	9.15	384	729	1,360	2,460	5,280	9,070	8,750	1,150
Average of selected[3] normalized estimates	--	276	510	919	1,620	3,320	--	--	--

[1]Area is the drainage area for the study reach (from table 18, in square miles).

[2]Normalized values were computed by dividing flow (in cubic feet per second) by area, raised to the 0.6 power.

[3]Average computed using the lower Rapid Creek reach (adjusted area), which is the drainage area between streamgages 06410500 and 06412500, both subreaches of Boxelder Creek, and Elk Creek.

documented flow was 8,500 ft^3/s from an unregulated drainage area of 32.5 mi^2 downstream from Deerfield Reservoir. This is the largest documented flow rate for high-elevation parts of the Black Hills (Driscoll and others, 2010). Scaling of the long-term 500-year quantile estimate for upper Rapid Creek (7,340 ft^3/s; table 18) to the location of the documented flow downstream from Deerfield Reservoir yields a quantile estimate of about 1,950 ft^3/s, which is much less than the documented flow of 8,500 ft^3/s. The drainage area ratio (32.5 to 292 mi^2, or 11 percent) for the sites involved in the scaling is substantially outside the range (75–150 percent) indicated by Burr and others (1996) and Sando (1998) as appropriate for such scaling. This example illustrates (1) possible pitfalls associated with extrapolation beyond appropriate ranges; (2) uncertainties regarding storm-generation processes for the high-elevation parts of the Black Hills; and (3) attenuation potential in this part of the Rapid Creek Basin—a peak flow of 1,520 ft^3/s for the 1955 flood (table S2–3) was recorded at the downstream streamgage (06410500) above Pactola Reservoir.

Scaled quantile estimates for the upstream and downstream streamgages (06422500 and 06423010) along Boxelder Creek (table 20) are similar and were scaled relative to results for the upstream and downstream subreaches (table 19). The largest differential is for the 500-year recurrence interval, which only differs by about 10 percent. For the upstream streamgage, recurrence intervals for the large 1907 and 1972 flows (16,400 and 30,800 ft^3/s, respectively; table 2) are slightly less than 200 and 500 years, respectively, based on the scaled quantile estimates (table 20). Flow estimates for 1907 and 1972 are not available for the downstream streamgage (06423010); however, the 1972 flow of 50,500 ft^3/s for the downstream paleoflood study subreach (table 18) exceeds the 500-year quantile estimate (37,400 ft^3/s; table 18) by about 35 percent.

The scaled quantile estimates for streamgage 06424000 along Elk Creek (table 20) are about 5 to 10 times larger than those from Sando and others (2008). The drainage area ratio (21.6 to 40 mi^2, or 54 percent) is outside the range (75–150 percent) indicated by Burr and others (1996) and Sando (1998) as appropriate for such scaling. However, the scaled estimates probably are more reliable than estimates by Sando and others (2008), which were based on a short period of record (1992–2001) that did not include the large floods of 1907 and 1972. Scaling of the quantile estimates for two other long-term streamgages (06425100 and 06425500) along Elk Creek (fig. 1, table 1) was not performed because of the large drainage areas (211 and 549 mi^2, respectively) for these streamgages and extensive floodplain areas in the intervening reaches. Recurrence intervals are slightly less than 100 years for the 1972 and 1907 flow estimates of 10,400 ft^3/s for both years (table 2) for the Elk Creek study reach (table 18, fig. 52*B*).

Summarizing estimates of recurrence intervals for 1972 flooding, the recurrence interval of nearly 100 years for the Elk Creek study reach is small relative to other study reaches along the eastern margin of the Black Hills and to the four large paleofloods (75,000–83,000 ft^3/s) recorded by stratigraphic deposits. The 1972 flow for the Spring Creek study reach was 21,800 ft^3/s, which corresponds with a recurrence interval of about 400 years. Recurrence intervals are about 500 years for the 1972 flood magnitudes along the lower Rapid Creek reach and the upstream subreach of Boxelder Creek. For the downstream subreach of Boxelder Creek, the large 1972 flood magnitude (50,500 ft^3/s) exceeds the 500-year quantile estimate by about 35 percent.

Extrapolation Beyond Study Basins

The similarities among normalized quantile estimates (table 19) for the area-adjusted reach of lower Rapid Creek, the two subreaches of Boxelder Creek, and Elk Creek provide a basis for expanding the approach for extrapolation of low-probability flood recurrence to be applicable for other drainage basins along the eastern flanks of the Black Hills. Table 19 provides averages of the normalized quantile estimates for these four reaches, which can be used as index values for deriving flood-quantile estimates for other drainage basins by multiplying by drainage area raised to the 0.6 power.

An example is provided by table 21, which shows computed quantile estimates for miscellaneous-record streamgage 440325103182500 at the mouth of Cleghorn Canyon (drainage area = 7.0 mi^2), which is a tributary at the downstream extent of the lower Rapid Creek study reach (fig. 16). Estimates derived by applying regression equations for “Subregion F” from Sando (1998), using the drainage area and a channel slope of 127 ft/mi (at points 10 and 85 percent of the channel length upstream) also are provided. Only two flows, both large, have been documented for this streamgage—2,920 ft^3/s in 1962 and 12,600 ft^3/s in 1972 (U.S. Geological Survey, 2010e; Driscoll and others, 2010). The 1962 and 1972 flows both exceed the 500-year quantile estimate derived from Sando’s (1998) regression equation (by a factor of more than 5 for the 1972 flow). Relative to the scaled quantile estimates, however, the 1962 and 1972 flows are similar to the 100- and 500-year recurrence intervals, respectively.

The index values (table 21) are most applicable for drainages in the eastern Black Hills in the vicinity of the study reaches and with physiographic settings and contributing drainage areas similar to those providing the source data (Elk Creek, Boxelder Creek, and the adjusted area for the lower reach of Rapid Creek), which span 40 to 112 mi^2 (table 18). Applicability beyond the study area and for small drainage areas such as Cleghorn Canyon (fig. 16) could not be evaluated; however, the example demonstrates that the index-value and scaling approach may provide reasonable estimates of flood recurrence for consideration with other approaches for flood-frequency analysis.

Table 20. Flood-frequency analyses scaled to drainage areas for selected streamgages.

[Scaled (area), peak-flow estimates for location of streamgage derived by scaling from peak-flow estimates and drainage areas, in square miles (mi²), for appropriate paleoflood study reaches from table 19, based on exponential (0.6 power) drainage-area adjustment; ft³/s, cubic feet per second]

Streamgage name, (streamgage number), and source of peak-flow estimates	Drainage area (square miles)	Peak-flow estimate, ft³/s, for associated recurrence interval (annual exceedance probability)				
		25 years (0.04)	50 years (0.02)	100 years (0.01)	200 years (0.005)	500 years (0.002)
Spring Creek drainage basin						
Spring Creek near Keystone, S. Dak. (06407500), scaled (171 mi²)	163	2,400	4,400	7,730	13,200	26,100
Spring Creek near Keystone, S. Dak. (06407500), from Sando and others (2008)	163	1,270	1,920	3,170	6,150	23,600
Spring Creek near Hermosa, S. Dak. (06408500), scaled (171 mi²)	206	2,760	5,060	8,900	15,200	30,100
Spring Creek near Hermosa, S. Dak. (06408500), from Sando and others (2008)	206	935	1,180	1,670	4,800	27,000
Lower Rapid Creek drainage basin						
Rapid Creek above Canyon Lake near Rapid City, S. Dak. (06412500), scaled[1] (81 mi²)	[1]54	3,460	6,230	11,000	18,900	37,900
Rapid Creek above Canyon Lake near Rapid City, S. Dak. (06412500), from Sando and others (2008)	[1]54	1,020	1,450	2,150	3,750	11,800
Rapid Creek at Rapid City, S. Dak. (06414000), scaled[1] (81 mi²)	[1]93	4,790	8,630	15,200	26,300	52,500
Rapid Creek at Rapid City, S. Dak. (06414000), from Sando and others (2008)	[1]93	2,400	3,380	4,760	7,240	17,900
Upper Rapid Creek drainage basin						
Rapid Creek above Pactola Reservoir at Silver City, S. Dak. (06410500), scaled[2] (201.6 mi²)	294	1,280	1,880	2,700	3,810	5,840
Rapid Creek above Pactola Reservoir at Silver City, S. Dak. (06410500), from Sando and others (2008)	294	1,640	2,540	4,260	7,950	27,100
Boxelder Creek drainage basin						
Boxelder Creek near Nemo, S. Dak. (06422500), scaled (98 mi²)	94.4	3,280	5,990	10,600	18,100	35,700
Boxelder Creek near Nemo, S. Dak. (06422500), from Sando and others (2008)	94.4	1,440	2,100	3,120	5,660	17,200
Boxelder Creek near Rapid City, S. Dak. (06423010), scaled (112 mi²)	127	3,460	6,380	11,400	19,900	40,200
Boxelder Creek near Rapid City, S. Dak. (06423010), from Sando and others (2008)	127	1,250	1,990	2,990	5,680	20,400
Elk Creek drainage basin						
Elk Creek near Roubaix, S. Dak. (06424000), scaled (40 mi²)	21.6	2,430	4,610	8,590	15,500	33,400
Elk Creek near Roubaix, S. Dak. (06424000), from Sando and others (2008)	21.6	530	696	967	1,870	6,980

[1]Scaled using unregulated area downstream from Pactola Dam, relative to an "adjusted" area of 81 mi² for the paleoflood study reach.

[2]Scaled using unregulated area downstream from Deerfield Dam.

Table 21. Summary of example flood-frequency computations for Cleghorn Canyon.

[--, not applicable]

Variable or computational approach	Drainage area (square miles)	Peak-flow estimate, in cubic feet per second, for associated recurrence interval (annual exceedance probability)				
		25 years (0.04)	50 years (0.02)	100 years (0.01)	200 years (0.005)	500 years (0.002)
Index values for unit drainage area (1.0 square mile) from table 19	1.0	276	510	919	1,620	3,320
Scaled quantile estimate[1] from extrapolation of paleoflood results	7.0	887	1,640	2,950	5,210	10,700
Regression equations of Sando and others (1998)	7.0	388	635	972	--	2,280

[1]Scaled quantile estimates computed by multiplying index values for peak-flow estimate times drainage area raised to the 0.6 power.

Outstanding Issues and Uncertainties

Several broad issues and uncertainties warrant consideration, beyond those already addressed regarding applicability of results, spatial variability, and regional characterization of low-probability flood recurrence for the Black Hills area. One inherent issue in development of paleoflood chronologies and associated hydraulic analyses is possible underestimation of numbers and magnitudes of floods. As described in the "Methods of Investigation" section, stratigraphic records are not always complete, and elevations of flood deposits securely provide only minimum indications of maximum flood stages. Although the investigation of multiple sites within each study reach in combination with specifying ranges of plausible flood magnitudes helps to minimize the bias of such factors, the actual errors remain unknown.

Another uncertainty owes to choice of statistical treatment, including the appropriateness of the log-Pearson Type III probability distribution as best characterizing the population of extreme floods. While the choice of an appropriate distribution is important and likely is readily testable, analysis of this factor was beyond the scope of this study. The rich paleoflood dataset acquired for the Black Hills area, however, provides an opportunity for further investigation of this question.

Especially germane is the question of how applicable is the paleoflood record, for most reaches spanning the last 1,000 to 2,000 years, to the modern risk of flooding. Broad-scale climate and watershed conditions could systematically affect the frequency of extreme floods. It is plausible that the frequency of mesoscale convective systems, similar to those associated with the largest floods within the historical record for the Black Hills area (Driscoll and others, 2010), has changed during the last ~2,000 years as a consequence of climate cycles of various spatial and temporal characteristics. Watershed conditions, and the consequent relation between precipitation and runoff, also may have changed in systematic, episodic, or cyclic manners for the period of time during which the paleoflood deposits accumulated.

An important factor is forest fire, which can enhance flood magnitudes (see section "Hydrology of the Study Area"). The abundant charcoal in some flood deposits, for example the numerous charcoal-rich deposits for the Lost Alcove in the lower Rapid Creek reach and the distinctive charcoal-rich deposits in the upper Boxelder Creek subreach, is evidence that some of the largest flood magnitudes in the paleoflood record possibly were enhanced by effects of fires. A converse example is the exceptional flooding of 1972, which is known to be independent of substantial effects of fire. Without more knowledge of past basin and climate conditions, it is not yet possible to assess potential for nonstationarity in the paleoflood records. As is the case for assessing the applicability of statistical models for flood-frequency analysis, however, the rich paleoflood dataset acquired for the Black Hills area offers excellent opportunities for further pursuit of these questions. Applicability of study results regarding future watershed conditions, which probably will be subject to future fire effects and enhanced runoff potential from expanding suburban development, is another important question.

Because of such issues and uncertainties, as is the case for application of all flood-frequency analyses, broad consideration of all factors and information will likely result in the most complete assessment of flood hazards. The results of the paleoflood investigations for Spring, Rapid, Boxelder, and Elk Creeks, however, provide better physically based information on low-probability floods than has been available previously, substantially improving estimates of the magnitude and frequency of large floods in these basins and reducing associated uncertainty.

Summary

Flood-frequency analyses for the Black Hills of western South Dakota are important because of severe flooding of June 9–10, 1972, along the eastern flanks of the Black Hills. Flooding was caused by a large mesoscale convective system and resulted in at least 238 deaths. Many 1972 peak flows are high outliers (by factors of 10 or more) in observational records that date back to the early 1900s for some streamgages. In appropriate environments, an efficient means of reducing uncertainties regarding probabilities of flood recurrence is to augment gaged records by using paleohydrologic techniques—typically using geologic and paleobotanical evidence to determine ages and magnitudes of previous large floods (paleofloods). This report summarizes results of paleoflood investigations that included analyses of stratigraphic evidence, timing, and magnitudes for large floods on Spring Creek, Rapid Creek (two reaches), Boxelder Creek (two subreaches), and Elk Creek. Cooperating agencies included the South Dakota Department of Transportation, Federal Emergency Management Agency, city of Rapid City, and West Dakota Water Development District. The stratigraphic records and resulting long-term flood chronologies, locally spanning more than 2,000 years, were combined with observed and adjusted peak-flow values (gaged records) and historical flood observations to derive flood-frequency estimates for each of the six study reaches. Results indicate that (1) floods as large as and even substantially larger than 1972 have affected most of the study reaches, and (2) incorporation of the paleohydrologic information reduced uncertainties substantially in estimating flood recurrence.

The primary paleoflood evidence consists of stratigraphic records formed of fine-grained sediment deposits that accumulate and record multiple floods where velocities are low (slack-water settings) and conditions are suitable for preservation. Numerous locations in canyons within outcrops of Paleozoic rocks along the eastern flanks of the Black Hills provided excellent environments for (1) deposition and preservation of stratigraphic sequences of late-Holocene flood deposits, primarily in overhanging ledges, alcoves, and small caves flanking the streams; and (2) hydraulic analyses for determination of associated flow magnitudes. Identification of flood deposits is enhanced by Precambrian metamorphic and igneous rocks in upstream reaches that produce micaceous sands that are unambiguously distinguishable within sediment accumulations from deposits of local tributaries, slopewash, or sediment spalling from cave and alcove ceilings and walls, none of which contain mica. The bedrock canyons ensure long-term stability of the channel and valley geometry, thereby increasing confidence in hydraulic computations of ancient floods from modern channel geometry.

This study focused on characterizing low-probability flood recurrence within the six study reaches. The approach consisted of (1) interpreting individual chronologies of flood stages from detailed stratigraphic analysis and age dating of slack-water deposits for multiple sites within each reach; (2) estimating flow magnitudes associated with flood evidence; (3) interpreting an overall paleoflood chronology for each reach; and (4) conducting quantitative flood-frequency analyses incorporating paleoflood information, observational records, and historical flood accounts.

Stratigraphic analysis involved excavating pits through slack-water deposits to bedrock or immovable rocks. Pit stratigraphy was examined to determine sequences of flood deposits that typically were separated by evidence of temporal hiatus, which is key to the stratigraphic interpretations—errors in inferences can lead to under- or over-estimation of the number of floods recorded in a sequence of deposits. Where possible, stratigraphy was examined at multiple elevations at individual sites, as well as multiple sites within reaches, in order to obtain the most complete and precise stratigraphic records. Stratigraphic ages were obtained using standard geochronologic approaches, including (1) radiocarbon analysis of paleobotanical evidence; (2) optically stimulated luminescence, which was especially useful for deposits less than about 300 years old and for deposits without sufficient organic material for radiocarbon dating; and (3) cesium-137 analysis, which provided a reliable means to distinguish 1972 flood sediments from those before the mid 1940s.

A reach-scale paleoflood chronology was interpreted for each study reach. This generally entailed selecting a “benchmark” site (typically with a particularly long and complete stratigraphic record), which was supplemented by stratigraphic records, age dating, and flow-magnitude information from other sites in the reach. Interpretations required correlation of flood evidence among multiple sites, chiefly based on relative position within stratigraphic sequences, unique textural characteristics, or results of age dating and flow estimation. A bias of underestimating the number of floods in the stratigraphic record for any reach was maintained by conservative approaches for interpretations. Flood-frequency analyses incorporated gaged records and historical flood accounts, which were adjusted to be comparable to the paleoflood records determined for each study reach.

Flow rates were derived from elevations of slack-water deposits or other flood evidence in conjunction with hydraulic calculations, primarily using the River Analysis System (HEC-RAS) hydraulic model developed by the Hydrologic Engineering Center of the U.S. Army Corps of Engineers. HEC-RAS models were applied for study reaches along Spring Creek, Boxelder Creek, and the downstream of two reaches for Rapid Creek. Models were calibrated for high-flow conditions using information from 1972 flooding, which allowed evaluation of Manning’s *n* values and provided confidence regarding digital topographic coverages and overall model functionality. Other approaches for flow estimation (critical-flow or Manning equations) were used for Elk Creek and an upstream reach of Rapid Creek, where HEC-RAS models were not justified because of sparse paleoflood information.

Two analytical models (FLDFRQ3 and PeakfqSA) with capabilities for incorporating paleoflood data were applied for flood-frequency analyses. Both models allow specification of dates, flow rates, and perception thresholds for peak-flow events. Perception thresholds provide constraining information regarding known (or presumed) exceedances (or non-exceedances) of especially large flood magnitudes within specified timeframes. Flood-frequency analyses were computed assuming log-Pearson Type III frequency distributions and were performed for as many as four flood-record scenarios: (1) analysis of gaged records only; (2) gaged records in combination with historical flow information (when available); (3) all available data, which may include gaged records, historical flows, paleofloods, and thresholds; and (4) the same as the third scenario, but "top fitting" the distribution by arbitrarily including only the largest 50 percent of the gaged peak flows. The Weibull plotting position was used for graphical representations of flood-frequency analyses. The PeakfqSA model is most consistent with procedures adopted by most Federal agencies for flood-frequency analysis and was (1) used for comparisons among results for study reaches, and (2) considered by the authors as most appropriate for general applications of estimating low-probability flood recurrence.

For each study reach, detailed paleoflood investigations involved hydraulic analyses, interpretation of paleoflood chronologies from stratigraphic records, and flood-frequency analyses, which together allowed understanding of the history and recurrence of low-probability floods. For Spring Creek, a chronology of at least five paleofloods with magnitudes approaching or exceeding the 1972 flow of 21,800 cubic feet per second (ft^3/s) was preserved by stratigraphic records dating back approximately (~) 1,000 years. The largest paleoflood was ~700 years ago with a flow range of 29,300–58,600 ft^3/s, which reflects the uncertainty regarding flood-magnitude estimates that was incorporated in the flood-frequency analyses. A paleoflood ~450 years ago had a flow of 18,200–36,400 ft^3/s, and three paleofloods had flows of 13,900–27,800 ft^3/s or smaller. Flood-frequency analyses were performed using the FLDFRQ3 and PeakfqSA flood-frequency models for three scenarios: (1) gaged records only, (2) all available data (including paleoflood chronologies and perception thresholds), and (3) top-fitting analysis (PeakfqSA only). The flood-quantile estimates derived using the PeakfqSA model (accounting for all gaged and paleoflood information without top fitting) were considered by the authors as most appropriate for general applications of estimating low-probability flood recurrence. For the PeakfqSA model, consideration of all available data (scenario 2) relative to scenario 1 (gaged records only) increased the magnitudes of the 100- and 500-year floods by about 27 and 29 percent, respectively, and reduced the associated 95-percent confidence intervals by about 90 and 95 percent.

The "lower" reach of Rapid Creek (downstream from Pactola Dam) is of primary interest; however, the paleoflood chronology for this reach pre-dates construction of Pactola Dam. Thus, detailed investigations also were conducted in an "upper" reach (upstream from Pactola Reservoir).

In the lower reach of Rapid Creek, two paleofloods in the last ~1,000 years exceeded the 1972 flow of 31,200 ft^3/s. The largest (~440 years ago) had a flow of 128,000–256,000 ft^3/s and another (~1,000 years ago) had a flow of 64,000–128,000 ft^3/s. Five smaller paleofloods of 9,500–19,000 ft^3/s occurred between ~200 and 400 years ago. Flood-frequency analyses for lower Rapid Creek included consideration of four historical floods (1878, 1883, 1907, and 1920) with flows of ~7,000 to 12,000 ft^3/s. The 100-, 200-, and 500-year quantile estimates for the analysis with all available data (PeakfqSA model) were substantially larger than for the analyses of the gaged records only and for gaged records plus historical data, reflecting the paleoflood evidence for this reach. The associated 95-percent confidence intervals were reduced by more than 80 percent, relative to analyses for gaged records only.

Two paleofloods of ~12,900 and 12,000 ft^3/s occurred along upper Rapid Creek ~1,000 and 1,500 years ago, respectively. Only one additional paleoflood (~800 years ago) that was similar in magnitude to the largest gaged flow of 2,460 ft^3/s was identified for inclusion in the paleoflood chronology. Compared to lower Rapid Creek and all other study reaches, the largest floods along upper Rapid Creek are substantially smaller. Because of the sparse evidence for large paleofloods, the 100-, 200-, and 500-year quantile estimates considering all available data (PeakfqSA model) are less than 10 percent larger than for the analyses of gaged records only. Because the paleoflood record spans at least 1,000 years, the corresponding 95-percent confidence intervals for the paleoflood analysis are much smaller than those from analyses of gaged records only, with reductions of 78 percent or more for recurrence intervals of 100 years and larger.

Boxelder Creek was treated as having two subreaches because of two relatively large tributaries that substantially affect peak-flow conditions. During the last ~1,000 years, two paleofloods in the upstream subreach have exceeded the 1972 peak flow of 30,800 ft^3/s—both occurred during the last ~500 years, with associated flow estimates 39,000–78,000 ft^3/s and 40,000–80,000 ft^3/s. One other paleoflood ~1,000 years ago was similar to the second largest flow of record (16,400 ft^3/s in 1907). Incorporation of all available data into the flood-frequency analyses (PeakfqSA model) reduced the 100-, 200-, and 500-year quantile estimates by about 50 to 65 percent, compared to the similar analysis of the gaged record only, and reduced the uncertainty in the estimates by more than 99 percent.

Two paleofloods in the last ~1,000 years have substantially exceeded the 1972 flood of 50,500 ft^3/s in the downstream subreach of Boxelder Creek. The largest (61,300–123,000 ft^3/s) was ~700 years ago and the second largest (52,500–105,000 ft^3/s) was ~900 years ago. Four additional paleofloods between ~450 and 1,000 years ago had flows between ~14,200 and 33,800 ft^3/s. The flood-quantile estimates (PeakfqSA model) are nearly identical to those independently determined for the upstream subreach and are

much smaller than those derived using the gaged records only. The quantile estimates are reduced by 60 percent or more for recurrence intervals of 100 years and larger, and the associated 95-percent confidence intervals are reduced by more than 99 percent.

The 1972 flow on Elk Creek (10,400 ft^3/s) has been substantially exceeded at least five times in the last 1,900 years. The largest paleoflood (41,500–124,000 ft^3/s) was ~900 years ago. Three other paleofloods between 37,500 and 120,000 ft^3/s occurred about 1,800, 1,700, and 1,100 years ago. A fifth paleoflood ~750 years ago had a flow of 25,500–76,500 ft^3/s. The magnitude of a 1907 historical flood is unknown, but for purposes of flood-frequency analysis, is inferred to be similar to that of 1972. Quantile estimates using all available data (PeakfqSA model) are more than twice as large as those derived using gaged records only for all recurrence intervals, and the 95-percent confidence intervals were reduced by 96 percent or more for the 100-, 200-, and 500-year recurrence intervals.

In total, the flood-frequency analyses for the 6 study reaches account for 29 large paleofloods inferred from examination and interpretation of stratigraphic records locally extending back 2,000 years and including 29 sites (19 primary sites and 10 supplemental sites). Collective examination of results provides insights regarding regional flood-generation processes and their spatial controls, enables approaches for extrapolation of results for hazard assessment beyond specific study reaches, and provides a millennial-scale perspective on the 1972 flooding.

Considering analyses for all available data for all six study reaches (including paleoflood information) from the PeakfqSA model, which accord most closely to established Federal procedures for flood-frequency analysis, the 95-percent confidence intervals about the low-probability quantile estimates (100-, 200-, and 500-year recurrence-intervals) were reduced by at least 78 percent relative to similar analyses of the gaged records only. In some cases, 95-percent uncertainty limits were reduced by 99 percent or more. For all study reaches except the two Boxelder Creek subreaches, quantile estimates for these long-term analyses were larger than for the short-term analyses. The 100- and 500-year quantile estimates increased by 61 and 73 percent, respectively, for lower Rapid Creek and by about 130 and 140 percent for Elk Creek. For Spring Creek and the upstream reach of Rapid Creek, increases in quantile estimates were smaller. The 100- and 500-year quantile estimates decreased by 48 and 65 percent for the upstream subreach of Boxelder Creek and decreased by 62 and 76 percent for the downstream subreach. The paleoflood chronologies for the two subreaches of Boxelder Creek were determined independently, and although the stratigraphic records cannot precisely be correlated between the two subreaches, the general similarities between results tend to affirm the overall study approaches.

All of the paleofloods plot within the bounds of a national envelope curve, indicating that the national curve represents exceedingly rare floods for the Black Hills area. Several Black Hills paleofloods plot above a regional envelope curve, which is poorly constrained. Elk Creek, lower Rapid Creek, and the downstream subreach of Boxelder Creek all had paleofloods that exceed the regional curve; in the case of Elk Creek, by a factor of nearly two. The Black Hills paleofloods represent some of the largest known floods, relative to drainage area, for the United States. Many of the other largest known United States floods are in areas with physiographic and climatologic conditions broadly similar to the Black Hills—semiarid and rugged landscapes that intercept and focus heavy precipitation from convective storm systems.

Previous investigators postulated that the eastern Black Hills are susceptible to intense orographic lifting associated with convective storm systems and also have high relief, thin soils, and narrow and steep canyons—factors favoring generation of exceptionally heavy rain-producing thunderstorms and promoting runoff and rapid concentration of flow into stream channels. In contrast, storm potential is smaller in and near the Limestone Plateau area, and storm runoff is reduced further by substantial infiltration into the limestone, gentle topography, and extensive floodplain storage. The 1972 precipitation and runoff patterns, previous analyses of peak-flow records, and results of the paleoflood investigations of this study support the hypothesis of distinct differences in flood generation within the central Black Hills study area.

Results of the paleoflood investigations are directly applicable only to the specific study reaches and in the case of Rapid Creek, only to pre-regulation conditions. Thus, approaches for broader applications were developed from inferences of overall flood-generation processes, and appropriate domains for application of results were described. Long-term quantile estimates and selected large flow values were normalized by dividing by drainage area raised to the 0.6 power. The normalized quantile estimates allow for extrapolation of low-probability flood recurrence within appropriate domains beyond the specific study reaches, especially along the eastern flanks of the Black Hills.

An appropriate approach for extrapolation is to use the normalized quantile estimates as index values that can be “scaled” to other locations of interest by multiplying by drainage area raised to the 0.6 power. Example applications of such scaling were provided by estimating flood quantiles for selected streamgages, which also allowed direct comparison with results of at-site flood-frequency analyses from a previous study and broader evaluation of recurrence intervals for the 1972 flooding and other large measured flows. Scaling of quantile estimates from the paleoflood investigations along upper Rapid Creek to an applicable drainage area for streamgage 06410500 (above Pactola Reservoir) reflected the absence of evidence for large paleofloods in this reach and were substantially smaller than those from a previous study. In all other example cases, the quantile estimates derived from the paleoflood studies and scaled to the streamgage areas were larger than those from a previous study.

The 1972 flow for the Spring Creek study reach (21,800 ft^3/s) corresponds with a recurrence interval of

~400 years. Recurrence intervals are ~500 years for the 1972 flood magnitudes along the lower Rapid Creek reach and the upstream subreach of Boxelder Creek. For the downstream subreach of Boxelder Creek, the large 1972 flood magnitude (50,500 ft^3/s) exceeds the 500-year quantile estimate by about 35 percent. The recurrence interval of ~100 years for 1972 flooding along the Elk Creek study reach is small relative to other study reaches along the eastern margin of the Black Hills.

An approach for extrapolation of low-probability flood recurrence to be applicable for other drainage basins along the eastern flanks of the Black Hills was developed. An example indicated recurrence intervals of about 100 and 500 years, respectively, for large flows of 2,920 ft^3/s in 1962 and 12,600 ft^3/s in 1972 for Cleghorn Canyon, which is a small tributary (drainage area = 7.0 mi^2) at the downstream extent of the lower Rapid Creek study reach.

Several broad issues and uncertainties were examined, including potential biases associated with stratigraphic records that inherently are not always complete, uncertainties regarding statistical approaches, and the unknown applicability of paleoflood records to future watershed conditions. Because of such issues and uncertainties, as is the case for application of all flood-frequency analyses, broad consideration of all factors and information is most likely to result in the most complete assessment of flood hazards. The results of the paleoflood investigations for Spring, Rapid, Boxelder, and Elk Creeks, however, provide much better physically based information on low-probability floods than has been available previously, substantially improving estimates of the magnitude and frequency of large floods in these basins and reducing associated uncertainty.

References Cited

Accelerator Mass Spectrometry Laboratory, 2011, Accelerator Mass Spectrometry Laboratory, University of Arizona, Tucson, Ariz., accessed June 2, 2011, at *http://www.physics.arizona.edu/ams*.

Agnew, William, Lahn, R.E., and Harding, M.V., 1997, Buffalo Creek, Colorado, fire and flood of 1996: Land and Water, v. 41, p. 27–29.

Baker, V.R., 1987, Paleoflood hydrology and extraordinary flood events: Journal of Hydrology, v. 96, p. 79–99.

Barnes, H.H., 1967, Roughness characteristics of natural channels: U.S. Geological Survey Water-Supply Paper 1849, 213 p.

Benson, M.A., and Dalrymple, T., 1967, General field and office procedures for indirect discharge measurements: U.S. Geological Survey Techniques of Water-Resources Investigations, book 3, chap. A1, 30 p.

Blong, R.J., and Gillespie, R., 1978, Fluvially transported charcoal gives erroneous ^{14}C ages for recent deposits: Nature, v. 271, p. 739–741.

Bradley, R.S., 1999, Paleoclimatology—Reconstructing climates of the Quaternary (2d ed.): Burlington, Mass., Harcourt Academic Press, p. 80–89.

Bronk Ramsey, Christopher, 2009, Bayesian analysis of radiocarbon dates: Radiocarbon, v. 51, no. 1, p. 337–360.

Bronk Ramsey, Christopher, van der Plicht, J., and Weninger, B., 2001, “Wiggle matching” radiocarbon dates: Radiocarbon, v. 43, no. 2A, p. 381–389.

Brown, P.M., and Sieg, C.H., 1996, Fire history in interior ponderosa pine communities of the Black Hills, South Dakota, USA: International Journal of Wildland Fire, v. 6, no. 3, p. 97–105.

Burr, M.J., and Korkow, K.L., 1996, Peak-flow frequency estimates through 1994 for gaged streams in South Dakota: U.S. Geological Survey Open-File Report 96–202, 407 p.

Carter, J.M., Williamson, J.E., and Teller, R.W., 2002, The 1972 Black Hills-Rapid City flood revisited: U.S. Geological Survey Fact Sheet FS–037–02, 6 p. (Also available at *http://pubs.usgs.gov/fs/fs-037-02/*.)

Center for Accelerator Mass Spectrometry, 2011, Center for Accelerator Mass Spectrometry, Lawrence Livermore National Laboratory, Livermore, Calif., accessed June 2, 2011, at *http://cams.llnl.gov.*

City of Rapid City, 2010, Pennington County-Rapid City GIS, accessed March 10, 2010, at *http://www.rcgov-gis.org/imf/sites/RapidMap/jsp/launch.jsp?popup_blocked=true*.

Cohn, T.A., Lane, W.L., and Baier, W.G., 1997, An algorithm for computing moments-based quantile estimates when historical flood information is available: Water Resources Research, v. 33, no. 9, p. 2,089–2,096.

Cohn, T.A., Lane, W.L., and Stedinger, J.R., 2001, Confidence intervals for expected moments algorithm flood quantile estimates: Water Resources Research, v. 37, no. 6, p. 1,695–1,706.

Costa, J.E., 1978, Holocene stratigraphy in flood frequency analysis: Water Resources Research, v. 14, no. 4, p. 626–632.

Costa, J.E., 1987, A comparison of the largest rainfall-runoff floods in the United States with those of the People’s Republic of China and the world: Journal of Hydrology, v. 96, p. 101–115.

Costa, J.E., and Jarrett, R.D., 2008, An evaluation of selected extraordinary floods in the United States reported by the U.S. Geological Survey and implications for future advancement of flood science: U.S. Geological Survey Scientific Investigations Report 2008–5164, 232 p., accessed April 6, 2011, at *http://pubs.usgs.gov/sir/2008/5164/*.

Covington, W.W., and More, M.M., 1994, Southwestern ponderosa forest structure—Changes since Euro-American settlement: Journal of Forestry, v. 92, p. 39–47.

Crippen, J.R., and Bue, C.D., 1977, Maximum flood flows in the conterminous United States: U.S. Geological Survey Water-Supply Paper 1887, 52 p.

Driscoll, D.G., and Carter, J.M., 2001, Hydrologic conditions and budgets for the Black Hills of South Dakota, through water year 1998: U.S. Geological Survey Water-Resources Investigations Report 01–4226, 143 p. (Also available at *http://pubs.usgs.gov/wri/wri014226/*.)

Driscoll, D.G., and Norton, P.A., 2009, Hydrologic characterization for Spring Creek and hydrologic budget and model scenarios for Sheridan Lake, South Dakota, 1962–2007: U.S. Geological Survey Scientific Investigations Report 2009–5059, 80 p. (Also available at *http://pubs.usgs.gov/sir/2009/5059/*.)

Driscoll, D.G., Bunkers, M.J., Carter, J.M., Stamm, J.F., and Williamson, J.E., 2010, Thunderstorms and flooding of August 17, 2007, with a context provided by a history of other large storm and flood events in the Black Hills area of South Dakota: U.S. Geological Survey Scientific Investigations Report 2010–5187, 139 p. (Also available at *http://pubs.usgs.gov/sir/2010/5187/*.)

Driscoll, D.G., Carter, J.M., and Ohlen, D.O., 2004, Hydrologic effects of the 1988 Galena fire, Black Hills area, South Dakota: U.S. Geological Survey Water-Resources Investigations Report 03–4323, 67 p. (Also available at *http://pubs.usgs.gov/wri/wri034323/*.)

Driscoll, D.G., Carter, J.M., Williamson, J.E., and Putnam, L.D., 2002, Hydrology of the Black Hills area, South Dakota: U.S. Geological Survey Water-Resources Investigations Report 02–4094, 150 p. (Also available at *http://pubs.usgs.gov/wri/wri024094/*.)

Driscoll, D.G., Hamade, G.R., and Kenner, S.J., 2000, Summary of precipitation data for the Black Hills area of South Dakota, water years 1931–98: U.S. Geological Survey Open-File Report 00–329, 151 p. (Also available at *http://sd.water.usgs.gov/pubs/reports/ofr00-329.pdf*.)

Duller, G.A.T., 2008, Luminescence dating—Guidelines on using luminescence dating in archeology: Swindon, United Kingdom, English Heritage, 44 p.

Ely, L.L., Enzel, Y., Baker, V.R., and Cayan, D.R., 1993, A 5000-yr record of extreme floods and climate change in the southwestern United States: Science, v. 262, p. 410–412.

Environmental Systems Research Institute, 2010, ArcGIS 9.3 software, accessed July 2009 at *http://www.ersi.com/*.

Enzel, Yehouda, Ely, L.L., House, K.P., Baker, V.R., and Webb, R.H., 1993, Paleoflood evidence for a natural upper bound to flood magnitudes in the Colorado River Basin: Water Resources Research, v. 29, no. 7, p. 2,287–2,297.

Enzel, Yehouda, Ely, L.L., Martinez-Goyre, J., and Vivian, R.G., 1994, Paleofloods and a dam failure flood on the Virgin River, Utah and Arizona: Journal of Hydrology, v. 153, p. 291–315.

Frances, Felix, Salas, J.D., and Boes, D.C., 1994, Flood frequency analysis with systematic and historical or paleoflood data based on the two-parameter general extreme value models: Water Resources Research, v. 30, no. 6, p. 1,653–1,664.

Grafe, Ernest, and Horsted, Paul, 2002, Exploring with Custer—The 1874 Black Hills Expedition: Custer, S. Dak., Golden Valley Press, 288 p.

Grant, G.E., 1997, Critical flow constrains flow hydraulics in mobile-bed streams—A new hypothesis: Water Resources Research, v. 33, p. 349–358.

Griffis, V.W., Stedinger, T.A., and Cohn, T.A., 2004, Log Pearson type 3 quantile estimators with regional skew information and low outlier adjustments: Water Resources Research, v. 40, no. 10, 17 p., citation number W07503, doi:10.1029/2003WR002697, accessed July 25, 2011, at *http://www.agu.org/pubs/crossref/2004/2003WR002697.shtml*.

Helsel, D.R., and Hirsch, R.M., 2002, Statistical methods in water resources: U.S. Geological Survey Techniques of Water Resources Investigations, book 4, chap. A3, 522 p.

Holmes, C.W., 1998, Short lived isotopic chronometers—A means of measuring decadal sedimentary dynamics: U.S. Geological Survey Fact Sheet FS–073–98, 1 p.

Honerkamp, J.R., 1978, At the foot of the mountain: Stickney, S. Dak., Argus Printers, 231 p.

Hortness, J.E., and Driscoll, D.G., 1998, Streamflow losses in the Black Hills of western South Dakota: U.S. Geological Survey Water-Resources Investigations Report 98–4116, 99 p. (Also available at *http://pubs.usgs.gov/wri/wri984116/*.)

Hosking, J.R.M., and Wallis, J.R., 1986, Paleoflood hydrology and flood frequency analysis: Water Resources Research, v. 22, no. 4, p. 543–550.

Hosman, K.J., Ely, L.L., and O'Connor, J.E., 2003, Holocene paleoflood hydrology of the lower Deschutes River, Oregon, *in* O'Connor, J.E., and Grant, G.E., eds., A peculiar river—Geology, geomorphology and hydrology of the Deschutes River, Oregon: American Geophysical Union Water Science and Application Series 7, p. 121–146.

Interagency Advisory Council on Water Data, 1982, Guidelines for determining flood flow frequency: Hydrology Subcommittee, Bulletin 17B, appendixes 1–14, 28 p.

International Association of Hydrological Sciences, 2003, World catalogue of maximum observed floods, compiled by Reg Herschy: Wallingford, Oxfordshire, U.K., IAHS Press, IAHS-AISH Publication 284, 285 p.

Jarrett, R.D., and England, J.F., Jr., 2002, Reliability of paleostage indicators for paleoflood studies, *in* House, P.K., Webb, R.H., Baker, V.R., and Levish, D.L., eds., Ancient floods, modern hazards—Principles and applications of paleoflood hydrology: Washington, D.C., American Geophysical Union's Water Science and Application Series, v. 5, p. 91–109, plus CD-ROM.

Kochel, R.C., and Baker, V.R., 1982, Paleoflood hydrology: Science, v. 215, p. 353–361.

Kochel, R.C., and Baker, V.R., 1988, Paleoflood analysis using slackwater deposits, *in* Baker, V.R., Kochel, R.C., and Patton, P.C., eds., Flood geomorphology: New York, John Wiley and Sons, p. 357–376.

Larimer, O.J., 1973, Flood of June 9–10, 1972, at Rapid City, South Dakota: U.S. Geological Survey Hydrologic Investigations Atlas HA–511, 1 sheet, scale 1:18,000.

Levish, D.R., 2002, Paleohydrologic bounds—Non-exceedance information for flood hazard assessment, *in* House, P.K., Webb, R.H., Baker, V.R., and Levish, D.L., eds., Ancient floods, modern hazards—Principles and applications of paleoflood hydrology: Washington, D.C., American Geophysical Union's Water Science and Application Series, v. 5, p. 175–190.

Miller, L.D., and Driscoll, D.G., 1998, Streamflow characteristics for the Black Hills of South Dakota, through water year 1993: U.S. Geological Survey Water-Resources Investigations Report 97–4288, 322 p. (Also available at *http://pubs.usgs.gov/wri/wri974288/.*)

O'Connell, D.R.H., 1999, FLDFRQ3 user's guide, release 1.1: U.S. Bureau of Reclamation, 19 p.

O'Connell, D.R.H., Ostenaa, D.A., Levish, D.R., and Klinger, R.E., 2002, Bayesian flood frequency analysis with paleohydrologic bound data: Water Resources Research, v. 35, no. 5, doi:10.1029/2000WR000028, accessed July 25, 2011, at *http://www.agu.org/pubs/crossref/2002/2000WR000028.shtml.*

O'Connor, J.E., and Costa, J.E., 2004, Spatial distribution of the largest rainfall-runoff floods from basins between 2.6 and 26,000 km^2 in the United States and Puerto Rico: Water Resources Research, v. 40, 11 p., citation number WR002247, doi: 10.1029/2003, accessed July 25, 2011, at *http://www.agu.org/pubs/crossref/2004/2003WR002247.shtml*.

O'Connor, J.E., and Driscoll, D.G., 2007, Applicability of paleoflood surveys to the Black Hills of western South Dakota: Completion report SD2005–12 submitted to South Dakota Department of Transportation, Office of Research, 59 p., accessed March 16, 2010, at *http://apps.sd.gov/Applications/HR19ResearchProjects/Projects/SD2005-12_Final_Report.pdf*.

O'Connor, J.E., and Webb, R.H., 1988, Hydraulic modeling for paleoflood analysis, *in* Baker, V.R., Kochel, R.C., and Patton, P.C., eds., Flood geomorphology: New York, John Wiley and Sons, p. 393–402.

O'Connor, J.E., Ely, L.L., and Wohl, E.E., 1994, A 4500-yr record of large floods on the Colorado River in the Grand Canyon: Journal of Geology, v. 102, p. 1–9.

Prescott, J.R., and Hutton, J.T., 1994, Cosmic ray contribution to dose rates for luminescence and ESR dating—Large depths and long-term time variations: Radiation Measurements, v. 23, no. 2–3, p. 497–500.

Progulske, D.R., 1974, Yellow ore, yellow hair, yellow pine—A photographic survey of a century of forest ecology: Brooking, S. Dak., Agricultural Experiment Station, South Dakota State University, Bulletin 616, 169 p.

Redden, J.A., and Lisenbee, A.L., 1996, Geologic setting, Black Hills, South Dakota, *in* Paterson, C.J., and Kirchner, J.G., eds., Guidebook to the geology of the Black Hills, South Dakota: Rapid City, S. Dak., South Dakota School of Mines and Technology Bulletin No. 19, p. 1–8.

Reimer, P.J., Baillie, M.G.L., Bard, E., Bayliss, A., Beck, J.W., Blackwell, P.G., Bronk Ramsey, C., Buck, C.E., Burr, G.S., Edwards, R.L., Friedrich, M., Grootes, P.M., Guilderson, T.P., Hajdas, I., Heaton, T.J., Hogg, A.G., Hughen, K.A., Kaiser, K.F., Kromer, B., McCormac, F.G., Manning, S.W., Reimer, R.W., Richards, D.A., Southon, J.R., Talamo, S., Turney, C.S.M., van der Plicht, J., and Weyhenmeyer, C.E., 2009, IntCal09 and Marine09 radiocarbon age calibration curves, 0–50,000 years cal BP: Radiocarbon, v. 51, no. 4, p. 1,111–1,150.

Sando, S.K., 1998, Techniques for estimating peak-flow magnitude and frequency relations for South Dakota streams: U.S. Geological Survey Water-Resources Investigations Report 98–4055, 48 p. (Also available at *http://pubs.usgs.gov/wri/wri98-4055/*.)

Sando, S.K., Driscoll, D.G., and Parrett, Charles, 2008, Peak-flow frequency estimates based on data through water year 2001 for selected streamflow-gaging stations in South Dakota: U.S. Geological Survey Scientific Investigations Report 2008–5104, 367 p., accessed March 13, 2010, at *http://pubs.usgs.gov/sir/2008/5104/*.

Schwarz, F.K., Hughes, L.A., Hansen, E.M., Petersen, M.S., and Kelly, D.B., 1975, The Black Hills-Rapid City Flood of June 9–10, 1972—A description of the storm and flood: U.S. Geological Survey Professional Paper 877, 47 p.

Sheffer, N.A., Rico, M., Enzel, Y., Benito, G., and Grodek, T., 2008, The paleoflood record of the Gardon River, France—A comparison with the extreme 2002 flood event: Geomorphology, v. 98, p. 71–83.

Strobel, M.L., Jarrell, G.J., Sawyer, J.F., Schleicher, J.R., and Fahrenbach, M.D., 1999, Distribution of hydrogeologic units in the Black Hills area, South Dakota: U.S. Geological Survey Hydrologic Investigations Atlas HA–743, 3 sheets, scale 1:100,000. (Also available at *http://pubs.usgs.gov/ha/ha743/*.)

South Dakota Department of Transportation, 2010, Application of paleoflood survey techniques in the Black Hills of South Dakota: South Dakota Department of Transportation, Office of Research, Project Synopsis for Project SD2008–01, accessed February 17, 2010, at *http://apps.sd.gov/Applications/HR19ResearchProjects/oneproject_search.asp?projectnbr=SD2008-01*.

Stedinger, J.R., and Baker, V.R., 1987, Surface water hydrology—Historical and paleoflood information: Review of Geophysics, v. 25, no. 2, p. 119–124.

Stedinger, J.R., and Cohn, T.A., 1986, Flood frequency analysis with historical and paleoflood information: Water Resources Research, v. 22, no. 2, p. 785–793.

Stuiver, Minze, and Polach, H.A., 1977, Discussion—Reporting of ^{14}C data: Radiocarbon, v. 19, no. 3, p. 355–363.

Taylor, R.E., 2001, Radiocarbon dating, *in* Brothwell, D.R., and Pollard, A.M., eds., Handbook of archaeological sciences: Chichester and New York, John Wiley, p. 23–24.

U.S. Army Corps of Engineers, 1973: Flood plain information, Rapid Creek, Rapid City, South Dakota: Department of the Army, Omaha District, 48 p., plus plates.

U.S. Army Corps of Engineers, 2008a, HEC-RAS River Analysis System user's manual, version 4.0: U.S. Army Corps of Engineers, variously paginated.

U.S. Army Corps of Engineers, 2008b, HEC-RAS River Analysis System hydraulic reference manual, version 4.0: U.S. Army Corps of Engineers, variously paginated.

U.S. Environmental Protection Agency, 2010, Radiation protection—Cesium, accessed March 3, 2010, at *http://www.epa.gov/radiation/radionuclides/cesium.html*.

U.S. Geological Survey, 2010a, History of flooding in the Black Hills, accessed May 11, 2010, at *http://sd.water.usgs.gov/projects/FloodHistory/floodhistory.html*.

U.S. Geological Survey, 2010b, Eastern Earth Surface Processes Team, Reston, Virginia, accessed March 22, 2010, at *http://geology.er.usgs.gov/eespteam*.

U.S. Geological Survey, 2010c, Luminescence Dating Laboratory, Lakewood, Colo., accessed March 22, 2010, at *http://crustal.usgs.gov/laboratories/luminescence_dating/index.html*.

U.S. Geological Survey, 2010d, Florida Integrated Science Center, accessed March 22, 2010, at *www.usgs.gov/state/state.asp?State=FL*.

U.S. Geological Survey, 2010e, National Water Information System (NWISWeb)—Peak streamflow for South Dakota: U.S. Geological Survey database, accessed March 22, 2010, at *http://nwis.waterdata.usgs.gov/sd/nwis/peak*.

Vogel, J.S., Southon, J.R., Nelson, D.E., and Brown, T.A., 1984, Performance of catalytically condensed carbon for use in accelerator mass spectrometry, nuclear instruments and methods in physics research, section B: Beam Interactions with Materials and Atoms, v. 5, issue 2, p. 289–293.

Walker, M., 2005, Quaternary dating methods: Chichester, England, John Wiley and Sons, Ltd., 286 p.

Webb, R.H., Blainey, J.B., and Hyndman, D.W., 2002, Paleoflood hydrology of the Paria River, southern Utah and Northern Arizona, USA, *in* House, P.K., Webb, R.H., Baker, V.R., and Levish, D.L., eds., Ancient floods, modern hazards—Principles and applications of paleoflood hydrology: Washington, D.C., American Geophysical Union's Water Science and Application Series, v. 5, p. 295–310.

Wells, J.V.B., 1962, Floods of 1955: U.S. Geological Survey Water Supply Paper 1455, 74 p.

Weibull, Waloddi, 1939, A statistical theory of the strength of materials: Handlingar, Ingeniors Ventenskaps Akademian, v. 151–3, p. 45–55.

Wohl, E.E., Webb, R.H., Baker, V.R., and Pickup, G., 1994, Sedimentary flood records in the bedrock canyons of rivers in the monsoonal region of Australia: Water Resources Papers, v. 107, 102 p.

Wolman, M.G., and Costa, J.E., 1984, Envelope curves for extreme flood events—Discussion: Journal of Hydraulic Engineering, v. 110, no. 1, p. 77–78.

Supplement 1. Age-Dating Tables

This supplemental section contains tables that present age-dating results for radiocarbon samples (table S1–1), optically stimulated luminescence samples (table S1–2), and cesium-137 samples (table S1–3).

Table S1–1. Results of laboratory analyses for radiocarbon samples.

[ID, identification number; ^{14}C yr BP, uncalibrated carbon-14 age in years before present (referenced to A.D. 1950) calculated using the Libby half-life of 5,568 years; $^{13}C/^{12}C$, ratio of carbon-13 to carbon-12; ±, plus or minus; --, analysis could not be performed; "Modern" results indicate a post A.D. 1950 age and are not calibrated; calibrated age ranges and median ages calculated on the basis of Oxcal 4.1 (Bronk Ramsey and others, 2001; Bronk Ramsey, 2009) using IntCal09 calibration dataset (Reimer and others, 2009)]

ID	Sample date	Field sample number	Laboratory identification number	Site or alcove and pit (if applicable)	Material sampled	^{14}C yr BP ±1-sigma error	$^{13}C/^{12}C$	Calibrated 2-sigma age ranges (fraction of probability density function)	Median age
Spring Creek study reach									
1	05/31/2006	3A(4)	ww6003	Hailstorm pit A	Twig fragment	599±33	--	A.D. 1296–1410 (0.95)	A.D. 1347
2	05/31/2006	3A(6)	ww5983	Hailstorm pit A	Charcoal fragment	2,205±34	--	382–192 B.C. (0.95)	284 B.C.
3	05/31/2006	3B(2)	ww6004	Hailstorm pit B	Stick fragment	625±32	--	A.D. 1289–1400 (0.95)	A.D. 1350
4	05/28/2008	3(1)	ww7068	Hailstorm	Seed shell	320±25	-23.31	A.D. 1486–1644 (0.95)	A.D. 1563
5	05/28/2008	3(2)	ww7587	Hailstorm	Driftwood	130±25	-23.98	A.D. 1678–1765 (0.35); A.D. 1799–1893 (0.45); A.D. 1906–1940 (0.15)	A.D. 1825
6	08/12/2008	2A(4)	ww7697	John Doe pit A	Charcoal	865±25	-24.61	A.D. 1048–1084 (0.10); A.D. 1122–1138 (0.03); A.D. 1150–1225 (0.82)	A.D. 1187
7	08/12/2008	2B(1)	ww7399	John Doe pit B	Charcoal	1,090±30	-25	A.D. 892–1014 (0.95)	A.D. 953
8	08/12/2008	2B(3)	ww7698	John Doe pit B	Charcoal	860±25	-25.35	A.D. 1052–1080 (0.07); A.D. 1152–1253 (0.88)	A.D. 1180
9	08/12/2008	2B(4)	ww7590	John Doe pit B	Charcoal	260±25	-27.81	A.D. 1522–1573 (0.20); A.D. 1628–1670 (0.63); A.D. 1780–1800 (0.12)	A.D. 1649
10	08/12/2008	1(1)	ww7070	Near Strike	Wood fragment	60±25	-24.91	A.D. 1694–1728 (0.23); A.D. 1812–1854 (0.21); A.D. 1866–1919 (0.52)	A.D. 1878
11	06/02/2006	1(2)	ww5981	Olympia	Charcoal clast	738±32	--	A.D. 1220–1295 (0.95)	A.D. 1270
12	05/28/2008	4(1)	ww7069	Superscour pit B	Bark fragment	225±30	-29.66	A.D. 1640–1684 (0.40); A.D. 1735–1806 (0.42)	A.D. 1764
13	06/01/2006	1A(4)	ww5976	Superscour pit A	Charcoal	672±32	--	A.D. 1272–1320 (0.54); A.D. 1350–1391 (0.42)	A.D. 1310
14	06/01/2006	1A(5)	ww6005	Superscour pit A	Ponderosa pine bark	95±32	--	A.D. 1682–1736 (0.27); A.D. 1804–1934 (0.68)	A.D. 1840
15	06/01/2006	1B(2)	ww5999	Superscour pit B	Bark fragment	138±32	--	A.D. 1669–1780 (0.42); A.D. 1798–1892 (0.38); A.D. 1908–1944 (0.15)	A.D. 1810
16	06/01/2006	1B(6)	ww6000	Superscour pit B	Organic detritus	Modern	--	Modern	--
17	06/05/2007	2(1)	ww6001	Temple of Doom	Driftwood	680±34	--	A.D. 1267–1320 (0.58); A.D. 1350–1392 (0.37)	A.D. 1303
Downstream reach of Rapid Creek									
18	09/05/2008	1(1)	ww7145	Black Socks	Charcoal	770±35	-24.92	A.D. 1209–1287 (0.95)	A.D. 1251
19	09/05/2008	1(14)	ww7148	Black Socks	Wood fragment	75±35	-25.98	A.D. 1684–1732 (0.26); A.D. 1807–1928 (0.70)	A.D. 1845
20	09/05/2008	1(2)	ww7704	Black Socks	Charcoal	480±35	-25	A.D. 1400–1466 (0.95)	A.D. 1431
21	09/05/2008	1(3)	ww7735	Black Socks	Charcoal	1,580±35	--	A.D. 410-558 (0.95)	A.D. 484
22	09/05/2008	1(5)	ww7749A	Black Socks	Charcoal	155±35	--	A.D. 1665–1710 (0.17); A.D. 1716–1785 (0.32); A.D. 1793–1891 (0.30); A.D. 1908–1952 (0.17)	A.D. 1784
23	09/05/2008	1(7)	ww7147	Black Socks	Charcoal	130±30	-27.87	A.D. 1675–1778 (0.38); A.D. 1798–1894 (0.43); A.D. 1905–1942 (0.15)	A.D. 1822
24	09/05/2008	1(9)	ww7146	Black Socks	Charcoal	125±35	-26.08	A.D. 1675–1778 (0.37); A.D. 1798–1942 (0.59)	A.D. 1825
25	08/04/2008	1(3)	ww7077	Church Mug	Charcoal	360±35	-24.38	A.D. 1450–1530 (0.47); A.D. 1538–1635 (0.49)	A.D. 1540
26	06/19/2009	1B(10)	ww7581	Lost	Charcoal	1,800±25	-23.6	A.D. 130–260 (0.87); A.D. 295–322 (0.09)	A.D. 215
27	06/19/2009	1B(11)	ww7702	Lost	Charcoal	1,740±30	-25	A.D. 234–389 (0.95)	A.D. 300
28	06/19/2009	1B(15)	ww7580	Lost	Charcoal	1,795±25	-26.82	A.D. 132–260 (0.82); A.D. 284–323 (0.14)	A.D. 224

Table S1–1. Results of laboratory analyses for radiocarbon samples.—Continued

[ID, identification number; ^{14}C yr BP, uncalibrated carbon-14 age in years before present (referenced to A.D. 1950) calculated using the Libby half-life of 5,568 years; $^{13}C/^{12}C$, ratio of carbon-13 to carbon-12; ±, plus or minus; --, analysis could not be performed; "Modern" results indicate a post A.D. 1950 age and are not calibrated; calibrated age ranges and median ages calculated on the basis of Oxcal 4.1 (Bronk Ramsey and others, 2001; Bronk Ramsey, 2009) using IntCal09 calibration dataset (Reimer and others, 2009)]

ID	Sample date	Field sample number	Laboratory identification number	Site or alcove and pit (if applicable)	Material sampled	^{14}C yr BP ±1-sigma error	$^{13}C/^{12}C$	Calibrated 2-sigma age ranges (fraction of probability density function)	Median age
Downstream reach of Rapid Creek—Continued									
29	06/19/2009	1B(16)	ww7584	Lost	Charcoal	1,550±25	-24.31	A.D. 430–566 (0.95)	A.D. 491
30	06/19/2009	1B(18)	ww7579	Lost	Charcoal	1,380±25	-26.38	A.D. 612–674 (0.95)	A.D. 652
31	06/19/2009	1B(21)	ww7694	Lost	Charcoal	1,190±30	-27.18	A.D. 720–742 (0.03); A.D. 769–898 (0.89); A.D. 921–944 (0.04)	A.D. 835
32	06/19/2009	1B(25)	ww7730	Lost	Charcoal	1,665±30	--	A.D. 258–298 (0.08); A.D. 319–434 (0.86)	A.D. 383
33	06/19/2009	1B(3)	ww7585	Lost	Charcoal	2,175±25	-24.71	360–272 B.C. (0.55); 262–166 B.C. (0.41)	295 B.C.
34	06/19/2009	1B(4)	ww7582	Lost	Charcoal	2,070±25	-26.02	172–37 B.C. (0.92); 11–2 B.C. (0.02)	89 B.C.
35	06/19/2009	1B(6)	ww7701	Lost	Charcoal	2,065±25	-24.86	169–36 B.C. (0.90); 31–19 B.C. (0.03); 12–1 B.C. (0.03)	84 B.C.
36	06/19/2009	1B(7)	ww7586	Lost	Charcoal	1,795±30	-24.85	A.D. 131–262 (0.79); A.D. 280–326 (0.17)	A.D. 224
37	06/19/2009	1B(9)	ww7583	Lost	Charcoal	2,240±25	-24.71	389–347 B.C. (0.27); 318–206 B.C. (0.67)	278 B.C.
38	05/29/2008	1(1)	ww7589	Meister	Charcoal from hearth	110±30	-27.68	A.D. 1680–1763 (0.30); A.D. 1801–1938 (0.66)	A.D. 1836
39	08/15/2008	1(2)	ww7142	Meister	Charcoal	1,195±35	-25	A.D. 708–748 (0.07); A.D. 766–898 (0.84); A.D. 920–947 (0.04)	A.D. 830
40	08/15/2008	1(3)	ww7379	Meister	Wood fragment	160±30	-27.54	A.D. 1664–1706 (0.17); A.D. 1720–1826 (0.48); A.D. 1832–1884 (0.13); A.D. 1914–1953 (0.18)	A.D. 1775
41	08/07/2008	2(1)	ww7078	Outhouse	Charcoal	895±35	-26.11	A.D. 1039–1215 (0.95)	A.D. 1131
42	08/07/2008	2(2)	ww7079	Outhouse	Charred wood	1,820±30	-23.85	A.D. 124–257 (0.92); A.D. 300–318 (0.02)	A.D. 189
43	08/7/2008	2(6)	ww7686	Outhouse	Wood fragment	245±25	-27.4	A.D. 1527–1552 (0.04); A.D. 1632–1673 (0.62); A.D. 1777–1800 (0.25); A.D. 1941–1954 (0.05)	A.D. 1659
44	08/13/2008	1(1)	ww7140	Spider	Stick fragment	960±35	-25.9	A.D. 1016–1160 (0.95)	A.D. 1095
45	08/13/2008	1(6)	ww7141	Spider	Charcoal	925±30	-24.56	A.D. 1026–1180 (0.95)	A.D. 1103
Upstream reach of Rapid Creek									
46	07/22/2008	1(1)	ww7076A	Blue Ribbon	Charcoal	795±30	-22.65	A.D. 1185–1278 (0.95)	A.D. 1232
47	08/22/2008	1A(1)	ww7143	Gage House	Charcoal	1,185±30	-25.88	A.D. 722–740 (0.02); A.D. 770–900 (0.88); A.D. 918–950 (0.06)	A.D. 839
48	08/22/2008	1A(3)	ww7144	Gage House	Organic detritus	Modern	-25	Modern	--
49	08/11/2008	1(3)	ww7139	Schist	Charcoal	1,070±30	-25.93	A.D. 895–925 (0.21); A.D. 936–1021 (0.74)	A.D. 958
Upstream subreach of Boxelder Creek									
50	05/20/2008	1A(3)	ww7054	Asphalt pit A	Charcoal	265±30	-23.55	A.D. 1516–1595 (0.35); A.D. 1617–1670 (0.50); A.D. 1780–1799 (0.09)	A.D. 1642
51	05/20/2008	1B(1)	ww7053	Asphalt pit B	Charcoal	190±30	-24.88	A.D. 1648–1694 (0.22); A.D. 1726–1813 (0.54); A.D. 1918–1954 (0.20)	A.D. 1772
52	05/21/2008	2A(5)	ww7056	Benchmark	Wood fragment	95±40	-25	A.D. 1680–1764 (0.30); A.D. 1800–1939 (0.65)	A.D. 1836
53	05/21/2008	2A(7)	ww7057	Benchmark	Wood fragment	85±30	-25.26	A.D. 1688–1730 (0.26); A.D. 1808–1926 (0.70)	A.D. 1844
54	05/23/2008	1A(1)	ww7058	Enob	Charcoal	270±30	-23.9	A.D. 1515–1598 (0.42); A.D. 1616–1669 (0.46); A.D. 1781-1798 (0.06)	A.D. 1633

Table S1–1. Results of laboratory analyses for radiocarbon samples.—Continued

[ID, identification number; ^{14}C yr BP, uncalibrated carbon-14 age in years before present (referenced to A.D. 1950) calculated using the Libby half-life of 5,568 years; $^{13}C/^{12}C$, ratio of carbon-13 to carbon-12; ±, plus or minus; --, analysis could not be performed; "Modern" results indicate a post A.D. 1950 age and are not calibrated; calibrated age ranges and median ages calculated on the basis of Oxcal 4.1 (Bronk Ramsey and others, 2001; Bronk Ramsey, 2009) using IntCal09 calibration dataset (Reimer and others, 2009)]

ID	Sample date	Field sample number	Laboratory identification number	Site or alcove and pit (if applicable)	Material sampled	^{14}C yr BP ±1-sigma error	$^{13}C/^{12}C$	Calibrated 2-sigma age ranges (fraction of probability density function)	Median age
Upstream subreach of Boxelder Creek—Continued									
55	05/23/2008	1A(3)	ww7693	Enob	Charcoal	140±30	-25.86	A.D. 1668–1780 (0.43); A.D. 1798–1891 (0.37)	A.D. 1808
56	08/01/2008	1B(10)	ww7064	Joan's pit B	Stick fragment	1,130±35	-26.4	A.D. 781–790 (0.02); A.D. 808–990 (0.94)	A.D. 923
57	08/01/2008	1B(2)	ww7703	Joan's pit B	Charcoal	1015±30	-25	A.D. 972–1047 (0.86); A.D. 1090–1122 (0.07); A.D. 1139–1149 (0.02)	A.D. 1013
58	08/01/2008	1B(7)	ww7678	Joan's pit B	Ponderosa pine bark	165±20	-25.51	A.D. 1666–1694 (0.17); A.D. 1726–1784 (0.47); A.D. 1795–1814 (0.11); A.D. 1917–1953 (0.19)	A.D. 1765
59	08/01/2008	1B(8)	ww7685	Joan's pit B	Charcoal	275±25	-25.21	A.D. 1520–1592 (0.46); A.D. 1619–1666 (0.48); A.D. 1784–1794 (0.02)	A.D. 1625
60	05/21/2008	1A()	ww7696	Snap-E Tom	Charcoal	2,030±35	-25.19	161–132 B.C. (0.05); 116 B.C.– A.D. 54 (0.90)	33 B.C.
61	05/21/2008	1A(4)	ww7706	Snap-E Tom	Charcoal	2,280±25	-24.51	400–353 B.C. (0.64); 291–231 B.C. (0.32)	370 B.C.
62	05/21/2008	1A(6)	ww7055	Snap-E Tom	Charcoal	2,145±30	-23.56	355–290 B.C. (0.25); 232–88 B.C. (0.68); 76–57 B.C. (0.02)	187 B.C.
Downstream subreach of Boxelder Creek									
63	09/23/2008	2(1)	ww7076 B	Custer Gap	Charcoal	1,190±30	-22.65	A.D. 720–742 (0.03); A.D. 769–898 (0.89); A.D. 921–944 (0.04)	A.D. 835
64	09/23/2008	2(4)	ww7691	Custer Gap	Charcoal	1,240±25	-24.26	A.D. 686–870 (0.95)	A.D. 763
65	05/24/2008	1A(5)	ww7745	Kitty's Corner pit A	Wood	925±30	--	A.D. 1026–1180 (0.95)	A.D. 1100
66	05/24/2008	1B(2)	ww7381	Kitty's Corner pit B	Charcoal	1,560±30	-24.08	A.D. 424–564 (0.95)	A.D. 488
67	05/24/2008	1C(1)	ww7059	Kitty's Corner pit C	Charcoal fragment	1,795±30	-25.32	A.D. 131–262 (0.79); A.D. 280–326 (0.17)	A.D. 224
68	05/24/2008	1C(10)	ww7683	Kitty's Corner pit C	Bark fragment	665±25	-24.58	A.D. 1278–1317 (0.50); A.D. 1354–1390 (0.45)	A.D. 1314
69	05/24/2008	1C(12)	ww7061	Kitty's Corner pit C	Wood fragment	440±30	-25.3	A.D. 1416–1490 (0.94); A.D. 1602–1609 (0.02)	A.D. 1445
70	05/24/2008	1C(13)	ww7062	Kitty's Corner pit C	Wood fragment	315±25	-26.06	A.D. 1490–1603 (0.74); A.D. 1611–1645 (0.21)	A.D. 1563
71	05/24/2008	1C(2)	ww7680	Kitty's Corner pit C	Charcoal	1,980±25	-24.11	40 B.C.– A.D. 70 (0.95)	A.D. 22
72	05/24/2008	1C(3)	ww7681	Kitty's Corner pit C	Wood fragment	1,250±30	-25	A.D. 676–870 (0.95)	A.D. 745
73	05/24/2008	1C(4)	ww7682	Kitty's Corner pit C	Wood fragment	920±25	-27.43	A.D. 1030–1173 (0.95)	A.D. 1099
74	05/24/2008	1C(7)	ww7060	Kitty's Corner pit C	Wood fragment	1,000±45	-25	A.D. 902–914 (0.02); A.D. 968–1158 (0.94)	A.D. 1035
75	05/24/2008	1C(9)	ww7734	Kitty's Corner pit C	Wood fragment	930±30	--	A.D. 1024–1169 (0.95)	A.D. 1098
76	06/22/2009	1C(1)	ww7744	Kitty's Corner pit C	Pine needle	190±35	--	A.D. 1646–1696 (0.22); A.D. 1725–1814 (0.50); A.D. 1835–1878 (0.05); A.D. 1916–1954 (0.19)	A.D. 1772
77	06/22/2009	1C(6)	ww7591	Kitty's Corner pit C	Charcoal	275±25	-24.18	A.D. 1520–1592 (0.46); A.D. 1619–1666 (0.48); A.D. 1784–1794 (0.02)	A.D. 1625
78	08/14/2008	1(2)	ww7066	Second Story	Stick fragment	740±35	-26.16	A.D. 1218–1296 (0.95)	A.D. 1268
79	08/14/2008	1(2)	ww7749B	Second Story	Packrat scat	1,195±35	--	A.D. 708–748 (0.07); A.D. 766–898 (0.84); A.D. 920–947 (0.04)	A.D. 830
80	05/27/2008	2(1)	ww7063	Trail	Wood fragment	1,325±35	-26.19	A.D. 648–728 (0.72); A.D. 736–772 (0.23)	A.D. 687
81	05/27/2008	2(2)	ww7677	Trail	Bark fragment	630±25	-27.58	A.D. 1288–1330 (0.39); A.D. 1340–1396 (0.57)	A.D. 1353
82	05/27/2008	2(4)	ww7378	Trail	Driftwood	870±30	-26.09	A.D. 1045–1095 (0.18); A.D. 1119–1142 (0.06); A.D. 1146–1227 (0.70); A.D. 1232–1252 (0.02)	A.D. 1176

Table S1–1. Results of laboratory analyses for radiocarbon samples.—Continued

[ID, identification number; ^{14}C yr BP, uncalibrated carbon-14 age in years before present (referenced to A.D. 1950) calculated using the Libby half-life of 5,568 years; $^{13}C/^{12}C$, ratio of carbon-13 to carbon-12; ±, plus or minus; --, analysis could not be performed; "Modern" results indicate a post A.D. 1950 age and are not calibrated; calibrated age ranges and median ages calculated on the basis of Oxcal 4.1 (Bronk Ramsey and others, 2001; Bronk Ramsey, 2009) using IntCal09 calibration dataset (Reimer and others, 2009)]

ID	Sample date	Field sample number	Laboratory identification number	Site or alcove and pit (if applicable)	Material sampled	^{14}C yr BP ±1-sigma error	$^{13}C/^{12}C$	Calibrated 2-sigma age ranges (fraction of probability density function)	Median age
Downstream subreach of Boxelder Creek—Continued									
83	06/22/2009	1(1)	ww7684	Trail	Charcoal	905±25	-25.49	A.D. 1039–1190 (0.92); A.D. 1196–1208 (0.03)	A.D. 1111
84	07/24/2008	1(1)	ww7065	Snow Shovel pit A	Charcoal	1,970±25	-24.96	40 B.C.– A.D. 79 (0.95)	A.D. 32
85	07/24/2008	1(3)	ww7592	Snow Shovel pit A	Charcoal	1,025±25	-26.37	A.D. 972–1036 (0.95)	A.D. 1007
86	07/24/2008	1(5)	ww7593	Snow Shovel pit A	Wood fragment	140±25	-25.74	A.D. 1669–1710 (0.16); A.D. 1716–1780 (0.27); A.D. 1797–1890 (0.37); A.D. 1909–1944 (0.16)	A.D. 1809
87	07/29/2008	1(3)	ww7398	Snow Shovel pit B	Charcoal	2,525±30	-24.11	795–722 B.C. (0.30); 694–540 B.C. (0.66)	653 B.C.
Elk Creek study reach									
88	09/24/2008	2(1)	ww7073	Dracula's Ledge	Charcoal	970±30	-26.42	A.D. 1016–1155 (0.95)	A.D. 1090
89	09/24/2008	2(11)	ww7072	Dracula's Ledge	Charcoal	1,845±30	-24.94	A.D. 85–238 (0.95)	A.D. 171
90	09/24/2008	2(5)	ww7380	Dracula's Ledge	Charcoal	1,115±30	-24.53	A.D. 869–1014 (0.95)	A.D. 935
91	09/24/2008	2(7)	ww7700	Dracula's Ledge	Charcoal	1,725±30	-25	A.D. 242–393 (0.95)	A.D. 315
92	09/24/2008	2(9)	ww7692	Dracula's Ledge	Charcoal	1,870±25	-25.05	A.D. 76–222 (0.95)	A.D. 134
93	09/24/2008	3(1)	ww7074	Dracula's Ledge, beaver-chewed log	Driftwood	760±30	-24.84	A.D. 1220–1284 (0.95)	A.D. 1259
94	08/25/2008	2(1)	ww7699	Bird's Nest	Charcoal	4,475±30	-23.34	3339–3205 B.C. (0.54); 3196–3084 B.C. (0.34); 3064–3028 B.C. (0.07)	3222 B.C.
95	08/27/2008	2(3)	ww7733	Flat Rock	Charcoal	5,775±30	--	4706–4546 B.C. (0.95)	4630 B.C.
96	08/27/2008	2(4)	ww7710	Flat Rock	Charcoal	5,540±30	-24.4	4450–4341 B.C. (0.95)	4389 B.C.
97	08/27/2008	2(5)	ww7690	Flat Rock	Charcoal	38,180±1,080	-24.95	42616–39384 B.C. (0.95)	--
98	08/27/2008	2(6)	ww7679	Flat Rock	Charcoal	5,255±30	-24.8	4229–4200 B.C. (0.12); 4170–4126 B.C. (0.14); 4121–4090 B.C. (0.7); 4082–3980 B.C. (0.56)	4060 B.C.
99	09/24/2008	1(2)	ww7071	Sand Wall	Charred wood	90±25	-23.67	A.D. 1690–1730 (0.25); A.D. 1810–1925 (0.70)	A.D. 1843

Table S1–2. Results of laboratory analyses for optically stimulated luminescence (OSL) samples.

[K, potassium content, in percent; U, uranium concentration; ppm, parts per million; Th, thorium concentration; Gy/ka, Grays per thousand years; Gy, (Grays) the absorption of 1 joule of ionizing radiation by 1 kilogram of matter; ±, plus or minus]

Sample information	Water content[1] (percent)	[2]K (percent)	[2]U (ppm)	[2]Th (ppm)	Cosmic dose[3] additions (Gy/ka)	Total dose additions (Gy/ka)	Equivalent dose (Gy)	Number[4]	Age[5] (years)	Calendar year[5]
9/17/08-OSL-1(3); High Alcove, Rapid Creek	8 (20)	2.14±0.12	3.36±0.17	12.7±0.32	0.32±0.02	4.23±0.08	2.73±0.06; 1.87±0.09	14 (15); 1 (15)	645±20; **440±25**	**A.D. 1545–1595**
5/29/08-OSL-1; Meister, 1972 flood, Spring Creek	17 (46)	1.73±0.02	3.04±0.13	7.82±0.30	0.31±0.02	3.23±0.07	1.06±0.01; 0.61±0.03	14 (15); 1 (15)	330±10; **190±20**	**A.D. 1800–1840**
5/28/08-OSL-1; Hailstorm Alcove, Spring Creek	22 (42)	2.10±0.06	2.80±0.05	13.7±0.08	0.25±0.01	3.93±0.08	15.8±5.53; 10.9±0.93	23 (25); 8 (25)	4,015±1,005; **2,765±255**	**1010–500 B.C.**
5/28/08-OSL-3; Superscour Alcove, Spring Creek	35 (41)	1.79±0.02	3.04±0.13	7.82±0.30	0.27±0.02	3.49±0.21	1.26±0.03; 0.73±0.04	10 (15); 1 (15)	360±25; **210±15**	**A.D. 1785–1815**
5/27/08-OSL-2; Kitty's Corner, pit C, Boxelder Creek	3 (30)	1.37±0.07	2.43±0.11	6.06±0.27	0.30±0.02	2.90±0.13	4.31±0.06; 2.94±0.09	28 (30); 4 (30)	1,485±70; **1,015±50**	**A.D. 945–1045**
5/27/08-OSL-3; Kitty's Corner, pit C, Boxelder Creek	2 (31)	1.55±0.10	3.26±0.44	4.26±0.54	0.30±0.02	3.01±0.18	2.17±0.37; 1.30±0.10	16 (18); 3 (18)	720±140; **435±60**	**A.D. 1515–1635**
5/27/08-OSL-8; Kitty's Corner, pit B, Boxelder Creek	6 (59)	1.44±0.02	3.09±0.24	8.10±0.72	0.25±0.01	2.78±0.13	1.12±0.02; 0.71±0.02	24 (35); 3 (35)	400±20; **255±15**	**A.D. 1740–1770**
5/27/08-OSL-5; Kitty's Corner, pit A, Boxelder Creek	3 (33)	1.63±0.03	3.42±0.25	8.26±0.45	0.24±0.01	3.27±0.11	3.67±1.03; 2.02±0.21	22 (24); 18 (24)	1,120±340; **620±80**	**A.D. 1310–1470**
5/27/08-OSL-6; Kitty's Corner, pit A, Boxelder Creek	12 (46)	1.59±0.02	3.39±0.26	9.28±0.44	0.29±0.02	3.26±0.10	1.10±0.28; 0.79±0.10	17 (20); 7 (20)	335±70; **245±35**	**A.D. 1730–1800**

[1]Field moisture, with numbers in parentheses indicating the complete sample saturation percent. Ages calculated using approximately 10 percent of saturation values.

[2]Analyses obtained using laboratory Gamma Spectrometry (low resolution sodium iodide detector).

[3]Cosmic doses and attenuation with depth were calculated using the methods of Prescott and Hutton (1994).

[4]Number of replicated equivalent dose estimates used to calculate the mean. Figures in parentheses indicate total number of measurements made including failed runs with unusable data. Second set of numbers indicates only those equivalent doses that fit into the lowest 10 to 15 percent of equivalent doses. If the data showed large positive skew, those doses were eliminated because of partial bleaching contamination.

[5]Age for fine-grained (90- to 250-micrometer) quartz sand. Linear plus exponential fit used on age, with errors to one standard deviation (very young samples only have linear fit). Age in **bold font** is age used for flood unit.

Table S1–3. Results of laboratory analyses for cesium-137 samples.

[dpm/g, disintegrations per minute per gram; ±, plus or minus; <, less than; ND, not detected; --; not applicable]

Sample identification	Depth, in inches, below top of unit	Sample weight (grams)	Cesium-137 (dpm/g)		Lead-210 (dpm/g)		Radium-226 (dpm/g)		Potassium-40	
			Activity	Error (±)	Activity	Error (±)	Activity	Error (±)	Activity	Error (±)
Trail Alcove Cs-6-22-09-2(1)	<0.5 below surface	50.00	0.44	0.04	2.28	0.18	1.63	0.06	28.09	1.17
Trail Alcove Cs-6-22-09-2(2)	<1.0 below top of intermediate unit	50.00	ND	--	1.36	.14	1.18	.05	8.46	.69
Kitty's Corner pit A Cs-6-22-09-1(2)	4.7 below surface	50.00	.06	.03	1.50	.16	1.56	.05	27.28	1.11
Kitty's Corner pit A Cs-6-22-09-1(3)	9.5 below surface	50.00	ND	--	1.47	.16	1.56	.05	27.78	1.04
Kitty's Corner pit A Cs-6-22-09-1(4)	16 below surface	50.00	ND	--	1.80	.15	1.49	.06	24.10	.91
Kitty's Corner pit A Cs-6-22-09-1(5)	21 below surface	50.00	ND	--	1.56	.17	1.56	.06	27.98	1.24
Kitty's Corner pit C Cs-Sample-2	2.8–3.9 below surface of unit II	50.00	ND	--	1.97	.15	1.67	.05	28.27	1.01
Kitty's Corner pit C Cs-Sample-4	0.2 below surface of unit I	50.00	.40	.04	2.32	.17	1.88	.08	33.26	1.18
Kitty's Corner pit C Cs-Sample-5	3.2–4.7 below surface	50.00	.66	.06	2.36	.25	1.70	.08	29.54	1.53
Kitty's Corner pit C Cs-Sample-6	5.5–7.9 below surface	50.00	.92	.06	2.62	.20	1.72	.07	28.81	1.32

Supplement 2. Modern Peak-Flow Chronologies

Details regarding development of modern peak-flow chronologies are presented within this section. Peak-flow records (including historical information) that were used in developing the chronologies are presented in tables S2–1 through S2–5.

Spring Creek

A modern peak-flow chronology (tables 2 and S2–1) was developed for the center of the Spring Creek study reach, which has a drainage area of 171 mi^2, relative to areas of 170 and 172 mi^2 at the upstream and downstream extents of the reach. This chronology includes 67 annual peak-flow values from 5 USGS streamgages (fig. 1, table S2–1), the earliest of which was from 1904.

Streamgage 06407500 is nearest the study reach and is most representative, from the standpoint of peak-flow potential. Peak-flow records for this streamgage are relatively short (table S2–1), but were extended to include 1950–2009, based primarily on least-squares regression analysis (Helsel and Hirsch, 2002) using concurrent records for 1987–2004 with downstream streamgage 06408500 (annual peak flow for streamgage 06407500, in cubic feet per second = 27.6 + 1.002 times annual peak flow for streamgage 06408500, in cubic feet per second; correlation coefficient = 0.85). Regression analysis was used because area-weighted adjustments resulted in unrealistically small values for the upstream streamgage, for cases with small downstream values, which owes to large streamflow losses that occur between the two streamgages (Hortness and Driscoll, 1998). The 1996 values (642 and 6,910 ft^3/s for streamgages 06407500 and 06408500, respectively) were excluded from the regression analysis because of the large differential between the values. The chronology for the center of the study reach for this period then was developed by applying drainage-area adjustments to the extended record, with two exceptions. The 1972 value is based wholly on an un-adjusted flow of 21,800 ft^3/s reported by Schwarz and others (1975) for streamgage 06408000. The 1996 value of 1,000 ft^3/s was arbitrarily selected as an appropriate value based on detailed knowledge of the storm pattern and radar imagery, as described by Driscoll and others (2010). The modern chronology was extended further using drainage-area adjustments to include 1938–40 (based on annual peak flows for streamgage 06407000) and 1946–47 and 1904–05 (based on annual peak flows for streamgage 06408000).

Rapid Creek

The reach of Rapid Creek downstream from Pactola Dam (fig. 1) is of primary interest for the paleoflood investigations because of its proximity to urban populations. However, the available paleoflood chronology pre-dates regulation from Pactola Dam; thus, detailed investigations also were conducted in a reach upstream from Pactola Reservoir to extract comparable paleoflood information.

The modern peak-flow chronology for the downstream (lower) reach of Rapid Creek (tables 2 and S2–2) was developed to estimate pre-regulation conditions for streamgage 06412500, which has a drainage area of 375 mi^2, relative to areas of 367 and 384 mi^2 at the upstream and downstream extents of the study reach. The drainage-area differential between the gage location and the upstream extent of the reach is about 2 percent and is considered inconsequential. About 321 mi^2 of the area has been regulated by Pactola Dam since August 1956, and 92.4 mi^2 has been regulated by Deerfield Dam since December 1945 (Miller and Driscoll, 1998). The modern chronology dates back to 1878 and includes area-adjusted values that are based on historical peak-flow values for 1878, 1883, 1907, and 1920 that were provided by the U.S. Army Corps of Engineers (1973) for the location of streamgage 06414000. The modern chronology also includes area-adjusted values based on annual peak flows for 1905–06 and 1943–46 from streamgage 06414000. The modern chronology was extended further using drainage-area adjustments to include 1915–17 (based on annual peak flows from streamgage 06412000) and 1929–42 (based on annual peak flows from streamgage 06411500). All of these drainage-area adjustments are for periods pre-dating construction of both dams; thus, unregulated areas were used. No adjustments were performed for 1947–55, which precedes construction of Pactola Dam; minor effects of storage in Deerfield Reservoir were considered inconsequential. Adjustments for 1956–2009 to account for effects of storage in Pactola Reservoir were made after scrutinizing individual annual and daily peak-flow records for (1) streamgages 06410500 and 06411500 to evaluate storage effects and (2) streamgages 06411500 and 06412500 to evaluate inflows downstream from Pactola Dam. Most adjustments were then made by adjusting annual peak-flow values for streamgage 06410500, relative to the unregulated area for streamgage 06412500 (multiplying by 375/295 raised to the 0.6 power); however, adjustments for shaded cells in table S2–2 were made through consideration of daily flow values for streamgages 06410500 and 06411500. The largest of all adjustments was an increase of about 1,770 ft^3/s, relative to the recorded annual peak flow of 614 ft^3/s for 1965.

Driscoll and others (2010) concluded from detailed examination of historical flood accounts that (1) the effects of storage in Pactola and Deerfield Reservoirs essentially have been inconsequential relative to large-scale flow events, and (2) with the exception of 1972 flooding, flows approaching the magnitudes of the historical peak-flow values (1878, 1883, 1907, and 1920) would not have occurred along lower Rapid Creek since 1920, regardless of storage effects. Driscoll and others (2010) further concluded that no exceptionally large flows have occurred in the reach of Rapid Creek upstream from Pactola Reservoir since 1929. The largest known peak-flow event in this upstream reach of Rapid Creek was in

1955, when a flow of 8,500 ft^3/s occurred along Castle Creek, upstream from Rapid Creek (Wells, 1962). This flow attenuated quickly in moving downstream, and resulted in a peak flow of only 1,520 ft^3/s (table S2–3) at streamgage 06410500 (above Pactola Reservoir).

Table 2 includes a modern chronology for the reach of Rapid Creek upstream from Pactola Reservoir at the location of streamgage 06410500, which has a drainage area of 294 mi^2, relative to areas of 290 and 294 mi^2 at the upstream and downstream extents of the reach (table 1). The drainage-area differential is considered inconsequential and no adjustments were made for the upstream extent of the reach. The modern chronology for streamgage 06410500 was extended to include 1929–42 and 1947–51 and 1953 using drainage-area adjustments based on annual peak flows from streamgage 06411500, for which the gaged records pre-date construction of Pactola Dam (table S2–3). The 1952 flow was affected substantially by storage in Deerfield Reservoir, so the 1952 adjustment was based on the annual peak flow from streamgage 06409000, which is located upstream from Deerfield Reservoir. The estimated value for 1952 is slightly larger than the largest recorded flow for streamgage 06410500 (2,060 ft^3/s in 1965) but is consistent with large flows along Rapid Creek, as described by Driscoll and others (2010). Flow adjustments were not made for other years because adjustments would require considerable speculation, and effects of storage were inconsequential relative to large-scale flow events. The extended chronology for streamgage 06410500 also includes pre-regulation values for 1915–17 that were based on drainage-area adjustments for annual peak flows from streamgage 06412000. Extension of the chronology to include the large historical values for streamgage 06414000 (1878, 1883, 1907, and 1920) was considered inappropriate and was not performed.

Boxelder Creek

Drainage areas for the Boxelder Creek reach increase from 98 to 112 mi^2 between the upstream and downstream extents of the reach, and potential exists for substantial differences in peak-flow characteristics from inflows of two relatively large tributaries within the reach. A 1972 peak flow (table S2–4) of 30,100 ft^3/s was recorded for streamgage 06422500 (drainage area = 94.4 mi^2), which is located just upstream from the reach, and a 1972 flow of 51,600 ft^3/s was recorded at streamgage 06422650 (drainage area = 116 mi^2), which is located just downstream from the reach. Adjusting the flow for the upstream streamgage to the area for the downstream streamgage yields a predicted flow of 34,060 ft^3/s and the opposite adjustment yields a flow for the upstream streamgage of 45,600 ft^3/s, which illustrates the effect of the intervening tributaries in 1972. Thus, modern chronologies were developed for two separate subreaches of Boxelder Creek (located upstream and downstream from the two tributaries; tables 2 and S2–4). Both chronologies were based primarily on gaged records for upstream streamgage 06422500, which were extended (based on drainage-area adjustments) to include 1904–05 values from streamgage 06423000. Subsequent adjustments for the two subreaches were primarily based on upstream and downstream areas of 98 and 112 mi^2. However, the 1972 value for the downstream subreach was derived from a drainage-area adjustment using downstream streamgage 06423000.

Elk Creek

The drainage area for the Elk Creek study reach is about 40 mi^2 (table 1). Upstream streamgage 06424000 (drainage area = 21.6 mi^2) is considered to be most representative, relative to peak-flow characteristics, but has only short-term records (table 1). Downstream streamgages 06425100 and 06425500 have much longer records (table S2–5); however, drainage areas are much larger (211 and 549 mi^2, respectively; table 1) and peak-flow values correlate poorly because of substantial hydrogeologic differences in the intervening drainage areas (Sando and others, 2008; Driscoll and others, 2010). Potential differences are well illustrated by the substantial attenuation of the 1972 flow values between streamgages 06424500 and 06425500 (11,600 and 1,880 ft^3/s, respectively). Thus, the modern peak-flow chronology for Elk Creek (tables 2 and S2–5) was derived by first extending records for upstream streamgage 06424000, based on least-squares regression analysis (Helsel and Hirsch, 1992) using concurrent records for 1982–2009 with long-term streamgage 06422500 that is located along Boxelder Creek near Nemo (annual peak flow for streamgage 06424000, in cubic feet per second = 52.0 + 0.32 times annual peak flow for streamgage 06422500, in cubic feet per second; correlation coefficient = 0.87). The chronology for the study reach was then obtained using a drainage-area adjustment. The 1972 value and values for 1945–47 were obtained using a drainage-area adjustment for the 1972 flow at downstream streamgage 06424500 (drainage area = 47.6 mi^2). Historical accounts (Driscoll and others, 2010) indicate that a very large flow occurred in 1907 that destroyed a railroad line within the Elk Creek study reach and which may well have been larger than the 1972 flow. One focus of paleoflood investigations within Elk Creek was a concerted effort to determine whether the 1907 or 1972 flow was larger; however, definitive evidence could not be found. Thus, the 1907 flow was arbitrarily assumed equal to the 1972 flow as a historical value for the modern chronology. Relatively large flows may have occurred within the Elk Creek reach during 1952, 1953, and 1962, based on flows for downstream streamgage 06425500 and historical accounts (Driscoll and others, 2010). However, extension of the modern chronology is considered inappropriate, as illustrated by the 1972 flow comparison, and as further illustrated by large flow differentials between streamgages 06425100 and 06425500 for many years of concurrent record (table S2–5) that include relatively large values.

Table S2–1. Selected information used in development of modern peak-flow chronology for the Spring Creek study reach.

[Gray-shaded rows signify a gap in the chronology. Area, drainage area in square miles; Date, dates shown are for systematic peak-flow records, entries without dates are derived values; Q, peak-flow value in cubic feet per second; E, estimated; --, not available]

Water year	06407000		435915103241200		06407500		06407500		Modern peak-flow chronology for Spring Creek study reach		06408000		06408500	
	Spring Creek near Hill City, S.Dak.		Spring Creek below Bitter Creek, S.Dak.		Spring Creek near Keystone, S.Dak.		Extended record for Spring Creek near Keystone				Spring Creek near Rapid City, S.Dak.		Spring Creek near Hermosa, S.Dak.	
	Area = 151		Area = 157		Area = 163		Area = 163		Area = 171		Area = 175		Area = 206	
	Date	Q	Date	Q	Date	Q	Date	Q	Date	Q	Date	Q	Date	Q
1904	--	--	--	--	--	--	--	--	--	493	07/13/1904	500	--	--
1905	--	--	--	--	--	--	--	--	--	641	08/01/1905	650	--	--
1938	04/16/1938	500	--	--	--	--	--	--	--	539	--	--	--	--
1939	08/26/1939	592	--	--	--	--	--	--	--	638	--	--	--	--
1940	06/22/1940	241	--	--	--	--	--	--	--	260	--	--	--	--
1946	--	--	--	--	05/03/1946	246	05/03/1946	246	--	346	06/18/1946	351	--	--
1947	--	--	--	--	06/23/1947	865	06/23/1947	865	--	690	06/23/1947	700	--	--
1950	--	--	--	--	--	--	--	97	--	100	--	--	08/12/1950	69
1951	--	--	--	--	--	--	--	30	--	30	--	--	06/19/1951	2.0
1952	--	--	--	--	--	--	--	609	--	627	--	--	05/23/1952	580
1953	--	--	--	--	--	--	--	233	--	240	--	--	06/19/1953	205
1954	--	--	--	--	--	--	--	406	--	418	--	--	08/12/1954	378
1955	--	--	--	--	--	--	--	29	--	29	--	--	03/30/1955	1.0
1956	--	--	--	--	--	--	--	32	--	33	--	--	07/03/1956	4.0
1957	--	--	--	--	--	--	--	330	--	340	--	--	05/25/1957	302
1958	--	--	--	--	--	--	--	32	--	33	--	--	06/13/1958	4.0
1959	--	--	--	--	--	--	--	30	--	30	--	--	05/30/1959	2.0
1960	--	--	--	--	--	--	--	32	--	33	--	--	03/19/1960	4.0
1961	--	--	--	--	--	--	--	29	--	29	--	--	07/08/1961	1.0
1962	--	--	--	--	--	--	--	529	--	544	--	--	07/13/1962	500
1963	--	--	--	--	--	--	--	378	--	389	--	--	06/15/1963	350
1964	--	--	--	--	--	--	--	86	--	88	--	--	06/20/1964	58
1965	--	--	--	--	--	--	--	379	--	390	--	--	06/19/1965	351
1966	--	--	--	--	--	--	--	53	--	54	--	--	08/19/1966	25
1967	--	--	--	--	--	--	--	801	--	825	--	--	06/07/1967	772

Table S2–1. Selected information used in development of modern peak-flow chronology for the Spring Creek study reach.—Continued

[Gray-shaded rows signify a gap in the chronology. Area, drainage area in square miles; Date, dates shown are for systematic peak-flow records, entries without dates are derived values; Q, peak-flow value in cubic feet per second; E, estimated; --, not available]

Water year	06407000		435915103241200		06407500		06407500		Modern peak-flow chronology for Spring Creek study reach		06408000		06408500	
	Spring Creek near Hill City, S.Dak.		Spring Creek below Bitter Creek, S.Dak.		Spring Creek near Keystone, S.Dak.		Extended record for Spring Creek near Keystone				Spring Creek near Rapid City, S.Dak.		Spring Creek near Hermosa, S.Dak.	
	Area = 151		Area = 157		Area = 163		Area = 163		Area = 171		Area = 175		Area = 206	
	Date	Q	Date	Q	Date	Q	Date	Q	Date	Q	Date	Q	Date	Q
1968	--	--	--	--	--	--	--	48	--	49	--	--	06/25/1968	20
1969	--	--	--	--	--	--	--	386	--	398	--	--	07/16/1969	358
1970	--	--	--	--	--	--	--	33	--	34	--	--	06/13/1970	5.0
1971	--	--	--	--	--	--	--	379	--	390	--	--	06/02/1971	351
1972	--	--	06/09/1972	14,900	--	--	06/10/1972	E20,000	06/10/1972	21,800	06/10/1972	21,800	06/10/1972	13,400
1973	--	--	--	--	--	--	--	124	--	127	--	--	05/10/1973	96
1974	--	--	--	--	--	--	--	32	--	33	--	--	08/14/1974	4.0
1975	--	--	--	--	--	--	--	42	--	43	--	--	06/19/1975	14
1976	--	--	--	--	--	--	--	389	--	401	--	--	06/16/1976	361
1977	--	--	--	--	--	--	--	368	--	379	--	--	06/12/1977	340
1978	--	--	--	--	--	--	--	198	--	204	--	--	05/20/1978	170
1979	--	--	--	--	--	--	--	33	--	34	--	--	11/16/1978	5.0
1980	--	--	--	--	--	--	--	406	--	418	--	--	06/14/1980	378
1981	--	--	--	--	--	--	--	31	--	31	--	--	05/17/1981	2.9
1982	--	--	--	--	--	--	--	383	--	394	--	--	07/25/1982	355
1983	--	--	--	--	--	--	--	217	--	223	--	--	05/07/1983	189
1984	--	--	--	--	--	--	--	275	--	283	--	--	06/15/1984	247
1985	--	--	--	--	--	--	--	42	--	43	--	--	03/20/1985	14
1986	--	--	--	--	--	--	--	41	--	42	--	--	04/26/1986	13
1987	--	--	--	--	04/29/1987	120	04/29/1987	120	--	123	--	--	03/06/1987	17
1988	--	--	--	--	03/29/1988	24	03/29/1988	24	--	25	--	--	03/21/1988	53
1989	--	--	--	--	05/20/1989	31	05/20/1989	31	--	32	--	--	03/27/1989	.35
1990	--	--	--	--	06/02/1990	93	06/02/1990	93	--	96	--	--	--/--/1990	.00
1991	--	--	--	--	06/07/1991	291	06/07/1991	291	--	299	--	--	06/08/1991	373
1992	--	--	--	--	06/28/1992	31	06/28/1992	31	--	32	--	--	11/10/1991	2.4
1993	--	--	--	--	06/08/1993	286	06/08/1993	286	--	294	--	--	08/06/1993	366
1994	--	--	--	--	05/16/1994	64	05/16/1994	64	--	66	--	--	03/01/1994	100
1995	--	--	--	--	05/09/1995	913	05/09/1995	913	--	940	--	--	07/18/1995	540

Table S2–1. Selected information used in development of modern peak-flow chronology for the Spring Creek study reach.—Continued

[Gray-shaded rows signify a gap in the chronology. Area, drainage area in square miles; Date, dates shown are for systematic peak-flow records, entries without dates are derived values; Q, peak-flow value in cubic feet per second; E, estimated; --, not available]

Water year	06407000		435915103241200		06407500		06407500		Modern peak-flow chronology for Spring Creek study reach		06408000		06408500	
	Spring Creek near Hill City, S.Dak.		Spring Creek below Bitter Creek, S.Dak.		Spring Creek near Keystone, S.Dak.		Extended record for Spring Creek near Keystone				Spring Creek near Rapid City, S.Dak.		Spring Creek near Hermosa, S.Dak.	
	Area = 151		Area = 157		Area = 163		Area = 163		Area = 171		Area = 175		Area = 206	
	Date	Q	Date	Q	Date	Q	Date	Q	Date	Q	Date	Q	Date	Q
1996	--	--	--	--	05/30/1996	642	05/30/1996	642	--	1,000	--	--	05/30/1996	6,910
1997	--	--	--	--	06/03/1997	516	06/03/1997	516	--	531	--	--	06/03/1997	512
1998	--	--	--	--	06/20/1998	306	06/20/1998	306	--	315	--	--	06/20/1998	292
1999	--	--	--	--	06/19/1999	306	06/19/1999	306	--	315	--	--	06/20/1999	457
2000	--	--	--	--	04/25/2000	106	04/25/2000	106	--	109	--	--	04/24/2000	59
2001	--	--	--	--	07/14/2001	66	07/14/2001	66	--	68	--	--	11/01/2000	5.8
2002	--	--	--	--	04/08/2002	31	04/08/2002	31	--	32	--	--	05/11/2002	5.5
2003	--	--	--	--	05/10/2003	62	05/10/2003	62	--	64	--	--	10/22/2002	1.3
2004	--	--	--	--	03/11/2004	14	03/11/2004	14	--	14	--	--	01/10/2004	2.5
2005	--	--	--	--	05/13/2005	27	05/13/2005	27	--	28	--	--	--	--
2006	--	--	--	--	03/30/2006	23	03/30/2006	23	--	24	--	--	--	--
2007	--	--	--	--	05/07/2007	34	05/07/2007	34	--	35	--	--	--	--
2008	--	--	--	--	05/24/2008	170	05/24/2008	170	--	175	--	--	--	--
2009	--	--	--	--	05/13/2009	69	05/13/2009	69	--	71	--	--	--	--

Table S2–2. Selected information used in development of modern peak-flow chronology for the lower Rapid Creek study reach.

[Gray-shaded rows signify a gap in the chronology. (H) indicates historical value obtained from U.S. Army Corps of Engineers (1973). **Bold font** indicates special computations for lower Rapid Creek as noted in the "Supplement 2. Modern Peak-Flow Chronologies" section. Area, drainage area in square miles; Date, dates shown are for systematic peak-flow records, entries without dates are derived values; Q, peak-flow value in cubic feet per second; E, estimated; --, not available]

Water year	06410500		06411500		06412000		06412500		06412500		06412500		06414000	
	Rapid Creek above Pactola Reservoir at Silver City, S.Dak.		Rapid Creek below Pactola Dam, S.Dak.		Rapid Creek at Big Bend near Rapid City, S.Dak.		Rapid Creek above Canyon Lake near Rapid City, S.Dak.		Rapid Creek above Canyon Lake—extended record		Rapid Creek above Canyon Lake—extended record adjusted for regulation effects (modern chronology)		Rapid Creek at Rapid City, S.Dak.	
	Area = 294		Area = 322		Area = 339		Area = 375		Area = 375		Area = 375		Area = 414	
	Date	Q	Date	Q	Date	Q	Date	Q	Date	Q	Date	Q	Date	Q
1878	--	--	--	--	--	--	--	--	--	7,060	--	7,060	06/11/1878	7,500 (H)
1883	--	--	--	--	--	--	--	--	--	7,900	--	7,900	05/17/1883	8,400 (H)
1905	--	--	--	--	--	--	--	--	--	2,350	--	2,350	07/26/1905	2,500
1906	--	--	--	--	--	--	--	--	--	922	--	922	08/02/1906	980
1907	--	--	--	--	--	--	--	--	--	12,200	--	12,200	06/12/1907	13,000 (H)
1915	--	--	--	--	06/26/1915	616	--	--	--	654	--	654	--	--
1916	--	--	--	--	05/24/1916	204	--	--	--	217	--	217	--	--
1917	--	--	--	--	06/04/1917	270	--	--	--	287	--	287	--	--
1920	--	--	--	--	--	--	--	--	--	7,540	--	7,540	05/12/1920	8,000 (H)
1929	--	--	06/03/1929	794	--	--	--	--	--	870	--	870	--	--
1930	--	--	04/09/1930	194	--	--	--	--	--	213	--	213	--	--
1931	--	--	04/08/1931	155	--	--	--	--	--	170	--	170	--	--
1932	--	--	04/24/1932	682	04/24/1932	694	--	--	--	747	--	747	--	--
1933	--	--	05/24/1933	1,540	05/24/1933	1,570	--	--	--	1,690	--	1,690	--	--
1934	--	--	02/11/1934	117	02/11/1934	119	--	--	--	128	--	128	--	--
1935	--	--	06/01/1935	437	05/01/1935	446	--	--	--	479	--	479	--	--
1936	--	--	04/13/1936	100	04/13/1936	102	--	--	--	110	--	110	--	--
1937	--	--	07/12/1937	84	07/12/1937	86	--	--	--	92	--	92	--	--
1938	--	--	04/16/1938	86	04/16/1938	88	--	--	--	94	--	94	--	--
1939	--	--	04/24/1939	62	04/24/1939	63	--	--	--	68	--	68	--	--

Table SS2–2. Selected information used in development of modern peak-flow chronology for the lower Rapid Creek study reach.—Continued

[Gray-shaded rows signify a gap in the chronology. (H) indicates historical value obtained from U.S. Army Corps of Engineers (1973). **Bold font** indicates special computations for lower Rapid Creek as noted in the "Supplement 2. Modern Peak-Flow Chronologies" section. Area, drainage area in square miles; Date, dates shown are for systematic peak-flow records, entries without dates are derived values; Q, peak-flow value in cubic feet per second; E, estimated; --, not available]

Water year	06410500		06411500		06412000		06412500		06412500		06412500		06414000	
	Rapid Creek above Pactola Reservoir at Silver City, S.Dak.		Rapid Creek below Pactola Dam, S.Dak.		Rapid Creek at Big Bend near Rapid City, S.Dak.		Rapid Creek above Canyon Lake near Rapid City, S.Dak.		Rapid Creek above Canyon Lake—extended record		Rapid Creek above Canyon Lake—extended record adjusted for regulation effects (modern chronology)		Rapid Creek at Rapid City, S.Dak.	
	Area = 294		Area = 322		Area = 339		Area = 375		Area = 375		Area = 375		Area = 414	
	Date	Q	Date	Q	Date	Q	Date	Q	Date	Q	Date	Q	Date	Q
1940	--	--	08/27/1940	245	08/27/1940	250	--	--	--	268	--	268	--	--
1941	--	--	06/11/1941	540	06/11/1941	552	--	--	--	592	--	592	--	--
1942	--	--	05/16/1942	409	05/16/1942	417	--	--	--	448	--	448	--	--
1943	--	--	--	--	--	--	--	--	--	882	--	882	06/13/1943	936
1944	--	--	--	--	--	--	--	--	--	254	--	254	06/12/1944	270
1945	--	--	--	--	--	--	--	--	--	359	--	359	08/01/1945	381
1946	--	--	--	--	--	--	--	--	--	942	--	943	07/18/1946	1,000
1947	--	--	06/23/1947	954	--	--	06/23/1947	950	06/23/1947	950	06/23/1947	950	06/24/1947	1,170
1948	--	--	06/22/1948	248	--	--	06/22/1948	245	06/22/1948	245	06/22/1948	245	08/13/1948	472
1949	--	--	06/02/1949	233	--	--	08/15/1949	290	08/15/1949	290	08/15/1949	290	08/15/1949	563
1950	--	--	04/15/1950	233	--	--	04/15/1950	209	04/15/1950	209	04/15/1950	209	04/16/1950	246
1951	--	--	06/14/1951	97	--	--	06/15/1951	77	06/15/1951	77	06/15/1951	77	10/09/1950	143
1952	--	--	05/22/1952	2,170	--	--	05/23/1952	2,600	05/23/1952	2,600	05/23/1952	2,600	05/23/1952	2,540
1953	--	--	06/15/1953	160	--	--	06/16/1953	152	06/16/1953	152	06/16/1953	152	06/19/1953	824
1954	05/23/1954	106	05/23/1954	94	--	--	08/12/1954	140	08/12/1954	140	08/12/1954	140	06/10/1954	172
1955	07/28/1955	1,520	07/29/1955	378	--	--	07/29/1955	326	07/29/1955	326	07/29/1955	326	08/10/1955	878
1956	03/24/1956	175	03/25/1956	178	--	--	05/29/1956	130	05/29/1956	130	--	203	10/15/1955	182
1957	05/25/1957	181	03/14/1957	55	--	--	07/14/1957	433	07/14/1957	433	--	**595**	07/14/1957	784
1958	05/31/1958	113	06/02/1958	84	--	--	05/30/1958	81	05/30/1958	81	--	131	07/19/1958	362
1959	09/25/1959	146	08/21/1959	90	--	--	06/30/1959	82	06/30/1959	82	--	169	12/11/1958	141
1960	03/23/1960	117	07/20/1960	112	--	--	07/16/1960	82	07/16/1960	82	--	135	06/20/1960	290
1961	07/07/1961	96	06/11/1961	111	--	--	07/01/1961	100	07/01/1961	100	--	111	06/14/1961	115
1962	06/15/1962	390	05/18/1962	67	--	--	07/13/1962	1,310	07/13/1962	1,310	--	**1,700**	07/13/1962	3,300
1963	06/16/1963	715	06/30/1963	184	--	--	06/06/1963	191	06/06/1963	191	--	827	06/05/1963	418
1964	06/09/1964	635	06/10/1964	266	--	--	06/11/1964	268	06/11/1964	268	--	735	06/13/1964	426

Table S2–2. Selected information used in development of modern peak-flow chronology for the lower Rapid Creek study reach.—Continued

[Gray-shaded rows signify a gap in the chronology. (H) indicates historical value obtained from U.S. Army Corps of Engineers (1973). **Bold font** indicates special computations for lower Rapid Creek as noted in the "Supplement 2. Modern Peak-Flow Chronologies" section. Area, drainage area in square miles; Date, dates shown are for systematic peak-flow records, entries without dates are derived values; Q, peak-flow value in cubic feet per second; E, estimated; --, not available]

Water year	06410500		06411500		06412000		06412500		06412500		06412500		06414000	
	Rapid Creek above Pactola Reservoir at Silver City, S.Dak.		Rapid Creek below Pactola Dam, S.Dak.		Rapid Creek at Big Bend near Rapid City, S.Dak.		Rapid Creek above Canyon Lake near Rapid City, S.Dak.		Rapid Creek above Canyon Lake—extended record		Rapid Creek above Canyon Lake—extended record adjusted for regulation effects (modern chronology)		Rapid Creek at Rapid City, S.Dak.	
	Area = 294		Area = 322		Area = 339		Area = 375		Area = 375		Area = 375		Area = 414	
	Date	Q	Date	Q	Date	Q	Date	Q	Date	Q	Date	Q	Date	Q
1965	05/15/1965	2,060	05/19/1965	547	--	--	05/19/1965	614	05/19/1965	614	--	2,380	06/11/1965	706
1966	03/16/1966	150	03/20/1966	147	--	--	03/22/1966	140	03/22/1966	140	--	174	07/26/1966	586
1967	06/16/1967	627	06/22/1967	406	--	--	06/15/1967	439	06/15/1967	439	--	726	06/15/1967	616
1968	06/09/1968	106	10/04/1967	311	--	--	10/04/1967	198	10/04/1967	198	--	123	06/09/1968	259
1969	07/20/1969	213	05/20/1969	306	--	--	05/20/1969	139	05/20/1969	139	--	246	07/23/1969	195
1970	04/19/1970	995	05/12/1970	304	--	--	06/14/1970	245	06/14/1970	245	--	1,150	06/12/1970	350
1971	04/25/1971	305	04/25/1971	338	--	--	04/26/1971	385	04/26/1971	385	--	353	04/26/1971	498
1972	07/06/1972	252	10/05/1971	505	--	--	06/09/1972	31,200	06/09/1972	31,200	06/09/1972	31,200	06/09/1972	50,000
1973	05/09/1973	169	05/08/1973	168	--	--	05/09/1973	173	05/09/1973	173	--	196	07/08/1973	282
1974	04/30/1974	54	07/04/1974	113	--	--	08/22/1974	516	08/22/1974	516	--	**476**	08/22/1974	1,040
1975	04/26/1975	219	06/07/1975	85	--	--	06/07/1975	92	06/07/1975	92	--	253	06/07/1975	1,500
1976	06/15/1976	614	06/29/1976	234	--	--	06/15/1976	636	06/15/1976	636	--	**1,220**	06/14/1976	1,400
1977	04/25/1977	187	05/05/1977	188	--	--	05/08/1977	194	05/08/1977	194	--	216	04/18/1977	209
1978	05/11/1978	430	06/01/1978	386	--	--	05/21/1978	433	05/21/1978	433	--	498	05/29/1978	602
1979	07/23/1979	173	06/16/1979	101	--	--	06/17/1979	150	06/17/1979	150	--	200	08/07/1979	451
1980	05/11/1980	75	07/15/1980	118	--	--	07/16/1980	119	07/16/1980	119	--	87	06/15/1980	265
1981	07/26/1981	83	05/02/1981	142	--	--	07/13/1981	132	07/13/1981	132	--	96	07/25/1981	409
1982	05/20/1982	332	07/03/1982	139	--	--	07/22/1982	264	07/22/1982	264	--	384	07/25/1982	2,000
1983	05/09/1983	262	05/13/1983	268	--	--	05/11/1983	283	05/11/1983	283	--	303	08/22/1983	411
1984	08/03/1984	198	05/12/1984	222	--	--	06/15/1984	249	06/15/1984	249	--	229	06/15/1984	414
1985	04/01/1985	75	05/10/1985	144	--	--	07/15/1985	134	07/15/1985	134	--	87	08/19/1985	300
1986	05/09/1986	123	06/03/1986	93	--	--	06/04/1986	89	06/04/1986	89	--	142	08/12/1986	919
1987	04/09/1987	99	07/31/1987	99	--	--	05/29/1987	99	05/29/1987	99	--	115	06/10/1987	388
1988	05/20/1988	69	08/01/1988	128	--	--	08/03/1988	126	08/03/1988	126	--	80	06/22/1988	201
1989	03/21/1989	55	07/12/1989	130	--	--	07/12/1989	111	07/12/1989	111	--	64	08/24/1989	1,360

Table S2–2. Selected information used in development of modern peak-flow chronology for the lower Rapid Creek study reach.—Continued

[Gray-shaded rows signify a gap in the chronology. (H) indicates historical value obtained from U.S. Army Corps of Engineers (1973). **Bold font** indicates special computations for lower Rapid Creek as noted in the "Supplement 2. Modern Peak-Flow Chronologies" section. Area, drainage area in square miles; Date, dates shown are for systematic peak-flow records, entries without dates are derived values; Q, peak-flow value in cubic feet per second; E, estimated; --, not available]

Water year	06410500		06411500		06412000		06412500		06412500		06412500		06414000	
	Rapid Creek above Pactola Reservoir at Silver City, S.Dak.		Rapid Creek below Pactola Dam, S.Dak.		Rapid Creek at Big Bend near Rapid City, S.Dak.		Rapid Creek above Canyon Lake near Rapid City, S.Dak.		Rapid Creek above Canyon Lake—extended record		Rapid Creek above Canyon Lake—extended record adjusted for regulation effects (modern chronology)		Rapid Creek at Rapid City, S.Dak.	
	Area = 294		Area = 322		Area = 339		Area = 375		Area = 375		Area = 375		Area = 414	
	Date	Q	Date	Q	Date	Q	Date	Q	Date	Q	Date	Q	Date	Q
1990	04/26/1990	93	07/02/1990	122	--	--	07/07/1990	124	07/07/1990	124	--	108	08/28/1990	231
1991	06/07/1991	421	08/29/1991	78	--	--	05/11/1991	201	05/11/1991	201	--	487	05/11/1991	659
1992	07/13/1992	55	05/21/1992	106	--	--	05/21/1992	105	05/21/1992	105	--	64	05/21/1992	152
1993	05/10/1993	867	06/19/1993	286	--	--	06/20/1993	328	06/20/1993	328	--	1,000	07/21/1993	500
1994	05/06/1994	196	04/27/1994	195	--	--	04/29/1994	198	04/29/1994	198	--	227	05/03/1994	670
1995	05/10/1995	879	05/15/1995	393	--	--	06/09/1995	479	06/09/1995	479	--	1,020	07/18/1995	786
1996	05/31/1996	711	06/07/1996	450	--	--	06/01/1996	652	06/01/1996	652	--	823	05/27/1996	880
1997	05/07/1997	524	06/11/1997	426	--	--	06/02/1997	1,050	06/02/1997	1,050	--	**1,090**	06/02/1997	3,190
1998	06/18/1998	1,290	07/02/1998	443	07/02/1998	481	06/24/1998	503	06/24/1998	503	--	1,490	09/13/1998	1,260
1999	06/15/1999	603	06/21/1999	444	06/17/1999	555	06/16/1999	642	06/16/1999	642	--	698	06/17/1999	708
2000	04/24/2000	228	05/18/2000	169	05/18/2000	175	05/20/2000	191	05/20/2000	191	--	264	05/17/2000	332
2001	04/07/2001	113	04/09/2001	101	07/11/2001	130	07/15/2001	107	07/15/2001	107	--	131	06/09/2001	533
2002	04/08/2002	137	07/04/2002	130	07/09/2002	112	07/06/2002	139	07/06/2002	139	--	159	07/20/2002	489
2003	03/15/2003	210	06/18/2003	111	06/19/2003	109	06/21/2003	115	06/21/2003	115	--	243	08/18/2003	166
2004	03/27/2004	58	08/19/2004	94	07/01/2004	102	07/01/2004	100	07/01/2004	100	--	67	07/03/2004	418
2005	05/13/2005	53	07/07/2005	105	07/07/2005	95	07/10/2005	104	07/10/2005	104	--	61	08/11/2005	274
2006	04/23/2006	90	06/30/2006	118	08/07/2006	110	08/07/2006	117	08/07/2006	117	--	104	08/07/2006	482
2007	06/02/2007	153	07/07/2007	107	07/09/2007	112	08/17/2007	159	08/17/2007	159	--	177	08/17/2007	535
2008	07/07/2008	1,640	07/17/2008	68	07/18/2008	80	05/24/2008	285	05/24/2008	285	--	**1,000**	05/24/2008	487
2009	04/24/2009	239	04/25/2009	220	04/26/2009	248	04/26/2009	243	04/26/2009	243	--	277	05/24/2009	342

Table S2–3. Selected information used in development of modern peak-flow chronology for the upper Rapid Creek study reach.

[Gray-shaded rows signify a gap in the chronology. Area, drainage area in square miles; Date, dates shown are for systematic peak-flow records, entries without dates are derived values; Q, peak-flow value in cubic feet per second; E, estimated; --, not available]

Water year	06409000		06410000		06410500		06410500		06411500		06412000	
	Castle Creek above Deerfield Reservoir near Hill City, S.Dak.		Castle Creek below Deerfield Dam, S.Dak.		Rapid Creek above Pactola Reservoir at Silver City, S.Dak.		Rapid Creek above Pactola Reservoir—extended record (modern chronology)		Rapid Creek below Pactola Dam, S.Dak.		Rapid Creek at Big Bend near Rapid City, S.Dak.	
	Area = 79.3		Area = 92.5		Area = 294		Area = 294		Area = 322		Area = 339	
	Date	Q	Date	Q	Date	Q	Date	Q	Date	Q	Date	Q
1915	--	--	--	--	--	--	--	566	--	--	06/26/1915	616
1916	--	--	--	--	--	--	--	187	--	--	05/24/1916	204
1917	--	--	--	--	--	--	--	248	--	--	06/04/1917	270
1929	--	--	--	--	--	--	--	752	06/03/1929	794	--	--
1930	--	--	--	--	--	--	--	184	04/09/1930	194	--	--
1931	--	--	--	--	--	--	--	147	04/08/1931	155	--	--
1932	--	--	--	--	--	--	--	646	04/24/1932	682	04/24/1932	694
1933	--	--	--	--	--	--	--	1,460	05/24/1933	1,540	05/24/1933	1,570
1934	--	--	--	--	--	--	--	111	02/11/1934	117	02/11/1934	119
1935	--	--	--	--	--	--	--	414	06/01/1935	437	05/01/1935	446
1936	--	--	--	--	--	--	--	95	04/13/1936	100	04/13/1936	102
1937	--	--	--	--	--	--	--	80	07/12/1937	84	07/12/1937	86
1938	--	--	--	--	--	--	--	81	04/16/1938	86	04/16/1938	88
1939	--	--	--	--	--	--	--	59	04/24/1939	62	04/24/1939	63
1940	--	--	--	--	--	--	--	232	08/27/1940	245	08/27/1940	250
1941	--	--	--	--	--	--	--	511	06/11/1941	540	06/11/1941	552
1942	--	--	--	--	--	--	--	387	05/16/1942	409	05/16/1942	417
1947	--	--	06/24/1947	151	--	--	--	903	06/23/1947	954	--	--
1948	--	--	06/30/1948	67	--	--	--	235	06/22/1948	248	--	--
1949	06/02/1949	48	04/05/1949	41	--	--	--	221	06/02/1949	233	--	--
1950	04/14/1950	108	04/15/1950	47	--	--	--	221	04/15/1950	233	--	--
1951	04/06/1951	55	05/14/1951	22	--	--	--	92	06/14/1951	97	--	--
1952	05/22/1952	1,120	05/22/1952	200	--	--	--	2,460	05/22/1952	2,170	--	--

Table S2–3. Selected information used in development of modern peak-flow chronology for the upper Rapid Creek study reach.—Continued

[Gray-shaded rows signify a gap in the chronology. Area, drainage area in square miles; Date, dates shown are for systematic peak-flow records, entries without dates are derived values; Q, peak-flow value in cubic feet per second; E, estimated; --, not available]

Water year	06409000		06410000		06410500		06410500		06411500		06412000	
	Castle Creek above Deerfield Reservoir near Hill City, S.Dak.		Castle Creek below Deerfield Dam, S.Dak.		Rapid Creek above Pactola Reservoir at Silver City, S.Dak.		Rapid Creek above Pactola Reservoir—extended record (modern chronology)		Rapid Creek below Pactola Dam, S.Dak.		Rapid Creek at Big Bend near Rapid City, S.Dak.	
	Area = 79.3		Area = 92.5		Area = 294		Area = 294		Area = 322		Area = 339	
	Date	Q	Date	Q	Date	Q	Date	Q	Date	Q	Date	Q
1953	08/15/1953	37	05/22/1953	30	--	--	--	152	06/15/1953	160	--	--
1954	05/23/1954	27	07/18/1954	65	05/23/1954	106	05/23/1954	106	05/23/1954	94	--	--
1955	04/16/1955	58	07/09/1955	60	07/28/1955	1,520	07/28/1955	1,520	07/29/1955	378	--	--
1956	05/28/1956	32	08/03/1956	53	03/24/1956	175	03/24/1956	175	03/25/1956	178	--	--
1957	08/27/1957	40	08/08/1957	42	05/25/1957	181	05/25/1957	181	03/14/1957	55	--	--
1958	07/18/1958	20	05/15/1958	69	05/31/1958	113	05/31/1958	113	06/02/1958	84	--	--
1959	04/16/1959	20	09/22/1959	128	09/25/1959	146	09/25/1959	146	08/21/1959	90	--	--
1960	03/28/1960	68	10/07/1959	31	03/23/1960	117	03/23/1960	117	07/20/1960	112	--	--
1961	06/13/1961	25	07/07/1961	90	07/07/1961	96	07/07/1961	96	06/11/1961	111	--	--
1962	04/15/1962	92	05/24/1962	11	06/15/1962	390	06/15/1962	390	05/18/1962	67	--	--
1963	06/05/1963	124	06/14/1963	14	06/16/1963	715	06/16/1963	715	06/30/1963	184	--	--
1964	06/09/1964	114	06/09/1964	64	06/09/1964	635	06/09/1964	635	06/10/1964	266	--	--
1965	06/17/1965	906	05/15/1965	90	05/15/1965	2,060	05/15/1965	2,060	05/19/1965	547	--	--
1966	03/31/1966	83	10/23/1965	55	03/16/1966	150	03/16/1966	150	03/20/1966	147	--	--
1967	03/29/1967	74	06/16/1967	59	06/16/1967	627	06/16/1967	627	06/22/1967	406	--	--
1968	07/17/1968	32	09/24/1968	39	06/09/1968	106	06/09/1968	106	10/04/1967	311	--	--
1969	07/17/1969	82	09/16/1969	40	07/20/1969	213	07/20/1969	213	05/20/1969	306	--	--
1970	04/27/1970	95	05/08/1970	74	04/19/1970	995	04/19/1970	995	05/12/1970	304	--	--
1971	04/17/1971	70	04/20/1971	61	04/25/1971	305	04/25/1971	305	04/25/1971	338	--	--
1972	05/10/1972	34	09/26/1972	40	07/06/1972	252	07/06/1972	252	10/05/1971	505	--	--
1973	05/05/1973	40	10/01/1972	40	05/09/1973	169	05/09/1973	169	05/08/1973	168	--	--
1974	03/28/1974	37	10/02/1973	26	04/30/1974	54	04/30/1974	54	07/04/1974	113	--	--
1975	04/23/1975	102	04/25/1975	46	04/26/1975	219	04/26/1975	219	06/07/1975	85	--	--
1976	06/15/1976	52	04/07/1976	28	06/15/1976	614	06/15/1976	614	06/29/1976	234	--	--

Table S2–3. Selected information used in development of modern peak-flow chronology for the upper Rapid Creek study reach.—Continued

[Gray-shaded rows signify a gap in the chronology. Area, drainage area in square miles; Date, dates shown are for systematic peak-flow records, entries without dates are derived values; Q, peak-flow value in cubic feet per second; E, estimated; --, not available]

Water year	06409000		06410000		06410500		06410500		06411500		06412000	
	Castle Creek above Deerfield Reservoir near Hill City, S.Dak.		Castle Creek below Deerfield Dam, S.Dak.		Rapid Creek above Pactola Reservoir at Silver City, S.Dak.		Rapid Creek above Pactola Reservoir—extended record (modern chronology)		Rapid Creek below Pactola Dam, S.Dak.		Rapid Creek at Big Bend near Rapid City, S.Dak.	
	Area = 79.3		Area = 92.5		Area = 294		Area = 294		Area = 322		Area = 339	
	Date	Q	Date	Q	Date	Q	Date	Q	Date	Q	Date	Q
1977	04/17/1977	27	10/15/1976	42	04/25/1977	187	04/25/1977	187	05/05/1977	188	--	--
1978	05/18/1978	64	05/18/1978	83	05/11/1978	430	05/11/1978	430	06/01/1978	386	--	--
1979	04/17/1979	30	02/09/1979	66	07/23/1979	173	07/23/1979	173	06/16/1979	101	--	--
1980	08/20/1980	28	09/08/1980	43	05/11/1980	75	05/11/1980	75	07/15/1980	118	--	--
1981	07/25/1981	20	07/31/1981	60	07/26/1981	83	07/26/1981	83	05/02/1981	142	--	--
1982	08/04/1982	148	08/04/1982	94	05/20/1982	332	05/20/1982	332	07/03/1982	139	--	--
1983	08/03/1983	87	05/08/1983	41	05/09/1983	262	05/09/1983	262	05/13/1983	268	--	--
1984	07/16/1984	122	06/16/1984	44	08/03/1984	198	08/03/1984	198	05/12/1984	222	--	--
1985	03/25/1985	34	07/25/1985	35	04/01/1985	75	04/01/1985	75	05/10/1985	144	--	--
1986	04/15/1986	34	09/21/1986	26	05/09/1986	123	05/09/1986	123	06/03/1986	93	--	--
1987	03/07/1987	31	04/10/1987	34	04/09/1987	99	04/09/1987	99	07/31/1987	99	--	--
1988	04/07/1988	57	05/18/1988	26	05/20/1988	69	05/20/1988	69	08/01/1988	128	--	--
1989	03/09/1989	23	08/11/1989	26	03/21/1989	55	03/21/1989	55	07/12/1989	130	--	--
1990	04/03/1990	33	04/26/1990	34	04/26/1990	93	04/26/1990	93	07/02/1990	122	--	--
1991	06/03/1991	106	06/06/1991	81	06/07/1991	421	06/07/1991	421	08/29/1991	78	--	--
1992	05/21/1992	30	03/10/1992	23	07/13/1992	55	07/13/1992	55	05/21/1992	106	--	--
1993	06/08/1993	113	06/10/1993	53	05/10/1993	867	05/10/1993	867	06/19/1993	286	--	--
1994	04/22/1994	65	05/13/1994	37	05/06/1994	196	05/06/1994	196	04/27/1994	195	--	--
1995	05/08/1995	153	06/14/1995	56	05/10/1995	879	05/10/1995	879	05/15/1995	393	--	--
1996	04/09/1996	271	05/31/1996	54	05/31/1996	711	05/31/1996	711	06/07/1996	450	--	--
1997	07/24/1997	116	--	--	05/07/1997	524	05/07/1997	524	06/11/1997	426	--	--
1998	06/18/1998	176	06/24/1998	87	06/18/1998	1,290	06/18/1998	1,290	07/02/1998	443	07/02/1998	481
1999	03/25/1999	198	--	--	06/15/1999	603	06/15/1999	603	06/21/1999	444	06/17/1999	555
2000	04/19/2000	291	04/29/2000	38	04/24/2000	228	04/24/2000	228	05/18/2000	169	05/18/2000	175

Table S2–3. Selected information used in development of modern peak-flow chronology for the upper Rapid Creek study reach.—Continued

[Gray-shaded rows signify a gap in the chronology. Area, drainage area in square miles; Date, dates shown are for systematic peak-flow records, entries without dates are derived values; Q, peak-flow value in cubic feet per second; E, estimated; --, not available]

Water year	06409000		06410000		06410500		06410500		06411500		06412000	
	Castle Creek above Deerfield Reservoir near Hill City, S.Dak.		Castle Creek below Deerfield Dam, S.Dak.		Rapid Creek above Pactola Reservoir at Silver City, S.Dak.		Rapid Creek above Pactola Reservoir—extended record (modern chronology)		Rapid Creek below Pactola Dam, S.Dak.		Rapid Creek at Big Bend near Rapid City, S.Dak.	
	Area = 79.3		Area = 92.5		Area = 294		Area = 294		Area = 322		Area = 339	
	Date	Q	Date	Q	Date	Q	Date	Q	Date	Q	Date	Q
2001	07/13/2001	56	07/16/2001	51	04/07/2001	113	04/07/2001	113	04/09/2001	101	07/11/2001	130
2002	03/09/2002	388	04/21/2002	32	04/08/2002	137	04/08/2002	137	07/04/2002	130	07/09/2002	112
2003	03/31/2003	288	09/17/2003	47	03/15/2003	210	03/15/2003	210	06/18/2003	111	06/19/2003	109
2004	03/27/2004	31	09/07/2004	34	03/27/2004	58	03/27/2004	58	08/19/2004	94	07/01/2004	102
2005	05/12/2005	22	05/18/2005	39	05/13/2005	53	05/13/2005	53	07/07/2005	105	07/07/2005	95
2006	05/23/2006	35	03/29/2006	43	04/23/2006	90	04/23/2006	90	06/30/2006	118	08/07/2006	110
2007	03/19/2007	35	08/20/2007	11	06/02/2007	153	06/02/2007	153	07/07/2007	107	07/09/2007	112
2008	07/06/2008	61	08/10/2008	13	07/07/2008	1,640	07/07/2008	1,640	07/17/2008	68	07/18/2008	80
2009	04/16/2009	48	04/16/2009	37	04/24/2009	239	04/24/2009	239	04/25/2009	220	04/26/2009	248

Table S2–4. Selected information used in development of modern peak-flow chronology for the Boxelder Creek study reach.

[Gray-shaded rows signify a gap in the chronology. Area, drainage area in square miles; Date, dates shown are for systematic peak-flow records, entries without dates are derived values; Q, peak-flow value in cubic feet per second; E, estimated; --, not available]

Water year	06422500 Boxelder Creek near Nemo, S.Dak. Area = 94.4		Boxelder Creek upstream subreach (modern chronology) Area = 98		Boxelder Creek downstream subreach (modern chronology) Area = 112		06422650 Boxelder Creek at Doty School near Blackhawk, S.Dak. Area = 116		06423000 Boxelder Creek at Blackhawk, S.Dak. Area = 126	
	Date	Q	Date	Q	Date	Q	Date	Q	Date	Q
1904	--	521	--	533	--	578	--	--	06/05/1904	620
1905	--	547	--	559	--	606	--	--	07/02/1905	650
1907	06/12/1907	16,000	--	16,400	--	17,700	--	--	--	--
1946	05/02/1946	1,180	--	1,210	--	1,310	--	--	05/02/1946	1,320
1947	05/23/1947	372	--	380	--	412	--	--	06/23/1947	395
1966	07/28/1966	30	--	31	--	33	--	--	--	--
1967	06/12/1967	950	--	972	--	1,050	--	--	--	--
1968	06/09/1968	62	--	63	--	69	--	--	--	--
1969	05/04/1969	144	--	147	--	160	--	--	--	--
1970	06/12/1970	648	--	663	--	718	--	--	--	--
1971	04/25/1971	221	--	226	--	245	--	--	--	--
1972	06/09/1972	30,100	--	30,800	--	50,500	06/09/1972	51,600	--	--
1973	04/20/1973	117	--	120	--	130	--	--	--	--
1974	04/19/1974	23	--	24	--	25	--	--	--	--
1975	07/30/1975	427	--	437	--	473	--	--	--	--
1976	06/15/1976	1,460	--	1,490	--	1,620	--	--	--	--
1977	04/17/1977	170	--	174	--	188	--	--	--	--
1978	05/11/1978	301	--	308	--	334	05/18/1978	251	--	--
1979	07/04/1979	97	--	99	--	107	--/--/1979	.00	--	--
1980	03/13/1980	35	--	36	--	39	--/--/1980	.00	--	--
1981	05/18/1981	26	--	27	--	29	--	--	--	--
1982	05/20/1982	272	--	278	--	301	--	--	--	--
1983	05/07/1983	178	--	182	--	197	--	--	--	--
1984	06/15/1984	215	--	220	--	238	--	--	--	--
1985	03/18/1985	129	--	132	--	143	--	--	--	--
1986	05/09/1986	82	--	84	--	91	--	--	--	--
1987	03/06/1987	123	--	126	--	136	--	--	--	--
1988	05/09/1988	33	--	34	--	37	--	--	--	--
1989	03/10/1989	30	--	31	--	33	--	--	--	--
1990	05/05/1990	29	--	30	--	32	--	--	--	--
1991	06/06/1991	401	--	410	--	444	--	--	--	--
1992	06/13/1992	53	--	54	--	59	--	--	--	--
1993	06/07/1993	293	--	300	--	325	--	--	--	--
1994	05/06/1994	125	--	128	--	139	--	--	--	--
1995	05/09/1995	1,140	--	1,170	--	1,260	--	--	--	--

Table S2–4. Selected information used in development of modern peak-flow chronology for the Boxelder Creek study reach.—Continued

[Gray-shaded rows signify a gap in the chronology. Area, drainage area in square miles; Date, dates shown are for systematic peak-flow records, entries without dates are derived values; Q, peak-flow value in cubic feet per second; E, estimated; --, not available]

Water year	06422500 Boxelder Creek near Nemo, S.Dak.		Boxelder Creek upstream subreach (modern chronology)		Boxelder Creek downstream subreach (modern chronology)		06422650 Boxelder Creek at Doty School near Blackhawk, S.Dak.		06423000 Boxelder Creek at Blackhawk, S.Dak.	
	Area = 94.4		Area = 98		Area = 112		Area = 116		Area = 126	
	Date	Q	Date	Q	Date	Q	Date	Q	Date	Q
1996	05/30/1996	826	--	845	--	915	--	--	--	--
1997	06/02/1997	463	--	474	--	513	--	--	--	--
1998	06/18/1998	607	--	621	--	673	--	--	--	--
1999	06/15/1999	327	--	334	--	362	--	--	--	--
2000	04/25/2000	178	--	182	--	197	--	--	--	--
2001	04/07/2001	52	--	53	--	58	--	--	--	--
2002	04/08/2002	47	--	48	--	52	--	--	--	--
2003	03/13/2003	100	--	102	--	111	--	--	--	--
2004	03/11/2004	19	--	19	--	21	--	--	--	--
2005	05/14/2005	24	--	25	--	27	--	--	--	--
2006	04/23/2006	103	--	105	--	114	--	--	--	--
2007	06/02/2007	200	--	205	--	222	--	--	--	--
2008	07/07/2008	646	--	661	--	716	--	--	--	--
2009	04/16/2009	368	--	376	--	408	--	--	--	--

Table S2–5. Selected information used in development of modern peak-flow chronology for the Elk Creek study reach.

[Gray-shaded rows signify a gap in the chronology. Area, drainage area in square miles; Date, dates shown are for systematic peak-flow records, entries without dates are derived values; Q, peak-flow value in cubic feet per second; E, value estimated on the basis of 1972 peak-flow value; --, not available]

Water year	06422500 Boxelder Creek near Nemo, S.Dak. Area = 94.4		06424000 Elk Creek near Roubaix, S.Dak. Area = 21.6		Extended record for Elk Creek near Roubaix (06424000) Area = 21.6		Elk Creek study reach (modern chronology) Area = 40		06424500 Elk Creek above Piedmont, S.Dak. Area = 47.6		06425100 Elk Creek near Rapid City, S.Dak. Area = 211		06425500 Elk Creek near Elm Springs, S.Dak. Area = 549	
	Date	Q	Date	Q	Date	Q	Date	Q	Date	Q	Date	Q	Date	Q
1907	06/12/1907	16,000	--	--	--	--	--	E10,400	--	--	--	--	--	--
1945	--	--	--	--	--	--	--	1,630	08/01/1945	1,810	--	--	--	--
1946	05/02/1946	1,180	05/02/1946	378	--	--	--	1,220	05/02/1946	1,350	--	--	--	--
1947	05/23/1947	372	06/22/1947	218	--	--	--	314	06/23/1947	348	--	--	--	--
1950	--	--	--	--	--	--	--	--	--	--	--	--	04/15/1950	852
1951	--	--	--	--	--	--	--	--	--	--	--	--	09/02/1951	328
1952	--	--	--	--	--	--	--	--	--	--	--	--	03/29/1952	8,540
1953	--	--	--	--	--	--	--	--	--	--	--	--	06/19/1953	5,250
1954	--	--	--	--	--	--	--	--	--	--	--	--	06/10/1954	838
1955	--	--	--	--	--	--	--	--	--	--	--	--	09/20/1955	270
1956	--	--	--	--	--	--	--	--	--	--	--	--	07/03/1956	48
1957	--	--	--	--	--	--	--	--	--	--	--	--	05/26/1957	2,690
1958	--	--	--	--	--	--	--	--	--	--	--	--	06/16/1958	616
1959	--	--	--	--	--	--	--	--	--	--	--	--	05/29/1959	16
1960	--	--	--	--	--	--	--	--	--	--	--	--	06/30/1960	796
1961	--	--	--	--	--	--	--	--	--	--	--	--	--/--/1985	.00
1962	--	--	--	--	--	--	--	--	--	--	--	--	05/29/1962	7,040
1963	--	--	--	--	--	--	--	--	--	--	--	--	06/17/1963	698
1964	--	--	--	--	--	--	--	--	--	--	--	--	06/08/1964	3,620
1965	--	--	--	--	--	--	--	--	--	--	--	--	05/16/1965	3,250
1966	07/28/1966	30	--	--	--	61	--	89	--	--	--	--	03/14/1966	775
1967	06/12/1967	950	--	--	--	352	--	510	--	--	--	--	06/16/1967	4,960
1968	06/09/1968	62	--	--	--	72	--	104	--	--	--	--	06/07/1968	1,020
1969	05/04/1969	144	--	--	--	98	--	141	--	--	--	--	07/17/1969	2,300
1970	06/12/1970	648	--	--	--	257	--	372	--	--	--	--	04/26/1970	2,920

Table S2–5. Selected information used in development of modern peak-flow chronology for the Elk Creek study reach.—Continued

[Gray-shaded rows signify a gap in the chronology. Area, drainage area in square miles; Date, dates shown are for systematic peak-flow records, entries without dates are derived values; Q, peak-flow value in cubic feet per second; E, value estimated on the basis of 1972 peak-flow value; --, not available]

Water year	06422500 Boxelder Creek near Nemo, S.Dak. Area = 94.4		06424000 Elk Creek near Roubaix, S.Dak. Area = 21.6		Extended record for Elk Creek near Roubaix (06424000) Area = 21.6		Elk Creek study reach (modern chronology) Area = 40		06424500 Elk Creek above Piedmont, S.Dak. Area = 47.6		06425100 Elk Creek near Rapid City, S.Dak. Area = 211		06425500 Elk Creek near Elm Springs, S.Dak. Area = 549	
	Date	Q	Date	Q	Date	Q	Date	Q	Date	Q	Date	Q	Date	Q
1971	04/25/1971	221	--	--	--	122	--	176	--	--	--	--	05/23/1971	3,510
1972	06/09/1972	30,100	--	--	--		--	10,400	06/09/1972	11,600	--	--	06/11/1972	1,880
1973	04/20/1973	117	--	--	--	89	--	129	--	--	--	--	04/22/1973	1,440
1974	04/19/1974	23	--	--	--	59	--	86	--	--	--	--	04/09/1974	54
1975	07/30/1975	427	--	--	--	187	--	271	--	--	--	--	04/27/1975	1,210
1976	06/15/1976	1,460	--	--	--	514	--	744	--	--	--	--	06/17/1976	2,230
1977	04/17/1977	170	--	--	--	106	--	153	--	--	--	--	06/14/1977	2,270
1978	05/11/1978	301	--	--	--	147	--	213	--	--	--	--	03/18/1978	2,830
1979	07/04/1979	97	--	--	--	83	--	120	--	--	08/08/1979	310	03/17/1979	92
1980	03/13/1980	35	--	--	--	63	--	91	--	--	06/14/1980	379	06/15/1980	437
1981	05/18/1981	26	--	--	--	60	--	87	--	--	07/02/1981	65	08/13/1981	124
1982	05/20/1982	272	--	--	--	138	--	200	--	--	05/20/1982	1,560	05/21/1982	5,300
1983	05/07/1983	178	--	--	--	108	--	157	--	--	10/10/1982	1,000	10/10/1983	1,940
1984	06/15/1984	215	--	--	--	120	--	174	--	--	06/10/1984	905	05/04/1984	890
1985	03/18/1985	129	--	--	--	93	--	134	--	--	03/17/1985	113	03/20/1985	73
1986	05/09/1986	82	--	--	--	78	--	113	--	--	02/26/1986	1,390	02/27/1986	4,960
1987	03/06/1987	123	--	--	--	91	--	132	--	--	05/24/1987	792	05/27/1987	718
1988	05/09/1988	33	--	--	--	62	--	90	--	--	03/30/1988	197	03/24/1988	101
1989	03/10/1989	30	--	--	--	61	--	89	--	--	05/17/1989	190	03/22/1989	11
1990	05/05/1990	29	--	--	--	61	--	89	--	--	05/24/1990	.66	09/02/1990	47
1991	06/06/1991	401	--	--	--	179	--	259	--	--	05/12/1991	995	05/28/1991	620
1992	06/13/1992	53	05/10/1992	15	--	15	--	22	--	--	--/--/1992	.00	06/21/1992	27
1993	06/07/1993	293	06/08/1993	154	--	154	--	223	--	--	05/08/1993	1,070	05/08/1993	3,660
1994	05/06/1994	125	05/05/1994	103	--	103	--	149	--	--	03/03/1994	90	06/08/1994	5,570
1995	05/09/1995	1,140	05/08/1995	515	--	515	--	745	--	--	05/09/1995	2,860	05/10/1995	4,580
1996	05/30/1996	826	05/30/1996	176	--	176	--	255	--	--	05/27/1996	3,120	05/28/1996	7,660
1997	06/02/1997	463	04/07/1997	200	--	200	--	289	--	--	05/26/1997	1,450	02/18/1997	3,000

Table S2–5. Selected information used in development of modern peak-flow chronology for the Elk Creek study reach.—Continued

[Gray-shaded rows signify a gap in the chronology. Area, drainage area in square miles; Date, dates shown are for systematic peak-flow records, entries without dates are derived values; Q, peak-flow value in cubic feet per second; E, value estimated on the basis of 1972 peak-flow value; --, not available]

Water year	06422500		06424000		Extended record for Elk Creek near Roubaix (06424000)		Elk Creek study reach (modern chronology)		06424500		06425100		06425500	
	Boxelder Creek near Nemo, S.Dak.		Elk Creek near Roubaix, S.Dak.						Elk Creek above Piedmont, S.Dak.		Elk Creek near Rapid City, S.Dak.		Elk Creek near Elm Springs, S.Dak.	
	Area = 94.4		Area = 21.6		Area = 21.6		Area = 40		Area = 47.6		Area = 211		Area = 549	
	Date	Q	Date	Q	Date	Q	Date	Q	Date	Q	Date	Q	Date	Q
1998	06/18/1998	607	06/18/1998	197	--	197	--	285	--	--	06/18/1998	357	06/19/1998	592
1999	06/15/1999	327	04/21/1999	133	--	133	--	192	--	--	04/22/1999	985	10/17/1999	5,150
2000	04/25/2000	178	05/11/2000	123	--	123	--	178	--	--	04/25/2000	881	04/19/2000	3,000
2001	04/07/2001	52	04/23/2001	39	--	39	--	56	--	--	03/04/2001	57	03/07/2001	1,200
2002	04/08/2002	47	04/08/2002	155	--	155	--	224	--	--	04/02/2002	16	04/29/2002	19
2003	03/13/2003	100	03/14/2003	100	--	100	--	145	--	--	05/05/2003	20	03/19/2003	61
2004	03/11/2004	19	03/27/2004	28	--	28	--	41	--	--	03/18/2004	10	05/23/2004	37
2005	05/14/2005	24	05/13/2005	45	--	45	--	65	--	--	--/--/2005	.00	05/12/2005	28
2006	04/23/2006	103	09/23/2006	153	--	153	--	221	--	--	04/28/2006	10	09/22/2006	2.4
2007	06/02/2007	200	06/07/2007	132	--	132	--	191	--	--	08/18/2007	68	08/24/2007	.58
2008	07/07/2008	646	08/06/2008	300	--	300	--	434	--	--	06/06/2008	2,390	06/06/2008	7,000
2009	04/16/2009	368	04/15/2009	130	--	130	--	188	--	--	04/13/2009	2,400	04/14/2009	5,090

Supplement 3. Schematic Diagrams

Stratigraphic investigations that were conducted for some sites along several of the study reaches were not incorporated in flood-frequency analyses. Schematic diagrams for such sites are not included within the main body of this report, but are provided in this section (figs. S3–1 through S3–10) as documentation for potential future purposes that may arise.

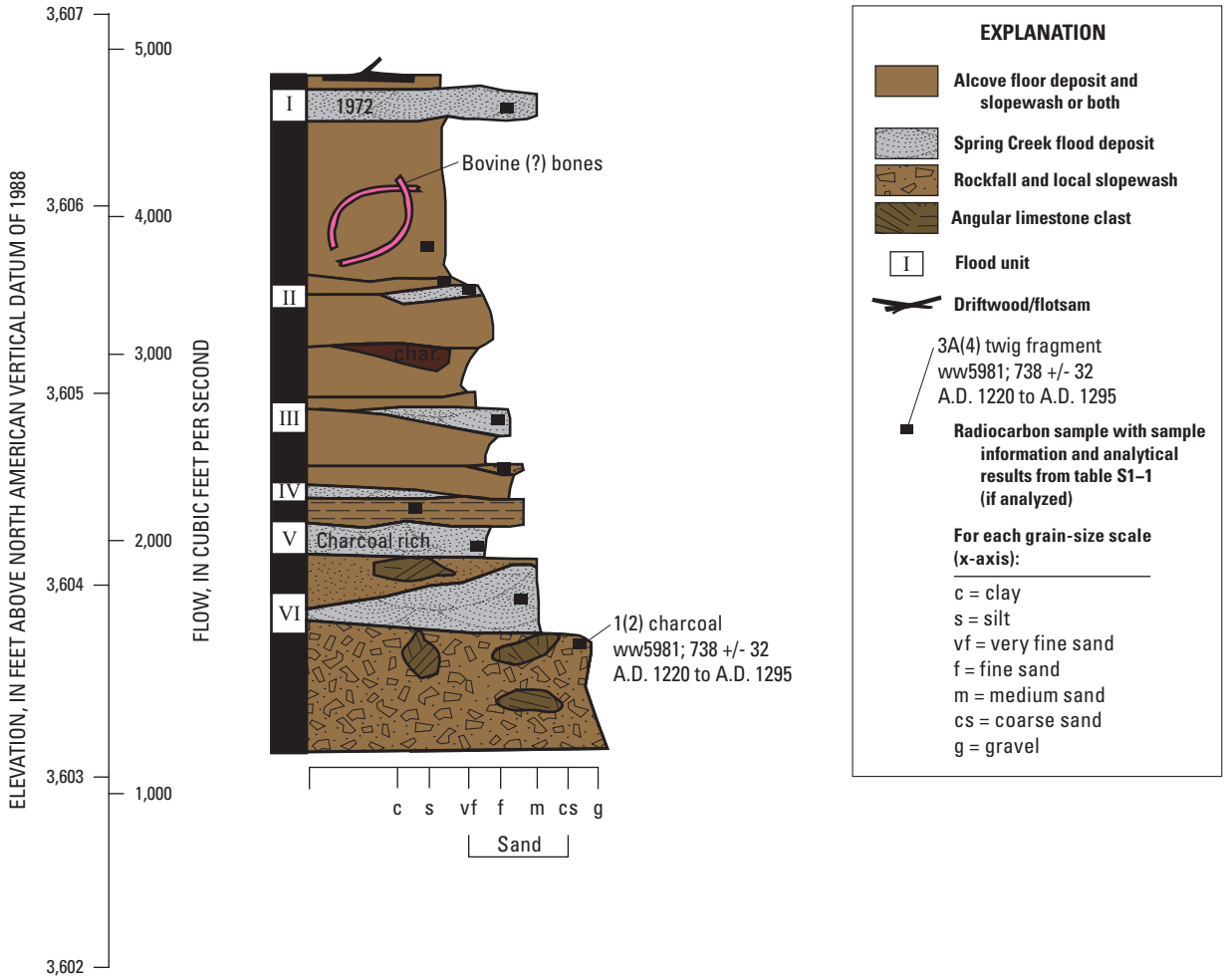

Figure S3–1. Schematic diagram showing paleoflood information for Olympia Alcove, Spring Creek.

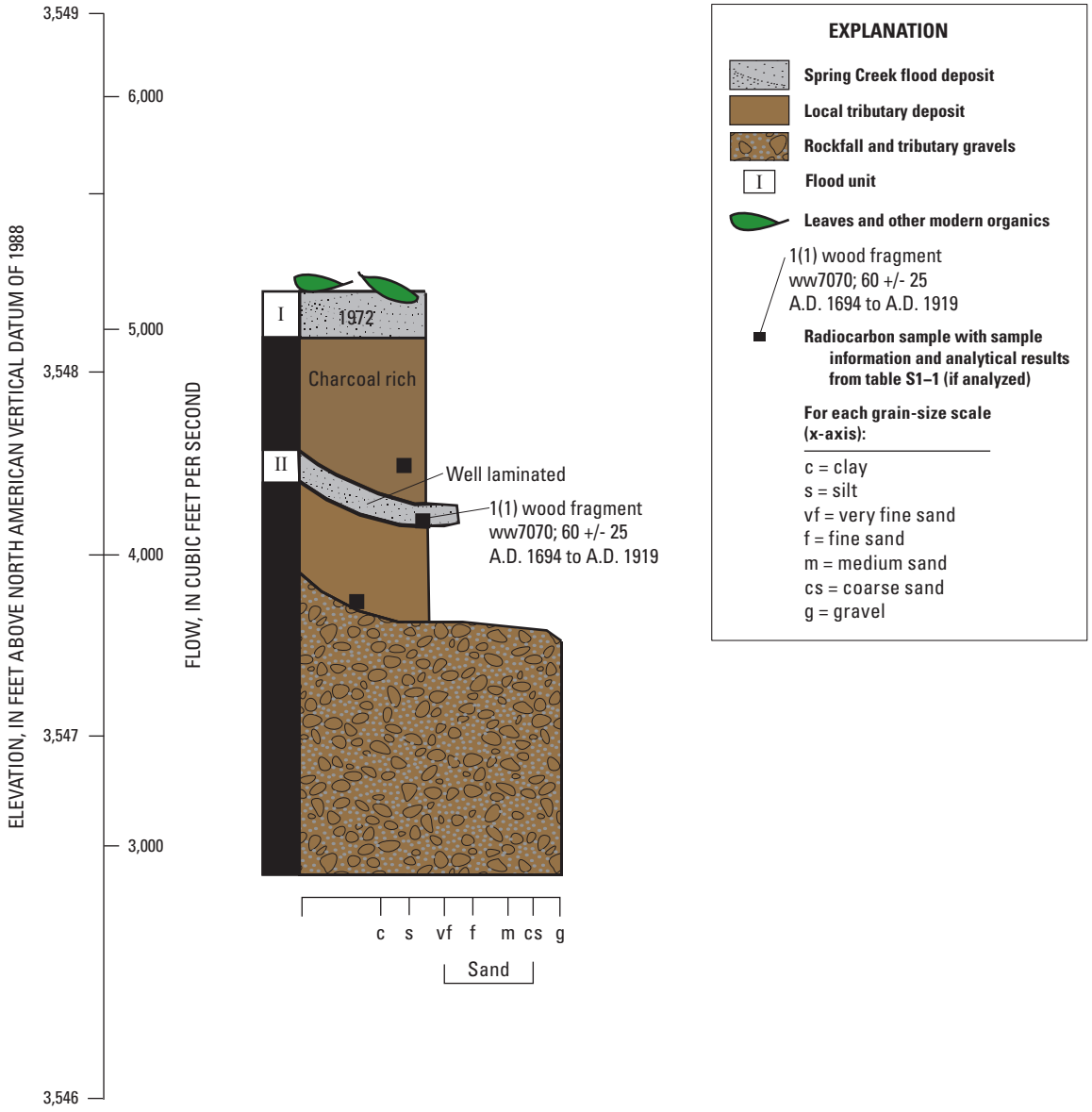

Figure S3–2. Schematic diagram showing paleoflood information for Near Strike Alcove, Spring Creek.

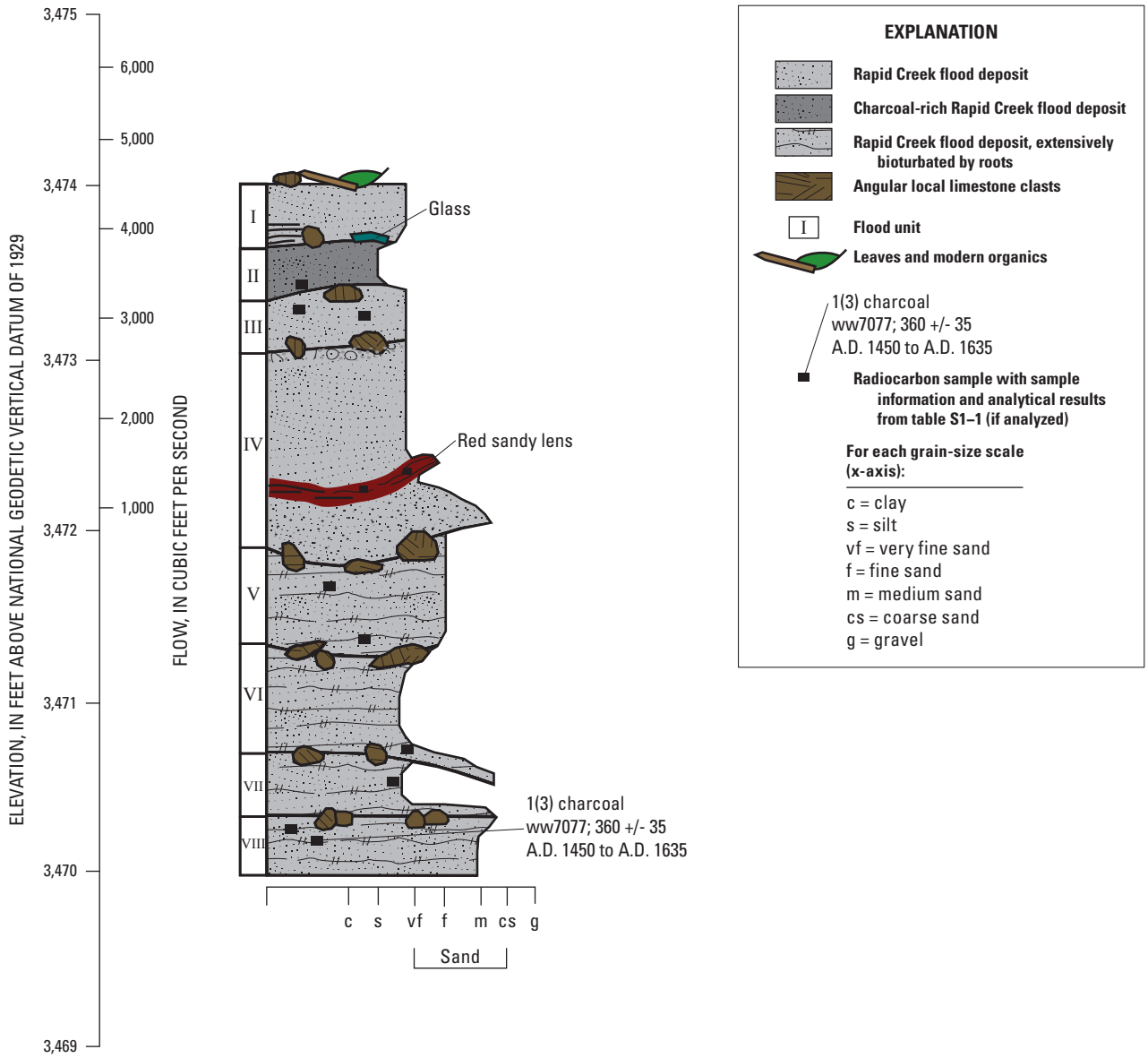

Figure S3–3. Schematic diagram showing paleoflood information for Church Mug Alcove, lower Rapid Creek.

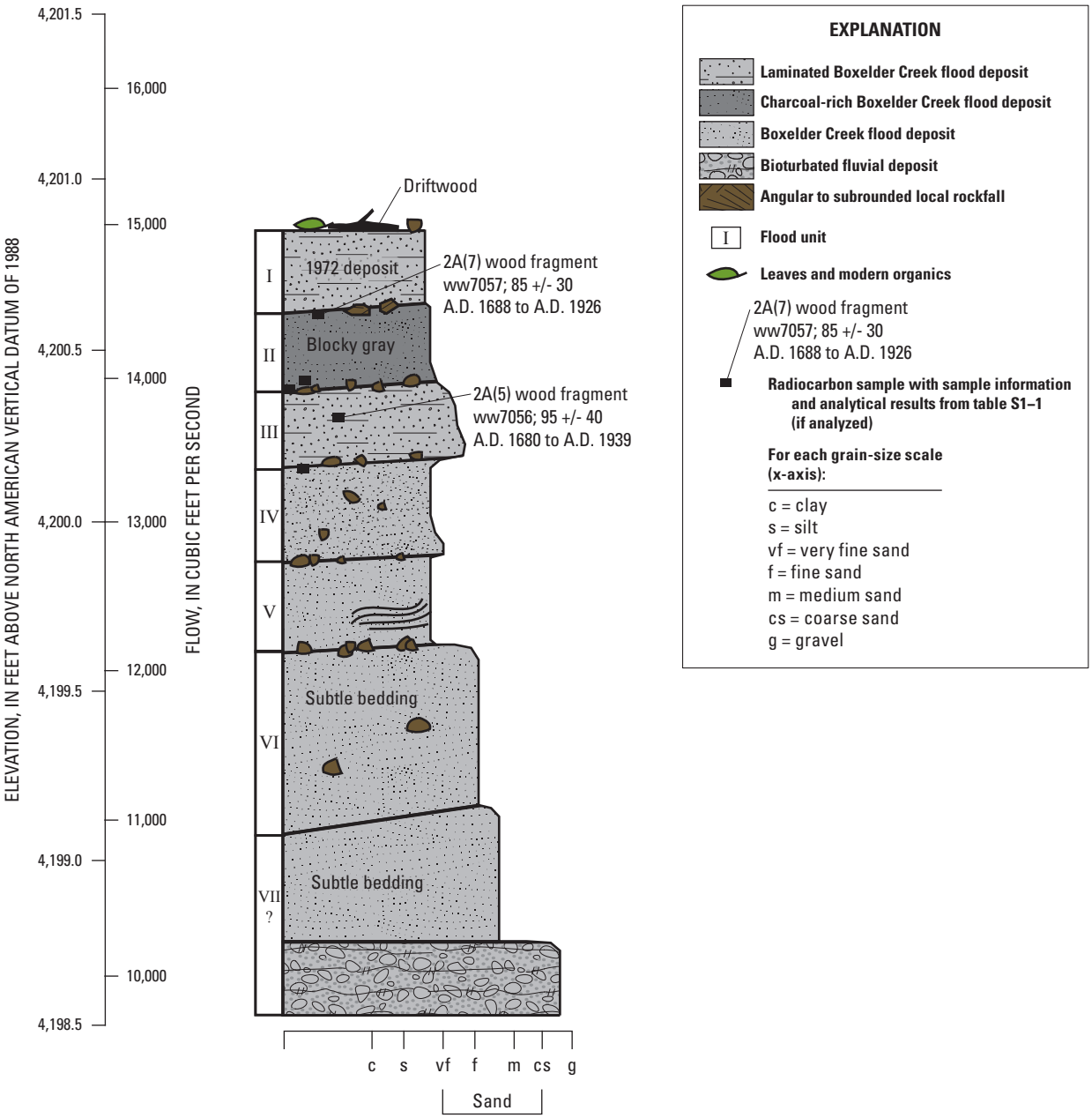

Figure S3–4. Schematic diagram showing paleoflood information for Benchmark Alcove, upstream subreach of Boxelder Creek.

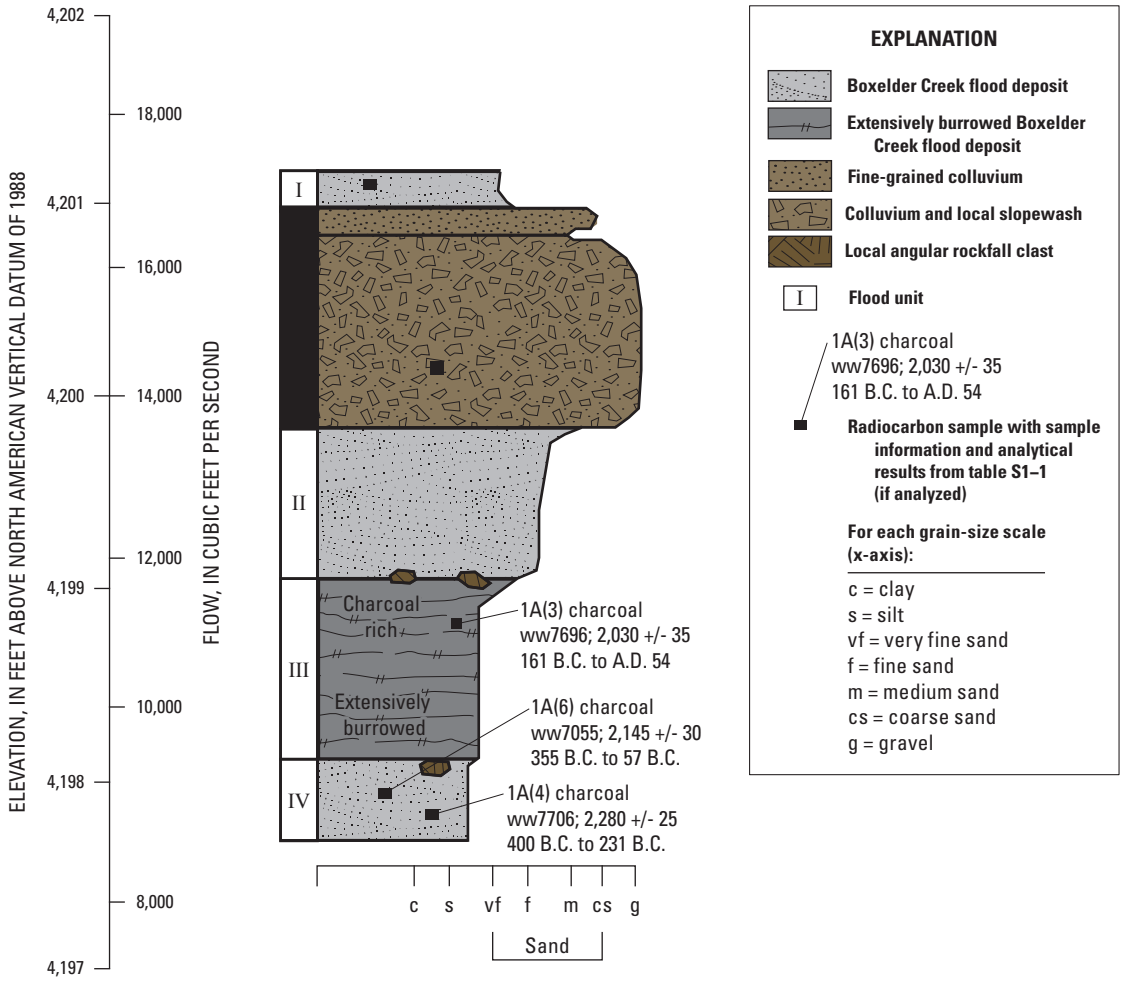

Figure S3–5. Schematic diagram showing paleoflood information for Snap-E-Tom Alcove, upstream subreach of Boxelder Creek.

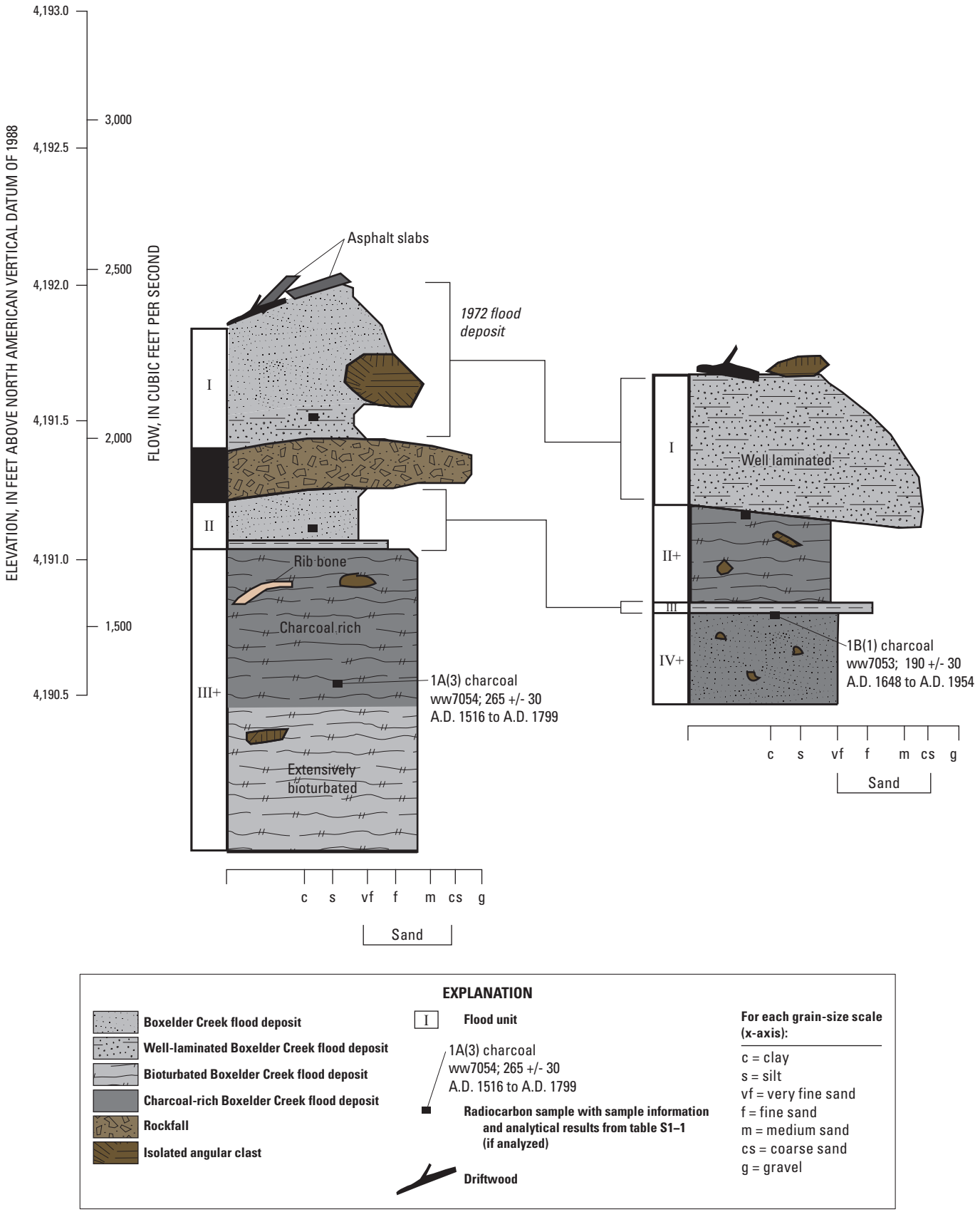

Figure S3–6. Schematic diagram showing paleoflood information for Asphalt Alcove, upstream subreach of Boxelder Creek.

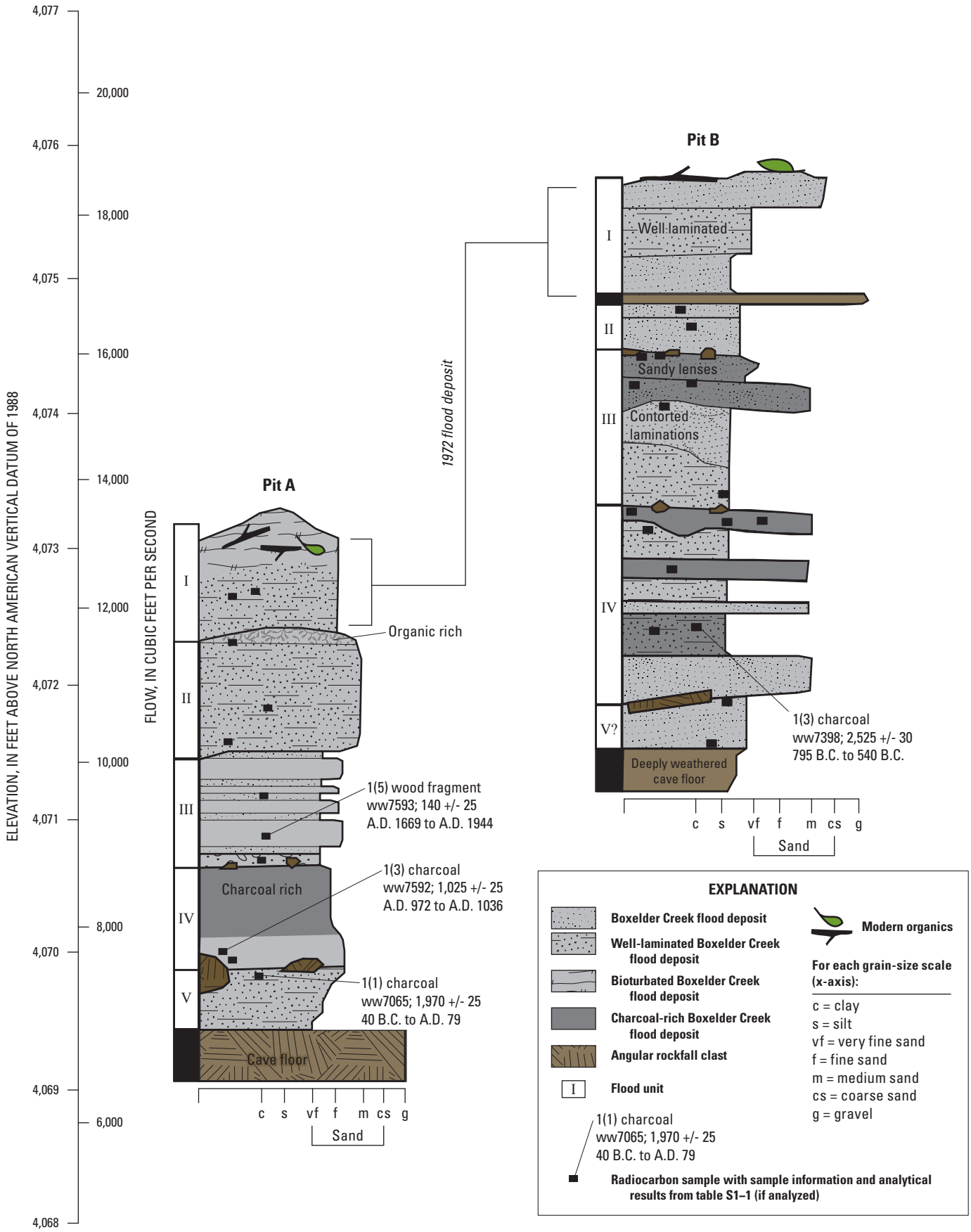

Figure S3–7. Schematic diagram showing paleoflood information for Snow Shovel Alcove, downstream subreach of Boxelder Creek.

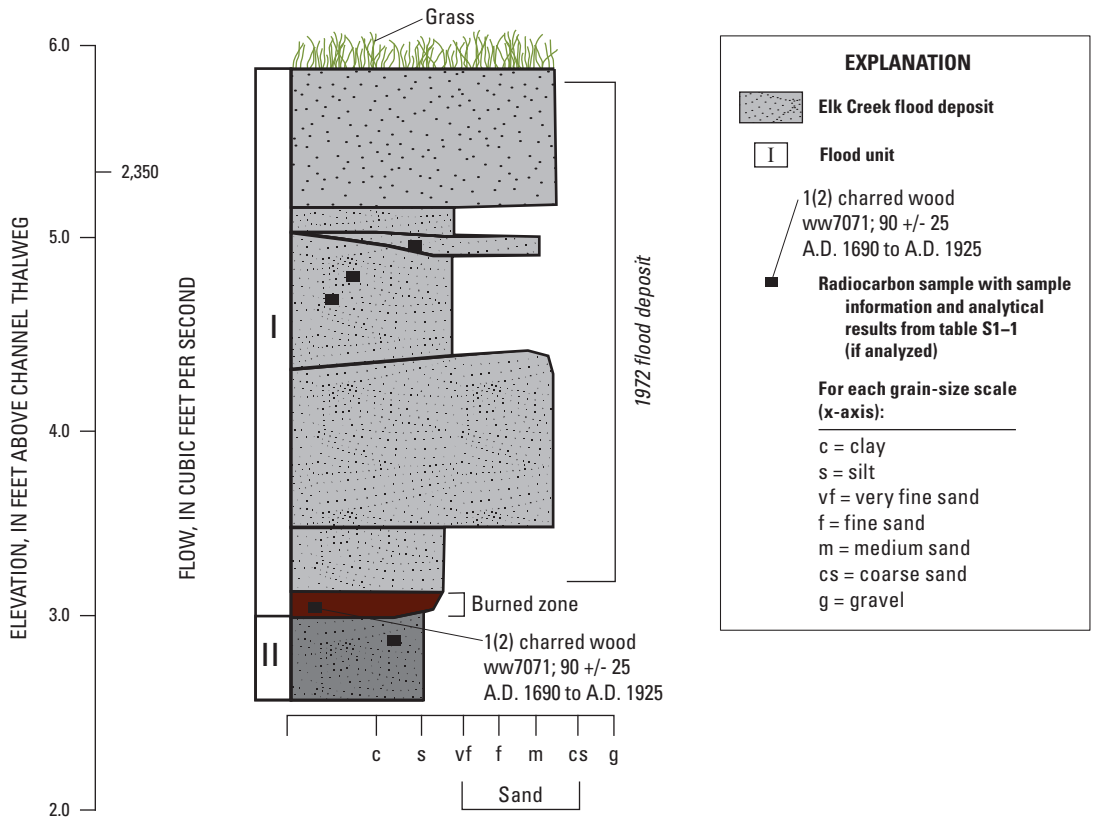

Figure S3–8. Schematic diagram showing paleoflood information for Sand Wall Alcove, Elk Creek.

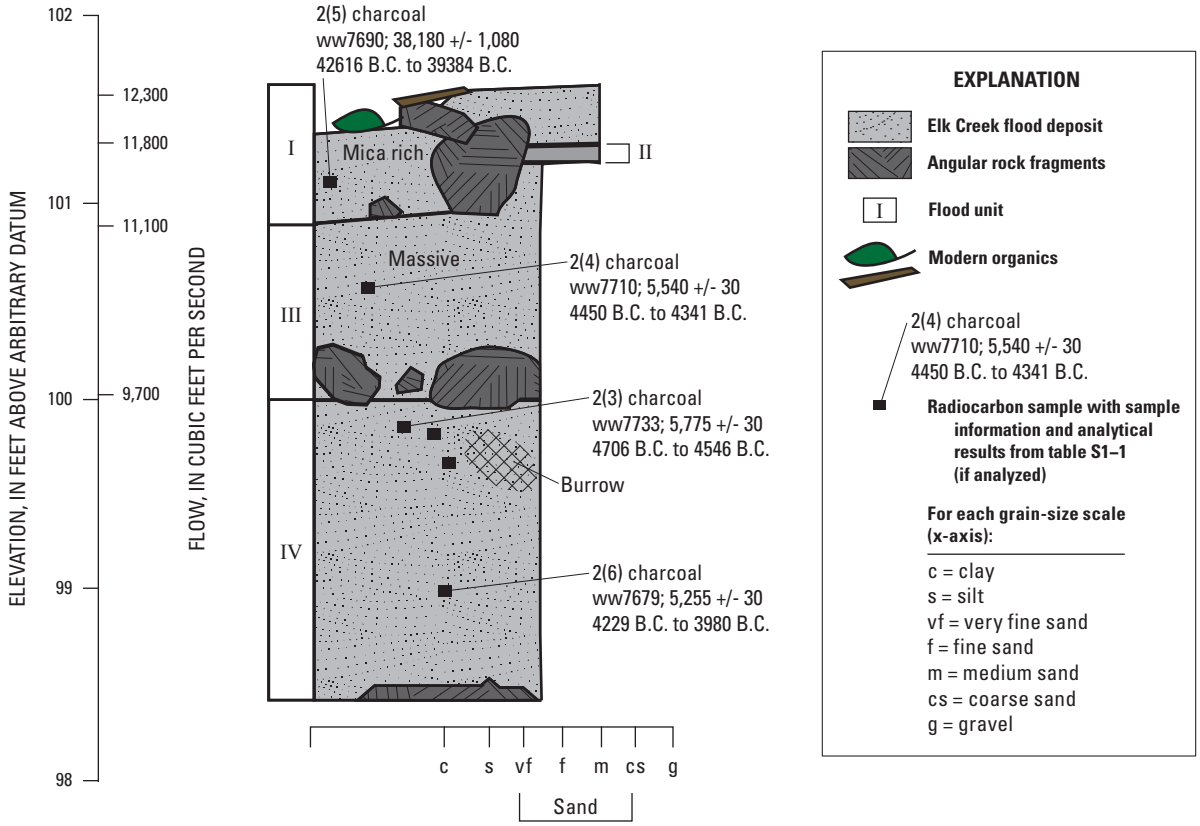

Figure S3–9. Schematic diagram showing paleoflood information for Flat Rock Alcove, Elk Creek.

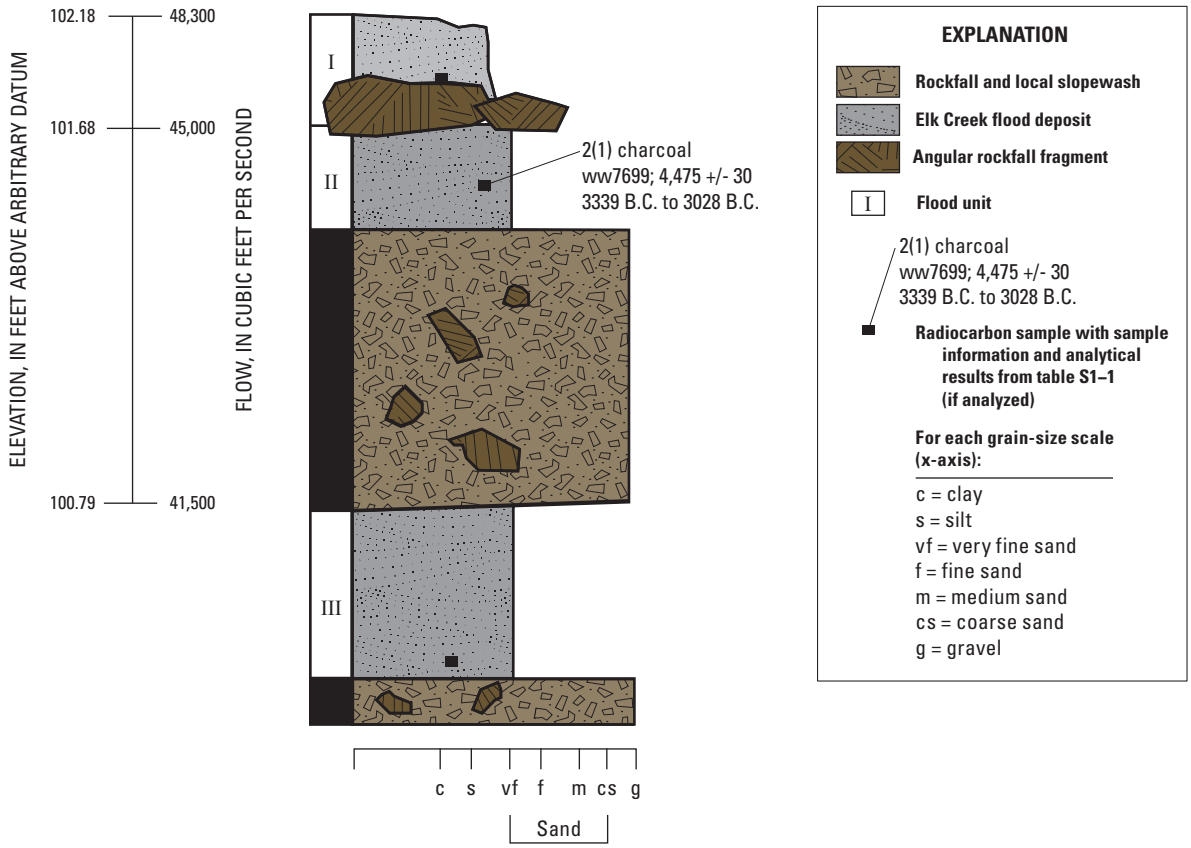

Figure S3–10. Schematic diagram showing paleoflood information for Bird's Nest Alcove, Elk Creek.

Publishing support provided by:
Rolla Publishing Service Center

For additional information concerning this publication, contact:
Director, USGS South Dakota Water Science Center
1608 Mt. View Rd.
Rapid City, SD 57702
(605) 394-3200

Or visit the South Dakota Water Science Center Web site at:
http://sd.water.usgs.gov

Back cover. Dracula's Ledge along Elk Creek, where four paleofloods of at least 75,000 cubic feet per second in the last 2,000 years have been recorded by flood deposits. A fifth flood of at least 51,000 cubic feet per second is recorded by a beaver-chewed driftwood log.

Inside back cover. Flood deposits for several Boxelder Creek locations shown in the inside front cover.

ISBN 978-1-4113-3230-0

Printed on recycled paper